UNIVERSITATEA DE ȘTIINȚE AGRICOLE ȘI MEDICINĂ
VETERINARĂ "ION IONESCU DE LA BRAD" IAȘI

LUCRĂRI ȘTIINȚIFICE

VOL. 59
MEDICINĂ VETERINARĂ

PARTEA 1

EDITURA "ION IONESCU DE LA BRAD" IAȘI 2016

on -line ISSN 2393 – 4603
ISSN–L 1454 – 7406

CUPRINS

CITOMORPHOLOGICAL DIAGNOSTIC OF MALIGNANT HISTIOCYTIC NEOPLASM IN DOGS

[1]Emilia BALINT, [2]Nicoale MANOLESCU, [1]Daniel LASTOFKA, [3]Andrei POPESCU

[1]The Faculty of Veterinary Medicine, Bucharest, Romania; [2]Bucharest Oncological Institute; [3]PhD Student at the Romanian Academy

emilia_balint@yahoo.com

Abstract

From the literature results that it can't be found information, for the canine species, about the cytomorfological differential diagnosis in the malignant histio-dendritical proliferations. In this paper the authors want to bring a series of exclusive cytomorphologic arguments for the positive diagnosis and differential diagnosis of canine malignat proliferations, which have as a proliferative cellular base, the histiocytic cell and the dendritic cell. In this study we discuss three cytomorphologic forms of malignant proliferations of the histiocytic and dendritic cell. Two of these forms, the dendritic sarcoma and the histiocytic sarcoma, belong to the malignant lymphoma category; these are solid tumors localized in the tegument, lymph nodes and spleen. The third histiocytic proliferation forms is the histiomonocytic leukemia, which belongs to the liquid forms, localized in the hematopoietic marrow, with permanent cytemic discharge in the peripheral blood. Between the dendritic sarcoma and the histiocytic sarcoma diagnosis confusions can be created. The differential diagnosis can be made with difficulty on the histopathological sample, but very easily on the cytomorphological ones. The differences obtained by the cytomorphological technique, which ensures at the end the differential diagnosis, are generated by two easily identifiable aspects: the first one consist in the presence of a large cytoplasm with multiple prolongations in dendritic sarcoma and total absence of this aspect in the histiocytic malignant cellular forms; the second aspect consists in the presence of a true syncytial cellular pointing out a veritable cytoplasmic mega-anastomosis in the dendritic sarcoma, and the lack of this aspect in the histiocytic proliferations. Histiomonocytic leukemia differs fundamentally from any other leukemia cell form by the the existence of a very high cellular polymorphism with cell gigantism and monstrosities. Finally, we make the assessment that besides the cytomorphological exam, there is no other methodology of these histiocytic proliferative variants except immunohistochemistry, which is an expensive and time consuming method. Histopathology can only provide the information that the malignant proliferation have as a cellular base, the histiocytic cell.

Keywords: *cancer, dendritic cell, histiocyte, histiomonocyte leukemia, sarcoma*

Introduction

Reviewing the literature of the past few years there were clearly outlined some aspects of general consensus. These aspects are: the relatively low incidence of histiocytic disease in dogs; this kind of neoplasia display very uncharacteristic clinical and pathological coarse of evolution exception being made by the cutaneous expressions; the diagnostic can be done by citology from fine needle aspiration of the lymph nodes or from peripheral blood smear which can be confirmed by histopathology or immunohistochemistry; the general cytomorphological aspects of these malignant proliferations resemble a lot the histiocytic cell; the differential diagnosis must be done between the histyomacrophagic and histyodendritic proliferations (1,2,3,4,5,6,7).

Materials and method

Our study was conducted within the Clinic of the Faculty of Veterinary Medicine in Bucharest on a number of 5 dogs, 4 of which presented with adenopathy, 2 of which were diagnosed with histiocytic sarcoma and 2 with dendritic sarcoma, the last one being diagnosed with acute histio-monocytic leukemia, an incidental finding at a routine hematologic exam.

The method comprised the citomorphological exam of peripheral blood and of fine needle aspirates from reactive lymph nodes. The smears obtained were stained in a panoptic fashion with May-Grunwald Giemsa.

Results and discussions

In the first section of this chapter we will make a brief cytomorphological description of each cell population in histiocytic proliferations from our cases as it follows:

- Histiocytic sarcoma is characterized by a monomorphous cell proliferation. The cells have relatively wide amphophylic cytoplasm with rare inclusions. The nucleus is round or oval, placed centrally or eccentrically, with spongy, quite lax chromatin. The nuclei may contain 1 or 2 prominent nucleoli, which in some cases have a gigantic aspect. In the smear can be identified rare huge cells, with only one nucleus but atypical.
- Dendritic sarcoma can be easily distinguished from the histiocytic sarcoma because the specific cell population is polymorphous with marked atypical morphology up to monster cells. Cells have basophilic cytoplasm which generates many expansions but have no inclusions. The nuclei are of various shapes and sizes with lax reticular chromatin and faded nucleoli. Little atypical mitosis can also be seen in large-sized cells. Clusters of 3 to 5 cells can be seen due to lack of cytoplasmic separation.
- Histio-monocytic leukemia is present in the peripheral blood with mixed proliferated cell population, both histiocytes and monocytes. The cells are large-sized, with slight basophilic cytoplasm (resembling cigar smoke). The nuclei can be round or irregular in shape, with stratified, quite lax chromatin. The nucleoli are all faded, not well contoured. Few microscope fields shown rare very large cells with strange shapes.

We consider that, by our cytomorphological architecture description of the cells population within each type of histiocytic malignant proliferation, the positive and differential diagnosis poses no great challenge or additional diagnostic investigations.

Next we will try to establish both consensus and divergences between literature and our cytomorphological data obtained from our cases.

Convergences are numerous and refer mainly to the validity of cytomorphogical exam in veterinary oncology as the first diagnostic tool of major importance for small animal cancer diagnostic. This statement is sustained by the fact that it is a fast and cheap method, and poses no additional risk for the patient. Referring to histiocytic proliferations all descriptions found in the literature resembled with our observations. Histopathology is of great use every time the cytomorphological exam in inconclusive. Speaking of immunohistochemistry, it is a significantly more laborious and a lot more expensive method, reason to be usually rejected by the owners.

There are also 2 contrary aspects between literature and the experience of our cytomorphology school. First is represented by the fact that simple classic cytology (May-Grunwald Giemsa staining) can establish a positive and differential diagnosis between the histiocytic and dendritic sarcomas (see the description above).

The second argument refers to the need of including the acute histio-monocytic leukemia within the histicytes pathology classifications. All of these cells, simple histiocytes or with macrophagic or dendritic orientation, originate from the medullary primordial stem cell, which, in its maturation process generates an intermediate stage called mielo-monocytic oriented stem cell.

Under this circumstances we believe that the histiocyte and its pathology has a much wider frame and thus we propose the following chart for a better understanding of tumoral and non-tumoral histiocytic pathology.

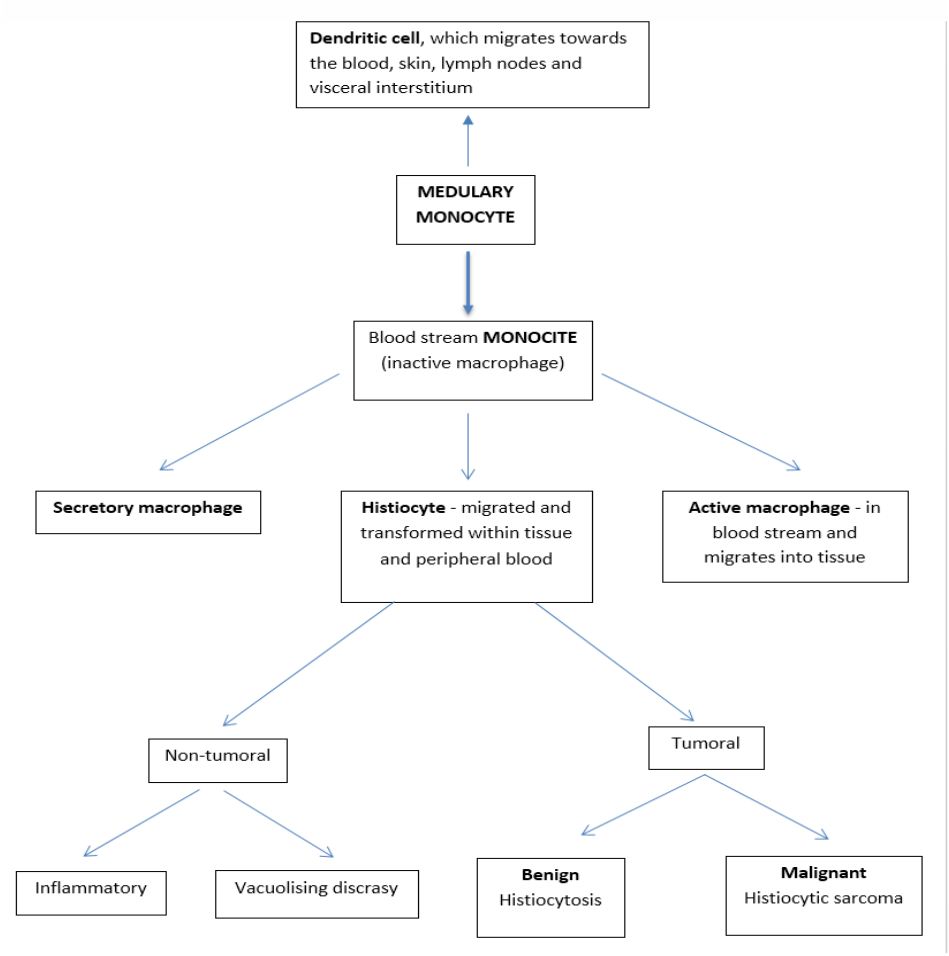

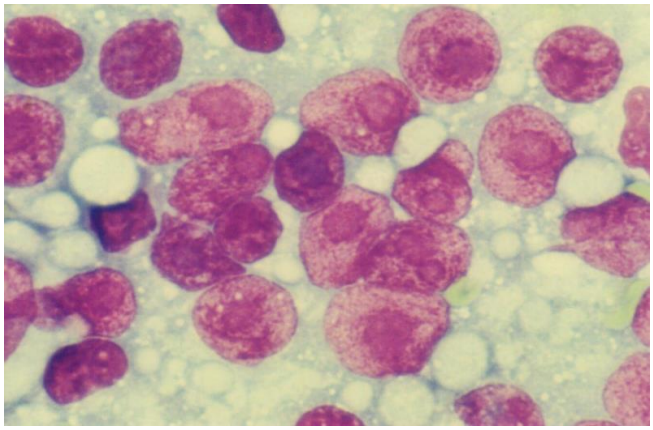

Fig. 1.

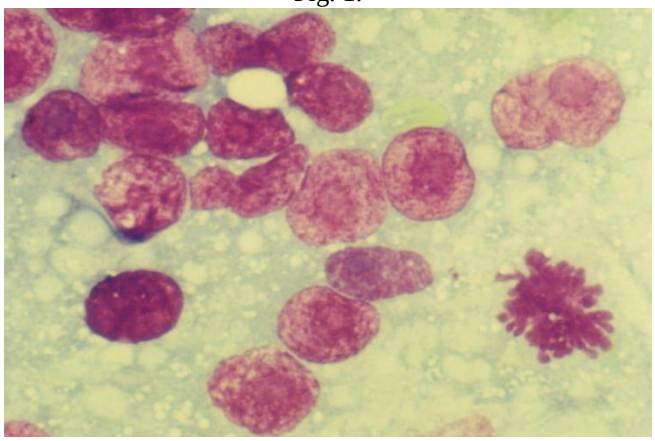

Fig. 2.

Fig. 1,2 - histiocytic blast cells from quasi-pure cell culture, describing large amfophilic cytoplasm with certain intracytoplasmic inclusions, large nuclei, relatively homogenous, with 1 or 2 nucleoli with lax chromatin

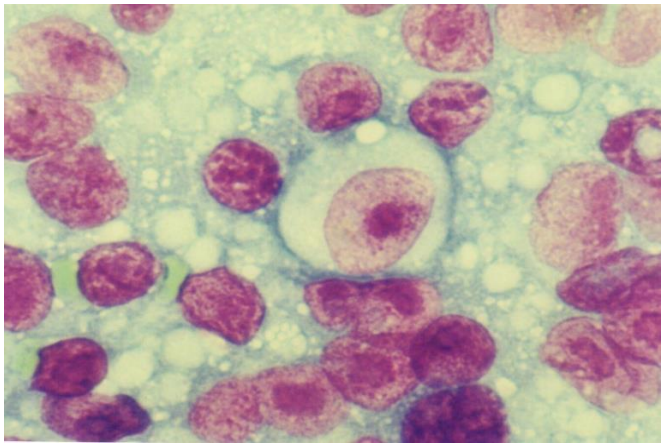

Fig.3 - histiocytic sarcoma - significant cell heterogeneity regarding size and shape and monster cells in a case of malignant histiocytic proliferation

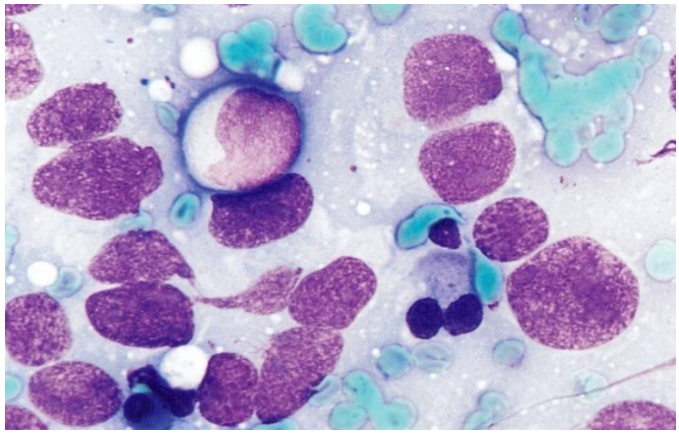

Fig. 4

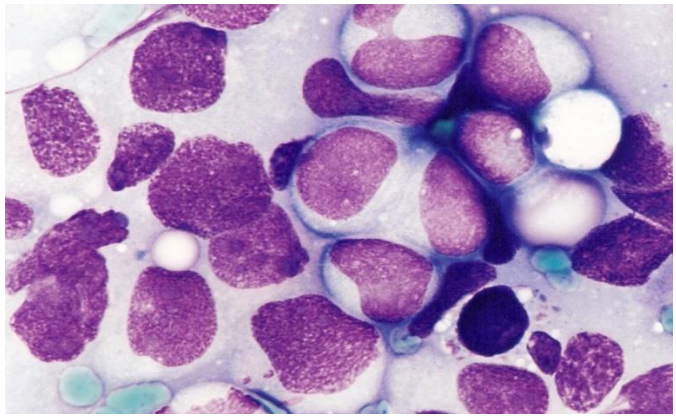

Fig. 5

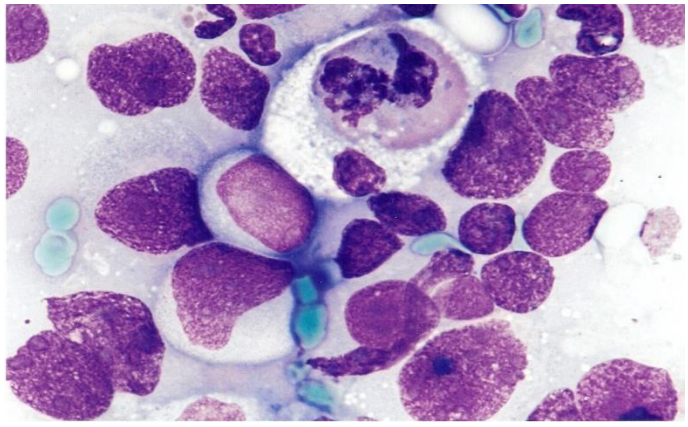

Fig.6

Fig. 4,5,6 - histio-monocytic leukemia; numerous atypical histiomonocytes (nulear and cytoplasmic criteria to include into malignant histiocytic proliferations)

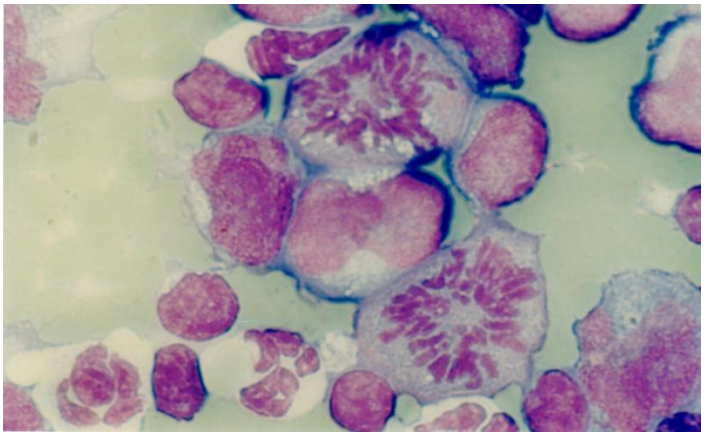

Fig. 7

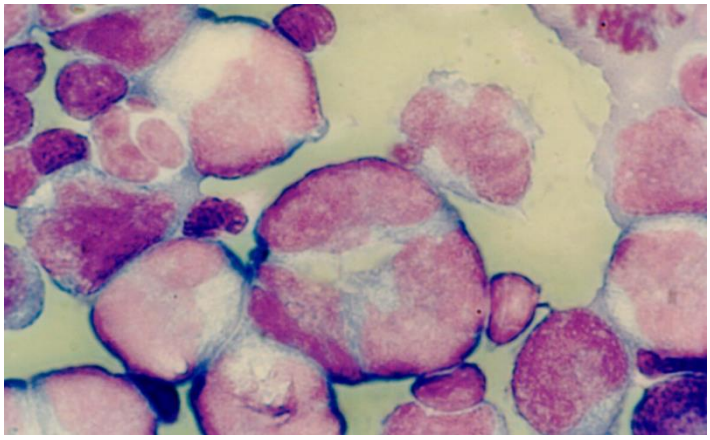

Fig. 8

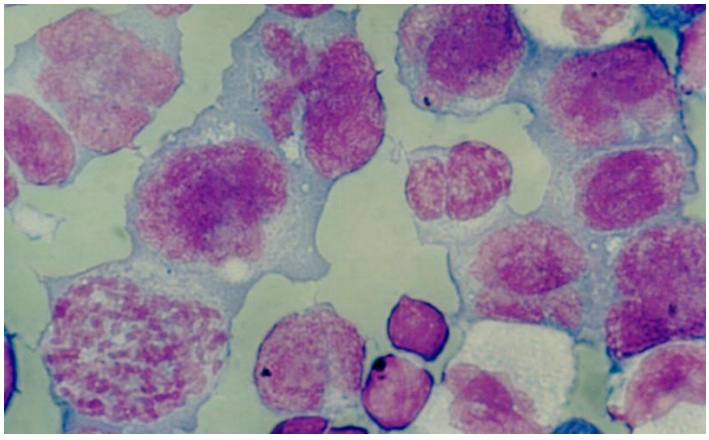

Fig. 9

Fig. 7,8,9 - dendritic sarcoma - cellular proliferation significantly different from histiocytes, marked by intense basophilic cytoplasm with multiple prominences, with large nuclei with numerous mitotic figures, frequent monster cells and sponge-like aspect chromatin.

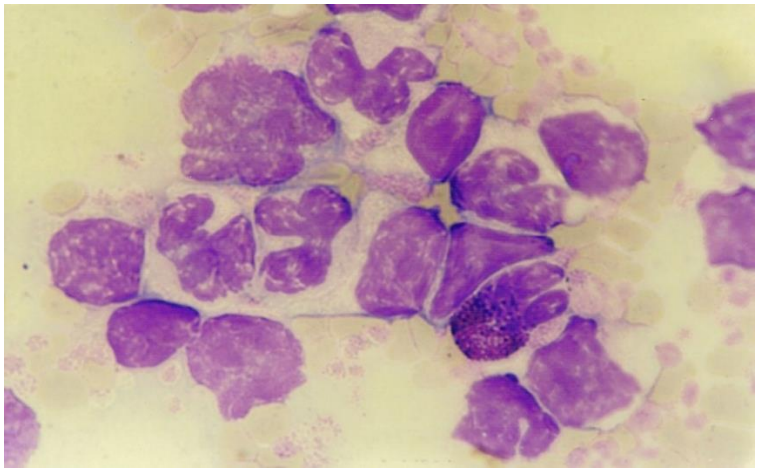

Fig.10 – Histio-monocytic leukemia

Conclusions

1. Cytomorphological exam is a great diagnostic tool for tumoral pathology of the histiocyte.
2. The cytmorphological exam can differentiate both histiocytic proliferative disease as well as non-tumoral histiocytic pathology.
3. We can differentiate the histiocytic sarcoma and the dendritic sarcom on the cytomorphological exam solely.
4. The histio-monocytic leukemia must be included within the histiocytic tumoral proliferative diseases.

References

1. A. R. Coomer, J.M. Liptak - Canine Histiocytic Diseases, Compend Contin Educ Vet. 2008 Apr;30(4):202-4, 208-16;
2. Amanda K. Fulmer and Glenna E. Mauldin - Canine histiocytic neoplasia: An overview, Can Vet J. 2007 Oct; 48(10): 1041–1050.
3. D. J. Argyle, M. J. Brearley, M. M. Turek; - Decision Making in Small Animal Oncology, Blackewell, 2008
4. R. Sapierzyński, D. Jagielski, I. Dolka, M. Fabisiak -Cytopathological diagnosis of visceral histiocytic sarcoma in five dogs, Polish Journal of Veterinary Sciences Vol. 15, No. 4 (2012), 751-758
5. Susan North, Tania Banks - Introduction to Small Animal Oncology, Saunders, Elsevier, 2009
6. V. K. AFFOLTER AND P. F. MOORE - Localized and Disseminated Histiocytic Sarcoma of Dendritic Cell Origin in Dogs, Vet Pathol 39:74–83 (2002)
7. WITHROW AND MACEWEN'S SMALL ANIMAL CLINICAL ONCOLOGY, Saunders Elsevier, 2007.

MICROANATOMY OF THE EYE STRUCTURES IN MERINO CROSSBREED LAMBS

Adrian Florin GAL, Vasile RUS, Flavia RUXANDA *, Bianca MATOSZ, Viorel MICLĂUŞ
University of Agricultural Sciences and Veterinary Medicine, Cluj-Napoca
flavia.ruxanda@gmail.com

Abstract

The information concerning the microanatomy of sensorial organs in mammals is scarce. The goal of our study was to present the microanatomy of the eye in Merino crossbreed lambs. The structure of eye was histologically evaluated in lambs (2 months old lambs, Merino crossbreed). The harvested samples were processed with the typical paraffin technique. Thus, the harvested samples were immersed in 10% buffered formalin, and then embedded in histological wax, sectioned at 5-µm thickness and mounted on microscopic slides. The obtained slides were stained using Goldner's trichrome staining procedure. The overall structure of the eye in lamb respects the general microanatomy of the human eye, with few differences. Thus, a similar distribution of melanocytes throughout the sclera, without observing a higher number of melanocytes in the inner part of sclera (lamina fusca) was noticed. The posterior epithelium of the ciliary body is simple squamous with few melanin granules in the cytoplasm, aspect somehow different from other species, where no melanin granules were noticed in the inner cellular epithelium of the ciliary body.

Keywords: *eye, melanin, melanosomes, melanocytes, histology.*

Introduction

The eye is an organ responsible with vision and it distinguishes light. A number of light-sensitive structures are found in a range of animals. The modest eyes do nothing but distinguish whether the environments are dark or light, whereas complex eyes can discern colors and shapes. Several animals, along with some mammals, birds, fish and reptiles, have two eyes, whose image basically overlap in order to permit better depth discernment (aspect known as binocular vision that occurs in humans). In some other species, for instance in rabbits and chameleons, eyes are positioned in such a way to minimalize the overlap (Moran and Rowley, 1988; Bacha W.J., Bacha L.M., 2000; Mills, 2007). Even if mammalian vision is not as exceptional as bird vision, in most of mammalian species it is at least dichromatic or even trichromatic in Hominidae (Bacha W.J., Bacha L.M., 2000; Ross and Pawlina, 2011).

The information concerning the microanatomy of sensorial organs in mammals is scarce. Most of histological details of the eye were attained from humans or a number of laboratory animals used in experiments (e.g. rats, mice etc.). According to that, the goal of our study was to present the microanatomy of the eye in Merino crossbreed lambs.

Materials and methods

The structure of eye was histologically evaluated in lambs (i.e., 2 months old lambs, Merino crossbreed). The harvested samples were processed using the typical paraffin technique. Thus, the harvested samples were immersed in 10% buffered formalin for 3 days. Afterwards, the obtained samples were embedded in histological wax, sectioned at 5-µm thickness and mounted on microscopic slides. The obtained slides were stained using Goldner's trichrome staining procedure. The photographs were obtained using the Olympus E-330 photocamera attached to an Olympus BX41 light microscope.

Results and discussion

In the present paper, the main histological features of the eyeball will be approached on each of the three layers, which are the fibrous tunic, vascular tunic, and neural tunic (Fig. 1).

As known, the fibrous tunic includes the sclera and cornea. The sclera displays a similar histological arrangement throughout its structure that is an irregular dense connective tissue made of collagenous fibers. Histologically, there is not a clear delimitation between the three layers of the sclera (i.e. episclera, stroma and lamina fusca). Melanocytes are scarce throughout the sclera, without observing a higher number of melanocytes in the inner part of sclera (lamina fusca) as suggested in some reports (Moran and Rowley, 1988; Bacha W.J., Bacha L.M., 2000; Kühnel and Kuhnel, 2003; Mills, 2007; Gal and Miclăuș, 2013). Melanocytes adopt here a spindle or dendritic shape appearance in the minute spaces created by the collagen fibers. Melanosomes have a granular or dot-like appearance in all the cytoplasm of melanocytes (Fig. 2). Concerning the cornea, it has a standard histological structure without any noticeable major differences. Accordingly, there is a non-keratinized squamous stratified epithelium (i.e. the anterior surface of the cornea), followed by a highly ordered avascular stroma (Fig. 3). The posterior corneal epithelium is simple squamous with a prominent basal membrane (or Descemet's membrane).

Concerning the vascular tunic (or uveal tract), we assessed the choroid, iris and ciliary body. As a comparison, while the epichoroid is an avascular structure with few melanocytes, the inner layers of choroid (i.e. vascular and choriocapillary layers) are highly pigmented and vascularized (Fig. 4). Melanocytes contain tiny granular melanosomes that often mask the nucleus of melanocytes. The melanocytes in choroid resemble the melanocytes located in sclera. Regarding the iris and ciliary processes of the ciliary body, they consist of the surface epithelium and the bulk of the iris and ciliary processes. The anterior epithelium is bistratified cuboidal to low columnar, but with no pigmentation in the upper epithelium and a highly pigmented basal epithelium (Fig. 5). In the pigmented epithelium, melanosomes have a granular or rod-like appearance, but are much bigger than the ones located in the sclera and choroid (Fig. 6). The sustaining stroma of the ciliary processes include large vascular spaces with young endothelial cells and discreet melanocytes in the connective tissue. The main bulk of ciliary body is made of dense irregular connective tissue, with some smooth muscle fibers, quite a number of dendritic or spindle shaped melanocytes and large blood vessels (Fig. 5). The posterior epithelium of the ciliary body and iris is simple squamous with melanin granules in the cytoplasm. However, there is a reduction concerning the number of melanin granules in the posterior epithelium of the iris and ciliary body in comparison to the one in the anterior epithelium (Fig. 7). The former aspect is different in comparison to some other reports in other species, which suggest no pigmentation in the posterior or inner cellular epithelium of the iris and ciliary body (Moran and Rowley, 1988; Bacha W.J., Bacha L.M., 2000; Kühnel and Kuhnel, 2003; Mills, 2007).

As regards the neural tunic represented by the retina (i.e. photosensitive part), no significant differences were noticed in comparison to the standard structure of the photosensitive retina in other mammals. As observed in Fig. 8, all ten layers are present (i.e. the pigmented epithelium, photoreceptor layer with cones and rods, external limiting membrane, outer nuclear layer, outer plexiform layer, inner nuclear layer, inner plexiform layer, ganglion cell layer, optic nerve fiber layer, and internal limiting membrane).

Fig. 1. Histological section of the eye in mix breed Merino lamb (A – sclera, B – choroid, C – retina); Goldner's tricrome stain.

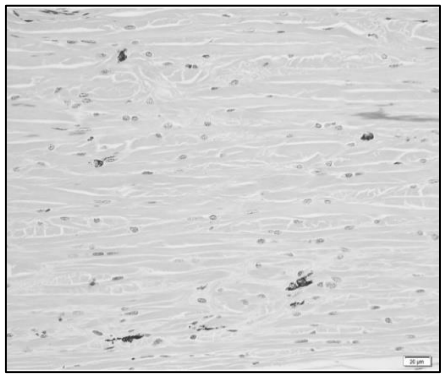

Fig. 2. Distribution of melanocytes in the sclera and the aspect of melanocytes and melanosomes; mix breed Merino lamb, Goldner's tricrome stain.

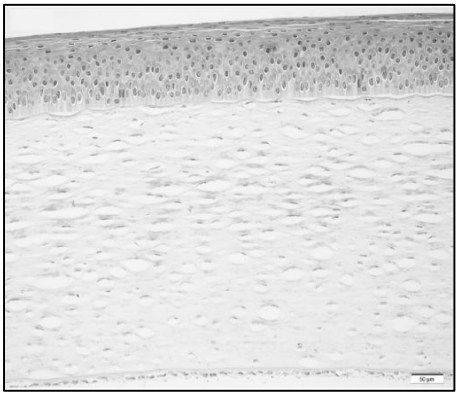

Fig. 3. The structure of cornea in mix breed Merino lamb; Goldner's tricrome stain.

Fig. 4. The inner layers of choroid (vascular and choriocapillary layers) include a high number of melanocytes (bottom); mix breed Merino lamb, Goldner's tricrome stain.

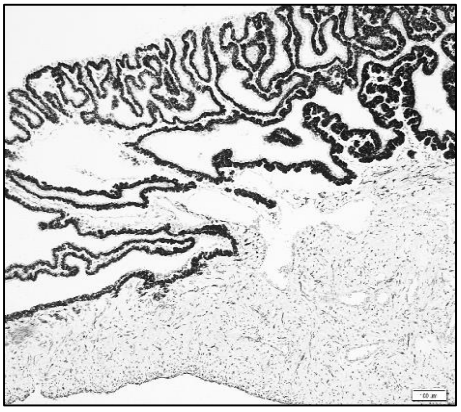

Fig. 5. General aspect of the ciliary processes and iris (bottom-left) that is highly pigmented, while the pigmentation degree decreases towards the posterior part of iris and ciliary body; Goldner's tricrome stain.

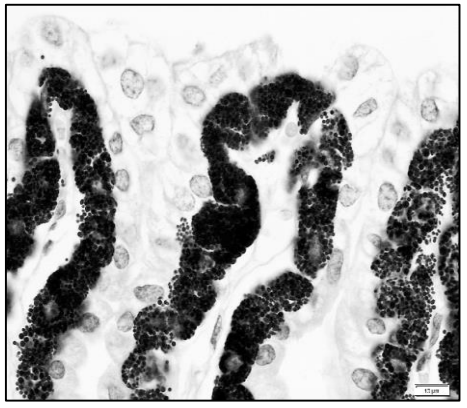

Fig. 6. The bistratified epithelium of the ciliary processes, with large melanin granules only in the basal layer; Goldner's tricrome stain.

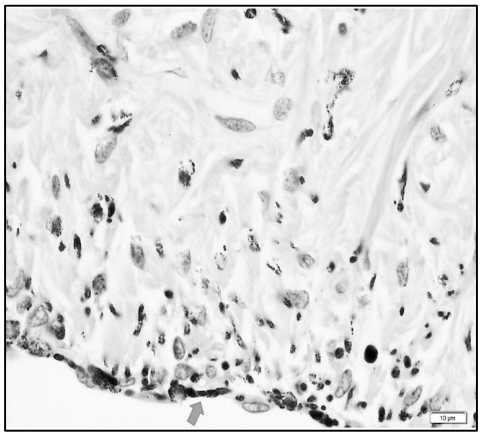

Fig. 7. The number of melanin granules in the posterior epithelium of the iris and ciliary body (arrow) diminish significantly in comparison to the anterior epithelium; Goldner's tricrome stain.

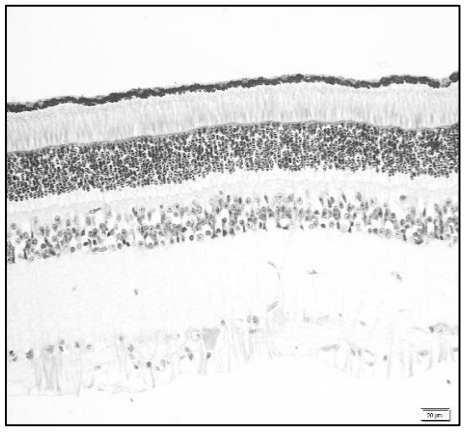

Fig. 8. Retina in lamb – the presence of all ten layers starting with the pigmentary cell layer (top); Goldner's tricrome stain.

The eye is a sensory organ that is composed of a lens and a wall that is divided into three layers, such as an outer fibrous tunic (corneoscleral layer), a central vascular tunic (uvea), and an internal retinal tunic (Moran and Rowley, 1988; Bacha W.J., Bacha L.M., 2000; Mills S.E., 2007).

The sclera includes compactly interwoven fascicles of collagenous fibers arranged parallel to the outer surface of the wall of the eye. There are also fibroblasts, some discreet elastic fibers, and disseminated melanocytes, especially in the deepest region of the sclera (Bacha W.J., Bacha L.M., 2000; Kühnel and Kuhnel, 2003; Mills, 2007). As observed in our paper, in lambs the melanocytes are somehow uniformly dispersed throughout the sclera, without observing a higher number of melanocytes in the inner part of sclera.

The cornea is an avascular structure, which has the anterior surface covered by non-keratinized stratified squamous epithelium. Below this coat is Bowman's membrane that is not evident in domestic mammals. The substantia propria (also called the stroma) is made of thin lamellae of collagen fibers set parallel to the corneal surface, with fibroblasts between fibers. Descemet's membrane is a thick membrane that splits the stroma from the posterior epithelium. The posterior epithelium is made of a single layer of squamous to low cuboidal cells (Bacha W.J., Bacha L.M., 2000; Mills, 2007; Miclăuş and Gal, 2010). In lambs, the cornea resembles the general histological features described above.

The ciliary body is a frontal extension of the choroid. The loose connective tissue of the stroma consists of smooth muscle, also called the ciliary muscle, which lies peripheral to an inner vascularized area. The epithelium of the ciliary body is called pars ciliaris retinae. It is a bilayer of cells containing a basal layer of pigmented cells and a superficial layer of non-pigmented columnar cells. Small folds of the posterior surface of the ciliary body become longer toward the iris and form ciliary processes, which project toward the lens. Zonular fibers spread from the processes to the capsule of lens near the equator of the lens (Moran and Rowley, 1988; Bacha W.J., Bacha L.M., 2000; Kühnel and Kuhnel, 2003; Mills, 2007). In lambs, the ciliary body presents a bistratified cuboidal to columnar epithelium. Additionally,

the basal pigmented epithelium encloses the largest melanin granules from all structures of the eye.

Retina is the deepest layer of the wall of the eye. The photosensitive zone lines the internal surface of the eye from the ora ciliaris retinae to the optic disc. The last one is the point of transition from the non-photosensitive retina to the photosensitive retina. From the ora ciliaris retinae, the non-photosensitive zone continues anteriorly as a bistratified epithelium, forming the pars ciliaris retinae and the pars iridica retinae (which cover the ciliary body and the rear surface of the iris). From the choroid to the cavity of the vitreous humor, the 10 layers of the photosensitive retina are (as in presented in lambs) the following: pigment epithelium, layer of rods and cones, outer limiting membrane, outer nuclear layer, outer plexiform layer, inner nuclear layer, inner plexiform layer, ganglion cell layer, nerve fiber layer and the inner limiting membrane (Moran and Rowley, 1988; Bacha W.J., Bacha L.M., 2000; Kühnel and Kuhnel, 2003; Mills, 2007; Gal and Miclăuș, 2013). No differences were noticed between the photosensitive retina in lambs and other mammals.

Conclusion

The overall structure of the eye in lamb respects the general microanatomy of the human eye, with few differences. Thus, a similar distribution of melanocytes throughout the sclera, without observing a higher number of melanocytes in the inner part of sclera (lamina fusca). The posterior epithelium of the iris and ciliary body is simple squamous with few melanin granules in the cytoplasm, aspect somehow different from other species where no melanin granules were noticed in the inner cellular epithelium of the ciliary body.

References

1. Bacha W.J., Bacha L.M., 2000. Color atlas of veterinary histology, 245-260.
2. Gal A.F., Miclăuş V., 2013. Histology, Ed. Risoprint, Cluj-Napoca, Romania, 339-347.
3. Kühnel W. and Kuhnel W., 2003. Color atlas of cytology, histology, and microscopic anatomy. Stuttgart; New York: Thieme, 458-480.
4. Miclăuş, V., Gal A.F., 2010. Histologie Specială și Embriologie Generală, Ed. Risoprint, Cluj-Napoca, 145-149 .
5. Mills S.E., 2007. Histology for pathologists. Philadelphia, 375-398.
6. Moran D.T. and Rowley J.C., 1988. Visual histology. Lea & Febiger, 236-244.
7. Ross MH, Pawlina W., 2011. Histology: A Text and Atlas (6th edition). Baltimore: Lippincott Williams and Wilkins, 896-928.

HISTOLOGICAL FINDINGS IN THE RETINA OF WISTAR ALBINO RATS

Adrian Florin GAL, Vasile RUS, Flavia RUXANDA *, Bianca MATOSZ, Viorel MICLĂUŞ
University of Agricultural Sciences and Veterinary Medicine, Cluj-Napoca
flavia.ruxanda@gmail.com

Abstract
The retina is the deepest of the three layers of the eyeball and is the tissue in charge of the reception and transduction of light stimuli. The general anatomy of the retina is comparable for all mammalian species, with a few key differences. The purpose of this study was to present some histological aspects of the retina in Wistar albino rats. Postmortem histologic analysis was performed with the intention to examine the structure of retina in Wistar albino rats in comparison to Brown Norway pigmented rats. The eye samples were processed using the standard paraffin technique and stained with Goldner's trichrome method. The multilayered structure of the rat retina was similar in the two rat breeds. However, a significant histological variation was observed in the pigmented layer of the retina in Wistar albino rats in comparison to the Brown Norway pigmented rats. Melanin granules were completely absent in the retina of Wistar albino rats. Pigments play a major role in vision. Accordingly, macular pigment (e.g., lutein and zeaxanthin) intercept blue light entering the eye, protecting against retinal injury. Melanin, acts as a screen against visible light and UV-radiation. The melanin distribution and quantity in the retina is of great importance in understanding the etiology of age-related macular degeneration (AMD) and also developing ways to identify and treat this condition. In conclusion, Wistar albino rats could be a useful animal model for the investigation of AMD in humans, which is a medical disorder that may result in unclear or loss of vision.
Keywords: *eye, retina, albino rats, histology.*

Introduction

The eye structures comprise four diverse basic pigments: zeaxanthin, lutein, lipofuscin and melanin. Concerning the location of the presented pigments, the zeaxanthin and lutein are built up in the retina (Kennedy et al., 1995; Sparrow et al, 2005; Baumann et al., 2015; Hu et al., 2008). Zeaxanthin is most abundant in the macula lutea and is responsible for the yellow color (from Latin, lutea = yellow), while lutein prevails in the peripheral retina (Johnson, 2014). Lipofuscin accumulates in the pigmented epithelium of the retina (PER). Melanin is present in the epithelium of iris, in the ciliary body, in the PER, and in the choroid. A combination of melanin and lipofuscin (i.e., melanolipofuscin) can also be found (Kennedy et al., 1995; Sparrow et al, 2005; Baumann et al., 2015; Hu et al., 2008).

The retina is the innermost of the three layers of the eyeball and is the tissue in charge with the reception and transduction of light stimuli. The general anatomy of the retina is comparable for all mammalian species, with a few key differences (Parker and Picut, 2016). The purpose of this study was to present some histological details of the retina in Wistar albino rats. Postmortem histologic analysis was performed with the aim to examine the structure of retina in Wistar albino rats in comparison to Brown Norway pigmented rats.

Materials and methods

The structure of retina was assessed in two rat strains (i.e., 2 months old Wistar albino rats and 2 months old Brown Norway pigmented rats). The eye samples were processed using the standard paraffin technique and stained by Goldner's trichrome method. Accordingly, the harvested eye samples were introduced in 10% buffered formalin for 3 days. Subsequently, the eye samples were embedded in paraffin, sectioned at 5-µm thickness and mounted on microscopic slides. The resulted slides were stained using Goldner's trichrome staining

technique. The microphotographs were obtained using the Olympus BX41 light microscope connected to an Olympus E-330 photocamera.

Results and discussion

The multilayered structure of the rat retina was similar in the two rat breeds. However, a significant histological variation was observed in the pigmented layer of the retina in Wistar albino rats in comparison to the Brown Norway pigmented rats. Melanin granules were completely absent in the retina of Wistar albino rats, whereas in Brown Norway pigmented rat strains the first layer of the retina had melanin granules. The pigmented cell layer was represented by a simple low cuboidal to squamous cells on top of rods and cones (in both rat strains). In Brown Norway pigmented rat strains, the cytoplasm of the pigmented cell layer of the retina presented tiny black granular or bacillar melanosomes. As suggested, some melanosomes had a more dot-like appearance, while some others adopted a rod-like appearance. In the pigmented cell layer, melanosomes were more numerous in the apical poles of these cells, while basal poles were occupied by their nuclei and a low number of melanosomes.

As known, pigments play a central role in vision. The macular pigment (i.e. lutein and zeaxanthin), may have significant antioxidative and anti-inflammatory roles. Some other pigments such as lutein and zeaxanthin may be involved in the protection against retinal damage by absorbing the blue light entering the eye. Regarding the melanin, it acts as photo-screen against ultraviolet radiation and visible light, and as an antioxidant (Hu et al., 2008). The PER lipofuscin accumulates with age and was associated with the development of age-related macular degeneration (AMD) (Kennedy et al., 1995; Sparrow et al, 2005). Recent years have witnessed a growing concentration on the development of procedures for assessing ocular pigmentation (Baumann et al., 2015).

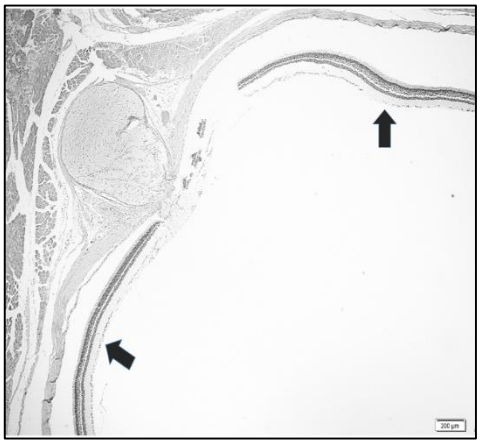

Fig. 1. Histological section of the eye in albino rat – retina (arrows); Goldner's tricrome stain.

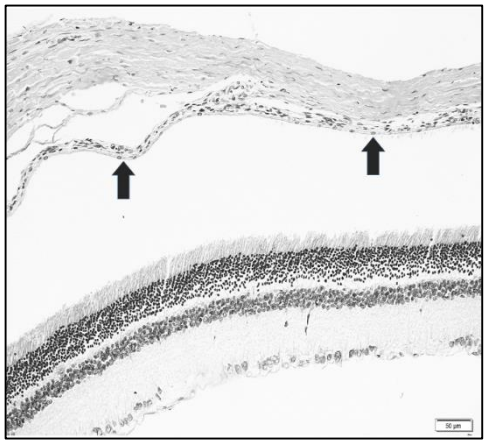

Fig. 2. Absence of melanin in the pigmented layer of the retina (arrows) - albino rat; Goldner's tricrome stain.

Fig. 3. Histological features of the retina in albino rat, showing the remained nine layers (except for the first pigmented layer suggested in Fig. 1); Goldner's tricrome stain.

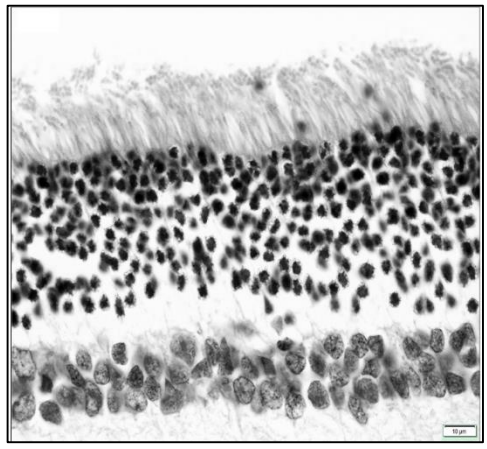

Fig. 4. Highly magnified image displaying the cones and rods in the retina of albino rat; Goldner's tricrome stain.

Melanin pigmentation is a central element for normal vision in humans. Histological arrangement of the ocular structures containing granules of melanin, namely the pigment epithelium and the uvea, and their implication in diseases such as age-related macular degeneration (AMD) have been subject to investigations using procedures ranging from fundus photography to electron microscopy (Delori et al., 1995; Feeney-Burns et al., 1984; Kornzweig, 1979; Srinivasan et al., 2008; Schmitz-Valckenberg et al., 2008; Spaide, 2009; Klein et al., 2011). Above all, the melanin-containing structures in the posterior eye (i.e. the PER and the choroid) are of major interest for understanding the pathogenesis and etiology of AMD and hence for the development of a number of methods for early diagnosis and treatment (Baumann et al., 2015; Schuetze et al., 2014).

Conclusion

The melanin distribution and quantity in the retina is of great importance for understanding the etiology of age-related macular degeneration (AMD) and afterwards for developing methods for AMD diagnosis and treatment. In conclusion, Wistar albino rats could be useful animal models for the investigation of AMD in humans, which is a medical disorder that may result in unclear or lack of vision.

References

1. Baumann B, Schirmer J, Rauscher S, Fialová S, Glösmann M, Augustin M, Pircher M, Gröger M, Christoph K. Melanin pigmentation in rat eyes: in vivo imaging by polarization-sensitive optical coherence tomography and comparison to histology. Invest Ophthalmol Vis Sci. 2015;56:7462–7472.
2. Delori FC, Dorey CK, Staurenghi G, Arend O, Goger DG, Weiter JJ. In vivo fluorescence of the ocular fundus exhibits retinal pigment epithelium lipofuscin characteristics. Invest Ophthalmol Vis Sci. 1995;36:718–729.
3. Feeney-Burns L, Hilderbrand ES, Eldridge S. Aging Human RPE - Morphometric analysis of macular, equatorial, and peripheral cells. Invest Ophthalmol Vis Sci. 1984;25:195–200.

4. Hu DN, Simon JD, Sarna T. Role of ocular melanin in ophthalmic physiology and pathology. Photochem Photobiol. 2008;84:639–644.
5. Johnson EJ. Role of lutein and zeaxanthin in visual and cognitive function throughout the lifespan. Nutr Rev. 2014;72: 605–612.
6. Kennedy CJ, Rakoczy PE, Constable IJ. Lipofuscin of the retinal pigment epithelium: A review. Eye. 1995;9:763–771.
7. Klein R, Chou C, Klein BK, Zhang X, Meuer SM, Saaddine JB. Prevalence of age-related macular degeneration in the US population. Arch Ophthalmol. 2011;129:75–80.
8. Kornzweig AL. Aging of the retinal pigment epithelium. In: Zinn KM, Marmor MF, eds. The Retinal Pigment Epithelium. Cambridge, MA: Harvard University Press; 1979:478–495.
9. Parker, G.A., and C.A. Picut, eds. Atlas of Histology of the Juvenile Rat. Academic Press, 2016, pp. 373-377.
10. Schmitz-Valckenberg S, Holz FG, Bird AC, Spaide RF. Fundus autofluorescence imaging - Review and perspectives. Retina-J Ret Vit Dis. 2008;28:385–409.
11. Schuetze C, Ritter M, Blum R, et al. Retinal pigment epithelium findings in patients with albinism using wide-field polarization sensitive optical coherence tomography. Retina- J Ret Vit Dis. 2014;34:2208–2217.
12. Spaide RF. Enhanced depth imaging optical coherence tomography of retinal pigment epithelial detachment in agerelated macular degeneration. Am J Ophthalmol. 2009;147: 644–652.
13. Sparrow JR, Boulton M. RPE lipofuscin and its role in retinal pathobiology. Exp Eye Res. 2005;80:595–606.
14. Srinivasan VJ, Monson BK, Wojtkowski M, et al. Characterization of outer retinal morphology with high-speed, ultrahighresolution optical coherence tomography. Invest Ophthalmol Vis Sci. 2008;49:1571–1579.

AGE ESTIMATION IN SHEEP BY RADIOGRAPHIC IMAGE OF RADIUS AND ULNA: MEDICOLEGAL STUDY

Gehan B.YOUSSEF*, BAKRY HH, El-SHWARBY R.M, NABILA M. Abd El-Aliem, Elham A El-SHEWY

Forensic medicine and Toxicology dept. Faculty of Veterinary Medicine,
*Educational hospital, Benha Univ. Egypt

Abstract

This work was done on 54 sheep (ram) which are apparently healthy and no anatomical deformities to evaluate the medicolegal importance of the radiographic images in determination the age of sheep. The age of the sheep was estimated through the measurement of the lengths and radiographic images of radius and ulna. The radius bone measured 10.69±0.07 cm at age of 2 months and reached the maximum length at age of 48 months 17.72±0.10 cm. The ulna bone measured 13.62±0.04 cm at age of 2 months and reached the maximum length at age of 48 months 22.94±0.08 cm. The radiolucent area appeared in the radius and ulna at age of 2-10 months in sheep. Partial union of radius started at age of 16 months in sheep and in ulna started at age of 18 months. The epiphyseal closure of the radius plate occurred at age of 28 months and ulna plate appeared at age of 30 months. The complete closure of the epiphyseal plates appeared at age of 42 month in radius and in ulna at age of 48 months.

Introduction

Sheep are widely spread in different areas in Egypt and adapted to different climatic conditions even in Delta or in South Egypt and are found in all different farming and production systems. It consume low amount of food because of their small body size if compared to large ruminants (Khalil et al., 2013).

Normal development of bones is very important to estimate the age in experimental animals and diagnose the skeletal diseases in growing animals (Fukuda et al., 1978). Several indicators for the age estimation such as body weight and bone length were also used

Radiology or sonography can play significant role in forensic medical investigation via usage of these images in assessment of forensic physicians, pathologists and anthropologists in mysterious cases related to the law. The radiographic images must be of a high quality for admission as credible evidence **i**n all legal uses of radiologic imaging (Kremer et al.,2008 and Myke et al.,2010). Image techniques are very important tools in forensic science .Although the forensic and medical examiner are not specialist than radiologist but they can judge the image to the medico legal side. The forensic specialists need the radiograph for additional proof or for presentation in the court (Kahana and Hiss, 2009).

The studies of the bone radiography play a new role in modern legal medicine/forensic medicine and archaeozoology now day's .Most of these studies focus on the bone ossification characters (Gudea and Stefan 2013).

The aim of the current study is to evaluate the age of the sheep via the radiographic image of the radius and ulna

Material and methods

This work was done on 54 male sheep (Ram), their age ranged from 2 months to 4 years (according to animal's records, ear tags and dentition). Three ram were used in each age. They were apparently healthy and not suffered from any diseases or anomalies by physical and clinical investigations sheep (Balady breeds) were collected from different small ruminant farms in Kalubia Governorate: Farm of Faculty of Veterinary medicine, Farm of Faculty of Agriculture, Benha University and Farm of Ministry of Agriculture at Moshtoher village.

X ray (Radiographic images)

The radiographic examinations were done for sheep of the present work. For radiographic shot, 100 kilovolts (kv), 60 milliAmperes (mAs) power x-ray digital device held in an accredited centre for diagnostic imaging in Toukh city, Kalubia Governorate for diagnostic imaging. The radiographic images were taken to the radius and ulna of sheep. Each sheep was assessed to ensure they were not lamed and their limbs were free from any external evidence injury or disease.

The images were analyzed using digital system (x-ray device) to determine the bone length (the distance between the proximal to the distal extremities of the bones). The bone length was measured using the digital device. For each image the sheep identity.

The radiography is taken to the sheep in lateral position according to Douglas et al. (1987). Before any examination; the sheep were dried and groomed because of the sheep fleece often contain a large amount of dirt which becomes radiopaque when wet.

Results

Radiography of sheep radius and ulna

The radius was a long bone situated between the humerus and the carpal bones. It composed of one shaft and two extremities. The proximal extremity formed the elbow joint with the humerus while the distal extremity formed the knee joint with the carpal bones. The radius was slightly oblique. The ulna was ill developed long bone; the distal end of the ulna was fused with the radius.

Age of 2-14 months:

The radiographic images of the radius and ulna showed radiolucent appearance in the epiphyseal plate at which no ossification occurred and the epiphyseal plate opened. This occurred at age of 2-10 months of sheep as shown in plate1 (Fig. A).

There were no significant changes appeared in the radiographic images of radius and ulna at age of 12-14 months compared to the age of 10 months. The differences were in the lengths of radius and ulna. The radius lengths were 15.97± 0.08 cm and 16.66± 0.18 cm at age of 12 and 14 months respectively. The lengths of ulna were 21.46± 0.26 cm and 21.67± 0.09 cm at age of 12 and 14 months respectively.

Age of 16-26 months

The appearance of radio opaque area in radiographic images of radius and ulna in the epiphyseal plate at which partial union occurred and this appeared at age of 16 months in radius and at age of 18 months in ulna of sheep as shown in plate 1(Fig .B).

There were no significant changes appeared in the radiographic images at age of 20-26 months compared to the age of 18 months. The lengths of radius and ulna were 17.13± 0.10 cm and 22.62± 0.19 cm at age of 26 months in radius and ulna respectively.

Age of 28-36 months

The radiographic images showed that appearance of radiopaque area and disappearance of radiolucent area in radiography of the radius and ulna. The epiphyseal closure (union) occurred between the epiphysis and diaphysis. This appeared at age of 28 months in radius and at age of 30 months in ulna of sheep as shown in plate 1 (Fig .C).

There were no significant changes appeared in the radiographic images at age of 36 months compared to the age of 30 months. The lengths of radius and ulna were 17.34± 0.08cm and 22.75± 0.07 cm at age of 36 months in radius and ulna respectively.

Age of 42-48 months

The complete closure of the growth or epiphyseal plate of the radius and ulna of sheep appeared in the radiographic images as complete union between the epiphysis and diaphysis of the radius and ulna and disappearance of the radiopaque line between the epiphysis and diaphysis.. The complete epiphyseal closure appeared at age of 42 months in radius and 48 months in ulna as shown in plate 1 (Fig .D).

The radius and ulna lengths

The total lengths of the radius of the sheep were measured as shown in (table 1 chart 1).The statistical analysis showed that a highly significant difference ($p< 0.01$) occurred in the measurement of the radius lengths. In all measurements, the radius lengths were increased with age increased. The radius was gradually increased from 10.69±0.07cm at the age of 2 months to reach 17.72±0.10 cm at the age of 48months of sheep.

The total lengths of the ulna of the sheep were measured as shown in (table 1 chart 2).There was a highly significant difference ($p< 0.01$) in the measurement of the ulna lengths. In all measurements, the ulna lengths increased with the age increased. The ulna lengths were gradually increased from 13.62±0.04 cm at the age of 2months till reached 22.94±0.08 cm at the age of 48 months.

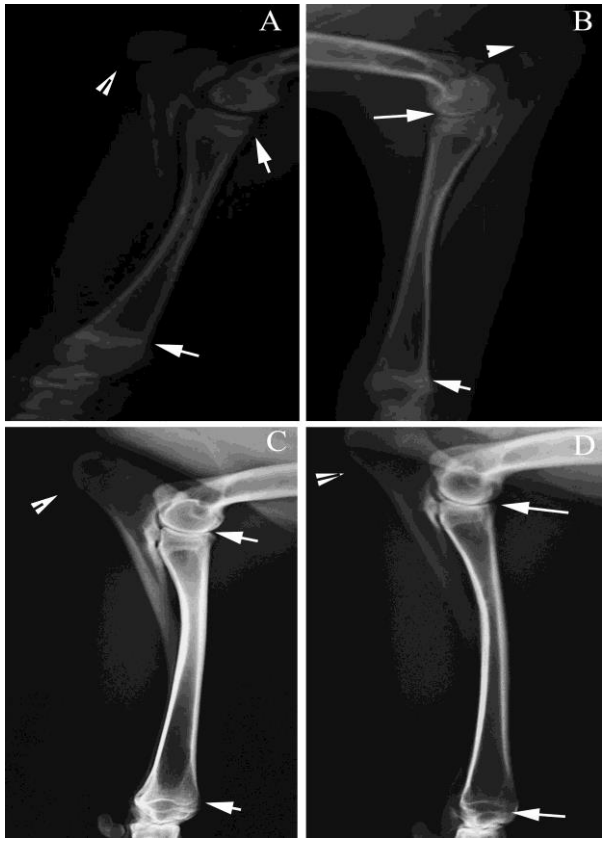

Plate 1(A,B,C,D) showed radiographic images of sheep radius and ulna.
Fig. A): The epiphyseal plates opened at age 2 months.
Fig .B): Partial epiphyseal union appeared at age of 16 months.
Fig .C): Disappearance of the radiolucent area at age 30 months.
Fig .D): Complete epiphyseal closure occurred at age 48 months

Table 1.

The length (cm) of the sheep forelimb bones (humerus-radius-ulna and metacarpal) in relation to their age

Age (month)	Radius(cm)	Ulna(cm)
2	10.69±0.07*	13.62±0.04*
4	13.44±0.14*	14.64±0.07*
6	13.99±0.05	16.68±0.22*
8	14.23±0.08*	19.02±0.06*
10	15.03±0.05	20.18±0.13*
12	15.97±0.08	21.46±0.26
14	16.66±0.18*	21.67±0.09
16	17.01±0.05*	21.92±0.09
18	17.13±0.02	22.34±0.07*
20	17.17±0.06	22.26±0.20
22	17.08±0.03	22.34±0.09
24	17.08±0.04	22.65±0.13
26	17.13±0.10	22.62±0.19
28	17.20±0.06	22.65±0.05
30	17.20±0.07	22.58±0.19
36	17.34±0.08	22.75±0.07
42	17.21±0.07	22.81±0.05
48	17.72±0.10*	22.94±0.08

Means values ±SD of fore limb bones in different ages of sheep represent significant difference. ($p < 0.01$)

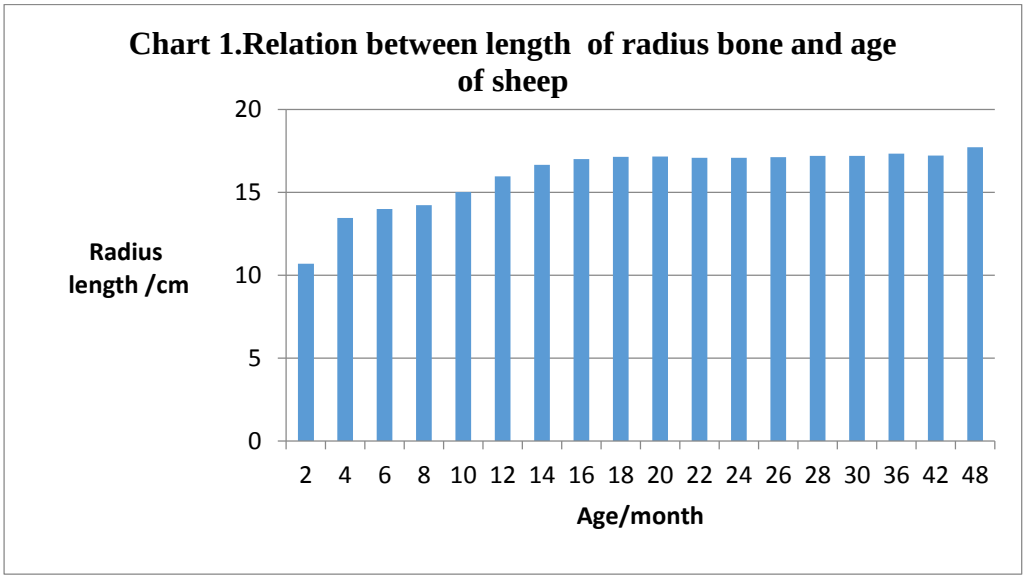

Chart 1: Showing the relation between length of radius bone and age of sheep

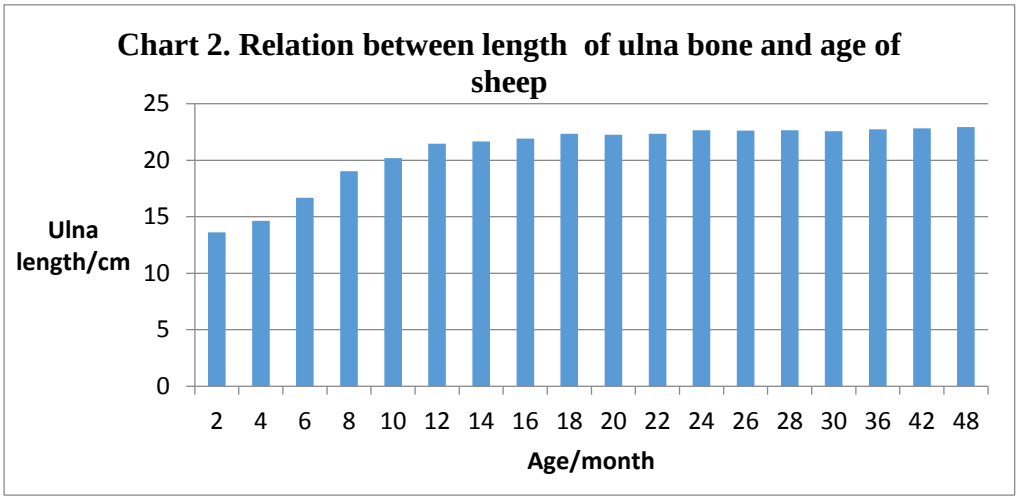

Chart 2: Showing the relation between length of ulna bone and age of sheep

Discussion

Radiological imaging is an effective method in estimation of the age of the animals through determination of the ossification and bone epiphyseal closure Asmius et al., 1995 and Genccelep et al., 2002.The endochondral ossification regions of the long bones are epiphyseal plates (growth plates). These epiphyseal plates are existed until the postnatal growth is completed and ossified after the process of postnatal growth (Aytekin 1993 and Aslanbey 2002). In the current work, the determination of the age of animals was done by radiographic examination of the radius and ulna of sheep.

The epiphyseal plates are appeared on radiographic images as radiolucent area between the epiphysis and diaphysis (Kealy and McAllister, 2000).The appearance of radiopaque area in the radiographic images in the epiphyseal plates was considered to be the first signs of epiphyseal closure and the ossification began to occur between the epiphysis and diaphysis of the radius and ulna of sheep.

In the present work, the complete closure of the epiphyseal plates appeared on the radiographic images as the appearance of radiopaque area and disappearance of radiolucent appearance between the epiphysis and diaphysis. This result was in agree with the study of Alpdogan and Genccelep (2012) while this result disagree with the studies of Asimus et al., (1995) and Todhunter et al., (1997) whom identified the complete closure of the epiphyseal plates by the displacement of radiopaque appearance with the radiolucent line between the epiphysis and diaphysis.

The present work was in agreement with the results of Choi et al., (2006) , Das et al., (2009) and Genccelep et al., (2012) in that the rate of bone growth in form of ossification and epiphyseal closure increased with age. The lengths of the the radius and ulna of sheep. In this work gradually increased with advancement of age and this similar to the result of Lochi et al., (2014).

The complete epiphyseal closure in the present work appeared at age of (42-48) months in radius and ulna in the sheep. While the result of Genccelep et al., (2012) recorded the complete epiphyseal closure appeared at the age of 33-35 months in radius and the complete closure of the ulna occurred at age 34-35 months in Mohair goats. Moreover, Saber et al., (1989) whom found that the union of the growth plate of ulna is appeared at the age of 13 months in sheep lambs and the result of Choi et al., (2006) whom recorded the fusion of the epiphyseal plates of the radius and ulna were found at 1 year or more than 1 year in Korean native goat and these differences could be attributed to species differences.

In the present work, the total lengths of the radius and ulna showed a highly significant difference and the radius lengths gradually increased with advancement of age from (10.69±0.07 to 17.72±0.10) cm in sheep. While the study of Genccelep et al., (2012) showed the radius lengths were increased from (7.90 ±0.17 cm to 15.18±0.25cm) in mohair goats.

In our work, the total lengths of the ulna gradually increased with advancement of age from (13.62±0.04 cm to 22.94±0.08 cm) in sheep. While the total lengths of the ulna studied by Genccelep et al., (2012) were increased from (10.75 ±0.025 to 19.76±0.30) cm in mohair goats.

References

1. Alpdogan, O. and Genccelep, M. 2012. Determination of the closure time of growth plates of tibia and fibula in colored Mohair goats kids by radiography .Asian Journal of Animal and Veterinary Advances,7(9),pp:860-867.
2. Asimus,E., Gauzy,J.S., Mathon,D., Urgeois,F., Darmana, R., Cahuzac, J. and Autefage,A.1995. Growth of the radius in sheep. An experimental model for monitoring activity of the growth plates. Rev. Med. Vet.146,pp:681–688.
3. Aslanbey, D. 2002. Veterinary Orthopedics and Traumatologie. Medipres Publishing House,Malatya,Turkey,pp:3-7.
4. Aytekin, Y.1993. Basic Histology.Baris Bookstore, Istanbul, Turkey, pp: 179-191.
5. Choi H., Shin, H., Kang, S., Lee H., Cho, J., Chang, D., Lee, Y., Jeong, S.M., Park, S. and Shin, S. T. 2006. A radiographic study of growth plate closure compared with age in the Korean native goat. Korean J.Vet.Res.vol.46(3): pp:285-289.
6. Das, R.K., Kanesh, J.S., Mandel, A.K. and Mishra, U.K.2009. Comparative radiographic study on the epiphyseal closure in long bones of hind limb in Black Bengal and Ganjam goats. Indian Journal of Veterinary Anatomy,vol.21,(2): pp:49-52.

7. Douglas, S.W., Herrtage, M.E. and Williamson, H.D.1987. Principals of veterinary radiography, Bailliere Tindall, London Philadelphia, Toronto, Mexico City ,Sydney, Tokyo, Hong Kong. 4th edition , part 2,pp:339.
8. Fukuda, S., Cho, F. and Honjo, S. 1978. Bone growth and development of secondary ossification centers of extremities in the cynomolgus monkey (MacacaFascicularis). Exp.Anim.,27, pp:387-397.
9. Genccelep, M., Bakir, B., Aslan, L., Atasoy, N. and Tas, A.2002. Determination of the closure time of growth plates of radius-ulna in Morkaraman lambs by radiography. YYU Vet. Fak. Derg.13: pp:1-7.
10. Genccelep, M., Karasu, A. and Alpdogan, O.2012. The determination of radius-ulna closure time of growth plates in mohair goat kids by radiography. Small Ruminant Research ,103 ,pp:182–186.
11. Gudea, A.I. and Stefan, A.C.2013. Histomorphometric ,fractual and lacunarity comparative analysis of sheep (Ovisaries), goat (Capra hircus) and roe deer (Capreoluscapreolus). compact bone samples. Folia Morphol,vol.72(3): pp:239-248.
12. Kahana, T.and Hiss, J.2009. The role of forensic anthropology in mass fatality incidents management. Forensic Science Policy & Management: An International Journal Volume 1, Issue 3.pp:144-149.
13. Kealy,J. K. and McAllister, H.2000. Bones and joints. In: Diagnostic Radiology and Ultrasonography of the Dog and Cat. W.B. Saunders Company, Philadelphia, pp.253–338.
14. Khalil, M. A. ,Sammour, H.B. and El-Wardani, M.A. 2013. socio-economic and technical evaluation of sheep and goat farms in north west coast of Egypt. Egyptian Journal of Sheep and Goat Sciences, Vol. 8 (1), pp: 29-42.
15. Kremer, C., Racette, S., Marton, D. and Sauvageau, A.2008. A Radiographs Interpretation by Forensic Pathologists .Am. J. Forensic Med. Pathol.29(4): pp:295-296.
16. Lochi, G. M.,Shah, M.G. , Kalhoro, I.B., Gandahi, J. A., Khan, M. S., Abdul Haseeb, Khushk, S.M., Oad, A. and Ansari, M. I.2014.Comparative osteometric differences in humerus of Bari goat and Dumbi sheep .Scientific Research and Essay,vol.9(6): pp:145-152.
17. Myke, K.R.T., Tersa, O.B.A and Lisa, K.B.A.2010. The state of forensic radiology in united states. American Society of Radiologic Technologists.pp:101-138.
18. Saber, A.S., Bolbol, A.E.and Schenksaber, B., 1989. A radiographic study of the development of the sheep carpus from birth to 18 months to age. Vet. Radol. Ultrasound 30, pp:189–192.
19. Todhunter, R.J., Zachos, T.A., Gilbert, R.O., Erb H.N., Williams, A.J., Burton –Wurster, and Lust, G. 1997 .Onset of epiphyseal mineralization and growth plate closure in radiographically normal and dysplastic labrador retrievers. J. Am. Vet. Med. Assoc., 210: pp:1458-1462.

THE IMPACT OF LOCAL REMEDY BIOR ON PROTEIN METABOLISM OF RECONDITIONED QUAILS

Vasile MACARI, Natalia PAVLICENCO, Ana ROTARU, Victor PUTIN
Faculty of Veterinary Medicine and Animal Science
State Agrarian University of Moldova Chişinău, R. of Moldova
E-mail: macvasile@mail.ru

Abstract

In aviculture, in the context of obtaining qualitative and safe products, a major concern is the usage of substances with antistress, adaptive, and obviously growth stimulator properties. Thus, in our research on adult quails during the reconditioning process, we tested for the first time the BioRremedy, an autochthon product of algalorigin, obtained from Spirulina platensis, with antistress and adaptive properties. The remedy was administered intramuscular to 4 experimental groups of quails, in different doses (0,25; 0,5; 1,0; 1,5 ml/head), 2 times consecutively: at the beginning of the study, and during the study. To the control group was administered – 0,5 ml of 0,9% sol. NaCl in the same consecutiveness. The biochemical tests, performed on the quails from the experimental groups, revealed an increase of the protein metabolism parameters: the total proteinserum, albuminserum, and creatinine levels as compared to the control group. While, regarding serum urea and serum uric acid levels, was recorded a decrease of these parameters in the quails treated with BioR, compared to the control group. According to the obtained results, we can conclude tha tthe studied bioremedy manages to improve the health indices, the parameters that reflect the protein metabolism, and the functional state of the liver in quails treated with BioR.

Keywords: *BioR remedy, quails, protein metabolism, albumin serum, creatinine.*

Introduction

Currently, in terms of livestock, particularly poultry and other species, several factors interfere that may negatively influence the health, welfare and productive performance [5, 10, 20]. However, lately, on both nationally and internationally levels the concept is focused on improving the quality of human life by providing qualitative and harmless to humans, animals and the environment products of animal origin. We declare that the international practice does not put at doubt the use of biologically active remedies with various influences on metabolism and productivity, giving priority to those of natural origin, in particular plant [1, 5, 10, 17, 18].

It is significant that in conditions of the Republic of Moldova an ecologically pure cure, universally accepted and recognized was obtained from the cyanobacterium Spirulina platensis [2, 11, 15]. This remedy has been studied on multiple laboratory animals, farm animals and man [1, 2, 5, 6, 8, 14, 15]. Meanwhile, the BioR's product impact on protein metabolism and bio parameters on quails has not been elucidated. In this context, in this work we aimed to study the BioR's remedy impact on the basic parameters of protein metabolism and productivity of quails put under reconditioning, in physiological conditions.

Material and methods

To elucidate the influence of BioR product on health and in particular on the markers' parameters of protein metabolism: total protein, albumin, creatinine, urea, uric acid and productivity, a study has been realized on five batches of 40 quails at the end of the laying cycle. The principles for achieving the experience, the regimen and dosage of administration of the BioR remedy on quails varied according to the experimental scheme, shown in Table 1.

The birds included in the study were homogeneous in terms of weight and analogous by physiological status and age, staying in the same shelter where all hygienic and technological parameters were identical: microclimate, hygiene and welfare of the birds,

feeding, watering and veterinary care. During the research the quails were monitored and reviewed in order to assess the health and highlight them numerically.

Table 1.

Scheme of administration of the BioR remedy on adult quails, 0,05% sol.

Animal groups	**Nr. of heads**	**The administration regimen**	**Dose, ml**	
			1 time	**2 time**
Control	40	2 times intramuscularly at the onset of the study and at day 7-10 after the first administration	0,5 ml 0,9% NaCl sol.	0,5 ml 0,9% NaCl sol.
Experimental 1	40		0,25	0,25
Experimental 2	40		0,5	0,5
Experimental 3	40		1,0	1,0
Experimental 4	40		1,5	1,5

At the onset of the investigations, body temperature and the number of respiratory movements per minute were measured on random 5 quail, and during investigations nominees parameters were assessed at 5 quail from each batch of birds involved in this study. Blood samples were taken from 5 birds in several steps: at the start of the study till the administration of the BioR remedy, and then 2 times: 1st collection (in the middle of the trial), and 2nd collection, at the end of investigations, from 5 quail from each batch by beheading them, in two standard tubes - with and without anticoagulant.

Determination of total protein, albumin, urea, uric acid and creatinine in the blood serum of quail was performed using sets of reagents of the company "Elitech", France, according to the enclosed instructions. Statistical evaluation of biochemical indices was performed using the criteria t-Student parameter with the veracity less than 0,05 ($p<0,05$).

Results and discussions

From the data in Table 2 we note that the total protein in quail's blood, at the 1st collection on the control group shows a downward trend from 10.7% compared to onset of the study ($p< 0,05$), which can be attributed to stressogenic factors that occurred during the study.

This assumption can be also justified by the analysed parameter investigated in all experimental groups treated with BioR cure, but with different doses. Thus, the serum proteins level of the first investigation on the experimental groups was amplified by 7,7 to 34,8% compared to the reference group, and conclusive differences were signaled in three experimental groups. Similar results were reported by us earlier, by administrating the product on young pigs and broilers reared in intensive conditions [8, 13]. This assumption can be confirmed at the end of research when the index rising trend is observed in all investigated groups, including the control one (+ 37,3%, $p< 0,001$ compared to control group at the 1st investigation). The monitoring of serum proteins in dynamic showed an increase of 6,1 to 22,8% in the groups treated with the BioR product compared to the reference group, there are also significant differences. Similar trends were reported by us earlier as a result of BioR's and Catosal administration on broilers [10].

Table 2.

Influence of the administration of BioR remedy on lipids' per oxidation and antioxidant system's indices in the blood serum of an adult quail

Value		Groups of animals				
		CG	EG 1	EG 2	EG 3	EG 4
Total protein, g/l, 1 collection 2 collection	45,24±1,27	40,39±1,58* 55,44±1,05***	43,48±1,82 58,79±4,04	49,09±1,72** 68,07±1,82***	54,44±2,13*** 63,30±2,86*	48,50±2,17* 65,64±2,72**
Albumin, g/l, 1collection 2 collection	17,52±1,15	16,5±0,48 16,27±0,50	15,38±0,49 17,43±0,52	16,24±0,45 17,05±0,34	15,79±0,25 16,22±0,36	16,47±0,33 17,37±0,31
Urea, mmol/l, 1 collection 2 collection	0,97±0,14	1,24±0,16 1,38±0,29	1,33±0,13 0,86±0,05	0,97±0,15 0,87±0,07	0,96±0,15 0,84±0,08	1,08±0,19 0,68±0,04*
Uric acid, µmol/l, 1 collection 2 collection	397,03±13,19	369,98±15,84 434,89±19,46*	393,78±15,93 394,86±17,63	394,86±19,12 403,52±14,76	397,03±9,68 428,4±12,74	401,35±23,22 401,35±7,74
Creatinine, µmol/l, 1 collection 2 collection	99,08±5,54	95,77±9,66 79,56±6,78	86,93±10,80 92,45±5,58	71,46±6,19 99,82±6,93	82,14±5,62 74,77±10,10	76,61±9,47 90,98±10,04

Note: *p< 0,05;**p<0,01 compared to control

The research results indicate that serum albumin's level of intact birds from the 1st investigation suffers similar changes as the total protein, decreasing by 5,8% compared with the beginning of experience. On the background of medication with the BioR product, the value of albumin, from the 1st collection do not show clear changes compared to group references. Meanwhile, at the end of the investigation, the BioR remedy induces a growing trend analyzed parameter from 4,9 to 7,1% compared to the control group in all three experimental groups. Thus, the manifestations of both investigated parameters (total protein and albumin) are relevant to the biology of quail, given that both parameters investigated are synthesized in the liver, and several studies have highlighted the beneficial impact of the BioR product on the functional status of the liver [5, 6, 8, 10, 11, 13, 14, 15]. The dynamics of the level of serum urea of quail in the 1st investigation is state of interest, it increased by 27,8% and respectively 37,1% compared to data reported in the study onset in the control group and the experimental group 1 (minimum dose of BioR). At the same time the serum urea within the other three groups treated with BioR, was maintained at the level obtained at the beginning of the research data. In the study conducted and at the end of the investigation, the growth trend of urea concerns only the birds from the control group, contrary to data reported in the groups treated with the BioR remedy. Thus, the tested remedy fortified the basal metabolism and especially the protein one, inducing beneficial metabolic changes at the end of the technological cycle of exploitation of birds within which the serum level of urea decreased by 1,6-2,0 times compared to group reference. It must specified the fact that in another study conducted by us on broilers during intensive growth, the BioR remedy on contrary induced a growing trend of serum urea, which

is explained by the ability of this medicinal product to also enhance the protein metabolism of young bodies [10].

The researches carried out (table 2) showed that prior to starting therapy with BioR the uric acid's level of quail at the end of the technological cycle was high. While the investigated parameter of intact birds in the first investigation shows a downward trend of 6.8% compared to the reference group, when BioR maintained the uremia's level at the level of the study onset. The monitoring in dynamic of the uric acid's level of the birds from the intact control group showed a significant increase compared to data reported in 1st investigation (with 17,5%, $p< 0,05$). The data in Table 3 show that during the study, the investigated parameter in both experimental groups (1 and 2) treated with low doses of BioR there was a decreasing moderately tendency of the uric acid in serum with 7,2 to 9,2 % compared to control group, while high doses do not certify any clear trend. Creatinine playes an important role in the metabolic processes of muscles and other tissues, its level in blood depends on the formation and its excretion and creatinine directly depends on the state of the formation of muscle [19]. These specifications are very important for reconditioned quail, because this metabolite reflects muscle mass. Our researches (tab. 2) demonstrated that adult quail's serum's level of creatinine is high, hovering the values' level of this parameter in broilers. „Cobb-500" [10, 14]. The first investigation of creatinine shows a downward trend in all groups, less palpable in intact birds from the control group by 3,3% compared with the beginning of the study. Meanwhile, on the background of medication of BioR remedy the creatinine's value was reduced by 9,2-25,4% compared to the control group, which probably can be explained by the beneficial incursion of the product from the study. This hypothesis can be confirmed at the end of the study, when creatinine's level from the control group was decreased by 16,9%, repeating "late" downward trend previously reported in the groups treated with BioR. The beneficial influence of the tested remedy was highlighted by amplifying the investigated parameter in the experimental groups 1 and 2, treated with low doses of BioR with 16,2 to 25,5% compared to control group, but without statistical significance. The given effect of the BioR product in broilers has already been reported [10, 14]. Similar results on the beneficial impact of other biologically active compounds: suspension of Chlorella, PPZ premix of a protein level of 22,0% compared to 20% [12, 16, 20]. In this context of statement we can probably consider that the cyanobacterial remedy BioR intensifies in adult quail the energy processes in muscle, which may reflect on the quality of the finished product. Based on biochemical indices registered in adult quail for reconditioning, treated twice with BioR product denotes stimulation of basal metabolism in general and especially of protein, manifested as hepatoprotectors therefore, antistressors and lasting adaptive test product.

Conclusion

1. The cyanobacterial product BioR produced by modern technologies from cyanobacteria Spirulina platensis, given to the adult quail has a very good local and general tolerance.
2. The cyanobacterial product BioR helps improve metabolism and especially the protein one, suggesting an intensification of the proteolytic synthetic processes in the liver.
3. The results are dependent on the product's administered dose on quail, but to determine the optimal dose and regime of use of BioR remedy for quail in reconditioning requires further investigation.

References

1. Brevet de invenţie. 4101 C1, MD. Procedeu de stimulare a productivităţii puilor-broiler/ Macari Vasile, Rudic Valeriu, Putin Victor, Macari Ana (MD). Cererea depusă 2010.06.01, BOPI nr. 3/2011.
2. Fala V. BioR – baza optimizării proceselor de regenerare tisulară. Ch.: Sirius, 2014, 256 p.
3. Macari A. Evoluţia ceruloplasminei şi a transferinei serice la prepeliţele recondiţionate şi tratate cu un produs cianobacterian autohton. În: Luc. ştiinţifice ale UASM, Medicină Veterinară, 2014, vol. 40, p. 40-43.
4. Macari A. Evoluţia ceruloplasminei şi a transferinei serice la prepeliţele recondiţionate şi tratate cu un produs cianobacterian autohton. În: Luc.ştiinţifice ale UASM, Medicină Veterinară, 2014, vol. 40, p. 40-43.
5. Macari A. Influenţa remediului BioR asupra unor parametri ai endotoxicozei şi dipeptidelorhistidinice în serul sanguin la puii broiler. În: Ştiinţa Agricolă, 2015, nr. 1, p. 101-105.
6. Macari A. ş. a. Impactul remediului BioR asupra unor parametri ai sistemului prooxidant (oxidant) – antioxidant la prepeliţele adulte. În: Studia UniversitatisMoldaviae. Ştiinţe reale şi ale naturii, 2015, nr. 1(81), p.67-73.
7. Macari A. ş. a. Impactul remediului BioR şi a Catosalului asupra sistemului pro-antioxidant la puii broiler crescuţi la pardosea. În: Lucrări ştiinţifice ale Universităţii Agrare de Stat din Moldova, Zootehnie şi Biotehnologii, 2015, vol. 44, p. 377-382.
8. Macari V. Aspecte fiziologico-metabolice ale acţiunii preparatului BioR de origine algală asupra organismului porcin. Autoref. tezei de dr. hab. în biologie. Chişinău, 2003. 49 p.
9. Macari V., Pavlicenco N., Macari A. Influenţa remediului cianobacterian asupra unor indici hematologici, biochimici şi ai statusului antioxidant la prepeliţe adulte. În: Integrare prin cercetare şi inovare. Tezele conf. ştiinţifice naţionale cu participare internaţională. Chişinău: CEP USM, 2014, p. 53-55.
10. Macari V. ş. a. Recomandări. Procedeu de ameliorare a sănătăţii şi stimulare a productivităţii la puii de carne. Chişinău: UASM. „Print-Caro”. 2014, 35 p.
11. Macari V. ş. a. Modificările conţinutului de bilirubină şi fracţiilor ei în serul sangvin la tineretul cunicul sub influenţa unui produs autohton. **În:** Lucrări ştiinţifice ale UASM, Medicină Veterinară, 2013**,**vol. 35,p. 20-24.
12. Oduguwa O. O. et all. Potency of twoproprietarymicronutrientpremixes for broilerchickens at marginally deficient proteincontents. *Archivos de Zootecnia*. 2000, vol. 49, nr. 188, pp. 433-444. ISSN 0004-0592.
13. Pavlicenco N. Impactul remediului BioR asupra activităţii pseudocolinesterazei serice la prepeliţele adulte. În: Lucrări ştiinţifice ale UASM, Medicină Veterinară, 2013,vol. 35, p. 93 – 96.
14. Putin V. Aspecte fiziologo-metabolice ale acţiunii preparatului BioR asupra puilor-broiler. Autoref. tezei. dr. în şt. biologie. Chişinău, 2014. 30 p.
15. Rudic V. ş. a. Ficobiotehnologie– cercetări fundamentale şi realizări practice. Ch.: Elena V.I., 2007. 365 p.
16. Берзиня Н. и др. Изменение редокс-статуса у цыплят в зависимости от длительности применения больших доз аскорбиновой кислоты. В: Актуальные проблемы современного птицеводства. Материалы XII Украинской конференции по птицеводству с международным участием. Харьков, 2011, с. 27-31.
17. Гунчак А. В. и др. Влияние фитопрепарата на антиоксидантый и витаминный статус организма японских перепелок и их продуктивность. В: Актуальные проблемы интенсивного развития животноводства. Сборник научных трудов. Горки, 2010, вып. 13, ч. 2, с 322-326.
18. Кирилов Б. Я. и др. Метаболический эффект от использования фитопрепарата в кормлении перепелов. В: Инновационные технологии в животноводстве: Жодино, 2010, часть 1, с. 253-255.
19. Назаренко Г. И., Кишкун А. А. Клиническая оценка результатов лабораторных исследований. М.: Медицина, 2000. 544 с.
20. Плутахин Г. и др. Хлорелла и её применение в птицеводстве. *Птицеводство.* 2011, № 05, с. 23-25.

PROTECTIVE EFFECT OF CAMEL MILK ON GENETIC AND HISTOPATHOLOGICAL CHANGES RETATED TO FERTITITY AND VISION IN DIABETIC WISTAR RATS

Mohamed Mohamed SOLIMAN[1,2*]; Hossam Fouad ATTIA[3]; Mohamed Abdo NASSAN[4]
Medical Laboratories Departments, Faculty of Applied Medical Sciences, Taif University, Saudi Arabia; [2]Biochemistry and [3]Histology Department, Faculty of Veterinary Medicine, Benha University, Egypt;
mmsoliman@tu.edu.sa; mohamed.soliman@fvtm.bu.edu.eg;
mhamedsoliman8896@yahoo.com

Abstract

Diabetes is a serious disease affects human health. Diabetes in advanced stages is accompanied by weakness in fertility and vision, general weakness, and alteration in fats and carbohydrates metabolism. Recently there are some scientific trends about the usage of camel milk (CM) in the treatment of diabetes or its associated alterations. Camel milk contains vital active material with insulin like action and reduce the complications associated with diabetes incidence (weakness in fertility and vision), but how these effects occur, still unclear and this is the aim of this study. 60 male rats were divided into four groups (15 rats per group), a control group (CNT); camel milk group (CM); diabetic group (D) and diabetic group supplemented with camel milk (D+CM). Rats were supplemented with camel milk for 4 consecutive months. At the end of the experiment design, rats were killed and blood was extracted for chemical analysis. Tissue samples from testis and eye were collected for RNA extraction, tissue histopathology and electron microscope. Tissues from liver and epididymal adipose tissue were taken for changes in gene expression of carbohydrate and lipid metabolism. Sperms were harvested from epididymis for spermogram. Results showed that induction of diabetes in rats for 4 months induced oligospermia, decrease in sperm live percent, weak motility and increase in sperm abnormalities. Also, diabetes induced alterations in kidney and liver functions, disruption in antioxidants levels and oxidative stress markers (MDA). Moreover a decrease in insulin, leptin, lipid profiles, reduced sex hormone level (testosterone) and luteinizing hormone (LH). Supplementation of CM to diabetic rats significantly reduced and ameliorated the damage and all alterations associated with the diabetes occurrence. At the genetic level, diabetes down-regulated gene expression of the genes associated with steroidogenesis such as steroid acute regulatory protein (StAR), Androgen Binding Protein (ABR), 3β-hydroxysteroid dehydrogenase (3β-HSD), 17□-HSD, cytochrome P450scc, $P450_{c17}$, androgen receptor (AR) and luteinizing hormone receptor (LHR). The results showed effective therapeutic role for camel milk in improvement the gene expression of altered genes using the semi-quantitative polymerase chain reaction (RT-PCR). Moreover, the occurrence of diabetes altered the expression of all examined aquaporins (AQPs). Aquaporins are genes found in the retina and cornea of the eye. AQPs play critical roles in controlling the water content in the eye. Diabetic rats showed alterations in AQPs expression that are ameliorated by CM. Moreover, genes of polyol pathway that affect level of glucose in the eye and change it to sorbitol to maintain good vision are normalized by CM. In parallel, the genetic changes of carbohydrates and lipids in liver and fat were affected by diabetes incidence and were ameliorated by camel milk supplementation. Finally, in testis the histopathology showed degenerated spermatogenic cells with odema and degranulation in the cytoplasm, while, in electron microscopy of diabetic rats supplemented with CM showed the ultrastructure of the spermatogenic cells that retained its fine structure. In eyes, the cornea of diabetic rats showed cytoplasm sparsely degranulation and vacuolation of some cells. The collagen bundles of the stroma showed irregular arrangement. In retina retinal ganglionic cells showed congestion in the retinal blood vessels and detachment of some ganglionic cells. The corneal inner epithelium in diabetic treated rats showed minor regeneration while the stromal collagen fibrills showed progressed regeneration. In retina CM in diabetic rats showed progressed regeneration in stromal collagen fibrills compared to the diabetic group. In conclusion, CM is good as a protective supplement that ameliorates the changes in testis and eye that are associated with diabetes incidence.

Introduction

Diabetes mellitus type 1 (T1D) is a complex disease resulting from the interplay of genetic, endocrine, epigenetic, and environmental factors [Hakonarson H, Grant 2011].1 Worldwide, the T1D represents an increasing global public health burden, and the incidence of

T1D among humans has been rising [Forlenza GP, Rewers, 2011]. Over the last few decades, there has been an overall increase in the incidence of T1D of ~3% to 5% per year, and it is estimated that there are ~65 000 new cases per year in children, 15 years old [Borchers et al., 2010]. Moreover, the number of peoples with diabetes will rise to 500 million within the next 20 years [Malik et al., 2012]. Africa will experience a largest increase in the next generation for diabetes incidence. But till now Middle East is characterized with high incidence of diabetes but Africa still the most affected [Al-Baghli et al., 2011]. It has been shown that affected diabetic cases experience sexual abnormalities like sexual dysfunction, impotence and infertility [Faid et al., 2015]. The relation between male infertility and diabetes mellitus without clear genetic explanation was conducted on streptozotocin (STZ) induced diabetic rats [Amaral et al., 2006 and Hakeem et al., 2008]. Diabetes is associated with an increase in the oxidative stress that is associated with hyperglycemic state, due to production of reactive oxygen species (ROS) and decrease in anti-oxidant enzyme defenses [Makker et al., 2009]. Diabetes mellitus is associated with induced hyperglycemia that impairs male fertility by altering cell function of testis [Faid et al., 2015].

Male reproductive function are affected and with deleterious degenerations due to diabetes mellitus [Glenn et al., 2003; Soudamani et al., 2005]. Spermatogenesis is severely altered in diabetic mice due to hyperglycemia that caused testicular alterations [Gnodos et al., 1998]. Moreover, hyperglycemia causes oxidative stress and an increase in reactive oxygen species (ROS) production, all cause testicular dysfunction and visual problems [Chaiban and Azar 2004; Faid et al., 2015]. The annoying aspect of diabetes is that it compromises many men at reproductive age, and most of them are not aware of their illness [Steger and Raber 1997]. Moreover, it has been shown that there is a decrease in testosterone secretion in diabetic patients [Pontes et al., 2011].

Regarding the effect of diabetes of eye, it has been reported that the most frequent complication of diabetes is diabetic retinopathy and is the cause of cataract and vision loss [Adachi-Uehara et al. 2006]. Surgery is the only treatment for diabetic cataract, but after surgery the progression of diabetic retinopathy is often accelerated by the breakdown of the blood–aqueous barrier [Chung et al., 2002]. Hyperglycemia triggers the activation of the aldose reductase (Ald-Red)/sorbitol pathway, non-enzymatic glycation of lens fibers and oxidative stress [Wolff et al., 1991]. In the lens, osmotic stress imposed by sorbitol accumulation has long been believed to be the major factor in the progression of diabetic cataract [Lee et al., 1995]. Activation of the Ald-Red /sorbitol pathway (polyol pathway) also increases oxidative stress by increasing levels of hydrogen peroxide and free radicals in the eye [Kubo et al., 1999]. So the decrease in production of reactive oxygen species is the target for diabetes therapy and recovery from diabetes related vision disorders.

It is believed that consumption of camel milk (CM) helps in prevention and control of diabetes, and its associated disorders and alterations [Agrawal et al., 2009, 2011, and 2013; Mohamad et al., 2009]. The exact mechanism of such regulation is still unclear. Camel milk proteins have variable molecules, including serum albumin, α-lactalbumin, immunoglobulin, lactophorin and peptidoglycan recognition protein [Kappeler et al., 2004]. Literature reviews [Agrawal et al., 2009 and 2011; Mohamad et al., 2009] suggest the following possibilities: i) insulin in camel milk possesses special properties that make absorption into circulation easier than insulin from other sources or cause resistance to proteolysis; ii) camel insulin is encapsulated in nanoparticles (lipid vesicles) that make its passage through stomach and entry into circulation possible; iii) some other elements of camel milk make it anti-diabetic.

Therefore, this project focused on examining the changes in fertility and vision associated genes and the biochemical alterations during diabetes incidence in diabetic rats and how to prevent or modulate their occurrence by camel milk supplementation. We examined: 1) the biochemical changes occurred in diabetes and possible protection by CM, 2) the expression of genes associated with normal eye vision and testis function, and 3) the histopathological changes using special stain and /or electron microscope occurred in diabetes and possible normalization and/or protection by CM supplementation.

Materials and Methods

Experimental Design

Animals and managements

Sixty male Wistar rats were divided into 4 groups, fifteen rats per group. Rats were exposed to 12h/12h day night cycle at temperature between 25-30 C. Group 1, will be negative control with free access to water and food. Group 2 is negative control with free access to food and camel milk. Group 3 is positive control diabetic rats with free access to food and water. Group4 is diabetic rats supplemented by camel milk for 4 consecutive months. Camel milk was given orally to group 2 and 4 in a dose of 100 ml /24 hours / cage (6 rats) based on study of Althnaian et al., 2013.

Induction of diabetes in Wistar rats

Rats were injected with streptozotocin (STZ) in a dose of 70 mg/kg body weight intraperitoneally in citrate buffer PH 4.5 after fasting for overnight. After injection of STZ glucose was supplemented in water for 12 hours to avoid hypoglycemic shock due to STZ action. Glucose concentration was measured 72 hours after STZ injection. Rats with glucose levels over 200 mg/dl considered diabetic and used for experimental continuation

Sampling

After the end of experimental schedule, rats were anesthetized after diethyl ether inhalation, sacrificed by decapitation after overnight fasting. Testes and eyes were preserved in Bouin's solution for histopathological examination and in Qiazol reagent for RNA extraction. Serum was extracted from blood after centrifugation for 10 minutes at 5000 rpm.

Retina extraction

Eye balls were dissected parallel to the limbus corneae and vitreous was removed. Retinae were carefully excised from the posterior eyecups, immediately stored in trizol at −20°C or in 10% neutral buffered formalin (NBF) at room temperature until further processing [Eberhardt et al., 2011].

Serum chemistry analysis

Kidney (creatinine and urea) and liver (GPT and GOT) function parameters together with and glucose levels were measured colorimetrically. Antioxidants such as superoxide dismutase (SOD), glutathione reducatse(GSH-R), malondialdehyde (MDA), and catalase were measured spectrophotometrically using commercial ELISA kits based on manufacture instruction manual and imported from *Biodiagnostic company, Dokki, Giza, Egypt*. Serum insulin and leptin levels were measured using commercial kits imported from abcam, Co, USA.

Serum hormone assays

Plasma changes in levels of testosterone were measured using commercial kits (Testosterone ELISA Kit from abcam, Tokyo, Japan Cat # ab108666) that purchased from *Clini Lab*., Al-Manial, Cairo, Egypt. Plasma prolactin levels were measured using Prolactin Human

Simple Step ELISA™ Kit (ab189570), Osaka, Japan. The instruction manual of each kite was followed as suggested by providers.

Sperm analysis (eosin-nigrosin stain)

The epididymal sperm was collected according to Blash et al. (2000) with some modification. The testes were removed from the scrotal sac within 5 to 10 minutes, placed in an insulator box and transported to laboratory and processed individually. The parietal tunic was removed leaving the tail of the epididymis exposed. A small lateral incision was made along the tail of the epididymis to open the convoluted tubules and put in petri dish with 3.025 g Tris, 1.7 g citric acid, 1.25 g fructose (TFC) supplemented with 5.5 mg tylosin, 27.5 mg gentamycin, 16.5 mg lincospectin, and 330 mg spectinomycin per 100 ml. Spermatozoa were sedimented by gentle centrifugation at 800 X g (1200 rpm) for 5 min at 30°C and the pellet was washed twice with TFC medium to remove contaminating epididymal plasma. The cells were dispersed in the same medium and this preparation of spermatozoa was used for the experiments. Individual sperm motility was assessed by bright field microscopy. Diluted sperm was examined microscopically using adjusted hot stage microscope at 38ºC. Individual sperm motility percent was determined on a subjective scale of 0–100% to the nearest 5% after examining several microscopic fields. The percentage of live and abnormal sperms was assayed by staining smears with eosin-nigrosin [Campbell et al., 1956]. A total of 200 sperm cells were examined randomly. Total sperm abnormalities and live percentage were recorded.

RNA extraction, cDNA synthesis and Semi-quantitative PCR analysis

For preparation of total RNA **[**Soliman et al., 2013], tissue samples (approximately 100 mg per sample) were collected from rats testis, eye, liver and epididymal adipose tissue, flash frozen in liquid nitrogen and subsequently stored at -80°C in 1 ml Qiazol. Frozen samples were homogenized using a Polytron 300 D homogenizer (Brinkman Instruments, Westbury, NY). Then 0.3 ml chloroform were added to the homogenates. The mixtures were shaken for 30 seconds followed by centrifugation at 4°C and 12,500 rpm for 20 min. The supernatant layer were transferred to a new set of tubes, and an equal volume of isopropanol will be added to the samples, shacked for 15 seconds and centrifuged at 4°C and 12,500 rpm for 15 min. The RNA pellets were washed with 70% ethanol, briefly dried up then, dissolved in Diethylpyrocarbonate (DEPC) water. The prepared RNA integrity will be checked by electrophoresis. RNA concentration and purity will be determined spectrophotometrically at 260 nm.

For cDNA synthesis, mixture of 3 µg total RNA and 0.5 ng oligo dT primer in a total volume of 11 µl sterilized DEPC water were incubated in the PeX 0.5 thermal Cycler (PCR machine) at 65°C for 10 min for denaturation. Then, 4 µl of 5X RT-buffer, 2 µl of 10 mM dNTPs and 100 U Moloney Murine Leukemia Virus (M-MuLV) Reverse Transcriptase were added in a total volume of 20 µl by DEPC water. The mixture were re-incubated in the thermal Cycler at 37°C for 1h, then at 90°C for 10 min to inactivate the enzyme.

Specific primers for genes of testes, eye, liver and epididymal adipose tissues (tables 1, 2, 3, and 4) were designed using Oligo-4 computer program and synthesized by Macrogen (Macrogen Company, GAsa-dong, and Geumcheon-gu. Korea). PCR were conducted in a final volume of 25 µl consisting of 1 µl cDNA, 1 µl of 10 picomolar (pM) of each primer (forward and reverse), and 12.5 µl PCR master mix (Promega Corporation, Madison, WI) the volume were brought up to 25 µl using sterilized, deionized water. The cycle sequence of PCR reaction was carried out at 94 °C for 5 minutes one cycle, followed by 27 cycles each of which consisted

of denaturation at 94 °C for one minute, annealing at the specific temperature corresponding to each primer (tables1, 2, 3, and 4) and extension at 72 °C for one minute with additional final extension at 72 °C for 7 minutes. As a reference, expression of glyceraldehyde-3-phosphate dehydrogenase (G3PDH) mRNA as housekeeping gene was expressed. PCR products were electrophorized on 1% agarose gel stained with ethidium bromide in TBE (Tris-Borate-EDTA) buffer. PCR products were visualized under UV light and subsequently photographed using an InGenius 3.0 gel documentation system (Syngene, Frederick, MD, USA). The band intensities were densitometrically quantified and calculated using ImageJ software version 1.47 (http://imagej.en.softonic.com/).

Histopathology and electron microscope

Small specimens from the wound were fixed in 10% neutral buffered formalin (NBF) for 24 h, then washed under running tap water and preserved in 70% ethanol. The samples were dehydrated in ascending grades of ethanol, cleared in xylene and embedded in Paraplast Plus®. (Leica Biosystems, Richmond, IL, USA) and cut at 5 µm thick sections. Tissue sections were mounted on glass slides and stained with hematoxylin and eosin (H&E) for general histology and Masson'n trichrome and toluidine blue techniques for special stains. Processing and staining methods are detailed in Bancroft and Gamble (2008). For electron microscopy, Very small pieces of Ixlxl mm were fixed in 2.5% glutaraldehyde in 1M phosphate buffer (pH. 7.3) for 24 hours then fixed in cold IM phosphate buffered 5% osmium tetroxide (pH. 7.3) for 3 hours, rinsed in phosphate buffer for 30 minutes then dehydrated. Semi-thin sections were stained by Toluidine blue. Ultra thin sections will be obtained and mounted on copper grids then stained with uranyl acetate and lead citrate [Bancroft and Gamble 2008].

Statistical analysis

The data are presented as the mean ± standard error of the mean. Analysis of variance and Fisher post-hoc descriptive test were used to analyze the data using SPSS software version 11.5 for Windows (SPSS, Inc., Chicago, IL, USA). Using the same software, regression analysis was performed. $P<0.05$ were considered to indicate a statistically significant difference.

Table 1.

PCR conditions and primer sequence for examined genes in the testis

Gene	Product size (bp)	Annealing (^{0}C)	Direction	Sequence (5'-3')
ABP	260	58	Sense	TCCGATACCACCAAGCACAAG
			Antisense	TCAGGAAAGCTGGGAACACTG
LHR	272	52	Sense	AGAGTGATTCCCTGGAAAGGA
			Antisense	TCATCCCTTGGAAAGCATTC
P450$_{scc}$	688	55	Sense	CGCTCAGTGCTGGTCAAAA
			Antisense	TCTGGTAGACGGCGTCGAT
P450$_{c17}$	302	55	Sense	GACCAAGGGAAAGGCGT
			Antisense	GCATCCACGATACCCTC
3□□ -HS	547	55	Sense	CCGCAAGTATCATGACAGA
			Antisense	CCGCAAGTATCATGACAGA
17□-HSI	653	55	Sense	TTCTGCAAGGCTTTACCAGG
			Antisense	ACAAACTCATCGGCGGTCTT
AR	570	55	Sense	TTACGAAGTGGGCATGATGA
			Antisense	ATCTTGTCCAGGACTCGGTG
StAR	389	58	Sense	TTGGGCATACTCAACAACCA
			Antisense	ATGACACCGCTTTGCTCAG
G3PDH	309	52	Sense	AGATCCACAACGGATACATT
			Antisense	TCCCTCAAGATTGTCAGCAA

Table 2.

PCR conditions and primer sequence for examined aquaporins in the eye

Gene	Product size (bp)	Annealing (^{0}C)	Direction	Sequence (5'-3')
AQ0	231	55	Sense	GCTCCTGCTATCCTCACCAG
			Antisense	CAGCTTTTACAGGGCCTGAG
AQ1	170	55	Sense	TTTGGGCACCTTTCAAACTC
			Antisense	GAATGAGCCTTTTCCAGCAG
AQ5	210	54	Sense	GCCCAGCTGGTGGGCGCCATT
			Antisense	TGGGGAGCCCACAGGGCTGGT
AQ6	240	55	Sense	GTCAACGTGGTCCACAACAG
			Antisense	TGCAAACTTCCCAACAATGA
AQ7	240	55	Sense	GCAGGTGGAGAACTGTTGGT
			Antisense	TGTGTTCATGCCTAGGGACA
AQ8	220	55	Sense	TGGAACCTGGAACTCCTTTG
			Antisense	AGTACGCATGGACTGGGTTC
AQ9	184	55	Sense	CTCAGTCCCAGGCTCTTCAC
			Antisense	ATGGCTCTGCCTTCATGTCT
AQ11	170	55	Sense	TTTGGGCACCTTTCAAACTC
			Antisense	GAATGAGCCTTTTCCAGCAG
AQ12	236	55	Sense	GGGAGCTCAGCGAACTACAC
			Antisense	AGGATTGAAGAAGGCAGACG

Table 3.

PCR conditions and primer sequence of genes of polyol pathway in the eye.

Gene	Product size (bp)	Annealing (^{0}C)	Direction	Sequence (5'-3')
Ald-Red	480	60	Sense	GTGGACACTTGGACGGCTAT
			Antisense	CACCCTCCAGTTCCTGTTGT
SDH	464	60	Sense	TTGACGAGCAGAAACACCAG
			Antisense	TTGTAGAAGCGGCAGAGGTT
MSRA	330	60	Sense	ATGATGGGCGACTCATCTTC
			Antisense	CTCAAAGCTGACGTGCTCTG

Table 4.

PCR conditions and primer sequence of genes of lipids and carbohydrates metabolism in liver and adipose tissue of diabetic rats and CM supplemented diabetic rats.

Gene	Product size (bp)	Annealing (^{0}C)	Direction	Sequence (5'-3')
PK	229	52	Sense	ATTGCTGTGACTGGATCTGC
			Antisense	CCCGCATGATGTTGGTATAG
PPAR-□	680	59	Sense	GAGGTCCGATTCTTCCACTG
			Antisense	ATCCCTGCTCTCCTGTATGG
GLUT 2	330	55	Sense	AAGGATCAAAGCCATGTTGG
			Antisense	GGAGACCTTCTGCTCAGTGG
FAS	345	61	Sense	CCAGAGCCCAGACAGAGAAG
			Antisense	GACGCCAGTGTTCGTTCC
HSL	313	61	Sense	TGCCCAGGAGTGTGTCTGAG
			Antisense	AGGACACCTTGGCTTGAGCG

Results and discussion

Protective effect of camel milk supplementation on spermogram, testosterone and LH levels,urea, creatinine, GPT, GOT, MDA and antioxidants in diabetic and camel milk supplemented diabetic rats

Induction of diabetes is rats after 4 months induced significant decrease in sperm motility, percentage of live sperms, and an increase in sperm abnormalities. Camel milk supplementation into diabetic rats normalized such abnormalities reported on diabetic rats alone (table 5). These finding gave a hope for diabetic patients for treatment of sexual impotency and lake of sexual desire. Parallel with changes in spermogram, a decrease in serum levels of testosterone and LH were reported that normalized after camel milk supplementation (table 6). It has been shown that both diabetic men and animal models, increases in oxidative stress, apoptosis of germ cells, inhibition of seminiferous epithelial cell proliferation, and alterations in pituitary–testicular hormonal axis collectively lead to decreases in sperm counts and a decrease in testosterone and LH levels [Kilarkaje and Al-Bader, 2015; Kilarkaje et al., 2014; Ko et al., 2014].

The decrease in sperm motility may be due to structural and functional changes during sperm tail morphogenesis as diabetes is known to induce sperm abnormalities [Kilarkaje et al., 2014]. The recovery of sperm count and motility to the control levels in camel milk- treated diabetic rats can be attributed to antioxidant properties of camel milk as supported by serum findings listed in table (7). As diabetes induced oxidative stress that are manifested by increase in MDA levels and a decrease in antioxidants activities represented by decrease in serum levels of SOD, GSH-R and catalase. Supplementation with camel milk showed the beneficial property of CM to normalize this decrease in antioxidants and the increase in MDA due to oxidative stress.

Camel milk inhibited oxidative stress by increasing the activities of SOD, catalase and glutathione reductase levels [Soliman et al., 2015; Zhu et al., 2016]. In parallel, diabetes induced alteration in all organs such as kidney and liver as reported by alteration in serum levels of urea, creatinine, GPT and GOT (table 7) that are ameliorated and normalized by camel milk supplementation. These findings are reported by ours and those of Althnaian et al., 2013.

Table 5.

The sperm characteristics of diabetic and CM supplemented diabetic rats

.

	Motility%	**Live %**	**Abnormality %**
Control	**75**.89 ± 1.82	84.44 ± 3.28	8.44 ± 1.09
CM	77.22 ± 1.21	89.44 ± 1.64	7.33 ± 0.38
Diabetes	51.3± 3.21	59.21± 5.67	21.33 ± 0.80
CM + diabetes	68.1± 4.3	71.8 ± 2.9	11.9 ± 1. 01

*Values are means ± standard error (SEM) for 10 different rats per each treatment. Values are statistically significant at *p<0.05 Vs. control and #p<0.05 Vs. diabetic rats.*

Table 6.

Protective effect of camel milk on serum changes of testosterone and LH levels in diabetic and CM supplemented diabetic rats.

	Testosterone (ng/ml)	LH (ng/ml)
Control	3.5 ± 0.3	1.7 ± 0.2
Camel Milk (CM)	3.6 ± 0.4	1.4 ± 0.1
Diabetic rats	1.2 ± 0.2*	0.6 ± 0.1*
Diabetics + CM	2.5 ± 0.2#	1.3 ± 0.1#

*Values are means ± standard error (SEM) for 10 different rats per each treatment. Values are statistically significant at *p<0.05 Vs. control and #p<0.05 Vs. diabetic rats.*

Table 7.

Protective effect of camel milk on serum changes of urea, creatinine, GOT, GPT, MDA, SOD, glutathione reductase (GSH-R) and catalase levels in diabetic rats and CM supplemented diabetic rats.

Parameter	Urea (mg/dL)	Creatinine (mg/dL)	GOT (U/l)	GPT (U/l)	MDA (nmol/g protein)	SOD (U/ g protein)	GSH-R (U/ g protein)	Catalase (U/ g protein)
Control	43.7 ± 5.9	0.8 ± 0.01	86 ±14	95.7 ± 3.5	5.4 ± 1.5	10.2 ± 0.2	10± 0.1	28.1 ± 2
Camel Milk (CM)	40.3 ± 1.5	0.8 ± 0.1	90 ± 4.3	95 ± 4.2	8.2 ± 1.7	10.9 ± 0.7	10.4± 0.4	31.4 ± 2
Diabetic rats	120.7± 6.4*	2.7 ± 0.1*	158.7±10.7*	190±19.5*	31.5 ± 1	3.4 ± 0.3	3.6± 0.3	8.7 ± 0.5
Diabetics + CM	67.3 ± 5.2#	0.9 ± 0.02#	111.3 ± 1.6#	107 ±10.8#	15.2±3.7#	8.9 ± 0.6#	9 ± 0.4#	32.3 ± 1.4#

*Values are means ± standard error (SEM) for 10 different rats per each treatment. Values are statistically significant at *p<0.05 Vs. control and #p<0.05 Vs. diabetic rats.*

Protective effect of camel milk supplementation glucose, insulin, leptin and dyslipidemia in diabetic and camel milk supplemented diabetic rats

Diabetes is a metabolic disease resulted from destruction of cells of pancreas. Therefore, insulin secretion is extremely affected and hyperglycemia occurs [Reddy et al., 2009]. Hyperglycemia leads to oxidative stress and increase in ROS and a decrease in antioxidants activities [Amaral et al., 2006 and Hakeem et al., 2008]. Increased ROS cause the oxidation of proteins, lipids and damage macro molecules like DNA [Paasch et al., 2004]. Moreover, it has been shown that changes in insulin are followed by similar changes on levels of energy associated hormones such as leptin [Mohamed-Ali et al., 1998]. Lipolysis during diabetes is increased and there is general dyslipidemia [Mohasseb et al., 2011]. Here we confirmed as seen in table (8) that diabetic rats showed an increase in glucose levels and a decrease in insulin levels that are coincided with a decrease in leptin secretion from white adipose tissue. Disorders in lipids metabolism resulted in general dyslipidemia that is characterized by hypercholesterolemia, hypertriglyceridemia and a decrease in high density lipoproteins (HDL) (table 8).

Table 8.
Protective effect of camel milk on serum changes of glucose, insulin, leptin, TG, cholesterol and HDL levels in diabetic rats.

Parameter	Glucose (mg/dL)	Insulin (µIU/ml)	Leptin (ng/ml)	TG (mg/dl)	Cholesterol (mg/dl)	HDL-C (mg/dl)
Control	85.7 ± 8.2	29.3 ±1.2	12.8± 2.1	65.3 ± 3.9	117 ± 4.6	21.7 ±1
Camel Milk (CM)	90.3 ± 3.9	34.7 ±3.8	10.7 ± .87	68.3 ± 2.4	128.3 ± 12.1	21.8 ± 0.9
Diabetic rats	410 ± 36.7*	14.2 ±0.9*	9.6 ± 0.6	135.7 ± 5.9*	313 ± 12.4*	10.1 ± 0.3*
Diabetics + CM	103 ± 12.5#	26.7± 3.8#	10.4 ± 0.2	83.3 ± 3.8#	170 ± 18.2#	19.3 ± 0.8#

*Values are means ± standard error (SEM) for 10 different rats per each treatment. Values are statistically significant at *p<0.05 Vs. control and #p<0.05 Vs. diabetic rats.*

Protective effect of camel milk supplementation on steroidogenesis related enzymes, AR and LHR in diabetic and camel milk supplemented diabetic rats

Semiquantitative RT-PCR analysis showed that induction of diabetes for 4 month was associated with down regulation in mRNA expression of ABP, StAR, 3β-HSD and 17β-HSD, (figure 1). Camel milk supplementation for diabetic rats for 4 months resulted in normalization of down regulated genes.

Chung et al., [2011] mentioned that, the Leydig cells, testosterone-producing cells located in the interstitial compartment of mammalian testis. In the testis, LH binds to Leydig cell receptors and initiates the activation of adenylate cyclase, resulting in an attendant increase in cAMP production. Luo and his collaborators **[**Luo et al., 2011**]** reported that**,** Steroidogenic Acute Regulatory protein (StAR) transfers cholesterol from the outer membrane to the inner mitochondrial membrane. Where, the enzyme cytochrome P450 side chain cleavage (P450scc) converts cholesterol into pregnenolone. Ultimately pregnenolone transferred to smooth endoplasmic reticulum. Where, the synthesis of testosterone takes place via the actions of 3β-hydroxysteroid dehydrogenase (3β-HSD), ($P450_{c17}$), and 17β-hydroxysteroid dehydrogenase (17β-HSD)**.** Moreover Wang et al. [2010] reported that, StAR is considered to be the rate limiting step in testosterone biosynthesis and reduced StAR is always found in testicular dysfunction. As known diabetes induce oxidative stress and increase in ROS as previously discussed. In parallel, diabetes produces erectile dysfunction and retrograde ejaculation in men [Rodriguez 1980] and many studies provided conflicting results with respect to the direct effects of diabetes on male fertility potential. While, Anderson et al., (1987) observed microscopic abnormalities in testicular morphology in Type 1 diabetic young men with erectile dysfunction. Our results confirmed same findings and confirmed till now the potential of camel milk usage for normalization of such diabetic defects as confirmed in figure 1 and 2. Figure 2 confirmed the down regulation of mRNA expression of other genes associated with male fertility in diabetic rats such as $P450_{scc}$ and $P450_{c17}$. Serum levels of testosterone and LH were decreased as shown in table (6) and was confirmed in figure 2 C and D as there are decrease in the mRNA expression of both androgen receptor (AR) and luteinizing hormone receptor (LHR). All are ameliorated to normal expression after camel milk supplementation for 4 months (Figure 2).

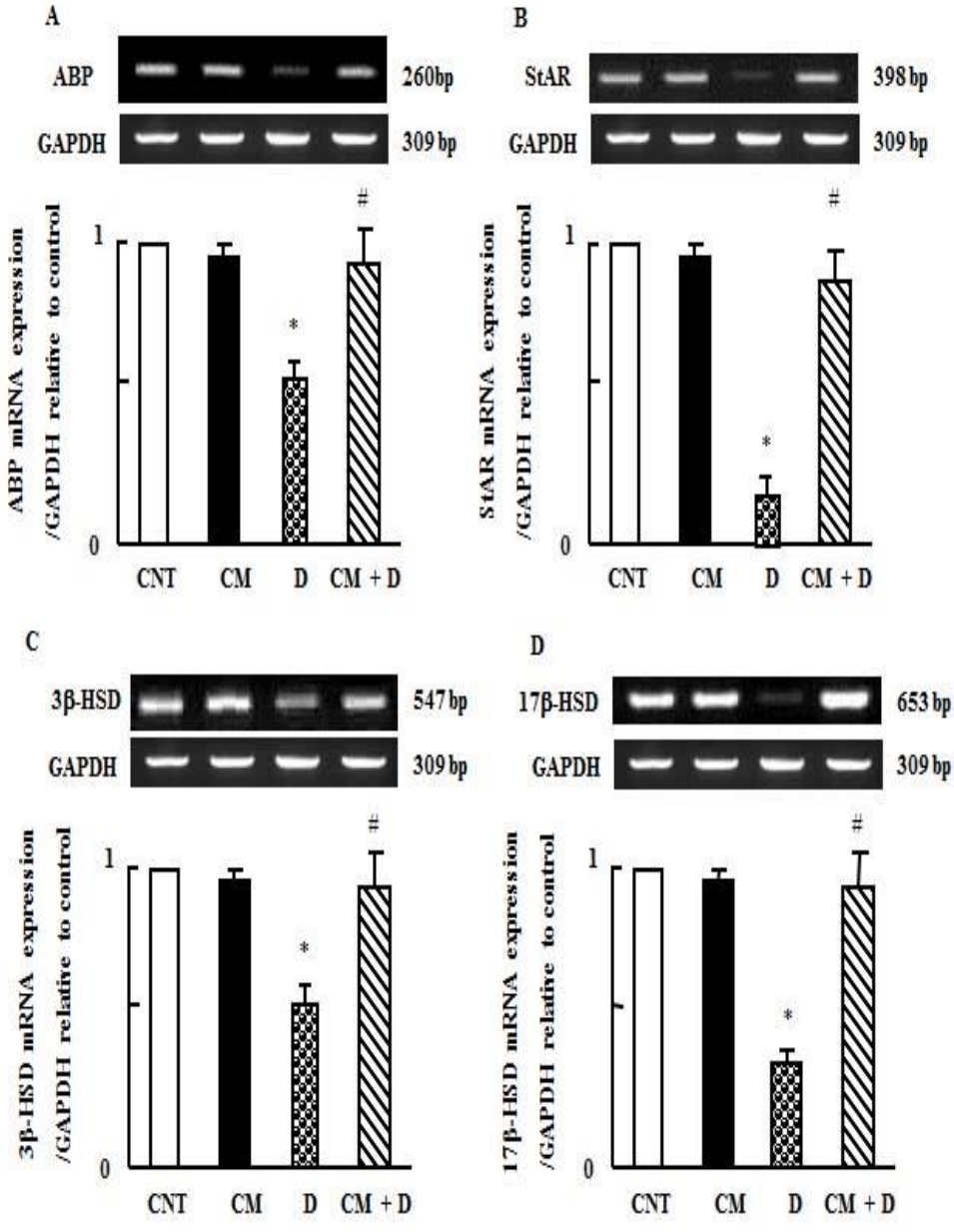

Figure.1. Semi-quantitative RT-PCR analysis of ABP (A), StAR (B), 3□□-HSD (c) and 17□-HSD (D) mRNA expressions and their corresponding GAPDH in the testis of diabetic and camel milk (CM) supplemented rats. Data presented as the mean ± standard error of values of 15 rats per group. *P<0.05 vs. the control (CNT) group; #P<0.05 vs. diabetic group (D). GAPDH, glyceraldehyde 3-phosphate dehydrogenase.

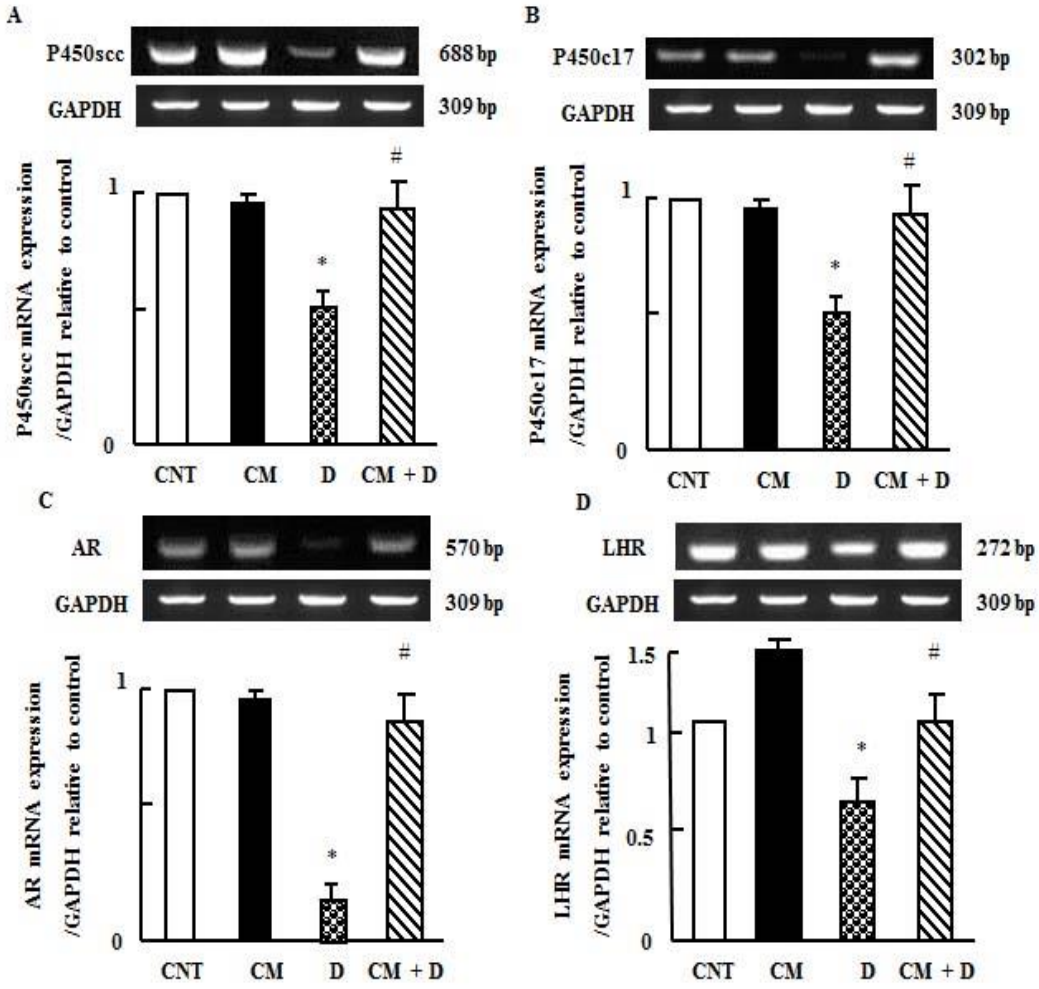

Figure.2. Semi-quantitative RT-PCR analysis of P450scc (A), P450c17 (B), AR (c) and LHR (D) mRNA expressions and their corresponding GAPDH in the testis of diabetic and camel milk (CM) supplemented rats. Data presented as the mean ± standard error of values of 15 rats per group. *P<0.05 vs. the control (CNT) group; #P<0.05 vs. diabetic group (D). GAPDH, glyceraldehyde 3-phosphate dehydrogenase.

Protective effect of camel milk supplementation on aquaporins mRNA expression in diabetic and camel milk supplemented diabetic rats

Aquaporins (AQPs) are a family of integral membrane proteins that allow water to cross the plasma membrane bi-directionally [Agre and Kozono, 2003]. They are critically involved in the maintenance of the ionic and osmotic balance in the central nervous system (CNS) in response to osmotic gradients and differences in hydrostatic pressure [Tait et al., 2008] due to the fact that the ionic transmembrane shift during neuronal activity must be accompanied by the movement of water across the membrane [Amiry-Moghaddam and

Ottersen, 2003]. The AQPs family is composed of aquaporin, which is selective for water, and aquaglyceroporin, which is also permeable to a wide variety of non-charged solutes, such as lactate and glycerol [Agre and Kozono, 2003; Tait et al., 2008; Verkman et al., 2008]. Among the 13 isoforms of the mammalian AQPs protein family identified so far, at least four AQPs (AQP-0, -1, -4, and -9) are reportedly expressed in the retina [Fukuda et al., 2010 and Naka et al., 2010].To date, at least 13 members of the AQP family (AQP0-12) have been identified in mammals [Agre et al., 2002]. Though the retina of the rat expresses gene transcripts of numerous AQPs [Hollborn **et** al., 2011; Tenckhoff et al., 2005], the presence of only four AQPs was hitherto demonstrated by immunohistochemistry. In our study we confirmed the expression of various AQPs in eye of diabetic rats. Using RT-PCR, we confirmed that AQ0 and 5 were up-regulated during diabetes and CM normalized such changes, While AQ6 was down regulated in dibetes and CM partially normalized it (Figure 3). In parallel, in figure 4, AQ-9 and AQ-12were up-regulated in diabetic rats and normalized after camel milk supplementation. In contrast, AQ 11 was down regulated in diabetic rats and normalized after CM supplementation (Figure 4). For our knowledge, our findings are the first showed expression of AQPs after CM supplementation in diabetic rats and in agreement with published papers in human study for the incidence of diabetes only but not for CM supplementation.

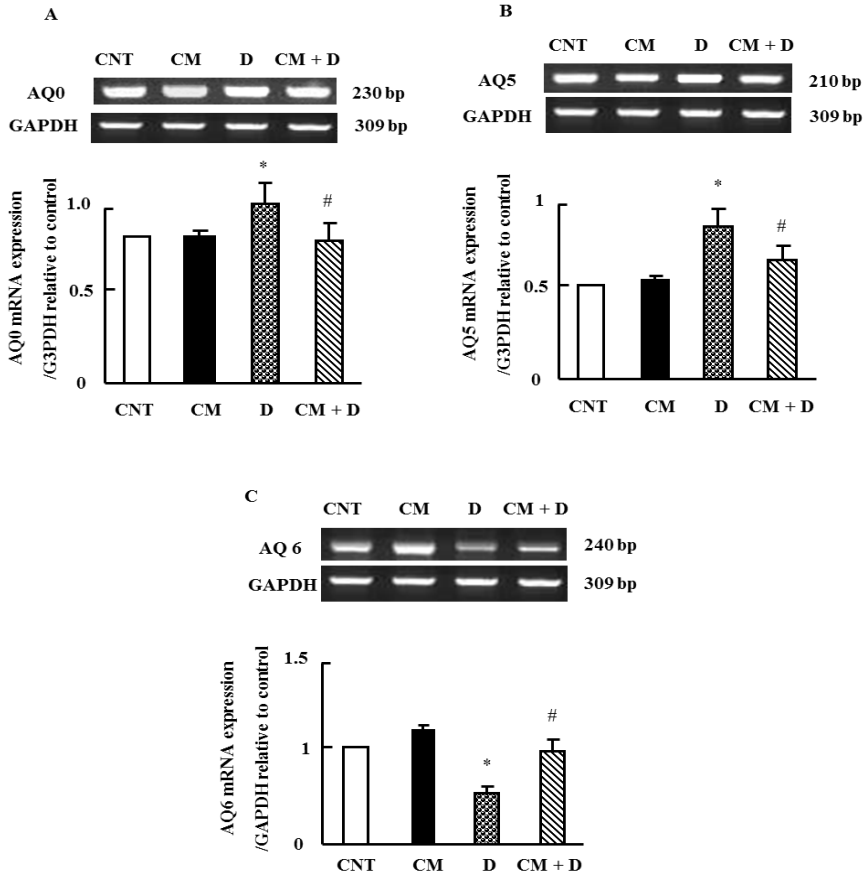

Figure.3. Semi-quantitative RT-PCR analysis of AQ0 (A), AQ5 (B), andAQ6 (D) mRNA expressions and their corresponding GAPDH in the eye of diabetic and camel milk (CM) supplemented rats. Data presented as the mean ± standard error of values of 15 rats per group. *P<0.05 vs. the control (CNT) group; #P<0.05 vs. diabetic group (D). GAPDH, glyceraldehyde 3-phosphate dehydrogenase.

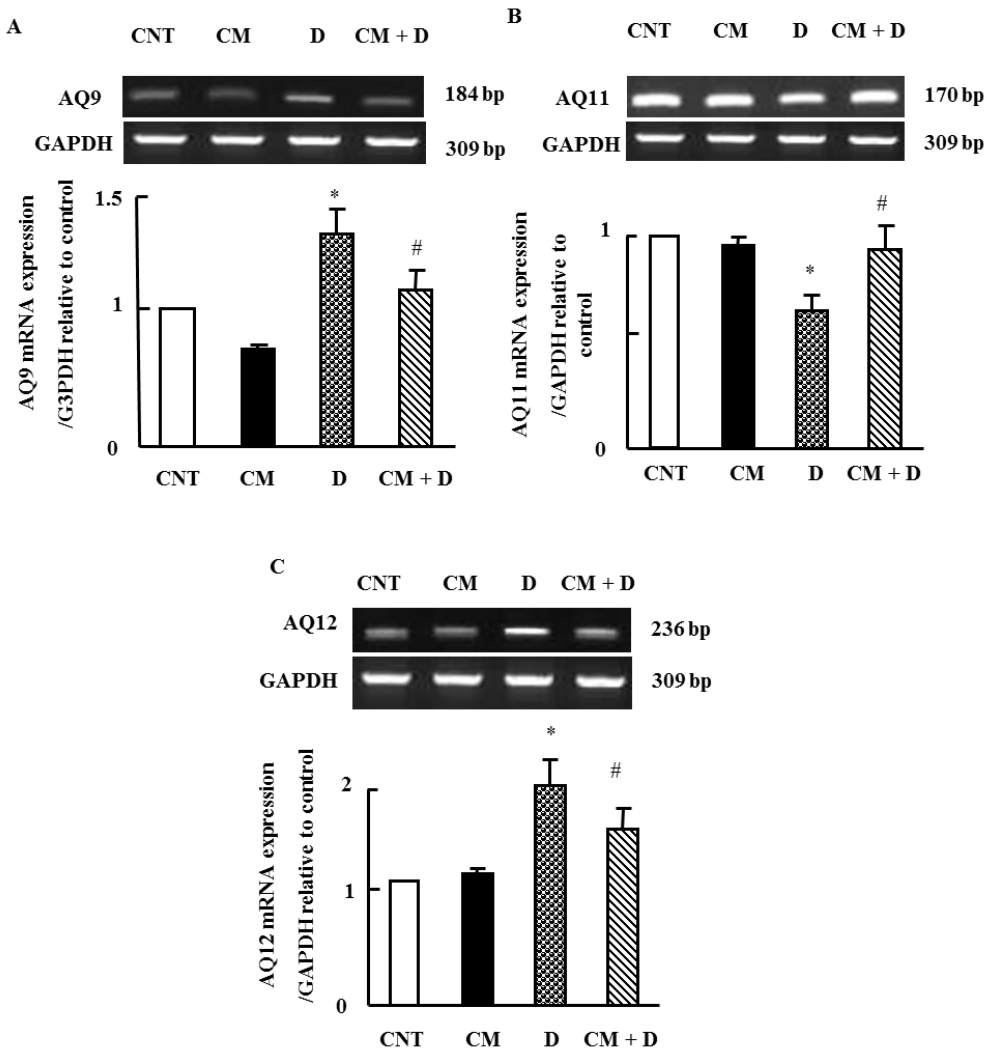

Figure.4. Semi-quantitative RT-PCR analysis of AQ9 (A), AQ11 (B), andAQ12 (D) mRNA expressions and their corresponding GAPDH in the eye of diabetic and camel milk (CM) supplemented rats. Data presented as the mean ± standard error of values of 15 rats per group. *P<0.05 vs. the control (CNT) group; #P<0.05 vs. diabetic group (D). GAPDH, glyceraldehyde 3-phosphate dehydrogenase.

Protective effect of camel milk supplementation on mRNA expression of polyol pathway genes in diabetic and camel milk supplemented diabetic rats

Diabetic rats after 4 month showed up-regulation in the mRNA expression of aldose reductase (Ald-Red), sorbitol dehydrogenase (SDH) and methionine sulofoxide reductase A. This increase is due to hyperglycemia and oxidative stress occurred in diabetic rats. CM supplementation ameliorated and normalized the expression of polyol pathway genes as shown in figure (5).

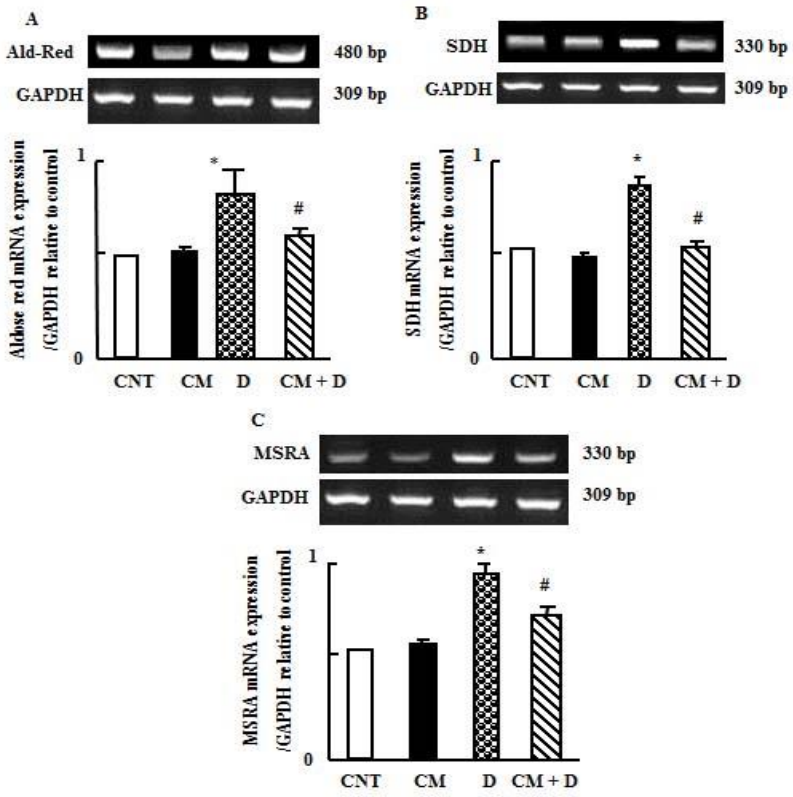

Figure.5. Semi-quantitative RT-PCR analysis of genes of polyol pathway in the eye. Ald-Red (A), SDH (B) and MSRA (C) mRNA expressions and their corresponding GAPDH in the eye of diabetic and camel milk (CM) supplemented rats. Data presented as the mean ± standard error of values of 15 rats per group. *P<0.05 vs. the control (CNT) group; #P<0.05 vs. diabetic group (D). GAPDH, glyceraldehyde 3-phosphate dehydrogenase.

Diabetes is characterized is associated with development of diabetes-specific pathology in the eye (refractive changes, cataract and retinopathy), peripheral nerve and kidneys (renal glomerulus) [Gabbay 1975; Giacco and Brownlee 2010]. The polyol pathway is based on the enzyme aldose reductase, when glucose concentration in the cell becomes too high; aldose reductase reduces that glucose to sorbitol. Sorbitol is then oxidised to fructose by the enzyme sorbitol dehydrogenase. Sorbitol is an alcohol, and is highly hydrophilic [Gabbay 1973; Brownlee 2001]. Therefore, it does not diffuse easily through the cell membrane and accumulate intracellularly [Lorenzi 2007; Mathebula 2015]. In animal models, treatment with Ald-Red inhibitors was shown to be effective in preventing the development of various diabetic complications, including cataract, neuropathy, and nephropathy [Oates and Mylari 1999]. It was thought that osmotic stress, from the accumulation of sorbitol, leads to diabetic lesions [Kinoshita and Nishimura 1988]. Sorbitol is more difficult to metabolise, and has damaging effects in cells, with possible osmotic damage and cataract formation [Gabbay 1975; Giacco and Brownlee 2010]. In cells when sorbitol dehydrogenase activity is high, an increase in

NADH/ NAD+ ratio occurs. A decreased NADH/NADP ratio can increase oxidative stress by decreasing regeneration of cellular antioxidant (reduced glutathione from oxidised glutathione) and by decreasing availability of NADPH, thereby decreasing the activity of catalase, the enzyme responsible for converting ROS and Hydrogen peroxide (H2O2) into water [Mathebula 2015] and confirmed in our results table (7). An elevated NADH/ NAD+ ratio could significantly affect the health of the retina [Baynes 1991]. It has been reported by Li et al., (2011), that the contents of methionine sulfoxide (MetO), in the lenses of STZ-induced diabetic mice after 14 days were significantly higher than that in the normal control.

Protective effect of camel milk supplementation on mRNA expression of genes of carbohydrate and lipid metabolism in diabetic and camel milk supplemented diabetic rats in liver and adipose tissue.

Next, we investigated the alteration in some enzymes regulating glucose metabolism including Pyruvate Kinase (PK) that is responsible for glycolysis and PPAR-□ that is associated with lipogenesis in liver. The expression of hepatic PK mRNA as estimated by RT-PCR analysis was significantly decreased in diabetic rats (figure 6a). Supplementation of CM to diabetic rats resulted in reversal PK expression. In contrast, PPAR-□□expression was increased in diabetic rats and normalized after CM supplementation (figure 6b).

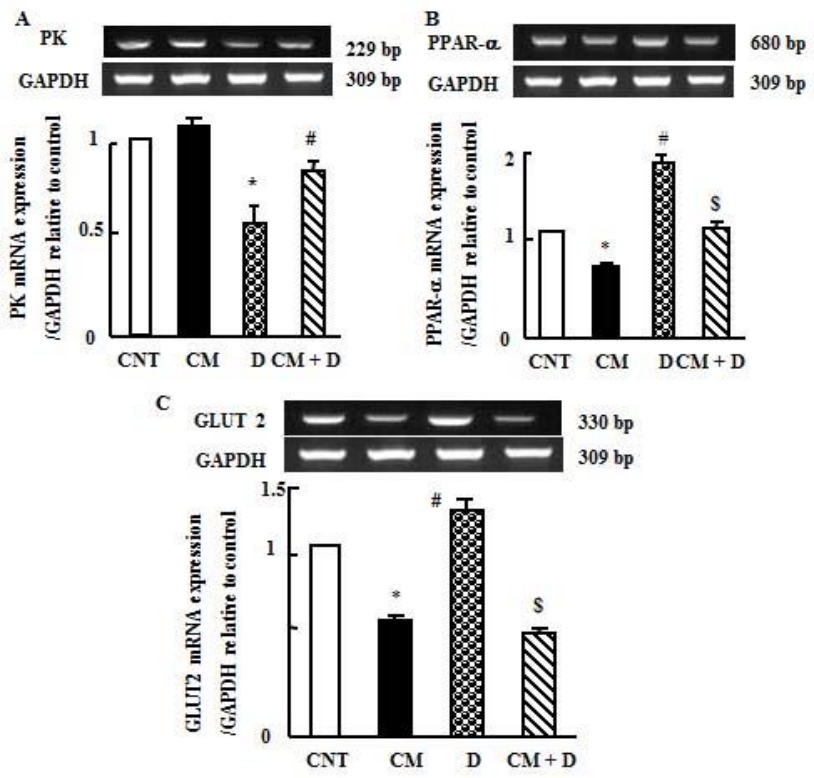

Figure.6. Semi-quantitative RT-PCR analysis of genes of carbohydrates metabolism in the liver. PK (A), PPAR-□ (B) and GLUT-2 (C) mRNA expressions and their corresponding GAPDH in the liver of diabetic and camel milk (CM) supplemented rats. Data presented as the mean ± standard error of values of 15 rats per group. *P<0.05 vs. the control (CNT) group; #P<0.05 vs. diabetic group (D). GAPDH, glyceraldehyde 3-phosphate dehydrogenase.

PPAR-alpha is a transcription factor and a major regulator of lipid metabolism in the liver. PPAR-alpha is activated under conditions of energy deprivation and is necessary for the process of ketogenesis, a key adaptive response to prolonged fasting [Kersten 1999]. Activation of PPAR-alpha promotes uptake, utilization, and catabolism of fatty acids by upregulation of genes involved in fatty acid transport, fatty binding and activation, and peroxisomal and mitochondrial fatty acid β-oxidation [Kersten 2014]. Simillar findings for GLUT-2 expression were reported as it increased by diabetes and normalized after camel milk supplementation (figure 6C). Glucose influx is inhibited in the absence of insulin and recovered on insulin treatment (Vats et al., 2004). GLUT-2 regulates passage of glucose between liver and blood and it is responsible for renal glucose reabsorption (Freitas et al., 2005]. Our findings show CM supplementation increases insulin levels and consequently participates in diabetes treatment.

In the adipose tissue we examined the expression of hormone sensitive lipase (HSL) and fatty acid synthase (FAS). As shown in figure 7, there is down regulation in mRNA expression of FAS and up-regulation in HSL expression. During diabetes there is alteration in lipid and carbohydrate metabolism. As lipolysis, and glycolysis enhanced while lipogenesis is impaired to overcome metabolic needs. Those processes are regulated by variable enzymes as PK, HSL and FAS as key enzymes for control of diabetes under CM supplementation.

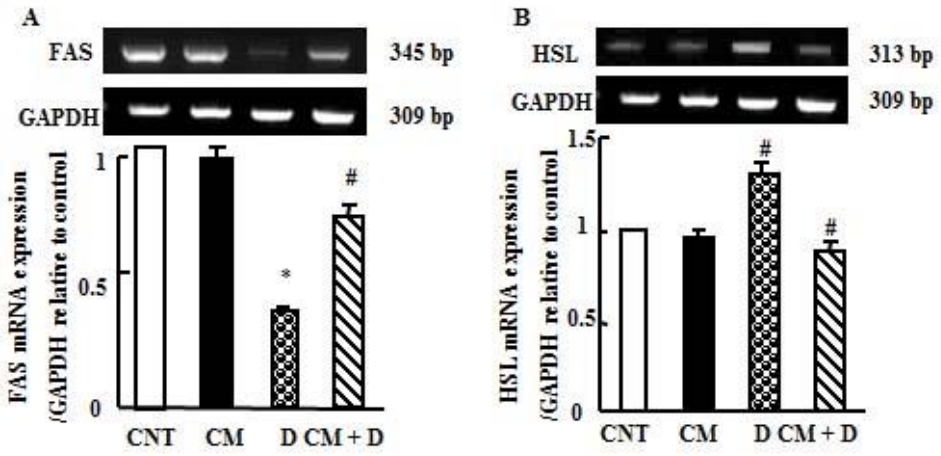

Figure.7. Semi-quantitative RT-PCR analysis of genes of lipids metabolism in the epidydimal adipose tissue. FAS (A), and HSL (B) mRNA expressions and their corresponding GAPDH in the epidydimal adipose tissue of diabetic and camel milk (CM) supplemented rats. Data presented as the mean ± standard error of values of 15 rats per group. *P<0.05 vs. the control (CNT) group; #P<0.05 vs. diabetic group (D). GAPDH; glyceraldehyde 3-phosphate dehydrogenase.

Histopathology of testis during diabetes and after CM administration for 4 consecutive months

The testis of the rats in the control group characterized by numerous seminephrous tubules which lined by spermatogonium cells, spermatocytes, spermatid and spermatozoa toluidine blue (Fig.8a). The cells were large polygonal with prominent nucleus and fine granular cytoplasm (Fig.8b). The testis of the camel milk group has the same histological characters of the control group. The interstitial cells were prominent as indicated by Masson

trichrome (Fig.8c) and the ultrastructure of the spermatogenic cells had the same criteria as that of the control (Fig.8d). The testis of the rats in the diabetic group had reduction in the number of the seminephrous tubules with appearance of numerous degenerated spermatogenic cells (Fig. 8e). Odema was prominent between the seminephrous tubules while the cell membranes showed separation Masson trichrome (Fig.8e). Some cells showed degranulation in the cytoplasm (Fig.8f). The testis of the rats in the CM treated group showed regression in the odema while some testicular blood vessels showed congestion H& E (Fig.8g). The ultrastructure of the spermatogenic cells retained its fine structure (Fig.8h).

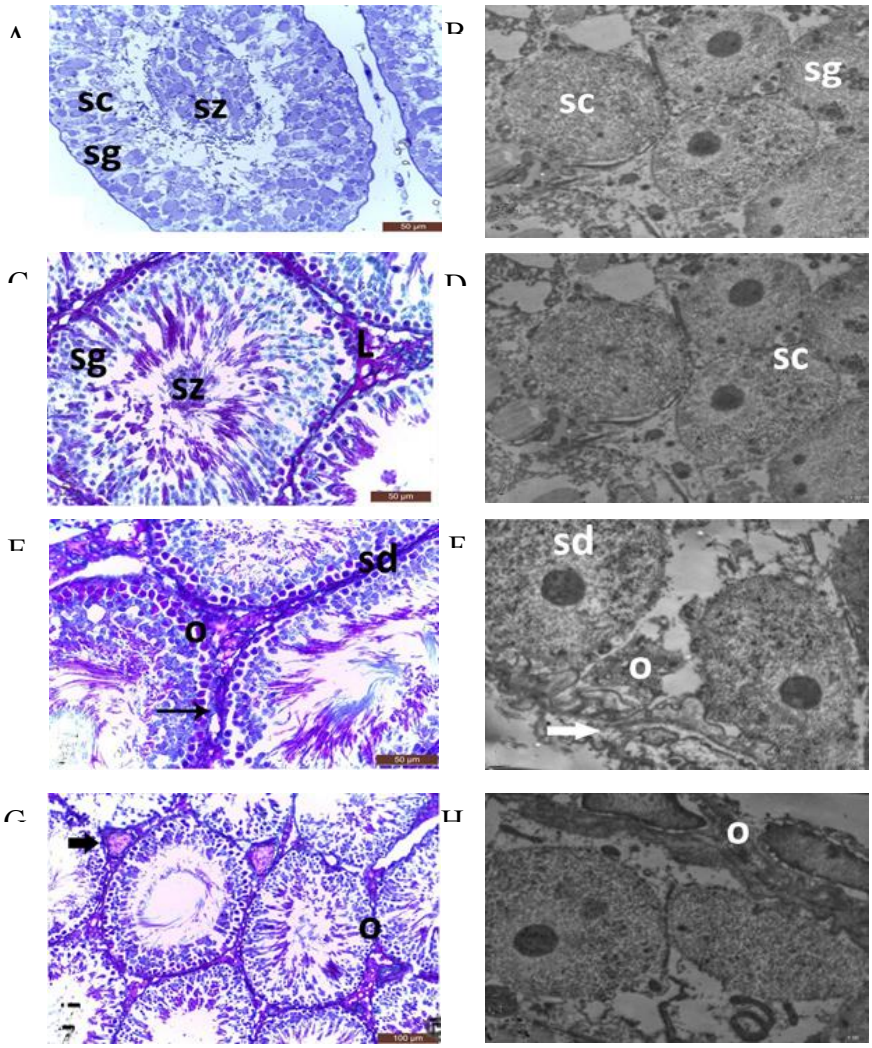

Fig.8. Light and electron microscopic examination of testis in control (A&B), CM (C &D), diabetic (E &F) and diabetic rats supplemented by CM (G &H). left column is light microscope while right one is Electron microscope. A is toluidine blue stain; C and E are Massson Trichrome and G is H& E stain. The magnification bare for light stains are written down right of each photo.

Histopathology of Eye during diabetes and after CM administration for 4 consecutive months

The histology of the eye (Figure 9) showed that eye cornea consisted of outer membrane which consisted of stratified squamous epithelium, outer bowman's membrane, stroma of collagen fibrils, inner descement's membrane and inner membrane which consisted of endothelial cells. Both of the outer and inner corneal membranes showed PAS positive reaction and negative alcianophilic fibers (Fig.9A).

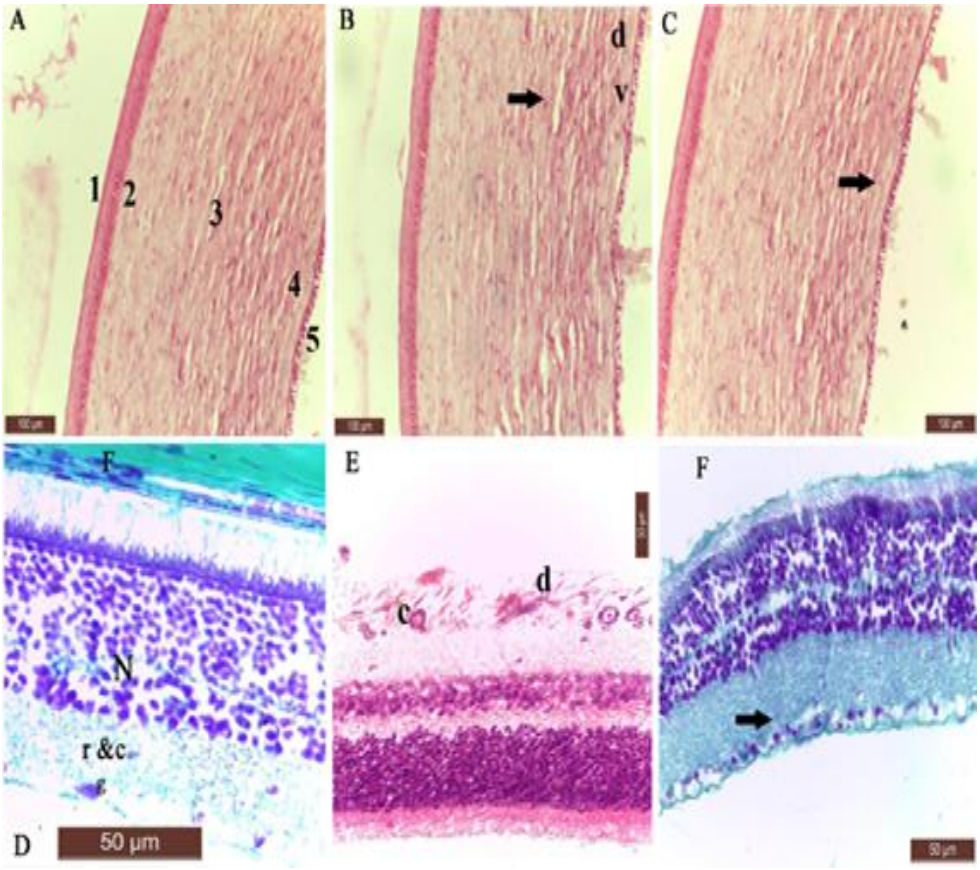

Figure 9. Light microscope of cornea and retina in diabetic and CM supplemented diabetic rats. In A; 1 is stratified squamous epithelium, 2 is outer bowman's membrane, 3 is stroma of collagen fibrils, 4 is inner descement's membrane and 5 is inner membrane with endothelial cells as shown by Periodic Acid Schiff (PAS). In B d is degeneration and v is vacuolation of some cells and irregular arrangements of some bundles in cornea. In C, CM induced minor regeneration in corneal epithelium and progress regeneration in collagen fibrils as indicated by arrow. In D, r&c are rods and cons, while N is bipolar cell nuclei and g is pigmented cell layer of retina. In diabetic group (E), c and d are congestion in the retinal blood vessels and detachment of some ganglionic cells. In CM supplemented diabetic rats (F), arrow is regeneration of retinal collaged fibrils.

The cells of the inner membranes was cuboidal in shape with centrally located nuclei and prominent mitochondria (Fig.9A). While In the diabetic group, the corneal inner endothelium showed cytoplasm sparsely degranulation and vacuolation of some cells. the collagen bundles of the stroma showed irregular arrangement and separation of the bundles from each other's (Fig.9B). In the treated group with camel milk, the corneal inner epithelium showed minor regeneration while the stromal collagen fibrills showed progressed regeneration in comparison to the diabetic group (Fig.9C).

In the retina consisted of ganglionic cell layer, outer and inner bipolar cell nuclei, inner and outer plexiform layer rodes and cones (nuclei and outer segments) and pigmented cell layer (Fig.9D). The retinal ganglionic cells showed congestion in the retinal blood vessels and detachment of some ganglionic cells (Fig.9E). The outer segments of rodes and cones appeared of normal structure as stacked cisterna of uniform structure (Fig.9E). In the treated group with camel milk, the retinal inner epithelium showed minor regeneration while the stromal collagen fibrills showed progressed regeneration in comparison to the diabetic group (Fig.9F).

Acknowledgement

The authors are greatly appreciating the financial and ethical support from King Abdulaziz City for Science and Technology (KACST) for the grant in aid for Mohamed Mohamed Soliman for Limited Grants (project # LG-35-046).

References

1. Adachi-Uehara N, Kato M, Nimura Y, Seki N, Ishihara A, Matsumoto E, Iwase K., Ohtsuka, S, Kodama H, Mizota A, Yamamoto S, Adachi-Usami E, Takiguchi M. (2006). Up-regulation of genes for oxidative phosphorylation and protein turnover in diabetic mouse retina. Exp. Eye Res., 83(4):849-57.
2. Agrawal RP, Dogra R, Mohta N, Tiwari R, Singhal S and Sultania S. (2009). Beneficial effect of camel milk in diabetic nephropathy. Acta Biomed., 80: 131-134.
3. Agrawal RP, Jain S, Shah S, Chopra A and Agarwal V. (2011). Effect of camel milk on glycemic control and insulin requirement in patients with type 1 diabetes: 2-years randomized controlled trial. Eur J Clin Nutr 65: 1048-1052.
4. Agrawal RP, Tantia P, Jain S, Agrawal R, Agrawal V. (2013) Camel milk: a possible boon for type 1 diabetic patients., Cell Mol Biol (Noisy-le-grand). 59(1):99-107.
5. Agre, P., Kozono, D., (2003). Aquqporin,. water channels: molecular mechanisms forhuman diseases. FEBS Lett. 555, 72e78.
6. Al-Baghli NA, Al-Ghamdi AJ., Al-Turki KA, Al Elq AH, El-Zubaier AG and Bahnassy A. (2011). Prevalence of diabetes mellitus and impaired fasting glucose levels in the Eastern Province of Saudi Arabia: results of a screening campaign. Singapore Med. J., 51: 923-930.
7. Althnaian T, Albokhadaim I and El-Bahr SM. (2013). Biochemical and histopathological study in rats intoxicated with carbon tetrachloride and treated with camel milk. Springerplus, 2(1):57.
8. Amaral S, Moreno AJ, Santos MS, Seiça R and Ramalho-Santos J. (2006). Effects of hyperglycemia on sperm and testicular cells of goto-kakizaki and streptozotocin-treated rat models for diabetes. Theriogenology, 66: 2056-2067.
9. Amaral S, Moreno AJ, Santos MS, Seiça R, Ramalho-Santos J. Effects of hyperglycemia on sperm and testicular cells of Goto-Kakizaki and streptozotocin-treated rat models for diabetes. Theriogenology. 2006; 66(9): 2056-67.
10. Amiry-Moghaddam, M., Ottersen, O.P., (2003). The molecular basis of water transport in the brain. Nat. Rev. Neurosci 4, 991e1001.
11. Anderson JE, Jones D, Penner SB and Thliveris JA. (1987). Primary hypoandrogenism in experimental diabetes in the Long-Evans rats. Diabetes, 36:1104–1110.
12. Bancroft JD, Gamble M. Theory and Practice of Histological Techniques. 6th ed. Churchill Livingstone Elsevier Philadelphia 2008; pp.126–127.

13. Baynes JW. (1991). Role of oxidative stress in development of complications in diabetes. Diabetes. 40:405–412. http://dx.doi.org/10.2337/diab.40.4.405
14. Blash S, Melican D, Gavin W. Cryopreservation of epididymal sperm obtained at necropsy from goats. Theriogenology. 2000;54 (6):899-905.
15. Borchers AT, Uibo R, Gershwin ME. (2010). The geoepidemiology of type 1 diabetes. Autoimmun Rev. 9(5):A355–A365.
16. Brownlee M. (2001). Biochemistry and molecular cell biology of diabetic complications. Nature.414:813–820.
17. Campbell RC, Dott HM, Glover TD. Nigrosin eosin as a stain for differentiating live and dead spermatozoa. J. Agricult. Sci., 1956; 48: 1–8.
18. Chaiban JT and Azar ST. (2004). Erectile dysfunction in diabetic patients. J. Med. Liban., 52, 217–219.
19. Chung J, Kim M-Y, Kim H-S, Yoo J-S and Lee Y-C. (2002). Effect of cataract surgery on the progression of diabetic retinopathy. J. Cataract Refract. Surg., 25: 626–630.
20. Chung, J.Y., Kim, Y.J., Kim, J.Y., Lee, S.G. Park, J.E., Kim, R.W., Yoon, Y.D., Yoo, K.S., Yoo, Y.H. and Kim, J.M. (2011). Benzo[a]pyrene Reduces Testosterone Production in Rat Leydig Cells via a Direct Disturbance of Testicular Steroidogenic Machinery. Environ Health Perspect., 119: 1569-1574.
21. Eberhardt C, Amann B, Feuchtinger A, Hauck SM, Deeg CA. Differential expression of inwardly rectifying K+ channels and aquaporins 4 and 5 in autoimmune uveitis indicates misbalance in Muller glial cell-dependent ion and water homeostasis. Glia. 2011;59:697–707.
22. Faid I, Al-Hussaini H, Kilarkaje N. (2015). Resveratrol alleviates diabetes-induced testicular dysfunction by inhibiting oxidative stress and c-Jun N-terminal kinase signaling in rats. Toxicol Appl Pharmacol. 289(3):482-94.
23. Forlenza GP, Rewers M. The epidemic of type 1 diabetes: what is it telling us? Curr Opin Endocrinol Diabetes Obes. 2011;18(4): 248–251.
24. Freitas, H.S., B.D. Schaan, P.M. Seraphim, M.T. Nunes and U.F. Machado, (2005). Acute and short-term insulin-induced molecular adaptations of GLUT2 gene expression in the renal cortex of diabetic rats. Mol. Cell. Endocrinol., 237: 49-57.
25. Fukuda M, Nakanishi Y, Fuse M, Yokoi N, Hamada Y, Fukagawa M, Negi A and Nakamura M. (2010). Altered expression of aquaporins 1 and 4 coincides with neurodegenerative events in retinas of spontaneously diabetic Torii rats. Exp. Eye. Res., 90: 17-25.
26. Gabbay KH. (1973). The sorbitol pathway and the complications of diabetes. New Engl J Med.288:831–836.
27. Gabbay KH. (1975). Hyperglycemia, polyol metabolism, and complications of diabetes mellitus. Ann Rev Med. 26:521–536.
28. Glenn DR, McClure N and Lewis SE. (2003). The hidden impact of diabetes on male sexual dysfunction and fertility. Hum. Fertil. Camb., 6:174–179.
29. Gnodos B, Rivikind Y and Jovaniivic L. (1998). Effect of increasing glucose concentration on sertoli cell viability in the non obese diabetic mouse (NOD mouse). Ann. Clin. Lab. Sci., 28: 236–241.
30. Hakeem P, Sani HA and Noor MM. (2008). Effects of Gynura procumbens extract and glibenclamide on sperm quality and specific activity of testicular lactate dehydrogenase in streptozotocin – induced diabetic rats. Malaysian J. Biochemistry and Molecular biology. 16: 10-14.
31. Hakonarson H, Grant S. (2011). Genome-wide association studies (GWAS): impact on elucidating the aetiology of diabetes. Diabetes Metab Res Rev. 27(7):685–696 2. 2.
32. Hollborn M, Stefanovic SD, Pannicke T, Ulbricht E, Reichenbach A, Wiedemann P, BringmannA, and Kohen L. (2011) Expression of Aquaporins in the Retina of Diabetic Rats. Current Eye Research, 36(9): 850–856.
33. Kappeler SR, Heuberger C, Farah Z and Puhan Z. (2004). Expression of the peptidoglycan recognition protein, PGRP, in the lactating mammary gland. J. Dairy Sci., 87:2660–2668.
34. Kersten S (2014). Integrated physiology and systems biology of PPARα. . Molecular Metabolism 3: 354 371.
35. Kersten S, Seydoux J, Peters JM, Gonzalez FJ, Desvergne B, Wahli W (1999). Peroxisome proliferator-activated receptor alpha mediates the adaptive response to fasting. J Clin Invest. 103 (11): 1489–98.

36. Kilarkaje, N., Al-Bader, M.M (2015). Diabetes-induced oxidative dna damage alters p53-p21CIP1/Waf1 signaling in the rat testis. Reprod. Sci. 22, 102–112.
37. Kilarkaje, N., Al-Hussaini, H., Al-Bader, M.M (2014). Diabetes-induced DNA damage and apoptosis are associated with poly (ADP ribose) polymerase 1 inhibition in the rat testis. Eur. J. Pharmacol. 737, 29–40
38. Kinoshita JH and Nishimura C. (1988). The involvement of aldose reductase in diabetic complications. Diabetes Metab. Rev., 4: 323–337.
39. Ko, E.Y., Sabanegh Jr., E.S., Agarwal, A (2014). Male infertility testing: reactive oxygen species and antioxidant capacity. Fertil. Steril. 102, 1518–1527.
40. Kubo E, Miyoshi N, Fukuda M and Akagi Y. (1999). Cataract formation through the polyol pathway is associated with free radical production. Exp. Eye Res. 68:457-464.
41. Lee AYW, Chung SK and Chung SSM. (1995). Demonstration that polyol accumulation is responsible for diabetic cataract by the use of transgenic mice expressing the aldose reductase gene in the lens. Proc. Natl. Acad. Sci. U S A. 92:2780-2784.
42. Li Y, Zhang W, Li P, Huang K. (2011). Effect of streptozocin-induced diabetes mellitus on expression of methionine sulfoxide reductases and accumulation of their substrates in mouse lenses. Experimental Eye Research, 92: 401-407.
43. Lorenzi M. (2007). The polyol pathway as a mechanism for diabetic retinopathy: attractive, elusive, and resilient. Exp Diabetes Res. 61038. doi: 10.1155/2007/61038. Review.
44. Luo, D.Y., Yang, G., Liu, J.J., Yang, Y.R., Dong, Q., (2011). Effects of varicocele on testosterone, apoptosis and expression of StAR mRNA in rat Leydig cells. Asian. J. Androl., 13: 287-291.
45. Makker, K., Agarwal, A and Sharma R. (2009). Oxidative stress and male infertility. Indian J. Med. Res., 129: 357-367.
46. Malik A, Al-Senaidy A, Skrzypczak-Jankun E, Jankun. (2012). A study of the anti-diabetic agents of camel milk. J. Int J Mol Med., (3):585-592.
47. Mathebula SD. (2015). Polyol pathway: A possible mechanism of diabetes complications in the eye. Afr. Vision Eye Health. 74(1), Art. #13, 5 pages. http://dx.doi.org/10.4102/ aveh.v74i1.13.
48. Mohamed RH, Zekry ZK, Al-Mehdar HA, et al., (2009). Camel milk as an adjuvant therapy for the treatment of type 1 diabetes: verification of a traditional ethnomedical practice. J. Med. Food, 12: 461-465.
49. Mohamed-Ali V, Pinkney JH and Coppack SW. (1998). Adipose tissue as an endocrine and paracrine organ. Int. J. Obesity, 22:1145–1158.
50. Mohasseb M , Ebied S, Yehia M and Hussein N. (2011). Testicular oxidative damage and role of combined antioxidant supplementation in experimental diabetic rats. J. Physiol. Biochem. 67:185–194.
51. Naka, M., Kanamori, A., Negi, A., Nakamura, M., (2010). Reduced expression of aquaporin-9 in rat optic nerve head and retina following elevated intraocular pressure. Invest. Ophthalmol. Vis. Sci. 51, 4618e4626
52. Oates PJ and Mylari BL. (1999). Aldose reductase inhibitors: Therapeutic implications for diabetic complications. Expert Opin Investig Drugs 8: 2095–2119.
53. Paasch U, Sharma RK, Gupta AK, Grunewald S, Mascha EJ, Thomas AJ Jr, Glander HJ and Agarwal A. (2004). Cryopreservation and thawing is associated with varying extent of activation of apoptotic machinery in subsets of ejaculated human spermatozoa. Biol. Reprod., 71: 1828-37.
54. Pontes D A, Fernandes GSA, Piffer RC, Gerardin D C, Pereira OM and Kempinas WG. (2011). Ejaculatory dysfunction in streptozotocin-induced diabetic rats: the role of testosterone. Pharamcological Reports, 63: 130-138.
55. Reddy PK, Singh BA, Puri A, Srivastava KA and Narender T. (2009). Synthesis of novel triterpenoid (lupeol) derivatives and their in vivo antihyperglycemic and antidyslipidemic activity. Bio. Med. Chem. Lett., 19: 4463-4466.
56. Rodriguez-Rigau LJ. (1980). Diabetes and male reproductive function. J. Androl., 1:105–110.
57. Soliman M M, Ahmed M M, El-Shazly S A. (2013). Cinnamon Regulates Gene Expression of Lipids and Carbohydrates in Streptozotocin Induced Diabetic Wistar Rats. American Journal of Biochemistry and Biotechnology, 9 (2): 172-182.
58. Soliman MM, Hassan MY, Mostafa SA, Ali HA, Saleh OM. (2015). Protective effects of camel milk against pathogenicity induced by Escherichia coli and Staphylococcus aureus in Wistar rats. Mol Med Rep. 2015 Dec;12(6):8306-12.

59. Soudamani S, Yuvaraj S, Malini T and Balasubramanian K. (2005). Experimental diabetes has adverse effects on the differentiation of ventral prostate during sexual maturation of rats. Anat. Rec. Discov. Mol. Cell. Evol. Biol., 287:1281– 1289.
60. Steger RW and Rabe MB. (1997). The effect of diabetes mellitus on endocrine and reproductive function. Proc. Soc. Exp. Biol. Med., 214: 1–11.
61. Tait, M.J., Saadoun, S., Bell, B.A., Papadopoulos, M.C. (2008). Water movements in the brain: role of aquaporins. Trends in Neurosci. 31, 37e43.
62. Tenckhoff S, Hollborn M, Kohen L, Wolf S, Wiedemann P, Bringmann A. (2005). Diversity of aquaporin mRNA expressed by rat and human retinas. Neuroreport 16:53–56.
63. Vats, V., S.P. Yadav and J.K. Grover, (2004). Ethanolic extract of Ocimum sanctum leaves partially attenuates streptozotocin-induced alterations in glycogen content and carbohydrate metabolism in rats. J. Ethnopharmacol., 90: 155-160.
64. Verkman, A.S., Ruiz-Ederra, J., Levin, M.H., 2008. Functions of aquaporins in the eye. Prog. Retin. Eye Res. 27, 420e433.
65. Wang, H., Wang, Q., Zhao, X.F., Liu, P., Meng, X.H., Yu, T., Ji, Y.L., Zhang, H., Zhang, C., Zhang, Y., Xu, D.X., (2010). Cypermethrin exposure during puberty disrupts testosterone synthesis via down regulating StAR in mouse testes. Arch. Toxicol., 84: 53-61.
66. Wolff SP, Jiang ZY and Hunt JV. (1991). Protein glycation and oxidative stress in diabetes mellitus and ageing. Free Radic. Biol. Med., 10:339–352.
67. Zhu WW, Kong GQ, Ma MM, Li Y, Huang X, Wang LP, Peng ZY, Zhang XH, Liu XY, Wang XZ. Short communication: Camel milk ameliorates inflammatory responses and oxidative stress and downregulates mitogen-activated protein kinase signaling pathways in lipopolysaccharide-induced acute respiratory distress syndrome in rats. J Dairy Sci. 2016 Jan;99(1):53-667.

RESEARCH REGARDING THE THICKNESS AND PROFILE OF MYOCYTES FROM SUPERFICIAL PECTORAL MUSCLE OF *ANAS PLATHYRYNCHOS* SPECIES

V. TEUSAN[1]; Anca TEUSAN[2]; M.R. RADU-RUSU[3]
[1]Animal Husbandry Faculty, University of Applied Life Sciences and Environment, Iasi
[2]Acad. I. Haulica"Research Institute Iasi; "Apollonia"University,
[3]Animal Husbandry Faculty, University of Applied Life Sciences and Environment, Iasi
e-mail:vasile.teusan@yahoo.com

Abstract

From a two years old female Anas plathyrynchos bird, with a live body weight of 1685 grams, we collected several samples histological from the Pectoralis superficialis muscle (PS). Samples were processed by the paraffin sectioning technique yielding a few histological slides with the muscle cross sections mentioned above with HEA coloration. The sections have been studied on an MC3 optical microscope (OM), which previously has been adjusted and calibrated. In microscopic field we made 1234 micrometer determinations, measuring both myocytes diameters (large and small) and their number of 17 primary muscle fascicles (PMF) within 5 secondary muscle fascicles (SMF).We determined the values of: myocytes average diameter and perimeter, and the size/shape index and their profile index.We have obtained the following results: the large diameter of myocytes of the 5 SMF ranged from 46.164μ to 53.862, with an average value of 49.759μ. The small diameter of myocytes from studied SMF was between 29.612μ and 34.84μ and the average value for this character was 31.808μ. The average diameter of myocytes from 5 SMF studied ranged between 38.359μ and 43.182μ, with an average value of 40.783μ. The myocytes average perimeter of the 5 SMF studied was 128.121μ, and for those two indicators that define the profile and format of myocytes (Fi = 1,614 / 1; Pi = 65.99 %), the mean of the 5 SMF indicate an cylindroid shape with the flattening tendency (oval shape). The differences between the average values of the five SMF studied for the 6 parameters analyzed were found to be very statistically significant at a rate of 46.67 % and statistically insignificant in proportion of 53.33 % .

Key words: *Anas plathyrynchos; Pectoralis superficialis; myocytes; thickness; profile*

Introduction

Increasing food needs for today's increasing demographic determine some financial, scientific and technological considerable efforts. Thus, new breeds and hybrids of birds are studied, in order to be grown and exploited extensively and intensively, knowing already that these animals grow relatively easy, with less costs and the products that they offer (meat, eggs, liver, fat) have a great demand in the market and they are requested by consumers.

After the granivores avian species (*Gallinaceae*), that hold the first place as numbers and as productions, come the ducks , which rank the second place on the podium , because they are easy to grow and maintain and their products (meat, eggs, liver, fat, feathers) have a high demand in the European market and worldwide [7].

Among the domestic ducks, it seems that the species *Anas plathyrynchos* (common duck) is best represented in poultry farming and animal husbandry in general and there are many different breeds and hybrids. In recent decades several farms and poultry complexes have been set up, that have as their object extensive and intensive growing rates. In this context it is natural that there is a pronounced interest for the scientific understanding of duck meat quality, quality appreciated by several parameters, including those related to the histological structure of the muscles of these birds carcasses.

Materials and methods

To organize and conduct such a scientific research, we aimed at knowing the histological structure of some somatic muscles, which requires different materials and several methods of scientific work. Thus, the materials we used can be classified into two major categories: biological and non-biologic materials. In the first category are histological samples, taken from the pectoral muscles, specifically from *Pectoralis superficialis* (PS) [2][4] from an *Anas plathyrynchos* female sex individual.

That bird had a body weight of 1685 grams, was 2 years old and weighed, at slaughter,1348 grams, which represents 80 % of the live weight [7]. The superficial pectoral muscles, right and left were weighing 117-118 grams each, so those two muscles together represented about 14-15 % of the live weight and about17-18% from the carcass weight [7]. The species studied by us has the following taxonomy :Kingdom *Animalia*, Phylum *Chordata*, Class *Aves*, Order *Anseriformes*, Family *Anatidae*, Genus *Anas* , Species *A. plathyrynchos*[17].

The histologicalsamples taken from the superficial pectoral muscles (left and right) were processed by sectioning in paraffin technique [3][6], using a device and specific anatomic and histologic instruments(forceps, scalpels, scissors, dissection needles, Slee Mainz -Cut-5062 semi-automated microtome, tissue processor, automated staining device, thermoregulation oven, laboratory glassware, reagents and histological dyes) [3][6]. Finally we obtained 10 histological blades with trichromic (HEA) histological cross-sections throughPS muscle [3][6] which were then studied using a MC3 type optical binocular microscope (fig. 6).

This microscope has been checked, tuned and calibrated prior to measurements and its calibration were done by the two associations of eyepieces (OC) and objectives (OB). The calibration of the microscope was done using the "Cotea" method, using for this purpose a calibration blade (micrometer lens) and an ocular micrometer. We calculated and used two micrometer values (MV), namely: one in association of OC10xOB6 = 15.0493µ per division; for other the association was OC10xOB10 = 9.0364µ per division. These micrometer values were used for the calculation of the muscle fibers diameters and of the muscle fibers diameters [11] [12].

In the microscopic field we highlighted, photographed and measured the cross-sectioned myocytes (using an ocular micrometer) and we calculated the three diameters (large, small and average) and their perimeter. By calculations we determined individual values for the two indices which define the profile of myocytes. In total we measured 617 myocytes that were part of 17 primary muscle fascicles (PMF) and 5 secondary muscle fascicles (SMF). To obtain the raw data we used the following mathematical relationship:

1) LD=MV x nr. Div.OC.,where: LD=large diameter of myocytes (µ); MV=micrometric value at OC10xOB10=9.0364µ/division; nr. Div.OC.= the number of divisions on the ocular micrometer, in the microscopic field.
2) Sd=MV x nr. Div.OC., where: Sd=small diameter of myocytes (µ); MV=micrometric value at OC10xOB10=9.0364µ/division; nr. Div.OC.=the number of divisions on the ocular micrometer, in the microscopic field.
3) Dx=(LD+Sd)/2, where: Dx=average diameter (µ); LD=large diameter (µ); Sd=small diameter (µ).
4) P=[(LD+Sd)/2]xπ, where: P=Perimeter of myocytes (µ); π=calculation coefficient for the lenght and surface of the circle=3,141592656.
5) If=LD/Sd, where: If= format index of myocytes (x/1).
6) Ip=(Sdx100)/LD, where: Ip=Profile index of myocytes (%)

All raw data obtained from micrometer measurements and calculations were tabulated and then interpreted statistically, first calculating generalstatistical indicators, such as: statistics mean, geometric mean, standard deviation , average deviation, standard error of mean, statistical variation and the coefficient of variation [10]. Subsequently, to test the statistical significance of differences between the 5 fascicles of muscle studied, we used the variance analysis, calculating the Fischer and Tukey test values, for all six indicators characterizing the fibers (myocytes) of the superficial pectoral muscle. For statistical calculations (general and specific) we used Instat Plus program. The data were statistically processed and graphically presented in tables and several microscopic images that are presented in this paper (fig. 6).

Results and discussions

The superficial pectoral muscle of *Anas plathyrynchos*has a structural organization similar to that found in other species of birds of the genus *Gallus* [8] [9] or the genus *Anser* [7] [17]. The similarity is that myocytes , which are almost cylindrical, are also grouped in primary fasciclesmuscle (PMF) and these form secondary muscle fascicles (SMF). Thus, we studied five SMF and their myocytes have different thicknesses , as they are presented in table 1 and in figure 1.

Regarding the situation in the SMF1, the large diameter of myocytes has an statistic average value of 47.107 ± 0.705μ, with limits of 27.3109μ and 67.773μ and with a coefficient of variation v = 17.07 % (table 1) (fig. 1). For small diameter of myocytes, the 130 values were found within limits such as 18.073μ and 45.182μ and their statistical average value was of 29.612 ± 0.445μ (v = 17.13 %) (table 1) (fig. 1).

For the average diameter, the 130 variables studied hadvalues between 26.205μ and 47.441μ, their statistical mean being of 38.359 ± 0.405μ (v = 12.04 %) (table 1) (fig. 1). The average perimeter of the SMF1 myocytes was 120.502 ± 1.271μ (v = 12.03 %), with the limits of variation between 82.325μ and 149.04μ (table 1) (fig. 1). In appearance, muscle myocytes in this secondary fascicle (SMF1) are almost cylindrical (with a slight roundness), as demonstrated by the values found for theformat index (1.00/1-3125/1), but mostly fromitsaverage value (Fi = 1.642 ± 0.037/1) (v = 25.78 %). The aspect mentioned above (cylindroid) is also confirmed by the average value of the profile index (Pi = 64.983 ± 1.443 %) (v = 25.33 %) (table 1) (fig. 4; 5).

Regarding the second muscle fascicle (SMF2) of the superficial pectoral muscle we measured 108 muscle fibers and their large diameter had average value of 51.524 ± 1.061μ, with a variability that is more accentuated than in the case of the first SMF1 (v = 21.41 %) (table 1). Compared with the first SMF, this statistical average value is 9.376 % higher. For the small diameter of myocytes in SMF2 were found values between 18.073μ and 54.218μ , their statistical average value being 34.84 ± 0.659μ (v = 19.64 %) (table 1) (fig . 1).

Table 1.

Statistical indicators regarding the thickness and profile of myocytes from the five secondary muscle fascicles (SMF) of the superficial pectoral muscle of *Anas plathyrynchos*

Specification		MU	n	Statistical indicators:					Variation limits	
SMF	Studied parameters of myocytes			$\bar{x}\pm s\bar{x}$	Geometric mean	Mean deviation	Standard deviation	V (%)	Min.	Max.
SMF1	Large diameter	μ	130	47.107±0.705	46.408	6.729	8.043	17.07	27.109	67.773
	Small diameter	μ	130	29.612±0.445	29.186	4.230	5.0715	17.13	18.073	45.182
	Average (mean) diameter	μ	130	38.359±0.405	38.081	3.923	4.617	12.04	26.205	47.441

	Muscle fibers perimeter	µ	130	120.502±1.271	119.628	12.335	14.494	12.03	82.325	149.04
	Format index	x/1	130	1.642±0.037	1.590	0.339	0.423	25.78	1.000	3.125
	Profile index	%	130	64.983±1.443	62.947	13.801	16.458	25.33	31.999	100.00
SMF2	Large diameter	µ	108	51.524±1.061	50.380	8.8834	11.031	21.408	31.627	81.328
	Small diameter	µ	108	34.84±0.659	34.1624	5.458	6.8434	19.64	18.073	54.218
	Average (mean) diameter	µ	108	43.182±0.722	42.522	6.0215	7.499	17.366	28.916	65.514
	Muscle fibers perimeter	µ	108	135.661±2.267	133.587	18.917	23.559	17.366	90.842	205.818
	Format index	x/1	108	1.514±0.036	1.475	0.2777	0.3766	24.869	1.000	3.000
	Profile index	%	108	69.437±1.394	67.815	11.5184	14.485	20.86	33.333	100.00
SMF3	Large diameter	µ	150	50.14±0.829	49.108	8.258	10.158	20.26	27.109	81.328
	Small diameter	µ	150	31.706±0.512	31.075	5.426	6.268	19.77	13.555	45.182
	Average (mean) diameter	µ	150	40.923±0.551	40.338	5.405	6.37433	16.478	20.332	54.219
	Muscle fibers perimeter	µ	150	128.563±1.73	126.727	16.9815	21.1845	16.478	63.875	170.334
	Format index	x/1	150	1.623±0.031	1.5803	0.304	0.385	23.724	1.000	3.000
	Profile index	%	150	64.921±1.192	63.2792	11.9272	14.593	22.478	33.334	100.00
SMF4	Large diameter	µ	115	46.164±0.785	45.430	6.664	8.413	18.22	31.627	72.291
	Small diameter	µ	115	31.816±0.501	31.3625	4.347	5.373	16.889	17.169	45.182
	Average (mean) diameter	µ	115	38.99±0.47	38.667	4.104	5.040	12.928	28.013	52.411
	Muscle fibers perimeter	µ	115	122.489±1.477	121.473	12.895	15.835	12.928	88.005	164.654
	Format index	x/1	115	1.493±0.036	1.4485	0.3084	0.3863	25.867	1.000	2.667
	Profile index	%	115	71.006±1.526	69.031	13.7034	16.369	23.053	37.500	100.00
SMF5	Large diameter	µ	114	53.862±0.914	52.974	7.646	9.758	18.12	27.109	81.328
	Small diameter	µ	114	31.065±0.585	30.490	5.118	6.246	20.11	20.784	54.218
	Average diameter	µ	114	42.463±0.55	42.069	4.710	5.873	13.831	27.109	58.737
	Muscle fibers perimeter	µ	114	133.392±1.727	132.155	14.787	18.445	13.827	85.165	184.528
	Format index	x/1	114	1.799±0.045	1.738	0.396	0.483	26.844	1.000	3.478
	Profile index	%	114	59.592±1.48	57.562	12.945	15.803	26.52	28.75	100.00

In this case we notice a difference from SMF1 which is of 17.655 %. For the average diameter of myocytes from SMF2, the statistical mean of the 108 values is 43.182 ± 0.722µ (v = 17.366 %) and their limits are 28.916µ, respectively 65.514µ (table 1) (fig. 1). Regarding the SMF2 myocyte perimeter, it has a statistical average value of 135.661 ± 2.267µ (v = 17.37 %) (table 1) (fig. 1). The appearance of SMF2 myocytes compared to that of SMF1 is a little closer to the cylindrical format because the format index has an average value of 1.514 ± 0.036/1, but the limits of the 108 values studied are very large (1/1 -3/1) (v = 20.86 %) (table 1) (fig . 5). The index profile for these myocytes evolved in the same way and the limits are: 33.333 % and 100%, and the average statistic value is 69.437 ± 1.394 % (v = 20.86 %) (table 1) (fig. 4).

Regarding SMF3 here myocytes components (150) have a large diameter of 50.14 ± 0.829µ, a small diameter of 31.706 ± 0.512µ and an average diameter of 40 923 ± 0.551µ (v = 16.478 % -19.77 % -20.26 %) (table 1) (fig. 1). The average perimeter of these myocytes has a value of 128.563 ± 1.73µ (v = 16.478 %), and their appearance is also cylindroid (1.623 ± 0.031/1) (Pi = 64.921 ± 1.192 %) (table 1) (fig. 1).

The 115 SMF4 muscle fibers had a thickness reduced by 7.93 % -4.72 %, compared to the SMF3 , but comparable to the SMF1 (table 1) (fig . 1). So the statistical average values for the 3 diameters of SMF4 myocytes were: 46.164 ± 0.785μ ; 31,816 ± 0.501μ and 38.99 ± 0.47μ (v = 12.93-16.89-18.22 %) (table 1) (fig . 1). Myocyte perimeter of SMF4 had an average value of 122.489 ± 1.477μ and their appearance was closer to the cylindrical shape (Fi= 1.493 ± 0.036/1) (Pi = 71.006 ± 1.526 %) (v = 23.053 %) (table 1) (fig. 5).

It seems that SMF5 has the thickest myocytes and the means of the 114 measured values were as following: 53.862 ± 0.914μ for the large diameter; of 31.065 ± 0.585μ for the smaller diameter and 42.463 ± 0.55μ for the average diameter (v = 13.83-18.12-20.11 %) (table 1) (fig. 1). If we compare the average diameter of myocytes in the first four to the one of SMF5, we find that it is higher by 10.69 % compared to SMF1; 3.76 % compared with SFM3; 8.90 % compared with SMF4and is comparable (with 1.67 % lower) with SMF2 (fig. 1).

Myocyte perimeter of SMF5 has an average statistic value of 133.392 ± 1.727μ (v = 13.83 %), and their appearance is cylindroid (a more pronounced oval), which is evidenced by the mean value of Fi = 1.799 ± 0.045/1 (v = 26.84 %) and that of Pi = 59.592 ± 1.48 % (v = 26.52 %) (table 1) (fig . 1, 3, 4, 5).The mean values of the 6 parameters studied, for the 5 secondary muscle fascicles were statistically processed and the resulting data was presented in tables 2 and 3 and in figures 2, 3 and 4. Thus we see that: the average value of the five secondary muscle fascicles for the large diameter of the 617 myocytes is 49 759 ± 1.415μ; for the small diameter is 31 808 ± 0.854μ; for the average diameter is 40.783 ± 0.94μ (v = 5.16-6.0-6.36 %) (tables 2 and 3) (fig . 2). Regarding the myocytes perimeter, the average statistic value of the five SMF is 128.121 ± 2.955μ (v = 5.16 %) and average values for the format and profile indices are: 1.614 ± 0.55/1 and 65.988 ± 2.002 % (v = 6.78-7.57 %) (tables 2 and 3) (fig. 3,4,5). The average number of muscle fibers existing in the 5 studied SMF is 123.4 ± 7.57 (v = 13.72 %) (table 2).

Table 2.

Statistical indicators regarding some parameters which characterizes the thickness and profile of myocytes from 5 secondary muscle fascicles (SMF) of the superficial pectoral muscle of *Anas plathyrynchos*

Specification		MU	n	Statistical indicators:					Variation limits	
No.	Studied parameters of myocytes			$\bar{x}\pm s\bar{x}$	Geometric mean	Mean deviation	Standard deviation	V (%)	Min.	Max.
1.	Large diameter	μ	5	49.759±1.415	49.679	3.124	3.164	6.36	46.164	53.862
2.	Small diameter	μ	5	31.808±0.854	31.763	1.520	1.909	6.00	29.612	34.840
3.	Average diameter	μ	5	40.783±0.94	40.740	2.109	2.103	5.16	38.359	43.182
4.	Muscle fibers perimeter	μ	5	128.121±2.955	127.985	6.626	6.607	5.16	120.502	135.661
5.	Format index	x/1	5	1.614±0.055	1.611	0.111	0.122	7.57	1.493/1	1.799/1
6.	Profile index	%	5	65.988±2.002	65.865	4.234	4.476	6.783	59.592	71.006
7.	Number of myocytes from SFM	n	5	123.4±7.574	122.521	16.600	16.935	13.724	108	150

Table 3.

Statistical average (mean) values for the thickness and profile of myocytes from the secondary muscle fascicles (SMF) of the superficial pectoral muscle of *Anas plathyrynchos*

Specification:		Secundary muscle fascicles studied for superficial pectoral muscle (average statistical values)					Average value of the five SMF*studied
Parameters studied at myocytes level	MU	SMF_1	SMF_2	SMF_3	SMF_4	SMF_5	
Large diameter	μ	47.107	51.524	50.140	46.164	53.862	**49.7594**
Small diameter	μ	29.612	34.840	31.706	31.816	31.065	**31.8078**
Average diameter	μ	38.359	43.182	40.923	38.990	42.463	**40.7834**
Perimeter of myocytes	μ	120.502	135.661	128.563	122.489	133.392	**128.1214**
Format index	x/1	1.642/1	1.514/1	1.623/1	1.493/1	1.799/1	**1.6142/1**
Profile index	%	64.983	69.437	64.921	71.006	59.592	**65.9878**

*SMF= secondary muscular fascicle.

Table 4.

Statistical significance of the differences between the five secondary muscle fascicles (SMF) of the superficial pectoral muscle of *Anas plathyrynchos*

Studied parameters of myocytes from superficial pectoral muscle	Differences between mean values of the five FMS	Tukey values (w=0.01)	Statistical significance	At 4; 612 LP, for:			
				P	p≤0.05	p≤0.01	p≤0.001
				Fα	**2.370**	**3.320**	**4.620**
Large diameter (LD) (μ)	SMF1-SMF2=4.417	3.3139	***	$\hat{F}$	**12.870678**		
	SMF1-SMF3=3.033	3.4522	n.s.				
	SMF1-SMF4=0.943	3.9387	n.s.				
	SMF1-SMF5=6.755	4.1273	***				
	SMF2-SMF3=1.384	3.2121	n.s.				
	SMF2-SMF4=5.360	3.8603	***				
	SMF2-SMF5=2.338	4.1314	n.s.				
	SMF3-SMF4=3.976	3.1548	***				
	SMF3-SMF5=3.722	3.5796	***				
	SMF4-SMF5=7.698	3.3637	***				
Small diameter (SD) (μ)	SMF1-SMF2=5.228	2.0726	***	$\hat{F}$	**11.7438022**		
	SMF1-SMF3=2.094	2.1590	n.s.				
	SMF1-SMF4=2.204	2.4633	n.s.				
	SMF1-SMF5=1.453	2.5812	n.s.				
	SMF2-SMF3=3.134	2.0089	***				
	SMF2-SMF4=3.024	2.4143	***				
	SMF2-SMF5=3.775	2.5838	***				
	SMF3-SMF4=0.110	1.9730	n.s.				
	SMF3-SMF5=0.641	2.2390	n.s.				
	SMF4-SMF5=0.751	2.1039	n.s.				
Average diameter ($D\bar{x}$) (μ)	SMF1-SMF2=4.823	2.1096	***	$\hat{F}$	**14.2176634**		
	SMF1-SMF3=2.564	2.1976	***				
	SMF1-SMF4=0.631	2.5073	n.s.				
	SMF1-SMF5=4.104	2.6274	***				
	SMF2-SMF3=2.259	2.0448	***				
	SMF2-SMF4=4.192	2.4575	***				

	SMF2-SMF5=0.719	2.6300	n.s.		
	SMF3-SMF4=1.933	2.0082	n.s.		
	SMF3-SMF5=1.540	2.2787	n.s.		
	SMF4-SMF5=3.473	2.1415	***		
Perimeter (P) (μ)	SMF1-SMF2=15.159	6.6267	***	$\hat{F}$	**14.2252184**
	SMF1-SMF3=8.061	6.9032	***		
	SMF1-SMF4=1.987	7.8761	n.s.		
	SMF1-SMF5=12.890	8.2532	***		
	SMF2-SMF3=7.098	6.4231	***		
	SMF2-SMF4=13.172	7.7193	***		
	SMF2-SMF5=2.269	8.2614	n.s.		
	SMF3-SMF4=6.074	6.3084	n.s.		
	SMF3-SMF5=4.829	7.1580	n.s.		
	SMF4-SMF5=10.903	6.7269	***		
Format index (Fi) (x/1)	SMF1-SMF2=0.128	0.1419	n.s.	$\hat{F}$	**9.98806**
	SMF1-SMF3=0.019	0.1479	n.s.		
	SMF1-SMF4=0.149	0.1687	n.s.		
	SMF1-SMF5=0.157	0.1768	n.s.		
	SMF2-SMF3=0.109	0.1376	n.s.		
	SMF2-SMF4=0.021	0.1653	n.s.		
	SMF2-SMF5=0.285	0.1769	***		
	SMF3-SMF4=0.130	0.1351	n.s.		
	SMF3-SMF5=0.176	0.1533	***		
	SMF4-SMF5=0.306	0.1441	***		
Profile index (Pi) (%)	SMF1-SMF2=4.454	5.3504	n.s.	$\hat{F}$	**9.454605**
	SMF1-SMF3=0.062	5.5737	n.s.		
	SMF1-SMF4=6.023	6.3591	n.s.		
	SMF1-SMF5=5.391	6.6636	n.s.		
	SMF2-SMF3=4.516	5.1860	n.s.		
	SMF2-SMF4=1.569	6.2326	n.s.		
	SMF2-SMF5=9.845	6.6703	***		
	SMF3-SMF4=6.085	5.0934	***		
	SMF3-SMF5=5.329	5.7794	n.s.		
	SMF4-SMF5=11.414	5.4313	***		

From the data we presented so far it can be noticed that there are notable differences between the 5 secondary muscle fascicles (of the superficial pectoral muscle) in all myocytes parameters that we studied, but they differ in statistical terms. Thus, in terms of the large diameter of muscle fibers, of the 10 possible comparisons, 6 (60 %) were found to be highly statistically significant and 4 (40 %) are not statistically significant (table 4). For the small diameter of myocytes the situation is reversed, meaning that only 4 (40 %) of these differences are very statistically significant and the rest of 6 (60 %) are not significant (table 4). For the average diameter and for the perimeter of myocytes, the situation is similar to that of the large diameter (table 4). Regarding the profile index and the format index, the differences between the 5 SMF are very significant in proportion of 30 % and statistically significant 70% (table 4).

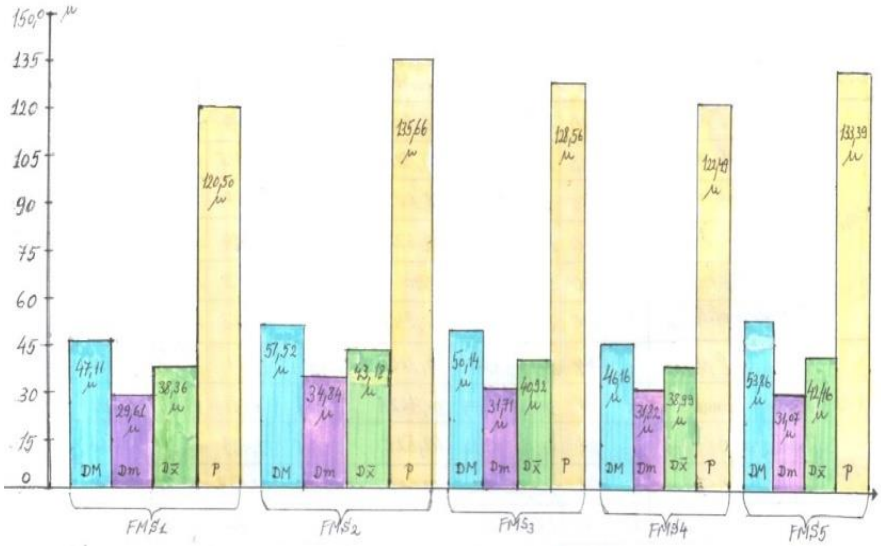

Fig. 1. Evolution of the thickness and the perimeter of myocytes from superficial pectoral muscle of *Anas plathyrynchos*

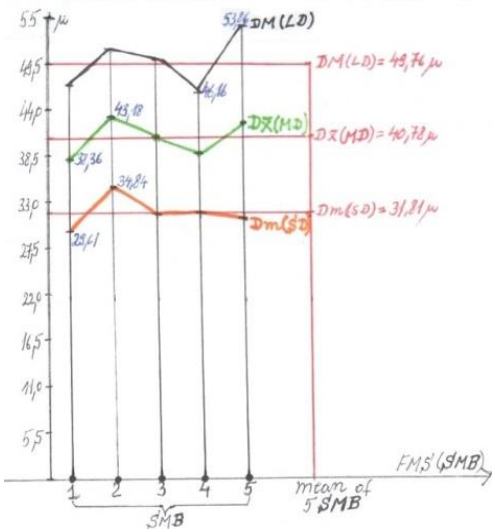

Fig. 2. Evolution of the myocytes thickness from the five SMF studied

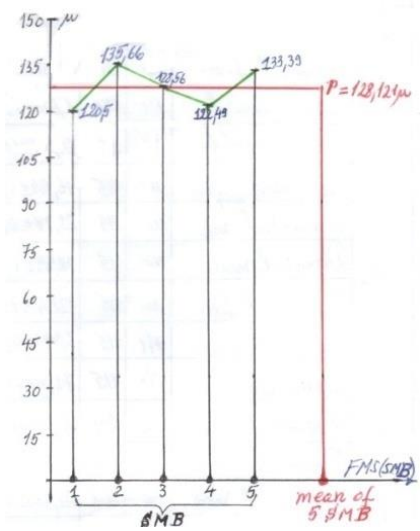

Fig.3. The perimeter of muscle fibers from the 5 SMF studied

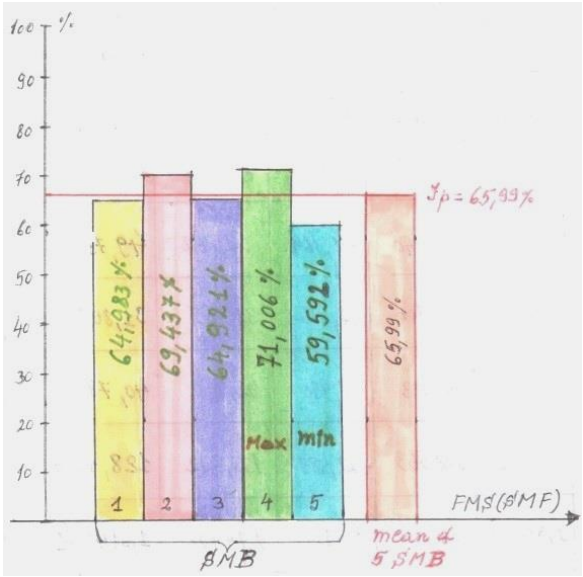

Fig. 4. Evolution of the profile index values for the SMF myocytes studied

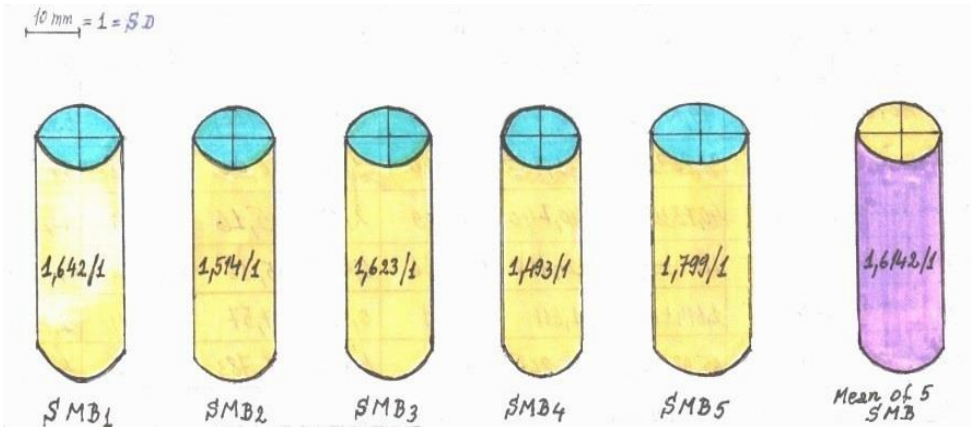

Fig. 5. Myocytes profile expressed through the format index (Fi) of the secondary muscle fascicles (bundles) (SMF/SMB) from the studied muscle of *Anas plathyrynchos*

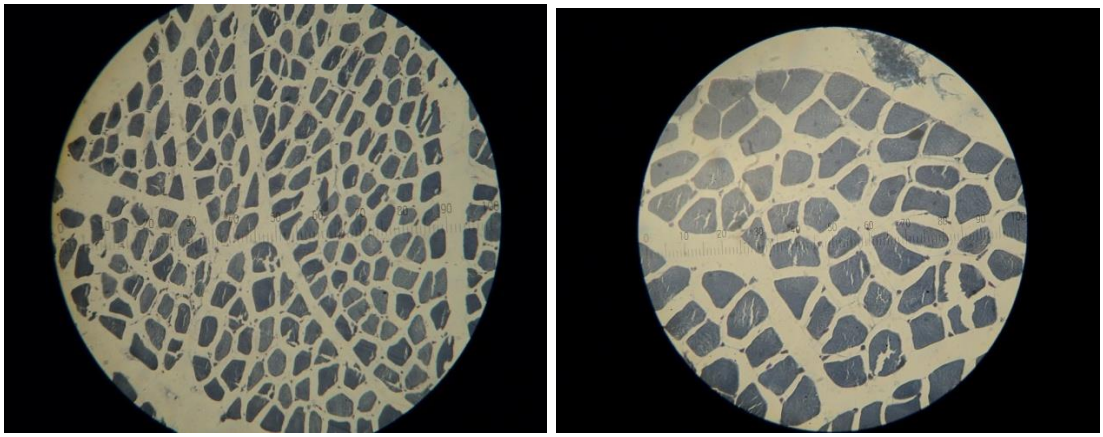

Fig.6. Cross section surface of the muscle fibers (microscopic view)

Conclusions

1. The large diameter of myocytes of the five secondary muscle fascicles (SMF) studied (617) from the superficial pectoral muscle, of *Anas plathyrynchos* is of 49.759 µ.
2. The small diameter of 617 myocytes studied of the five secondary muscle fascicles from the superficial pectoral muscle, of *Anas plathyrynchos* is of 31.808 µ.
3. The average (mean) diameter of 617 myocytes of the five secondary muscle fascicles from the superficial pectoral muscle, of *Anas plathyrynchos* is of 40.783 µ.
4. The myocytes perimeter of the five secondary muscle fascicles studied has a value of 128.121µ
5. The 617 myocytes from the secondary muscle fascicles from the superficial pectoral muscle of the studied species have a cylindroid shape (Fi=1.614/1; Pi=65.99%).
6. The number of myocytes from the five SMF studied varied between 108 and 150 and their average value is of 123.4 m.f./SMF
7. The differences found between the five secondary muscle fibers, for the six studied parameters are very statistically significant, in proportion of 46.67 % and insignificant in proportion of 53.33 %

References

1. Cotea C.V., 2014 – *Biologie celulara, Histologie și Embriologie generală și specială*, EdituraTehnopress, Iaşi.
2. Cotofan V. and colab., 2000 – 2007 – *Anatomia animalelor domestice*, vol. I si II, Editura Orizonturiuniversitare, Timisoara.
3. Diaconita Gh. and colab., 1953 – *Tehnica histopatologica*, Editura de Stat pentru Literatura Stiintifica, Bucuresti.
4. Ghetie V., Chitescu St., Cotofan V., Hillebrand A., 1976 – *Atlas de anatomie a pasarilor domestice*, EdituraAcademiei RSR.
5. Nickel R., Schummer A., Seiferle E., 1977 – *Anathomy of domestic birds*, EdituraVerlag Paul Parey, Berlin, Hamburg, Germany.
6. Niculae Al., 1995 – *Investigatia histologica in diagnosticul veterinar*, Editiaa I-a, Editura „L.C.S.V.”, Bucuresti.

7. Radu-Rusu R.M., Teusan V., 2005 – *Cercetari privind morfologia sistemului muscular somatic la palmipedeledomestice*, U.S.A.M.V. Iasi – Facultatea de Zootehnie, lucrare de licenta.
8. Radu-Rusu R.M., Teusan V., AncaTeusan, 2007 – *Comparative researches concerning some histometric features of the myocytes in somatic musculature of the domestic chicken and waterfowl (I). Pectoral muscles*, Lucr. Stiintif. U.S.A.M.V. Iasi, SeriaZootehnie, vol. 50, pg. 115-120.
9. Radu-Rusu R.M., 2009 – *Contributii la cunoasterea morfologiei, structuriisi a insusirilorfizico-chimice ale unor muschi somatici, proveniti de la puii broiler de gaina*, U.S.A.M.V. Iasi, Facultatea de Zootehnie, teza de doctorat, pg. 117-123.
10. Sandu Gh., 1995 – *Metode experimentale în Zootehnie*, Editura Coral Sanivet, Bucureşti, pg. 86-91,134-138, 225-228, 300-302, 317-319, 327-328.
11. Teusan V., 2000 – *Cercetari privind raportul dintre finetea si densitatea fibrelor musculare in diferiti muschi somatici la specia Gallus domesticus*, Lucr. Stiint. SeriaZootehnie, Nr. 43-44, U.S.A.M.V. Iasi, pg. 1001-1008.
12. Teusan V., Radu-Rusu R.M., AncaTeusan, 2009 – *Investigations on the histological structure of the superficial pectoral muscle in Cobb-500 commercial meat-type hybrid hen*, Agricultural Research Stations from Moldavia, ISSN 0379-5837, vol. XLII, No 4 (140), pg. 75-83.
13. Teusan V., AncaPrelipcean (Teusan), Prelipcean A., 2012 – *Researches on the thickness and profile of superficial pectoral muscle myocytes of meat-type hybrid hen Cobb-500, slaughtered at different ages*, Lucr. Stiin. USAMV Iasi, ISSN 1454-7366, pg. 651-658.
14. Teusan V., AncaPrelipcean (Teusan), Prelipcean A., 2012 – *Cercetari privind structura muschiului Pectoral superficial, la hibridul comercial de gaina, pentru carne Cobb-500, in functie de sex si de varsta de sacrificare*, Revista de Zootehnie, anul IX, Nr. 3-4- (Iulie-Decembrie), ISSN 1842-1334, pg. 46-57.
15. Teusan V., AncaPrelipcean (Teusan), 2013 – *Investigations on the histological structure of the superficial pectoral muscle in Cobb-500 commercial meat-type hybrid hen slaughtered at different ages*, Lucr. Stiint. USAMV Iasi, SeriaMedicina-Veterinara, vol. 56, ISSN 1454-7366.
16. Tudor Despina, Constantinescu Gh.M., Constantinescu Ileana, Cornilă N., 2010 – *Nomina Histologica et Embriologica Veterinaria*, Ediţie bilingvă, EdituraVergiliu, Bucureşti.
17. ***Hamlyn Guide - Determinator de pasari ilustrat – *Pasarile din Romania si Europa* – SocietateaOrnitologicaRomana, 1999, pg. 52 – 54.

CHEMICAL COMPOSITION AND ANTIOXIDANT ACTIVITY OF SOME FERMENTED VEGETABLE JUICES COMPARED TO FRESH VEGETABLE JUICES

Corina PREDESCU[1], Camelia PAPUC[1], Valentin NICORESCU[1], Izabela NICORESCU[2], Georgeta ȘTEFAN[1]

University of Agronomic Sciences and Veterinary Medicine of Bucharest,
[2]Institute of Hygiene and Veterinary Public Health, Bucharest, Romania
durduncorina@yahoo.com

Abstract

The aims of this study were to evaluate (1) the conversion rate of nitrate to nitrite in red pepper and tomato juices, and (2) the total polyphenols content (TPC), total carotenoid content (TCC) and antioxidant activity (AA) of fresh compared to fermented juices obtained from red pepper (Capsicum annuum L.) and tomato (Solanum lycopersicum L.). Red pepper and tomato juices were obtained from frozen fruits and fermentation was made in the presence of Staphylococcus xylosus ATCC strain 29971 (10^8 CFU/mL). The nitrate and nitrite concentration (ppm) was determined from 6 to 6 hours for 30 hours. For nitrate and nitrite determination, colorimetric methods were used. After 30 hours of incubation at 37°C, it was found a conversion rate of nitrate to nitrite of 85.10 % for red pepper, and 81.87 % for tomato. Fermented juices of red pepper and tomato showed similar conversion yield of nitrate to nitrite. The TPC, TCC and AA were determined for fresh and fermented juices using colorimetric methods. TPC, expressed as mg gallic acid equivalents/100 mL (mg GAE/100 mL) and TCC, expressed as mg β carotene equivalents/100 g wet weight (mg β-CarE/100g WW), varied considerably between unfermented and fermented sterilized juices, with highest concentrations in the unfermented pepper and tomato juices (42.34 ± 2.82 and 57.92 ± 3.86, respectively) for polyphenols, and (31.85 ± 2.12 and 61.76 ± 4.12, respectively) for carotenoids. AA was expressed as % Inhibition of DPPH•. After fermentation, the antioxidant activity decreased for both juices, the decrease rate was 39.50% for red pepper and 32.18% tomato juice.

Keywords: *fermented juice, nitrate, nitrite, polyphenols, carotenoids*

Introduction

Over the past two decades, consumers, researchers and food manufacturers became more and more interested in phytonutrients (George et al., 2004). Human consumption of phytochemicals such as polyphenols and carotenoids within fruit vegetables has been associated with the decrease of various inflammation and oxidative stress related chronic diseases, which may be due to direct antioxidant effects. The health effects of polyphenols and carotenoids depend on the amount consumed and on their bioavailability (Toor and Savage, 2005). The interest has increased considerably in finding naturally occurring antioxidants which can be used in food industry to replace synthetic antioxidants, which are being restricted due to their side effects (Stewart et al., 2000). The main reasons for the recognition of the antioxidant properties of polyphenols are their great abundance in our diet and their important role in the prevention of various diseases associated with oxidative stress, such as cancer and cardiovascular and neurodegenerative diseases (Arabbi et al., 2004; Slimestad and Verheul, 2005). Polyphenols, which constitute the most active substances found in dietary vegetable, have antioxidant properties and modulate the activity of a wide range of enzymes and cell receptors (Le Gall et al., 2003). In addition, polyphenols have multiple other specific biological actions that are yet poorly understood (Materska and Perucka, 2005)

Carotenoids are a group of phytochemicals responsible for different colours (yellow, orange and red). They are playing an important role in the prevention of human diseases and maintaining good health (Marin et al., 2004). Carotenoids are recognized as potent antioxidants and also contribute to dietary vitamin A. There are scientific reports of the beneficial properties

of those phytochemicals in the prevention of several chronic diseases. The chemical structure of carotenoids has been studied extensively, their bioavailability, metabolism and biological functions are not completed clarified (Rao and Rao, 2007).

The nitrate ion, NO_3^-, is absorbed and plays essential rolls for the development of plants. High nitrate concentrations are found in vegetables which can be used as sources of natural nitrites for meat conservation (Predescu et al., 2015).

Red peppers and tomatoes have important quantities of ascorbic acid and their attractive red colour is due to several carotenoid pigments which are exclusive to these fruits and have proven to be effective at scavenging free radicals (Igbokwe et al., 2013). Red peppers and tomatoes also contain large quantities of phenolic compounds. The consumption of these sources of bioactive compounds provide beneficial effects to human health due to their antioxidant properties, which protect cells against oxidative damage and thus prevent the development of common degenerative diseases (Blanco-Ríos et al., 2013; Nour et al., 2013).

The aim of this study was to obtain nitrite-rich juices by fermentation of vegetal materials containing nitrate, and to assay their chemical composition and antioxidant activity. Fermented juice containing nitrites can be used in food industry to obtain meat products.

Red peppers and tomatoes fermented juices were obtained using *Staphylococcus xylosus* ATCC 29971, a bacterial strain capable to produce nitrate reductase to reduce nitrate to nitrite.

Materials and methods

Chemicals. All chemicals and reagents used in the study were of analytical grade and purchased from Sigma chemicals (Romania). *Staphylococcus xylosus* ATCC 29971 strain used for vegetable juice fermentations was purchased from BioMerieux**.**

Vegetable juice obtaining. Selected vegetables were red peppers and tomatoes. Fresh ripe samples of tomatoes and red peppers were bought from a local market and frozen until analyses. Unfrozen plant material was cut into pieces and chopped in a laboratory blender. The fresh juices were sterilized for 15 min at 121ºC. After sterilization, the juices were filtrated and kept in refrigeration condition, at 4 ºC, until analyzes were done.

Bacterial strains. *Staphylococcus xylosus* ATCC 29971 strain used for vegetable juice fermentations was incubated in nutritive broth for 24 hours and then was used as nitrate reductase source.

Vegetable juice fermentation. Each composition containing sterilised tomato or red pepper juice, to which 0.3 % yeast extract was added, was inoculated with *S. xylosus* in concentration of 10^8 CFU/mL. The strain of *S. xylosus* used for vegetable juice fermentations is coagulase-negative and non-toxigenic. The nitrate and nitrite concentration (ppm) was determined from 6 to 6 hours for 30 hours, for each composition.

Determination of nitrate concentration in vegetable juices. For nitrate determination, it was used a colorimetric method described by Cataldo et al. (1975). The complex formed by nitration of salicylic acid under highly acidic conditions absorbs maximally at 410 nm in alkaline (pH>12) solutions. An aliquot of 0.200 mL of juices or standard nitrate was pipetted into a 50 mL Erlenmayer flask. There were added 0.8 mL of 5% (w/v) salicylic acid in concentrated H_2SO_4 and the reaction mixture was gently homogenized. After 20 minutes at room temperature, 19 mL of 2 N NaOH were added to raise the pH above 12, and the tubes were left to cool at room temperature. In parallel it was prepared a blank of 0.200 mL extraction solvent (H_2O) with the same reagents. The absorbance was measured at 410 nm. Absorbance

values of the samples were compared with absorbance values for standard solutions, and the result was expressed as ppm nitrate.

Determination of nitrite concentration in vegetable juices. Nitrite ions react with Griess reagent and the purple colour that developed after 20 min was read spectrophotometrically at 538 nm. 10 mL of juices were pipetted into a 50 mL volumetric flask and water was added up to 30 mL. 5 mL of sulphanilamide solution followed by 3 mL of concentrated HCl were then added and the solution was left in the dark for 5 min. After adding of 1 mL of NED solution, the mixture was left for 15 min. in the dark and then it was diluted to mark with water. The absorbance of the solution was measured using a spectrophotometer at a wave length of about 538 nm (Giustarini et al. 2008). Absorbance values of the samples were compared with absorbance values for standard solutions, and the result was expressed as ppm nitrite.

Determination of total phenolic content (TPC). Tomato and red pepper juices (1 g) were extracted with 10 ml of ethanol solution. The solution was vortexed for 5 min, followed by centrifugation at 3000 rpm for 10 min. The extraction was repeated three times. The supernatant was collected for the analysis. TPC was measured using the Folin–Ciocalteu colorimetric method (Singleton and Rosi, 1965). 0.5 mL of extract (prepared for TPC) were mixed with 7.0 mL of distilled water and 0.5 mL of Folin–Ciocalteu reagent and then incubated at room temperature for 30 min. Following the addition of 2 mL of 20% sodium carbonate to the mixture, total polyphenols were determined after 1 h of incubation at room temperature. The absorbance of the resulting blue colour was measured at 765 nm. The results were expressed as milligrams of gallic acid equivalents/100 mL juice (mg GAE/100 mL).

Determination of total carotenoids content (TCC). The total carotenoid analysis was performed according to Zhang and Hamauzu method (2004). The extraction of carotenoids from 1.0 g juice was performed with a mixture of acetone and petroleum ether (1:1, v/v) using a Glas-Col Potter homogenizer until no more colour was extracted. The upper phase was collected and combined with crude extract after being washed several times with water. The extract was made up to a known volume with petroleum ether. TCC was determined by recording the absorbance at 450 nm with a spectrophotometer UV-VIS, Jasco 670. The TCC was expressed as milligrams of β-carotene equivalents /100 g wet weight (mg β-Car E/100 g WW).

Determination of total antioxidant activity (AA). The antioxidant activity of the extracts was evaluated using the scavenging activity of the stable DPPH free radical, which was measured according to the method of Burits and Bucar (2000) with some modifications. Aliquots of 1.95 mL of 0.2 mM DPPH ethanolic solution were mixed with 50 μL of the samples. The mixture was shaken vigorously and then kept at room temperature for 30 min in the dark. The absorbance was measured at 517 nm. The DPPH radical scavenging activity was expressed as % Inhibition.

Results and discussions

Determination of nitrate and nitrite in vegetable juices. Researchers share the idea that the nitrate concentration of the edible parts of vegetables is determined genetically and may vary depending on climatic and agricultural conditions (Wierzbicka and Majkowska-Gadomska, 2005). The nitrate content of the edible parts of vegetables is also influenced by temperature and precipitations.

Nitrate concentration at the beginning of the fermentation was 631.24 ± 30.50 ppm for red pepper juice and 342.11 ± 15.44 ppm for tomato juice (Fig. 1). It can be observed that the highest nitrate concentration was found for fresh red pepper juice. Also, nitrite was not detected in fresh juices of tomato and red pepper. Similar results were obtained by Majkowska-Gadomska et al. (2009).

In table 1 are presented the results for nitrate to nitrite conversion rate in red pepper and tomato juices during 30 hours of fermentation. The highest conversion rate after 30 hours of fermentation was noted for red pepper juices (84.83%). Tomato juices conversion rate was 81.82%.

The highest conversion rates were registered for red pepper juice from 24 to 30 hours (from 40.38% to 59.62%) and for tomato juice from 12 to 18 hours (from 38.34% to 59.68%).

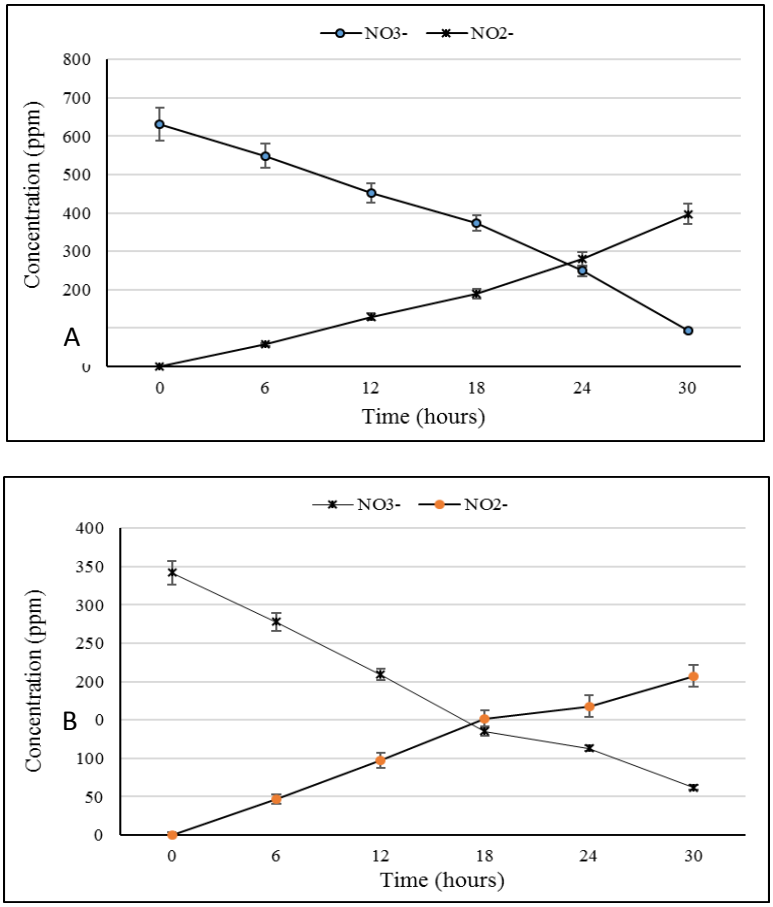

Figure 1. Nitrate and nitrite concentration during 30 hours of Fermentation in the presence of *Staphylococcus xylosus*, for red pepper (A) and tomato (B) juices

Table 1.

Nitrate to nitrite conversion rate (%) in red pepper and tomato juices during 30 hours of fermentation

Time (hours)	Nitrate to nitrite conversion rate (%)	
	Red pepper juice	Tomato juice
0	0.00	0.00
6	13.00	18.71
12	28.53	38.89
18	40.89	60.53
24	60.54	66.96
30	85.10	81.87

Determination of TPC and TCC in vegetable juices. In table 2 are presented total polyphenolic content (TPC) and total carotenoid content (TCC) of fresh and fermented red pepper and tomato juices. Tomato juice contained the highest concentrations of TPC and TCC (57.92±3.86 mg GAE/100 mL and 61.76±4.12 mg β-Car E/ 100 g FW). Comparing the results obtained for fresh with the results obtained for fermented juices, the concentrations decreased for both red pepper and tomato juices. The decrease was higher for polyphenols concentration, and the decreases were almost the same for the two plants (41.09% for tomatoes and 41.26% for red pepper). Carotenoid decreases were 24.82% for tomatoes and 22.39% for red pepper juices. The carotenoids seemed to be more stable then polyphenols and maybe carotenoids were protected by polyphenols during fermentation. The interdependence between juices phytochemical components such as carotenoids and polyphenols could determine the possibility that polyphenols may sacrificially protect carotenoids ().

Table 2.

Total polyphenolic content (TPC) and total carotenoid content (TCC) of unfermented and fermented red pepper and tomato juices

Fermentation time (hours)	Red pepper juice		Tomato juice	
	TPC (mg GAE/ 100 mL)	TCC (mg β-CarE/ 100 g WW)	TPC (mg GAE/ 100 mL)	TCC (mg β-CarE/ 100 g WW)
0	42.34 ± 2.82	31.85 ± 2.12	57.92 ± 3.86	61.76 ± 4.12
30	24.87 ± 1.66	24.72 ± 1.65	34.12 ± 2.27	46.43 ± 3.10

Determination of total antioxidant activity (AA) of juices. Total antioxidant activity is an important parameter in establishing the health functionality of a product that contains antioxidant compounds. AA was expressed as % inhibition of DPPH•. DPPH radical scavenging activity ranged from 76.85% for fresh red pepper to 81.38% for fresh tomato juices. After fermentation, the antioxidant activities decreased for red pepper (46.49%) and tomato juices (55.19%). The antioxidant activity decrease rates were 39.50% for red pepper and 32.18% for tomato juice.

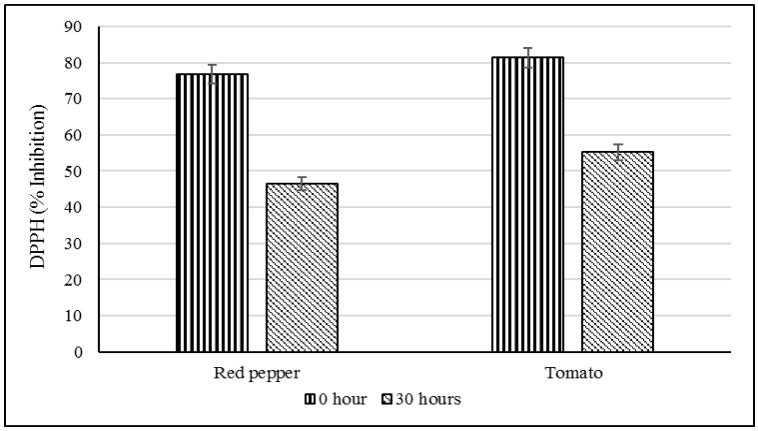

Figure 2. Antioxidant activity (expressed as % Inhibition of DPPH•)
of red pepper and tomato juices at the beginning and after 30 hours of fermentation

Conclusions

Fresh red pepper and tomato juices contain high concentration of nitrate. Red pepper contains the highest concentration of nitrate. After 30 hours of fermentation, the conversion rate of nitrate to nitrite was over 80% for both juices. Tomato juice contains the highest concentrations of phenolics and carotenoids; the carotenoids seem to be more stable than polyphenols during fermentation. The total antioxidant activity was higher for tomato juices compared to red pepper juices.

Acknowledgments: This work was carried out through Partnerships in priority areas Program – PN II, implemented with the support of MEN – UEFISCDI (Romania), project nr. 149/2014.

References

1. Arabbi, P. R., Genovese, M. I. & Lajolo, F. M. (2004). Flavonoids in vegetable foods commonly consumed in Brazil and estimated ingestion by the Brazilian population, Journal of Agricultural and Food Chemistry. 52, 1124-1131.
2. Blanco-Ríos, A.K., Medina-Juarez, L.A., González-Aguilar, G.A., & Gamez-Meza, N. (2013). Antioxidant activity of the phenolic and oily fractions of different sweet bell peppers. Journal of Mexican Chemical Society. 57, 137–143.
3. Burits, M., & Bucar, F. (2000). Antioxidant activity of Nigella sativa essential oil. Phytotherapy Research, 14(5), 323-328.
4. Cataldo DA, Haroon LE, Schrader LE, Youngs VL (1975). Rapid colorimetric determination of nitrate in plant tissue by nitration of salicylic acid. Communications in Soil Science and Plant Analysis 6, 71–80.
5. George, B., Kaur, C., Khurdiya, D. S. & Kapoor, H. C. (2004). Antioxidants in tomato (Lycopersicon esculentum) as a function of genotype, Food Chemistry. 84, 45-51.
6. Giustarini D, Rossi R, Milzani A, Dalle-Donne I. (2008). Nitrite and nitrate measurement by Griess reagent in human plasma: evaluation of interferences and standardization. Methods in Enzymology 440:361-80.

7. Igbokwe, G.E., Aniakor, G.C., & Anagonye, C.O. (2013). Determination of β-Carotene & Vitamin C content of Fresh Green Pepper (Capsicum annnum), Fresh Red Pepper (Capsicum annum) and Fresh Tomatoes (Solanum lycopersicum) Fruits. Bioscientist. 1, 89–93.
8. Le Gall, G., DuPont, M. S., Mellon, F. A., Davis, A. L., Collins, G. J., & Colquhoun, I. J. (2003). Characterization and content of flavonoid glycosides in genetically modified tomato (Lycopersicon esculentum) fruits, Journal of Agricultural and Food Chemistry. 51, 2438-2446.
9. Li, H., Deng, Z., Liu, R., Loewen, S. (2014). Bioaccessibility, in vitro antioxidant activities and in vivo anti-inflammatory activities of a purple tomato (Solanum lycopersicum L.). Food Chemistry, 159, 353–360.
10. Majkowska-Gadomska, J., Arcichowska, K., & Wierzbicka, B. (2009). Nitrate content of the edible parts of vegetables and spice plants. Acta Scientiarum Polonorum Hortorum Cultus. 8(3), 25-35.
11. Marin, A., Ferreres, F., Tomas-Barberan, F. A. & Gil, M. I. (2004). Characterization and quantitation of antioxidant constituents of sweet pepper (Capsicum annuum L.), Journal of Agricultural and Food Chemistry. 52, 3861-3869.
12. Materska, M. & Perucka, I. (2005). Antioxidant activity of the main phenolic compounds isolated from hot pepper fruit (Capsicum annuum L.), Journal of Agricultural and Food Chemistry. 53, 1750-1756.
13. Nour, V., Trandafir, I. & Ionica, E.M. (2013). Antioxidant compounds, mineral content and antioxidant activity of several tomato cultivars grown in southwestern Romania. Notulae Botanicae Horti Agrobotanici Cluj-Napoca. 41, 136–142.
14. Predescu, N.C., Papuc, C., Nicorescu, V. & Dobrea, M. (2015). Optimization of fermentation parameters for vegetable juices with nitrate content to obtain natural nitrites. Lucrări Ştiinţifice USAMV Ion Ionescu de la Brad Iaşi Seria Medicină Veterinară, 58(17)-I, 76-82.
15. Rao, A.V. & Rao L.G. (2007). Carotenoids and human health. Pharmacological Research. 55, 207–216.
16. Singleton, V.L. & Rosi, J.A. (1965). Colorimetric of total phenolics with phosphomolybdic-phosphotungstic acid reagents. American Journal of Enology and Viticulture. 16, 144–158.
17. Slimestad, R. & Verheul, M. J. (2005). Seasonal variations in the level of plant constituents in greenhouse production of cherry tomatoes, Journal of Agricultural and Food Chemistry. 53, 3114-3119.
18. Stewart, A. J., Bozonnet, S., Mullen, W., Jenkins, G. I., Lean, M. E. & Crozier, A. (2000). Occurrence of flavonols in tomatoes and tomato-based products, Journal of Agricultural and Food Chemistry. 48, 2663-2669.
19. Toor, R. K. & Savage, G. P. (2005). Antioxidant activity in different fractions of tomatoes, Food Research International. 38, 487-494.
20. Wierzbicka B., Majkowska-Gadomska J., (2005). The effect of cultivation season and selected sorbents on the field and nitrate content of butterhead lettuce (Lactuca sativa L. var. Capitata L.). Polish Journal of Natural Sciences. 18(1) Y, 15–21.
21. Zhang, D.L. & Hamauzu, Y. (2004). Phenolics, ascorbic acid, carotenoids and antioxidant activity of broccoli and their changes during conventional and microwave cooking. Food chemistry. 88, 503-509.

RESEARCH ON THE MYOCYTES DENSITY AND PROPORTION OF MAIN TISSUE CATEGORIES, FROM SUPERFICIAL PECTORAL MUSCLES, OF *ANAS PLATHYRYNCHOS* SPECIES

Anca TEUȘAN[2] ; V. TEUȘAN[1] ; Teodora TEUȘAN[3]
[1]Acad. I. Haulica"Research Institute Iasi; "Apollonia"University,
[2]Animal Husbandry Faculty, University of Applied Life Sciences and Environment, Iasi
[3]"Gr.T. Popa"University, Iași; University Hospital „Sf. Spiridon" Iași.
e-mail:vasile.teusan@yahoo.com

Abstract

From a two years old female Anas plathyrynchos bird, common breed, weighing 1685 grams, we collected several histological samples from Pectoralis superficialis muscle (PS).Samples were processed by the paraffin sectioning technique yielding a few histological slides with the muscle cross sections mentioned above with HEA coloration. The sections have been studied on an MC3 optical microscope (OM), which previously has been adjusted and calibrated. In the microscopic field were made over 1200 myocytes micrometer measurements and 170 determinations of 17 primary muscle bundles (PMB) within 5 secundary muscle bundles (SMB/SMF).We determined: the average diameter; perimeter; profile and format index of the primary muscle fascicles (bundles). Also we determined the ratio of the myocytes density from muscle and connective tissue. We have obtained the following results: the average diameter of PMF of the 5 SMF ranged 285.936µ and 338.609µ, with an average value of 313.653µ. PMF average perimeter of the 5 SMF studied was 985.369µ , and for those two indicators that define the profile and format PMF (Fi= 1.8464 / 1; Pi = 62.0232 %), the mean value of the 5 SMF, indicating a cylindroid shape with a flattening tendency (oval shape). The myocytes density varied between 460.831 and 596.577mf/square milimeters, with an average value of 525.933mf/mm².The proportion of muscle tissue was of 64.904 % and the proportion of 35.096 %. The differences between the average values of the five SMF studied for the 12 parameters analyzed, were found to be very statistically significant at a rate of 5% and not statistically significant in a proportion of 95 %.

Key words :*Anas plathyrynchos; Pectoralis superficialis; myocytes; density; muscle tissue.*

Introduction

Because of the demographic explosion, featured in the last decades, an exponential increase in food needs appeared, which led to livestock farmers orientation towards new species, breeds and hybrids of mammals, birds and fish. Birds are animals very valuable because they grow easily, with relatively low costs and can deliver three to four main productions, namely: meat, fat, eggs and liver, which have a great demand in all markets.

There are many species of birds bred in large and very large flocks, both extensively and especially in intensive systems, first of these for the chickens and then for ducks. The latter are very interesting birds, because they are easier to grow than chickens and they consume and convert forage and other resources than cereals.Ducks provide approximately 7-8 % of the total production of poultry produced worldwide. Among the types of ducks, *Anas plathyrynchos* is one of the most well known and breed, but there are many broiler breeds and hybrids of high productivity. The largest producer of duck meat in the world is China, followed by France and then by other countries. In general, poultry meat can successfully compete with other meats in the consumer preferences, because it presents a series of histological, physical, chemical, technological and especially organoleptic and dietetico - nutritional characteristics which are very valuable. It is therefore understandable why there is a growing interest for newscientific research studies in the fields of knowledge that compete in defining the concept of good quality

meat. In this context we can sign in our research, in which we approach issues of histological structure of one of the most valuable of *Anas plathyrynchos's* muscles.

Materials and methods

The organisation and conduct, in good condition,of our research has requested the use of at least two categories of material and several specific methods of study. Thus, the biological material was represented by samples of *Pectoralis superficialis dexter* muscle [10] [11] from *Anas plathyrynchos* (common breed) two years old female sexindividual, with a body weight of 1685 grams. At slaughter, the resulting carcass had aweight of 1348 grams, representing 80% of the live weight. The superficial pectoralmuscle had a total weight of 117 grams, which represents 6.94 % of the live weight (LW) and 8.68 % of carcass weight (CW) [3].Both superficial pectoral muscles represent about 14 % of LW and 17% of CW. The studied species has the following systematic classification: Kingdom - *Animalia*; Phylum - *Chordata*; Class - *Aves*; Order -*Anseriformes*; Family - *Anatidae*; Genre - *Anas*; species - *A. plathyrynchos* [14]. *Pectoralis superficialis* muscle samples were processed by paraffin sectioning technique [12] [13], using anatomic and histologic specific instruments (forceps, scalpels, scissors, dissection needles, "SLEE-MAINZ-CUT-5062 " semiautomatic microtome,tissue processor, automated staining device, thermoregulation oven, glassware, reagents and histological dyes [12][13].After completing the specific steps of the method mentioned above, we obtained 10 histological sampleswith cross sections of superficial pectoral muscle, which were stained using HEA method of coloring [12] [13]. Subsequently these blades were studied using a MC3binocular optical microscope which has been previously calibrated for two associations of oculars (OC) and objectives (OB). In the process of calibration we used "Cotea - 1979" method, using an objective micrometer (calibration blade or scale) and an ocular micrometer, calculating two micrometer values (MV), namely: MV = 15.0493μ/division, with the association OC10xOB6 and VM = 9,0364μ/division, with the association OC10xOB10 [12] [13]. In the microscopic field we measured, by using the ocular micrometer incorporated into MC3 binocular microscope, the large and small diameters of the myocytes and of the primary muscle fascicles (PMF). All myocytes in the composition of PMF were counted, 98,93 % of them being measured. The most suggestive images of microscopic field were photographed with a "SONY STEADY-SHOT DSC-S-2100" digital camera, of which are outlined in the iconography of this study (fig. 9). We determined: the average diameter and perimeter of myocytes and of PMF; the profile and format index for these muscle structures; the cross-sectional area and density of myocytes and of PMF [6]. Also, we determined the proportion of muscle and connective tissue in the muscle studied [8]. The following mathematical relationships were used:

7) $D\bar{x}=(LD+SD)/2$, where: $D\bar{x}$=Mean diameter; LD=large diameter of myocytes and of PMF (μ); SD=small diameter of myocytes and of PMF (μ)
8) $P=(LD+SD)/2x\pi$, where: P=myocytes and PMF perimeter; π=coefficient for calculating the circumference and area of a circle, with the value of 3,141592656.
9) Fi=LD/SD, where: Fi=format index (x/1)
10) Pi=(SDx100)/LD, where: Pi=profile index (%)
11) $C.s.s=[(LDxSD)/4]x\pi$, where: C.s.s.=Cross section surface of myocytes and of PMF (μ^2).
12) $MfD=(nx1000x10^3)/C.s.s.$ PMF, where: MfD=muscle fibers density (mf/mm^2); n=number of myocytes from PMF.

13) MTP=(nx C.s.s.m.f. x100)/C.s.s. FMP, where: MTP=muscle tissue proportion (%).

14) CTP=100-MTP, where : CTP=connective tissue proportion (%).

All data from micrometer measurements and calculations were statistically interpreted using general statistic indicators, such as: the statistical mean (average values); geometric mean; the mean deviation; standard deviation; variance and the coefficient of variation [5]. Then, to test the statistical significance of the differences between the five secondary muscle fascicles (SMF), weproceeded the analysis of variance by calculating Fischer (F) and Tukey (W) tests [5]. We also calculated the coefficients of correlation (r) and their error (Sr) of the morphological parameters studied for PMF and we used Instat Plus for statistical interpretation of data.

Results and discussions

The pectoral muscles of birds are more developed than in other regions of the body and along with the thigh and calf muscles, are the regions most valuable of carcasses. And for the species we studied, *Anas plathyrynchos*, the superficial pectoral muscles from which histological samples were collected, represented about 14 % of the live weight and about 16-17 % from the carcass weight [4] [5]. Of course, compared to chickens, meaning theCobb-500 hybrid, the superficial muscles represent 25-30% from the total carcass weight and this number islower in ducks.

Table 1.

Statistical indicators regarding some morphological parameters of the 5 secondary muscle fascicles (bundles) studied for the superficial pectoral muscle of *Anas plathyrynchos* species

Specification			MU	n	Statistical indicators:					Variation limits	
Species and sex	Muscle name	Studied parameters of PMF* from SMF**			$\bar{x} \pm s\bar{x}$	Stand.dev. (s)	Geometric mean	Average dev.	V (%)	Min.	Max.
Anas plathyrynchos; females	*Pectoralis superficialis*	Large diameter	µ	17	393.052±20.07	82.751	384.452	73.255	21.05	255.838	541.775
		Small diameter	µ	17	229.281±14.912	61.484	221.498	56.656	26.82	135.444	331.085
		Average diameter	µ	17	311.166±11.595	47.808	307.668	42.492	15.36	233.264	391.282
		PMF perimeter	µ	17	977.558±36.427	150.194	966.567	133.493	15.36	732.820	1229.249
		Format index	x/1	17	1.861±0.18	0.743	1.736/1	0.630	39.52	1.056/1	3.556/1
		Profile index	%	17	61.414±5.215	21.503	57.614	19.576	35.01	28.125	94.736
		Total number of myocytes from PMF	n	17	36.765±3.319	13.686	34.646	11.081	37.23	22	65
		Number of myocytes from the measured PMF	n	17	36.294±3.239	13.355	34.256	11.029	36.80	22	63
		Measured myocytes proportion from total number of myocytes	%	17	98.932±0.802	3.309	98.876	1.869	3.34	86.486	100.00
		Cross section surface of PMF	μ^2	17	70230.447± 5592.81	23059.746	66880.679	19945.87	32.84	42334.988	117399.333

PMF* = primary muscle fascicle; SMF**= secondary muscle fascicle.

From histologically point of view, the superficial pectoral muscle, for this species of bird (duck) does not have a particularly structural organization, meaning that the muscle fibers (myocytes) have a cylindrical or rather cylindroid aspect; are associated in primary, secondary and tertiary muscle bundles/fascicles and these are covered and protected by some connective elements such as endomissium, internal perimissium and external perimissium [7].Superficial pectoral muscle myocytes had a statistic mean value of 50.02 ± 0,837μ for the large diameter; one of 31.948 ± 0,664μ for the small diameter and 40.984 ± 0.571μ , for the average diameter. Variability of the data for these parameters was relatively low (v = 5,743-6,896-8,568 %) (tab. 2) because the number of values in the statistical calculation was low (n = 17), but each of them represents the average of 108- 153 myocyte variables.

Table 2.

Statistical indicators regarding the myocytes density and the proportion of the two principal categories of muscles from the superficial pectoral muscle of *Anas plathyrynchos* species

Specification				MU	n	Statistical indicators:					Variation limits	
Species and sex	Muscle name		Studied parameters of myocytes and of PMF*			$\bar{x} \pm s_{\bar{x}}$	Stand.dev. (s)	Geometric mean	Average dev.	V (%)	Min.	Max.
Anas plathyrynchos; females	*Pectoralis superficialis*	Myocytes level	Large diameter	μ	17	50.02±0.837	3.4495	49.908	2.9613	6.896	43.743	56.515
			Small diameter	μ	17	31.948±0.664	2.737	31.836	2.3737	8.568	27.733	36.070
			Average diameter	μ	17	40.984±0.571	2.354	40.920	1.9504	5.743	36.654	44.820
			Cross section surface	μ^2	17	1259.791±36.548	150.689	1251.221	123.769	11.961	1008.738	1516.47
		PMF level	Myocytes density	fm** /mm^2	17	519.219±19.20	80.483	513.621	58.407	15.50	364.378	742.081
			Muscle tissue proportion	%	17	64.70±1.752	7.223	64.342	5.856	11.164	55.361	81.447
			Connective tissue proportion	%	17	35.30±1.752	7.223	34.461	5.856	20.463	18.553	44.639

PMF* = primary muscle fascicle; m.f.**= muscle fibers.

Compared to the *Gallus domesticus* species, meaning the Cobb -500 meat hybrid, for the female sex at the same superficial pectoral muscle, where myocytes have a large diameter of 35.85μ; a small diameter of 27.35μ and an average diameter of 31.60μ [4] [5] [6] [7], whilethe species studied here (*Anas plathyrynchos*) their muscle fibers myocytes are thicker with 39.53 %; 16.81 % and 29.70 % respectively. Myocyte cross-sectional area of the studied musclehas a statistical average value of 1259.791 ±36.548μ^2 (v = 11.96 %) (table 2).Regarding the number of myocytes from primary muscle fascicles (PMF), their number ranged between 22 and 65 the statistical mean value of the 17 FMP investigated in this study, being of 36.765 ± 3.319 (v = 37.23 %). 98.932 ± 0.8 % of them were measured (table 1) (fig. 1).Myocytes density for this muscle has a statistical average valueof 519.219 ± 19,2fm / mm^2 (v = 15.5 %) (table 2) (fig. 2). Regarding the parameters studied in the primary muscle fascicles (PMF), they are displayed in table, where we see a statistical average of 393.052 ± 20,07μ for the large diameter; one of 229.281 ± 14,912μ, for the small diameter and one of 311.166±11.595μ for the average diameter (fig. 3).The variability for this trait has values from 15.36 to 26.82 % (table 1).

Compaired with *Gallus domesticus*(Cobb -500 meat type hybrid), for the same muscle, which have a PMF thickness of 452.5μ; of 255,5μ and 354μ respectively, for *Anas plathyrynchos* species differences were: 13.14 % for the large diameter; 10.26 % for the small

diameter and 12.1% for the average diameter. Therefore , in the case of the superficial pectoral muscle in ducks, the primary muscle fascicle (PMF) are thinner (with 10.26 to 13.13 %), but their fiber component (myocytes) are larger (with 16.81 to 39.53 %), compared to the case of the meat type hybrid Cobb -500.In terms of appearance (profile) these PMF are cylindroid with a pronounced oval shape, so we found a statistical average format index value of 1.861 ± 0.18/1 (v = 39.52 %) , and within the 5 SMF, the index has ranged from 1,239/1 to 2.139/1, their average value being of 1.8464/1 (table 3) (fig. 4).

Table 3.

Average statistical values for indicators such as the thickness and profile of PMF and also for myocytes density and for principal muscle category proportion from superficial pectoral muscle of *Anas plathyrynchos*

Specification:		SMF** studied from superficial pectoral muscle (statistical mean/average value)					Average value of the 5 SMF studied
Histological parameters studied for PMF*	MU	SMF_1	SMF_2	SMF_3	SMF_4	SMF_5	
Large diameter	µ	426.397	383.757	376.232	411.348	376.2325	**394.7933**
Small diameter	µ	240.789	188.1165	300.986	210.690	221.977	**232.5117**
Average diameter	µ	333.593	285.9365	338.609	311.019	299.105	**313.6525**
PMF perimeter	µ	1048.013	898.297	1063.773	977.095	939.665	**985.3686**
Format index	x/1	1.908/1	2.045/1	1.239/1	2.139/1	1.901/1	**1.8464/1**
Profile index	%	62.690	49.643	81.235	52.50	64.048	**62.0232**
Total number of myocytes from PMF	n	45.00	27.00	51.00	38.33	28.50	**37.966**
Cross section surface of PMF	$µ^2$	77910.608	56832.053	91429.272	67237.922	64213.994	**71524.7698**
Myocytes density	fm*** /mm^2	552.731	476.902	542.624	596.577	460.831	**525.933**
Muscle tissue proportion	%	60.445	67.447	69.407	68.334	58.889	**64.9044**
Connective tissue proportion	%	39.555	32.553	30.593	31.666	41.111	**35.0956**

PMF* = primary muscle fascicle; SMF**= secondary muscle fascicle; m.f.**= muscle fibers (myocytes)

This cylindroid - oval aspect was also found the species *Gallus domesticus*, where the index format for PMF had an average value of 1.87 ± 0.15/1.The cylindroid - oval format of the PMF, it is given also by the profile index, which has a statistical average value of 61.414 ± 5.215 % (v = 35.01 %) (table 1) (fig. 5).

PMF perimeter of the muscle studied has a statistical mean valueof 977.558 ± 36,427µ (v = 15.36 %) (table 1) (fig. 6). Regarding the cross-sectional area of the PMF, it has an average statistical value 70230.447 ± 5592.81$µ^2$ (v = 32.84 %) (table 1) (fig. 7) and it is lower by 21.72 % than the similar found at PMF, for *Gallus domesticus* muscle (89717,99$µ^2$).In terms of the proportion of muscle and connective tissue in the Pectoral superficial muscle, the values ranged between 55.361 % and 81.447 % for the muscle tissue and values between 18.553 % and 44.639 % for connective tissues group. Thus, the statistical average, in the case of muscle tissue, was of 64.70 ± 1.752 %, andin the case of connective tissues, it was of 35.30 ± 1.752 % (table 2) (fig. 8). Since the 17PMFwe studied from the pectoral superficial muscle were parts of the 5 secondary muscle fascicles (SMF), we looked to see if there are differences between them in terms of parameters addressed in this study. Thus, the data in table 3 highlights

these differences, which can be smaller or larger, but the arithmetic averages of the 5 FMS, are very close to statistical average values (table 1). So for large diameter of PMF, the mean value of the five FMS is 394.7933µ; for the small diameter it is 232.5117µ; the average diameter is 313.6525µ and the PMF perimeter is of 985.3686µ (table 3) (fig. 6). For the two indices which define the format of PMF, the average values are of 1.8464/1 and those of 62.0232% (table 3) (fig. 5). The number of myocytes has was of 37.966m.f./PMF; their density has an average value of 525.933f.m. /mm²; the cross-section of the PMFis 71524.7698µ² and the proportion of the tissue is: 64.9044% muscle tissue and 35.0956% connective tissue (table 3) (fig. 8). The differences found between the 5 SMF were tested to see whether they are or not statistically significant.

Table 4.

Statistical significance of the differences between the five (5) secondary muscular fascicles of the superficial pectoral muscle of *Anas plathyrynchos* species, regarding the thickness and profile of myocytes from PMF.

Studied parameters of PMF* from SFM**	Differences between average values of the 5 SMF compared	Tukey values(W=0,01)	Statistical significance	At 4; 12 LL (liberty levels), for:			
				P	p≤0.05	p≤0.01	p≤0.001
				Fα	3.260	5.410	9.630
Large diameter of PMF(µ)	SMF_1-SMF_2= 42.640	193.064	n.s.	$\hat{F}$	0.194350		
	SMF_1-SMF_3=50.165	240.793	n.s.				
	SMF_1-SMF_4=15.049	262.770	n.s.				
	SMF_1-SMF_5=50.1645	260.994	n.s.				
	SMF_2-SMF_3=7.525	193.064	n.s.				
	SMF_2-SMF_4=27.591	225.241	n.s.				
	SMF_2-SMF_5=7.5245	227.566	n.s.				
	SMF_3-SMF_4=35.116	206.394	n.s.				
	SMF_3-SMF_5=0.0005	225.241	n.s.				
	SMF_4-SMF_5=35.1155	193.064	n.s.				
Small diameter of PMF (µ)	SMF_1-SMF_2= 52.6725	143.445	n.s.	$\hat{F}$	1.953195		
	SMF_1-SMF_3=60.197	178.908	n.s.				
	SMF_1-SMF_4=30.099	195.236	n.s.				
	SMF_1-SMF_5=18.812	193.917	n.s.				
	SMF_2-SMF_3=112.8695	143.445	n.s.				
	SMF_2-SMF_4=22.5735	167.353	n.s.				
	SMF_2-SMF_5=33.8605	169.080	n.s.				
	SMF_3-SMF_4=90.296	153.349	n.s.				
	SMF_3-SMF_5=79.009	167.353	n.s.				
	SMF_4-SMF_5=11.287	143.445	n.s.				
Average diameter of PMF (µ)	SMF_1-SMF_2= 47.6565	111.540	n.s.	$\hat{F}$	0.697210		
	SMF_1-SMF_3=5.016	139.115	n.s.				
	SMF_1-SMF_4=22.574	151.812	n.s.				
	SMF_1-SMF_5=34.488	150.785	n.s.				
	SMF_2-SMF_3=52.6725	111.540	n.s.				
	SMF_2-SMF_4=25.0825	130.388	n.s.				
	SMF_2-SMF_5=13.1685	131.473	n.s.				
	SMF_3-SMF_4=27.590	119.241	n.s.				
	SMF_3-SMF_5=39.504	130.130	n.s.				
	SMF_4-SMF_5=11.914	111.540	n.s.				
Perimeter of PMF (µ)	SMF_1-SMF_2= 149.716	350.413	n.s.	$\hat{F}$	0.697213		
	SMF_1-SMF_3=15.760	437.042	n.s.				
	SMF_1-SMF_4=70.918	476.930	n.s.				
	SMF_1-SMF_5=108.348	473.707	n.s.				
	SMF_2-SMF_3=165.476	350.413	n.s.				
	SMF_2-SMF_4=78.798	409.626	n.s.				
	SMF_2-SMF_5=41.368	413.034	n.s.				

	SMF_3-SMF_4=86.678	374.607	n.s.		
	SMF_3-SMF_5=124.108	408.815	n.s.		
	SMF_4-SMF_5=37.430	350.413	n.s.		
Format index of PMF (Fi)(x/1)	SMF_1-SMF_2= 0.137	1.7334	n.s.	$\hat{F}$	0.634234
	SMF_1-SMF_3=0.669	2.1619	n.s.		
	SMF_1-SMF_4=0.231	2.3593	n.s.		
	SMF_1-SMF_5=0.007	2.3433	n.s.		
	SMF_2-SMF_3=0.806	1.7334	n.s.		
	SMF_2-SMF_4=0.094	2.0223	n.s.		
	SMF_2-SMF_5=0.144	2.0432	n.s.		
	SMF_3-SMF_4=0.900	1.8531	n.s.		
	SMF_3-SMF_5=0.662	2.0223	n.s.		
	SMF_4-SMF_5=0.238	1.7334	n.s.		
Profile index of PMF (Pi)(%)	SMF_1-SMF_2= 13.047	50.1678	n.s.	$\hat{F}$	1.114413
	SMF_1-SMF_3=18.545	62.5702	n.s.		
	SMF_1-SMF_4=10.190	68.281	n.s.		
	SMF_1-SMF_5=1.358	67.8194	n.s.		
	SMF_2-SMF_3=31.592	50.1678	n.s.		
	SMF_2-SMF_4=2.857	58.5291	n.s.		
	SMF_2-SMF_5=14.405	59.1331	n.s.		
	SMF_3-SMF_4=28.735	53.6316	n.s.		
	SMF_3-SMF_5=17.187	58.5291	n.s.		
	SMF_4-SMF_5=11.548	50.1678	n.s.		

Table 5.

Statistical significance of the differences between the five (5) secondary muscular fascicles of the superficial pectoral muscle of *Anas plathyrynchos* species, regarding the number and density of myocytes and the proportion of main tissue categories

Studied parameters of PMF* from SFM**	Differences between average values of the 5 SMF compared	Tukey values(W=0,01)	Statistical significance	At 4; 12 LL (liberty levels), for:			
				P	p≤0.05	p≤0.01	p≤0.001
				Fα	3.260	5.410	9.630
Total number of myocytes from PMF (n)	SMF_1-SMF_2= 18.00	31.9312	n.s.	$\hat{F}$	2.901000		
	SMF_1-SMF_3=6.00	39.8251	n.s.				
	SMF_1-SMF_4=6.67	43.4501	n.s.				
	SMF_1-SMF_5=16.50	43.1662	n.s.				
	SMF_2-SMF_3=24.00	31.9312	n.s.				
	SMF_2-SMF_4=11.33	37.253	n.s.				
	SMF_2-SMF_5=1.50	37.6375	n.s.				
	SMF_3-SMF_4=12.67	34.1358	n.s.				
	SMF_3-SMF_5=22.50	37.253	n.s.				
	SMF_4-SMF_5=9.83	31.9312	n.s.				
Cross-section surface of myocytes (μ^2)	SMF_1-SMF_2= 326.223	127.7083	***		At 4; 612 LL (liberty levels), for:		
	SMF_1-SMF_3=172.681	133.0371	***	P	p≤0.05	p≤0.01	p≤0.001
	SMF_1-SMF_4=60.754	151.7854	n.s.	Fα	2.370	3.320	4.620
	SMF_1-SMF_5=222.879	159.0529	***	$\hat{F}$	14.769995		
	SMF_2-SMF_3=153.542	123.7846	***				
	SMF_2-SMF_4=265.469	148.7647	***				
	SMF_2-SMF_5=103.344	159.2119	n.s.				
	SMF_3-SMF_4=111.927	131.7117	n.s.				
	SMF_3-SMF_5=50.198	137.9468	n.s.				
	SMF_4-SMF_5=162.125	129.6379	***				
Myocytes density from PMF (fm/mm^2)	SMF_1-SMF_2= 75.829	187.771	n.s.		At 4; 12 LL (liberty levels), for:		
	SMF_1-SMF_3=10.107	234.192	n.s.	P	p≤0.05	p≤0.01	p≤0.001
	SMF_1-SMF_4=43.846	255.566	n.s.	Fα	3.260	5.410	9.630
	SMF_1-SMF_5=91.900	253.839	n.s.	$\hat{F}$	2.192858		
	SMF_2-SMF_3=65.722	187.771	n.s.				
	SMF_2-SMF_4=119.675	19.066	n.s.				
	SMF_2-SMF_5=16.071	221.327	n.s.				

	SMF_3-SMF_4=53.953	200.736	n.s.		
	SMF_3-SMF_5=81.793	219.066	n.s.		
	SMF_4-SMF_5=135.746	187.771	n.s.		
Cross-section surface of PMF (μ^2)	SMF_1-SMF_2= 21078.555	53799.923	n.s.	$\hat{F}$	1.18895999
	SMF_1-SMF_3=13518.664	67100.265	n.s.		
	SMF_1-SMF_4=10672.686	73224.496	n.s.		
	SMF_1-SMF_5=13696.614	72729.526	n.s.		
	SMF_2-SMF_3=34597.219	53799.923	n.s.		
	SMF_2-SMF_4=10405.869	62766.577	n.s.		
	SMF_2-SMF_5=7381.941	63414.303	n.s.		
	SMF_3-SMF_4=24191.350	57514.513	n.s.		
	SMF_3-SMF_5=27215.278	62766.577	n.s.		
	SMF_4-SMF_5=3023.928	53799.923	n.s.		
Muscle tissue proportion of PMF (%)	SMF_1-SMF_2= 7.002	16.853	n.s.	$\hat{F}$	1.918634
	SMF_1-SMF_3=8.962	21.019	n.s.		
	SMF_1-SMF_4=7.889	22.937	n.s.		
	SMF_1-SMF_5=1.556	22.782	n.s.		
	SMF_2-SMF_3=1.960	16.853	n.s.		
	SMF_2-SMF_4=0.887	19.622	n.s.		
	SMF_2-SMF_5=8.558	19.864	n.s.		
	SMF_3-SMF_4=1.073	18.016	n.s.		
	SMF_3-SMF_5=10.518	19.661	n.s.		
	SMF_4-SMF_5=9.445	16.853	n.s.		
Connective tissue proportion of PMF (%)	SMF_1-SMF_2= 7.002	16.853	n.s.	$\hat{F}$	1.9186395
	SMF_1-SMF_3=8.962	21.019	n.s.		
	SMF_1-SMF_4=7.889	22.937	n.s.		
	SMF_1-SMF_5=1.556	22.782	n.s.		
	SMF_2-SMF_3=1.960	16.853	n.s.		
	SMF_2-SMF_4=0.887	19.662	n.s.		
	SMF_2-SMF_5=8.558	19.864	n.s.		
	SMF_3-SMF_4=1.073	18.016	n.s.		
	SMF_3-SMF_5=10.518	19.662	n.s.		
	SMF_4-SMF_5=9.445	16.853	n.s.		

Thus, in tables 4 and 5 are calculated some Fischer (F) and Tukey (w) test values for all 12 parameters studied. It is noted that the vast majority (95%) of thetested differences are statistically insignificant and only a few (5%) are highly statistically significant (table 4) (table 5).

Table 6.

Simple correlations between different morphological parameters of PMF and of myocytes from superficial pectoral muscle of *Anas plathyrynchos*

For PMF:				For muscle myocytes:			
Morphological parameters between which we calculated the correlation coefficients	n	Correlation coefficient	Correlation coefficient error	Morphological parameters between which we calculated the correlation coefficients	n*	Correlation coefficient	Correlation coefficient error
Large diameter and small diameter	17	-0.1460	±0.255	Large diameter and small diameter	17	+0.1466	±0.2446
Large diameter and average diameter	17	+0.7726	±0.1012	Large diameter and average diameter	17	+0.8180	±0.083
Large diameter and perimeter	17	+0.7720	±0.101	Large diameter and perimeter	17	+0.8180	±0.083
Small diameter and average diameter	17	+0.5167	±0.0703	Small diameter and average diameter	17	-0.5715	±0.168
Small diameter and perimeter	17	+0.8116	±0.0853	Small diameter and perimeter	17	+0.4355	±0.203

Average diameter and perimeter	17	+0.999	±0.0003	Average diameter and perimeter	17	+1.000	±0.00001
Format index and profile index	17	-0.9504	±0.0242	Format index and profile index	17	-0.9937	±0.00314
Number of myocytes and their density	17	+0.3920	±0.212	Number of myocytes and their density	17	-0.6377	±0.148
Number of myocytes and the muscle tissue proportion	17	+0.2380	±0.236	Number of myocytes and the muscle tissue proportion	17	+0.9694	±0.0151
Muscle and connective tissue proportions	17	-0.10004	±0.0002	Muscle and connective tissue proportions	17	-	-

*n=represents the average values of: 135, 108, 153, 115, 114 myocytes determinations.

To complete the study we calculated a number of correlation coefficients between various morphological indices (parameters), both at myocytes level and at primary muscle fascicles level. Thus, in the myocytes we found positive correlation coefficients with large values between:thelarge and average diameters (r = + 0.818 ± 0.083); between the large diameter and the perimeter (r = + 0.818 ± 0.083); between the mean diameter and the perimeter (r = + 1.000 ± 0.00001) and between the mean diameter and cross sectional area of myocytes (r = + 0.9694 ± 0.0151) (table 6). Also in the myocytes case there are negative correlation coefficients between the mean diameter and density (r = -0.6377 ± 0.148) and between the format and profile indices(r = -0.9937 ± 0.00314) (table 6).

Regarding the primary muscle fascicles (PMF) there are some positively correlated parameters, such as: the large and average diameters (r = + 0.7716 ± 0.1012); the large diameter and perimeter (r = + 0.772 ± 0.101); the small diameter and the average diameter (r = + 0.5167 ± 0.0703); the small diameter and the perimeter (r = + 0.8116 ± 0.0853); average diameter and their perimeter (r = + 0.999 ± 0.0003); the number of myocytes and their density (r = + 0.392 ± 0.212) and the number of myocytes and the proportion of muscle tissue (r = + 0.238 ± 0.236). Some of the indices are negatively correlated in the case of PMF, such as: the profile index and the format index (r = -0.9504 ± 0.0242) and the proportion of muscle tissue and connective tissue (r = -0.1004 ± 0.0002) (tab. 6).

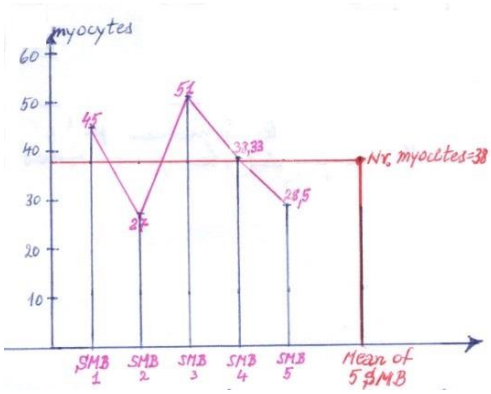

Fig.1. Number of myocytes from SMB (SMF)

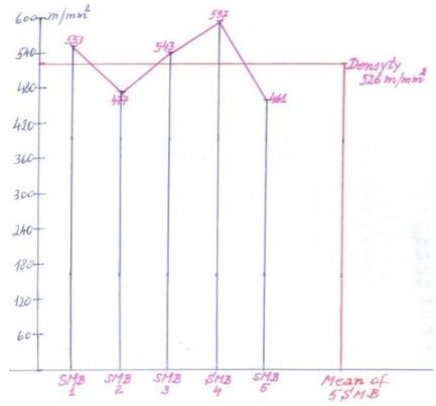

Fig.2. Myocytes density from the 5 SMB

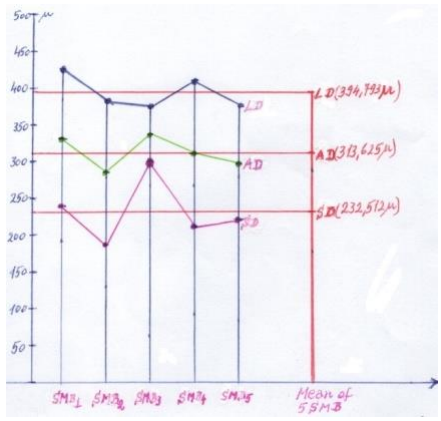

Fig.3. The thickness of the 5 PMF

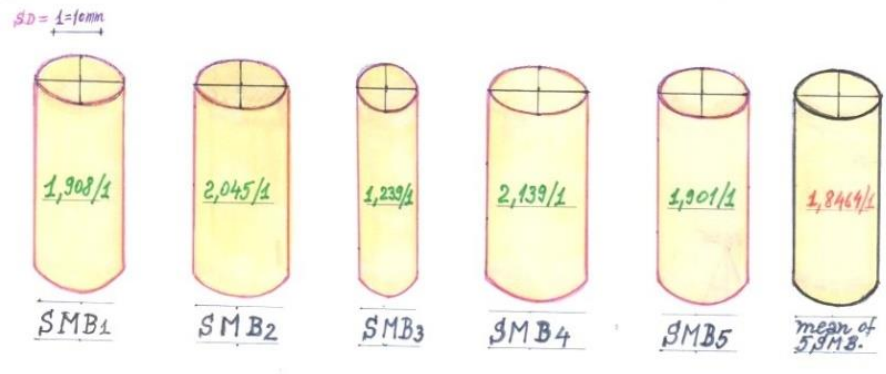

Fig.4. Format index of the PMF from the 5 SMF (SMB) studied

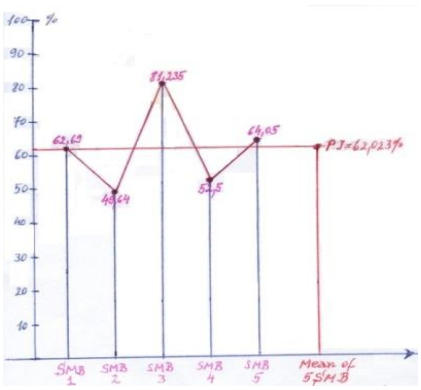

Fig.5. The evolution of the profile index

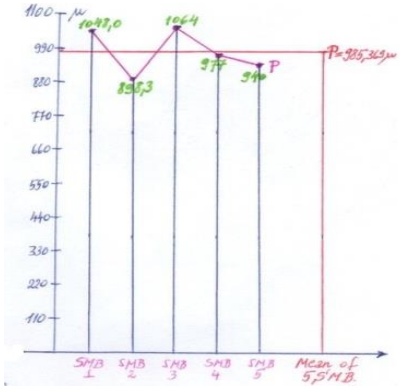

Fig.6. The evolution of the perimeter of muscle fascicles

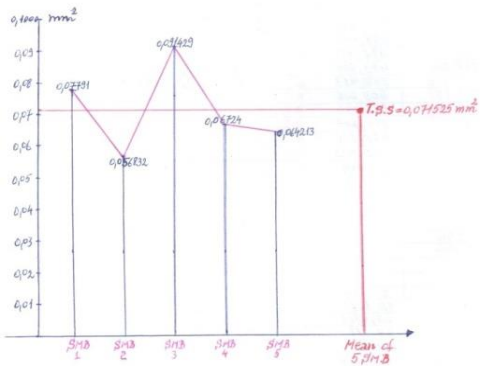

Fig.7. Cross section surface of the muscle fibers

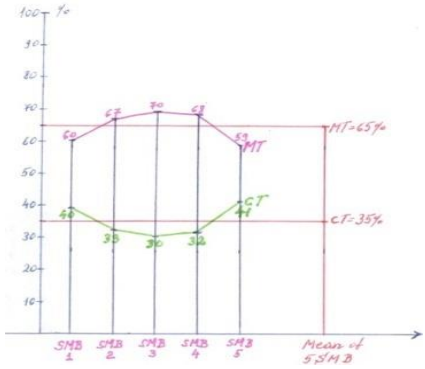

Fig.8. Muscle and connective tissue proportion

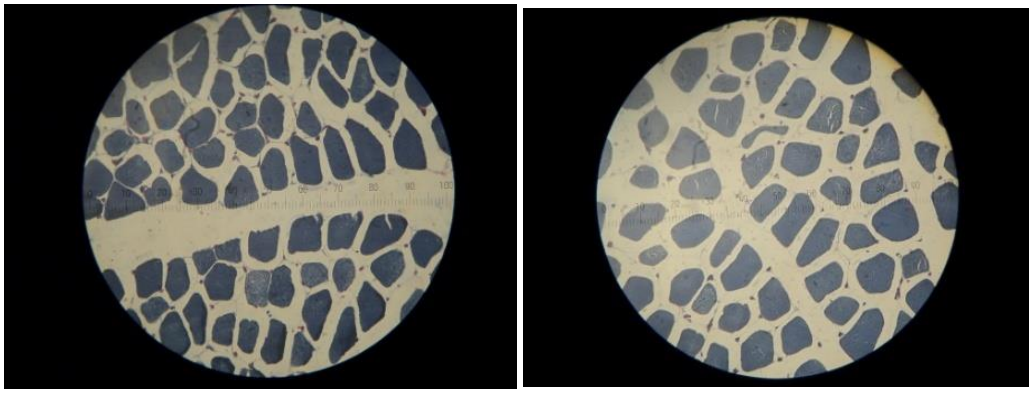

Fig.9. Cross section surface of the muscle fibers (microscopic view)

Conclusions

1. Superficial pectoral muscle myocytes, for the studied species, have an average thickness of 40.98µ and a surface cross-section of 1259.791µ² .
2. Superficial pectoral muscle myocytes density has an average value of 519.219m.f. / mm².
3. The average proportion of muscle tissue is 64.7 %, and the connective tissue represents 35.3 %.
4. The primary muscle fascicles (PMF) from the superficial pectoral muscle studied has an average thickness of 311.166µ and a cross-sectional aria of 70230.447µ².
5. The format of PMF from the studied muscle of *Anas plathyrynchos* species is an oval cylinder (Fi=1.861/1) (Pi=61.414%).
6. The number of myocytes from PMF of the studied muscle is of 36.765.
7. Most of the differences (95 %) of the average values of parameters that characterize the morphology of the PMF, in the SMF are statistically insignificant.
8. The correlation coefficients between different parameters of the muscle fibers and of PMF have positive or negative values , smaller or larger, depending on the way they are associated and determined.

References

1. Cotea, C.V.-2014-*„Biologie celulară; Histologie și Embriologie generală și specială”,* Editura ”Tehnopress”, Iași.
2. Nickel, R. ; Schummer,A.; Seiferle, E.-1977-*„Anathomy of domestic birds”*, Editura „Verlag Paul Parey”, Berlin, Hamburg, Germany.
3. Sandu, Gh.-1995-*„Metode experimentale în Zootehnie”,*Editura Coral-Sanivet, București, pg. 86-91; 134-138; 225-228; 300-302; 317-319; 327-328.
4. Radu-Rusu, R.M.; Teușan, V.; Voicu, P.-2006*„Researches concerning the thickness and cross-section area of the myocytes in the domestic waterfowl s pectoral muscles”* , Lucr.Științ. USAMV Iași, Seria Zootehnie, vol.49, pg. 156-164.5
5. Radu-Rusu, R.M.; Teușan, V.; Anca, Teușan-2007 *„Comparative researches concerning some histometric features of the myocytes in somatic musculature of the domestic chicken and waterfowl (I). Pectoral muscle.”* Lucr.Științ. USAMV Iași, Seria Zootehnie, vol.50, pg. 115-120.
6. Teușan, V.; Anca, Teușan; A.Al. Prelipcean-2012 *-„Researches regarding the surface on transversal section and density of sperficial pectoral muscle of meat-type hybrid hen Cobb-500, at different age stages”*, Lucr.Științ. USAMV Iași, Seria Medicină Veterinară, vol.55(1-2), ISSN 1454-7406, pg. 133-143.
7. Teușan, V.; Anca, Teușan-2013-*„Investigations on the histological structure of the pectoralis superficialis muscle in Cobb-500 meat-type hybrid hen, slaughtered at different ages”,*Lucr.Științ. USAMV Iași, Seria Medicină Veterinară, vol.56(1-2), ISSN 1454-7406, pg. 30-44.
8. Teușan, Anca-2014-*“Researches regarding the fineness and density of myocytes as well as the proportion of main tissue categories from the lateral gastrocnemius muscle of avian hybrid-Cobb-500, by sex and age of slaughter”,* Lucr.Științ. USAMV Iași, Seria Medicină Veterinară, vol.57(4), ISSN 1454-7406, pg. -.
9. Teușan, V.; Anca, Teușan-2014-*„Cercetări privind structura histologică, a mușchiului Gastrocnemian lateral, la hibridul comercial de găină pentru carne-Cobb-500, în funcție de sex și vârsta de sacrificare”,*Revista de Zootehnie, anul XI, nr 3-4(Iulie- Decembrie) 2014, ISSN 1842-1334, pg. 26-35.
10. Tudor, Despina; Constantinescu, Gh. M.-2002 *„Nomina Anatomica Veterinaria*” Ediție Bilingvă, Editura „Vergiliu”, București.
11. Tudor, Despina; Constantinescu, Gh. M.; Constantinescu, Ileana; Cornilă, N.-2010-*„Nomina Histologica et Embriologica Veterinaria”*, Ediție Bilingvă, Editura „Vergiliu”, București.
12. ****** -1953-*„Tehnica histopatologică”, Editura de Stat pentru literatură științifică, București.*
13. ******-1995--*„Investigația histologică în diagnosticul veterinar”*, Ediția a-I-a, Editura „LCSV”, București.
14. ******Hamlyn Guide -Determinator de pasari ilustrat – *Pasarile din Romania si Europa* – Societatea Ornitologica Romana (S.O.R.), 1999, pg. 52 – 54.

COMPARATIVE STUDY ON CERTAIN PARAMETERS OF THE SKULL OF SOME CATS SPECIES GROWN IN CAPTIVITY IN ROMANIA

B. Georgescu[1], G. Predoi[1], Petronela Mihaela Roșu[1], C.Belu[1], Oana-Margarita Ghimpețeanu[1], Letiția Purdoiu[1], C. Vișoiu[2], C. Petrescu[2], P.B. Matei[3]

[1]University of Agronomic Sciences and Veterinary Medicine of Bucharest, Faculty of Veterinary Medicine; [2]Zoo Bucharest; [3] "Grigore Antipa" National Museum of Natural History

georgescubogdi@yahoo.com

Abstract

In Romania, 5 of the 6 species covered by this study - tiger (Panthera tigris), lion (Panthera leo), jaguar (Panthera onca), cheetah (Acinonyx jubatus) and puma (Puma / Felis concolor) - are present only in circuses or zoos, and the sixth species - the European wildcat (Felis silvestris silvestris) is present in our country in wild. The studied specimens were born and bred in captivity and have slightly smaller dimensions than wild specimens. The skulls come from the Anatomy museum, Faculty of Veterinary Medicine in Bucharest. There are not known the subspecies of tiger, lion, jaguar, cheetah or cougar from which the skulls belonged. The bodies of these cats that died of natural causes (old age) were donated by Bucharest-Baneasa Zoo and Circus N & Variete Globus Bucharest (cheetah and one tiger). Our measurements are based on studies conducted on wild cat skulls by Clara Stefen D. Heidecke (2012) and skulls of several species of mammals from archaeological sites by Angela von den Driesch (1976). Based on the measurements, the facial index, the cranial index, the skull volume, and the cranial cavity volume were calculated. It was observed that only the tiger and the wild cat facial and cranial indexes are close, while for the other species the facial index is higher than the head one. The biggest difference between the volume of the skull and cranial cavity volume is observed in tiger, and the smallest difference at the wildcat. Even if they are part of different kinds of cats, the cheetah (big cats category) and the puma (small cats category) presented similar values for the cranial cavity and cranial volume area.

***Key words**: big cats, small cats, cranial cavity volume, skull volume, cranial index, facial index*

Introduction

The main objective of this work is to provide for professionals working in gardens and zoos, officers and other interested specialists tools for morphological recognition of endangered species based on particular aspects of the skull.

The research carried out in developing this work is justified concerns of many authors to ascertain the skeletal morphology on cats in zoos. However, in these areas there are still things less known or even unclear.

Cats' bones and especially skulls often appear as evidence in casuistry forensic on wildlife (especially in the United States and in most European countries) to imports of trophies, which are: cheetah, jaguar, leopard, puma, snow leopard/irbis, lion and tiger. Because these species have different degrees of protection under international law, it requires a thorough examination to identify the right species.

Comparative skeletal morphology is a classical method to study the degree of similarity between species, especially for taxonomic classification and differentiation.

Skulls of the big cats are overlapping and can be hard to find, especially when you do not know their geographic area. Articles about felids taxonomy and systematic (phylogenetic relationships) contain little information about comparative morphology, especially for the skulls (Werdein, 1985; Garcia-Perea, 1994). Angela von den Driesch (1976) described, designed and made standard measurements of the skulls of cats. Seymour (1999) compares the morphology of the skulls of small felids from South America and adds applicable features that were investigated in this study. Skull morphology of the small wild cats was described by

Lekagul and McNeely, 1988; de Oliveira, 1998; Garcia-Perea, 2002). Skull cats morphology in North America was described by Currier, 1983; Tumlison, 1987; Seymour, 1989; Lariviere and Walton, 1997; Murray and Gardner, 1997; de Oliveira, 1998 etc. Cat skull morphology of medium and large genus Panthera was partially described by Todd, 1966; Werdelin, 1983; Lamerichs, 1985; Seymour, 1989; Larsen 1997.

In Romania we have found only a few disparate data on skeleton description of some species of cats found in zoos or circuses menageries.

Materials and methods

The study was conducted on three tiger skulls (*Panthera tigris*), two lion skulls (*Panthera leo*) and one jaguar skull (*Panthera onca*), one cheetah skull (*Acinonyx jubatus*), one puma/cougar skull (*Puma/Felis concolor*) and one European wildcat skull (Felis silvestris silvestris) in the Department of the Anatomy Museum at the Faculty of Veterinary Medicine in Bucharest. The studied skulls are from specimens born and bred in captivity and have dimensions slightly smaller than specimens from the wild. There is not known the subspecies to which the tiger, lion, jaguar, cheetah or cougar skulls belonged. The bodies of these cats that died of natural causes (old age) were donated by Bucharest-Baneasa Zoo and Circus N & Variete Globus Bucharest (cheetah and one tiger). Description of skulls, identifying formations and their homologation was performed according to Nomina Anatomica Veterinaria (N.A.V.), 2005. The measurements were performed on pieces of bone (skull and jaw). For physical measurements there were used livestock compass, ruler and caliper (classical and electronic). Based on the measurements, there were calculated facial index, cranial index, skull volume index, and cranial cavity volume.

In zootechnical studies the cephalic index is the ratio of head length and breadth of its low orbit (zygomatic arches). According to this report the skulls are narrow (index of less than 43%), normal (index values between 44-45%) and large (cephalic index greater than 46%). Total facial index is the ratio between the bizygomatic diameter and the maximum vertical diameter of the face. According to this index, the skulls are systematized in dolichocephalic (narrow and high), mesocephalic (average) and brachycephalic (flat and wide). In Felids the skull can be outlined by an ellipsoid.

Starting from the 3D calculation of the volume of this geometric figure, we can find the skull volume, using standard margin of error of 0.12345 (6), the calculation formula that is $4/3\ \pi$ abc (a = half the maximum length of the skull, b = half the height of the skull and c= half the skull width in the zygomatic arch), and where $\pi = 3.14159$. The cranial cavity volume, which has also the shape of an ellipsoid, was calculated from measurements made on radiological images, using the formula $4/3\ \pi$ abc, with a (1/2 of anterior-posterior diameter), b (1/2 the dorsal-ventral diameter) and c (1/2 of the transverse diameter). Following the two types of measurements (total skull volume and cranial cavity volume) of the skull, for the studied skulls it can be calculated how much of the skull volume is the cranial cavity volume. Linear measurements were performed according to research on various species of cats conducted by Clara Stefen and Heidecke D. (2012). These measurements comply with the utmost anthropological references.

Radiographs were made at the Faculty of Veterinary Medicine, Radiology Service which is equipped with a Philips Bucky Diagnost FS Standard device for digital radiography which has a program of measurements (which we used for measuring parameters used in calculating cranial cavity volume).

Results and discussions

Nine felids skulls were morphometrically examined - belonging to both main categories (big cats - tiger, lion, jaguar, cheetah and small cats – puma and European wild cat).

Cranial measurements included those used on different species of felines by Clara Stefen and Heidecke D. (2012).

According to S. Larson (1997), studying both basal-condyle length and other morphological aspects of the skull, like canines' length, length and aspect of nasal profile, width of the skull, etc., can contribute to a more accurate determination of the origin of any studied skull.

Parameters were measured on lateral, dorsal, ventral and aboral (occipital) sides of the nine skulls. Some of the measured parameters were used to calculate the cranial and facial index of each studied skull. Also, by using some of the measured parameters, it was calculated the volume of each skull, and, on the basis of the radiologically measured parameters on the head cavity, it was calculated the volume of each head cavity. For the lion and tiger skulls there was calculated the average for each parameter.

The results are presented below in tabular form and suggestive graphics.

Table 1.

Parameters used to calculate the facial index, cranial index, cranial volume and cranial cavity volume

Measurements	Cats species					
	Tiger - Media	Lion - Media	Jaguar	Cheetah	Puma /Cougar	European wild cat
kliob	6.7	6.0	5.6	4.6	3.8	1.2
ln_1	12.0	7.5	6.0	4.9	4.3	2.3
zw	21.5	19.5	17.0	12.9	13.4	7.0
gsl	35.8	35.9	29.8	20.2	18.6	9.8
shbull	12.33	9.45	9.1	8.4	7.0	4.7
Facial index	55.83	80.0	74.66	93.87	88.37	52.17
Cephalic index	60.05	54.31	57.04	63.86	72.04	71.42
Skull volume	4955.5	3489.7	2408.7	1143.6	911.59	168.46
anterior-posterior diameter of the cranial cavity	10.0	8.5	9.2	7.1	9.0	5.1
Dorso-ventral diameter of the cranial cavity	6.4	5.45	6.3	4.9	5.9	3.3
Transversal diameter of the cranial cavity	8,6	7.4	7.2	6.1	7.5	4.1
Cranial cavity volume	291.26	178.05	183.4	110.8	201.03	36.05
Report skull volume/cranial cavity volume	5.37	5.16	7.61	9.68	22.05	21.39

Legend:

- **kliob** = interorbital width measured at the level of the smallest distances between orbits,
- **ln_1** = nasals length of the median suture,
- **zw** = maximum width of the skull at zygomatic arch,
- **gsl** = maximum length of the skull,
- **shbull** = skull height vertically measured from the tympanic bubble.

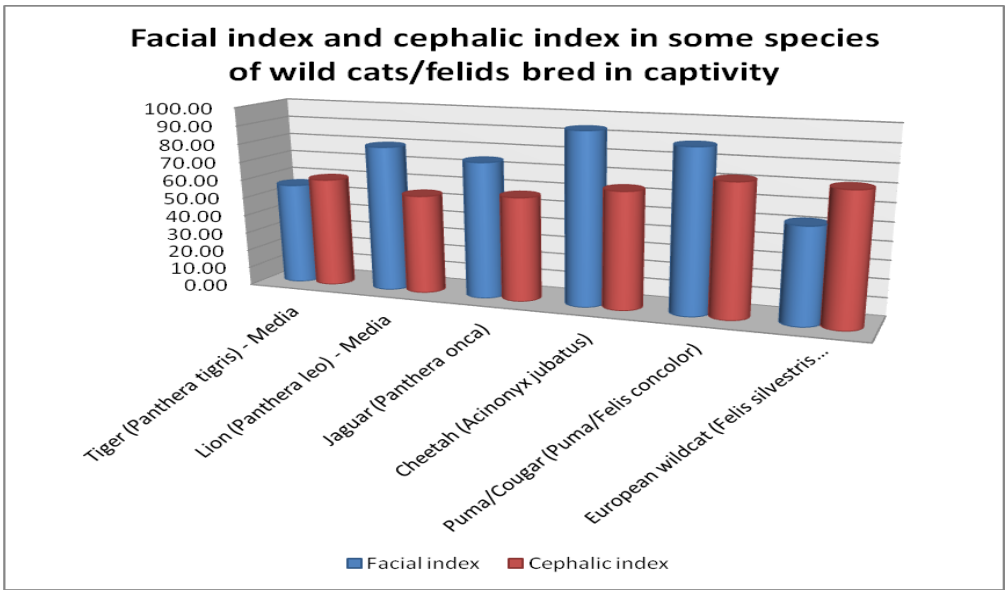

Graphic 1. Facial index and cephalic index in some species of wild cats/felids bred in captivity

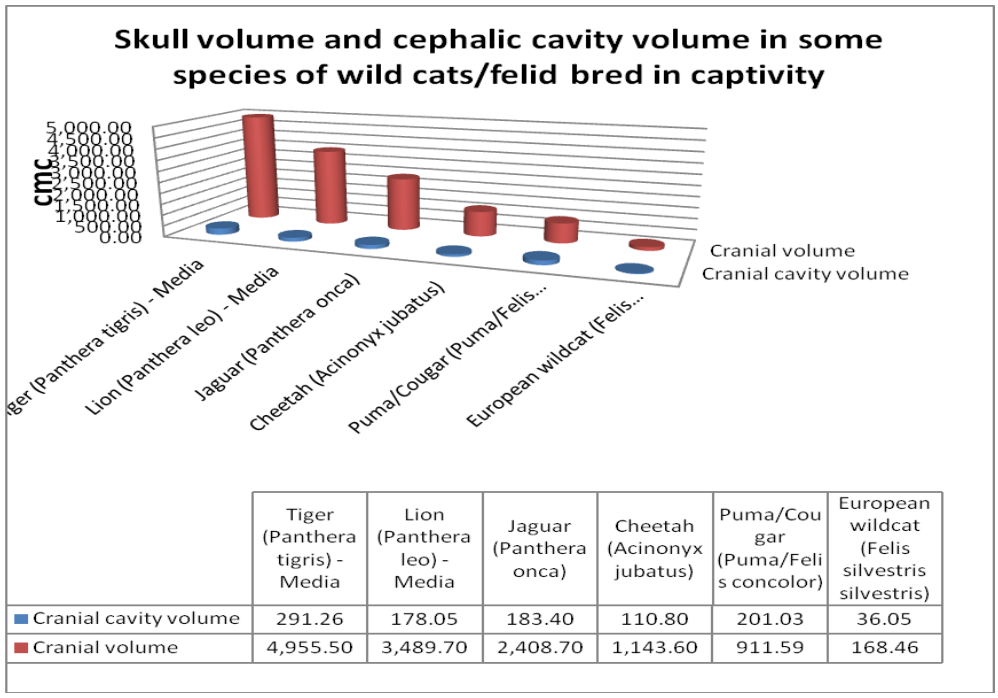

	Tiger (Panthera tigris) - Media	Lion (Panthera leo) - Media	Jaguar (Panthera onca)	Cheetah (Acinonyx jubatus)	Puma/Cougar (Puma/Felis concolor)	European wildcat (Felis silvestris silvestris)
Cranial cavity volume	291.26	178.05	183.40	110.80	201.03	36.05
Cranial volume	4,955.50	3,489.70	2,408.70	1,143.60	911.59	168.46

Graphic 2. Skull volume and cephalic cavity volume in some species of wild cats/felids bred in captivity

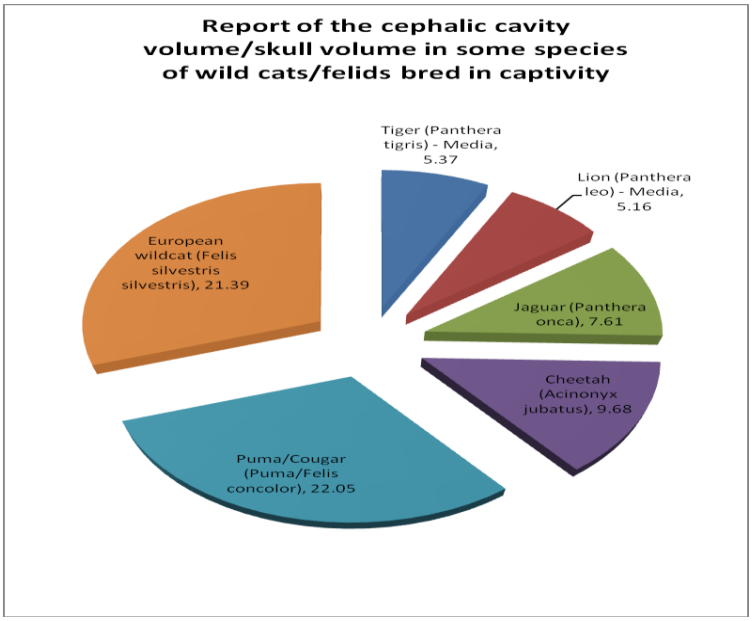

Graphic 3. Report of the cephalic cavity volume/skull volume in some species of wild cats/felids bred in captivity

It appears that only the tiger and the wild cat facial and cranial indexes are close in value, for other species the facial index is higher than the head one. The biggest difference between the volume of the skull and cranial cavity volume is observed at the tiger, and the smallest difference at the wildcat. Even if part of different kinds of cats, cheetah (big cats category) and puma (small feline category) presented close values of the cranial cavity and cranial volume area.

Conclusion

Based on measurements, the facial index, the cranial index, skull volume, cranial cavity volume were calculated.

1. It was observed that only the tiger and the wild cat facial and cranial indexes are close, while for the other species facial index is higher than the head one.
2. The biggest difference between the volume of the skull and cranial cavity volume is observed in tiger, and the smallest difference at the European wildcat.
3. Even if they are part of different kinds of cats, cheetah (big cats category) and puma (small cats category) presented similar values of the cranial cavity and cranial volume area.
4. It appears that there are similarities between the different measured parameters to felids born and bred in the wild.
5. Parameters of the specimens born and bred in captivity have dimensions slightly smaller than wild specimens (cage effect).

References

1. Alberch, P - (1980) Ontogenesis and morphological diversification. Am Zool. 20; 653-667.
2. Barone, R. – (1966). Anatomie comparée des mammiferes domestiques, Tome premier - Osteologie, Imprimerie des Beaux – Arts s.a. - J. Tixier & fils, Lyon,1966.
3. Bertrand, Anne-Sophie, Morisot, A. - (2012) Neotropical Spotted Cat Species Discrimination Using Morphometrics. Natureza & Conservação 10(1): 40-44.
4. Bright,M., Jen Green, Robin Kerrod, Rhonda Klevansky, Barbara Taylor – (2006) Hunters of the wild. Annes Publishing Ltd., Hermes House, London.
5. Cotta, V., Bodea, M., Mincu, I. (2008) – Vânatul și vânătoarea în România. Tehnica ocrotirii și recoltării vânatului. Ed. Ceres.
6. Coţofan, V., Predoi; G. (2003) – Anatomia topografică a animalelor domestice – Ed. BIC All, 2003, Bucureşti.
7. Christiansen, P., Adolfssen, J.S. (2005) – Bite forces, canine strength and skull allometry in carnivores (Mammalia, Carnivora). J. Zool. Lond. 266: 133-151.
8. Garcia, Karla, Ortiz, J.C., Marcela Vidal, Rau, J.R. (2010) – Morphometric of the Tracks of *Puma concolor*: Is It Possible to Differentiate the Sexes Using Measurements from Captive Animals. Zoological Studies 49(4): 577-582.
9. Georgescu, B., Predoi, G., Belu, C., Letiția Purdoiu, Mărgărita Ghimpețeanu, Marilena Chereji, Petronela Mihaela Roșu, Ancuța Elena Oprea, Vișoiu, C., Florica Bărbuceanu – *Biodiversitatea morfometrică a craniului la jaguar (Panthera onca). Studiu de caz.* Revista Română de Medicină Veterinară, București, 2014, vol. 24, nr.4, pp.29-42
10. Georgescu, B., Predoi, G., Belu, C., Letiția Purdoiu, Tudon, N., Ștefania Raita, Dumitrescu, I., Ciobanu, M.L., Florica Bărbuceanu – *Caracterele morfologice ale craniului la tigru (Panthera tigris).* Revista Română de Medicină Veterinară, București, 2015, vol. 25, nr.1, pp.27-44
11. König, H.E., Liebich, H.G. (2004) – Veterinary Anatomy of Domestic Mammals. Schattauer GmbH, Stuttgart, New York.
12. Künzel, W., Breit, S., Oppel, M. (2003) – Morphometric investigations of breed-specific features in feline skulls and considerations on their functional implications. Anatomy, Histology, Embryology 32(4): 218-223.
13. Meachen-Samuels, Julie, Van Valkenburgh, B. (2009) – Craniodental indicators of prey size preference in the Felidae. Biological Journal of the Linnean Society 96: 784-799.
14. Petrov, L., Nikolov, H., Gerasimov, S (1992) – Craniometrical sex determination of wild cat *Felis silvestris* in Bulgaria. Acta Theriologica 37(4): 381-396.
15. Predoi, G., Georgescu, B., Belu, C., Dumitrescu, I., Anca Şeicaru, Petronela Roşu (2011) – Anatomia comparată a animalelor domestice. Osteologie, artrologie, miologie. Ed. Ceres, Bucureşti.
16. Sunquist, M.; Sunquist Fiona (2002) – Wild cats of the world. The University of Chicago Press, Chicago.
17. Sims, Margaret (2012) – Cranial morphology of five felids: Acinonyx jubatus, Panthera onca, Panthera pardus, Puma concolor, Uncia uncia. Russian J. Theriol 11(2): 157-170.
18. Stefen, Clara, Heidecke, D. (2012) – Ontogenetic changes in the skull of European wildcat (Felis silvestris SCHREBER, 1777). Vertebrate Zoology 62(2): 281-294.
19. Tiwari, Y., Taluja, J.S., Vaish, R. (2011) – Biometry of Mandible in Tiger (Panthera tigris). Annual Review & Research in Biology 1(1): 14-21.
20. Turner, A. (1996) - The Big Cats and their fossil relatives. Columbia University Press, New York.
21. * * * - Nomina Anatomica Veterinaria, Fifth edition, Published by the Editorial Committee Hannover, Columbia, Gent, Sapporo, 2005.

CONTRIBUTIONS TO THE STUDY ON DIFFERENT PARAMETERS OF THE CARPATHIAN LYNX (*Lynx lynx ssp. carpathicus*) SKULLS FROM ROMANIA

B. Georgescu[1], G. Predoi[1], Petronela Mihaela Roșu[1], Ștefania Mariana Raita[1], Florica Bărbuceanu[1], Oana-Margarita Ghimpețeanu[1],M. Ciobanu[1], C. Vișoiu[2], C. Petrescu[2]

[1]University of Agronomic Sciences and Veterinary Medicine of Bucharest, Faculty of Veterinary Medicine; [2]Bucharest Zoo

georgescubogdi@yahoo.com

Abstract

This species is not included on the I.U.C.N. Red List, but in Romania, due to the relative high number of individuals, it is considered to be a protected species by governmental acts. During certain periods, in exchange of a tax, hunting is accepted for a limited number of individuals. Five skulls of Eurasian lynx, owned by the Department of Anatomy Museum of the Faculty of Veterinary Medicine of Bucharest, were morphometrically examined. The dimensions of the five skulls were compared with the literature in order to fit into the subspecies called Carpathian lynx (Lynx lynx ssp. carpathicus). Cranial measurements were performed using electronic digital calipers reading a tenth of a millimeter. Cranial measurements were compared with those made by Angela von den Driesch (1976). Generally, it was observed that the results regarding the dimensions of the skulls can be compared with the results obtained by G.E. Predoiu (2011). But there are four parameters, maximum width of the skull between the orbits, the width of the canine teeth socket, maximum length of skull and length of the mandible, larger than the subspecies described by G.E. Predoiu. These dimensional differences can be explained by the fact that some of the 5 skulls from the Anatomy Department belonged to an outstanding specimen. The C.I.C. score (the value of trophy hunting that can be awarded) for 4 of the 5 studied cases show that the skulls belonged to an outstanding specimen with Gold Medal.

Key words: Carpathian lynx, cranial measurements, value trophy hunting

Introduction

Research undertaken in developing this paper are the justified concerns of many authors in discovering aspects of the cats skull morphology in zoos and national parks, but also in veterinary forensic medicine. Loss of habitat, reduced food sources and intensive hunting (there was a period in Romania, the '50s – '60s of last century, when it was considered a harmful species for herbivorous species that were being hunted – red deer, roe deer, chamois etc.) were causes that may explain the reduction of population in Romania of the Eurasian lynx subspecies known as Carpathian lynx (*Lynx lynx ssp. carpathicus*) in the Carpathian Mountains.

Due to this situation and given the Order of the Romanian Government 20/2014 and 31/2014 Emergency Ordinance of the Romanian Government, the Carpathian lynx is considered a species requiring strict protection in Romania.

Comparative skull morphology is a classical method to study the degree of similarity between species for taxonomic classification and differentiation.

Considering this situation and the fact that there is limited literature regarding the anatomical parlicularities of this species, we consider that a description of the skull of the Carpathian lynx, which is regarded as a valuable hunting trophy, would be useful.

This study contains comparative data between feline species, but only measurements and issues that may be identified at the species *Lynx lynx ssp. carpathicus* and comparisons of skull dimensions to other subspecies of lynx.

The literature is limited regarding the skulls identification based on their morphology, depending on the geographical area and size, mostly due to the erroneous identification of species in their home countries.

Most biologists are not yet familiar with the connection between morphology and feline zoo archeological and paleontological literature describing many distinctive features of skulls (Meriam & Stock – 1932, Schmid – 1940, Seymour - 1993). Comparative morphology of the skulls, teeth and morphometry characteristics of dentition can be found in the monography by German E.Schmid (1940) „Variationsstatisische Untersuschungen am Gebis pleistozaner und rezenter Leoparden und anderer Feliden".

In 1976, Angela von den Driesch designed and described standard measurements for skulls of different species, including cats. Later, in 1999, Seymour compares skull morphology of small feline from South America and adds applicable features that were investigated in this study. Cat skull morphology of medium and large genus Panther was partially described by Todd, 1966; Werdelin, 1983; Lamerichs, 1985; Seymour, 1989; Larsen 1997.

Materials and methods

The study was performed on five Carpathian lynx skulls (*Lynx lynx ssp. Carpathicus*) of the Department of Anatomy Museum at the Faculty of Veterinary Medicine in Bucharest, skulls that are present in the museum for over 40 years. One of the skulls is incomplete. It is not known the sex which the skulls belonged to, but according to literature, dimensional differences are not significant in the skulls of the two sexes. The area from which these samples were taken is also unknown.

The description of skulls, identification and homologation of formations were performed according to Nomina Anatomica Veterinaria (N.A.V.), 2005.

Measurements were performed on pieces of bone (skull and jaw). Physical measurements were made using livestock compass, ruler and caliper (classical and electronic).

Results and discussions

The five Eurasian lynx skulls were examined morphometrically. The dimensions of the five skulls were then compared with the literature in order to fit them into the subspecies. The cranial measurements included those used by Angela von den Driesch (1976). As a result of studies performed on a larger number of lynx skulls (*Lynx lynx*), G.E. Predoiu (2011) managed to create the taxonomic classification of the studied specimens, based on measurements of length. Data was taken to be compared with those obtained in this study. According to S. Larson (1997), the study of both basal condyle length and other morphological aspects, like the length of the canine teeth, length and aspect of the nasal profile, width of the skull, etc. it can contribute to a more accurate determination of the origin of all studied skulls. In order to compare the parameters of the five studied skulls the mean of each parameter was made. The mean of each parameter was compared to the mean of each parameter of the study conducted by G.E. Predoiu (2011) on other subspecies of the Eurasian lynx. The results obtained are presented below in tabular form and suggestive charts (Table 1).

It is noted that in general, the 5 studied skulls fit into the dimensions of the Carpathian lynx skull (*Lynx lynx ssp. Carpathicus*) studied by G.E. Predoiu (2011).

However, there are four parameters that are larger than the subspecies of lynx studied by G.E. Predoiu (2011), these parameters being: the maximum width of the skull between the

orbits (4.64 cm), width of the skull to the socket canine teeth (6.64 cm), the maximum length of skull (17.24 cm) and the total length of the mandible (10.66 cm).

Table 1.

Craniometry main measurement values - discipline Anatomy-FMV Bucharest, Romania (after G.E. Predoiu, 2011), Slovakia (after G.E. Predoiu, 2011), Russian Federation (after G.E. Predoiu, 2011)(in cm)

Nr.crt.	Skull measurements	Location of the measured skulls			
		media/ 5 skulls dep. Anatomy, FMV	Romania/51 skulls	Slovakia/ 81 skulls	Russian Federation/ 19 skulls
1	the width of the skull to the mastoid process	5.46	6.40	6.35	6.54
2	maximum width of the skull between the orbits – Entorbitale-Entorbitale	4.64	3.39	3.13	3.44
3	the width of the skull to the socket canine teeth	6.64	4.14	4.27	4.18
4	the maximum length of the skull – Akrokranion / external occipital protuberance – Prosthion	17.24	15.10	14.80	15.50
5	condylobazal length - from the edge of the occipital condyles at Prosthion/incisor labial slot	12.88	13.50	13.30	14.00
6	The total length of the jaw - the condyle to infradental / rostral edge of central incisors alveoli	10.66	10.00	9.80	10.50

These dimensional differences can be explained by the fact that perhaps some of the five skulls of the Anatomy Department belonged to outstanding examples of possible trophies with high score, score that will be calculated and presented in this subchapter.
The trophy hunting score (C.I.C. score) is calculated by adding two values, the skull width and skull length (Table 2).

Table 2.

Scoring C.I.C. and medals that could be awarded

Measurements	Lynx 1	Lynx 2	Lynx 3 – incomplete skull	Lynx 4	Lynx 5
The maximum length of the skull	13,0	19,6	17,6	18,7	17,3
skull width at the zygomatic arch	9,0	11,4	10,6	11,7	9,1
C.I.C. scoring	22	31	28,2	30,4	26,4
The medal that could be awarded	-	gold	gold	gold	gold

The C.I.C. scoring which 4 of the 5 skulls (between 26,4 and 31 points, respectively) of the Anatomy Department fall into shows that these skulls belonged to outstanding examples which can be classified as trophies that might be awarded the Gold Medal (over 26 points).

It is known that Prof. DHC Vasile Gheţie, who founded the Department of Anatomy Museum of the Faculty of Veterinary Medicine Bucharest, was an avid hunter and perhaps even those animals were hunted by the teacher and kept due to their beauty and size.

Conclusion

1. The five studied skulls fit in the dimensions of the Carpathian lynx (*Lynx lynx ssp. Carpathicus*), dimensions determined by G.E. Predoiu (2011).
2. Four parameters are larger than the subspecies of lynx studied by G.E. Predoiu (2011). These parameters are the maximum width of the skull between the orbits (4.64 cm), width of the skull to the socket canine teeth (6.64 cm), the maximum skull length (17.24 cm) and the total length of the mandible (10.66 cm).
3. These dimensional differences can be explained by the fact that perhaps some of those five skulls from the Anatomy department belonged to outstanding examples of possible trophies with high C.I.C scoring.
4. The C.I.C. scoring which 4 of the 5 skulls (between 26,4 and 31 points, respectively) of the Anatomy Department fall into shows that these skulls belonged to outstanding examples which can be classified as trophies that might be awarded the Gold Medal (over 26 points).

References

1. Atalar, O.; Ustundag, Y.; Yaman, M.; Ozdemir, D., 2009. Comparative Anatomy of the Neurocranium in Some Wild Carnivora. Journal of Animal and Veterinary Advances. Vol. 8, Issue 8, p. 1542-1544.
2. Barone, R., 1966. Anatomie comparée des mammiferes domestiques, Tome premier - Osteologie, Imprimerie des Beaux –Arts S.A. - J. Tixier & Fils, Lyon.
3. Bertrand, Anne-Sophie, Morisot, A. , 2012. Neotropical Spotted Cat Species Discrimination Using Morphometrics. Natureza & Conservação 10(1): 40-44.
4. Breitenmoser, Christine; Breitenmoser-Würsten, U.; Cop, J.; Frkovic, A., 1998. The re-introduction of the lynx in Slovenia and its present status in Slovenia and Croatia. Hystrix, the Italian Journal of Mammalogy, Vol 10, No 1 (1998) ISSN 1825-5272 (electronic version)
5. Christiansen, P., Adolfssen, J.S., 2005. Bite forces, canine strength and skull allometry in carnivores (Mammalia, Carnivora). J. Zool. Lond. 266: 133-151.
6. Coţofan, V., Predoi, G., 2003. Anatomia topografică a animalelor domestice, BIC All, Bucureşti.
7. Cotta, V., Bodea, M., Micu, I., 2008. Vânatul și vânătoarea in România – Tehnica recoltării și ocrotirii vânatului. Ed. Ceres, Bucureşti.
8. Gheţie, V., Hillebrand, A., 1971. Anatomia animalelor domestice, vol. I – Aparatul locomotor. Ed. Academiei Republicii Socialiste România, București.
9. Gomerčic, T. and al., Cranial morphometry of the European lynx (Lynx lynx L.) from Croatia. Veterinarski Arhiv, 2010, vol. 80 (3), p. 393-410.
10. Haimovici S., Contribuțiuni la studiul morfologiei râsului Felis (Lynx) lynx L. (1964). Analele Științifice ale Universității Al.I. Cuza, sII, a.Biologie, tom 10, fasc.2, p. 359-368
11. Hriţcu, A.C., 2006. Criterii morfologice de diferenţiere intre oasele provenite de la unele specii de vânat si animale domestice, utile in expertiza sanitară veterinară. Teza de doctorat, USAMV „Ion Ionescu de la Brad" Iași.

12. König, H.E., Liebich, H.G., 2004. Veterinary Anatomy of Domestic Mammals. Schattauer GmbH, Stuttgart, New York.
13. Künzel, W., Breit, S., Oppel, M., 2003. Morphometric investigations of breed-specific features in feline skulls and considerations on their functional implications. Anatomy, Histology, Embryology 32(4): 218-223.
14. Ommundsen, P.D., Morphological Differeces Between Lynx and Bobcat Skulls. Northwest Science, 1991, vol. 65, No. 5, p. 248-250.
15. Predoi, G., Georgescu, B., Belu, C., Dumitrescu, I., Şeicaru Anca, Roșu Petronela, 2011. Anatomia comparată a animalelor domestice. Osteologie, artrologie, miologie. Ed. Ceres, Bucureşti.
16. Predoiu, G.E., 2011. Aspecte privind biologia și bazele managementului râsului (Lynx lynx Linnaeus 1758) din România. Teză, Universitatea Transilvania din Brașov.
17. Stephen, Clara, Heidecke, D., 2012. Ontogenetic changes in the skull of European wildcat (Felis silvestris). Vertebrate Zoology, 62(2):281-294.
18. Sunquist, M., Sunquist, Fiona, 2002. Wild cats of the world. The University of Chicago Press, Chicago.
19. Șelaru, N., 2006. Trofee de vânat european – preparare, evaluare, clasificare. Ed. Cynegis, București.
20. Wiig, O., Andersen, T., 1986. Sexual Size Dimorphism in the Skull of Norwegian Lynx. Acta Theriologica, vol. 31, 12, p. 147-155.
21. Zheltuchin, A.S.,1992. Distribution and numbers of lynx in the Soviet Union. Pp. 19-22 in The situation, conservation needs and reintroduction of lynx in Europe. Proc. symp. 17- 19 October, Neuchatel. Council of Europe, Strasbourg.
22. * * * - Nomina Anatomica Veterinaria, Fifth edition, Published by the Editorial Committee Hannover, Columbia, Gent, Sapporo, 2005.

RESEARCH ON SWINE STOMACH HISTOLOGICAL STRUCTURE

Valerica DANACU[1], Stefania Mariana RAITA[1], Viorel DANACU[2], Carmen IONIȚĂ[1], Alexandra Valentina MINCU[1]
[1]FMV Bucharest; [2]ANSVSA Bucharest
valericadanacu@yahoo.com

Abstract

Following research we noticed that swine stomach lining presents numerous longitudinal folds with many cuts bounded by deep ditches. With 4x objective there is an overview of the stomach wall consisting of four tunics: mucosa, submucosa, muscular and serous. Lamia propria composed of loose connective tissue infiltrated by lymphocytes and mucosal muscle is composed of smooth muscle fibres. In histological examination we noticed that submucosa is composed of loose connective tissue with large blood vessels and contains nerves, Meissner submucosal plexus. Simple prismatic epithelium consists of two types of cells: high prismatic, located in the third round with core basal cells that are grouped in the bottom of the crypts. We observed high prismatic cells with apical microvilli and basal cells from pole to pole dilated basal and apical pole tapered, narrower allowing their location at the base of the crypts. Fundic glands are most numerous, straight appear in the upper and lower third bifurcated and these appears sectioned obliquely. Composed glands enter several types of cells: main basophils, parietal cells, oxintic, delomorfe and undifferentiated cells. With 40x objective is noted that the principal cells are located at the base of the gland appear grouped into nests and are the most numerous cells. These cells are cubic, small has basophil cytoplasm, nucleus euchromatic, small and round. Predominated gland parietal cells in the body are round or oval, large that protrudes outside the gland. Muscle lining is made of two layers of smooth muscle, organized on two levels: internal circular and external longitudinal. In histological examination we noticed that submucosa is composed of loose connective tissue with large blood vessels and contains nerves, plexus submucosal Meissner.

Key words*: simple prismatic epithelium, gastric glands, gastric parietal cells, the main cells.*

Material and methods

The research was performed on clinicaly healthy swine stomach. The tissues have been histologicaly prepared, sectioned, stained and examined . Large sections were stained on slides after staining following methods: hematoxylin eosin, staining and Mallory (Bancroft, J.D. and A. Stevens, 1986).

The examination of the microscopic preparates was performed using: the laboratory's Nikon optic microscope; Olympus micoscope equiped with a photographic device, later the computerized integration

Results and discussion

Following research we noticed that swine stomach has a lining with numerous pleats having longitudinal folds bounded by deep ditches. 4x objective there is an overview of the stomach wall consisting of four tunics : mucosa, submucosa, muscular and serous. We examined the lining and noticed that consists of epithelium and lamina propria of mucous glands and musclaris mucosae (Figure 1, 2, 3).

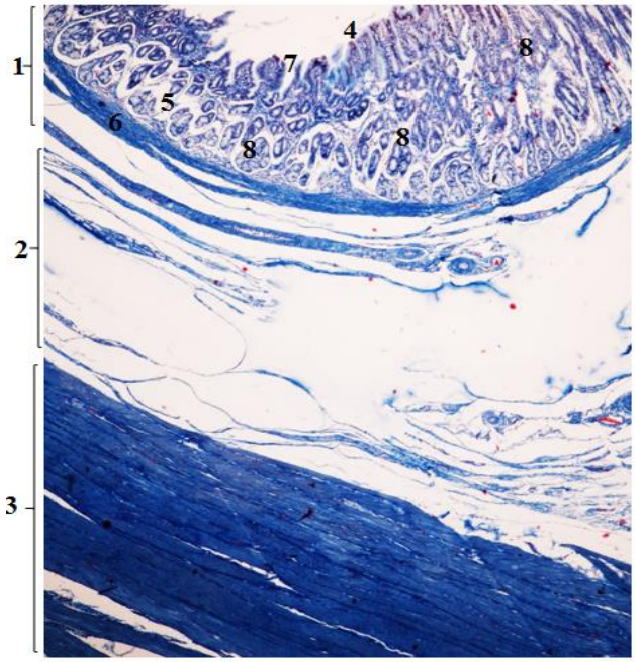

Fig. 1 Overall image of swine stomach, Mallory stain, 4x objective; 1-mucosa; 2-submucosa; 3-muscularis; 4-simple prismatic epithelium; 5 –lamina propria; 6-muscularis mucosae; 7-gastric crypts; 8-gastric glands.

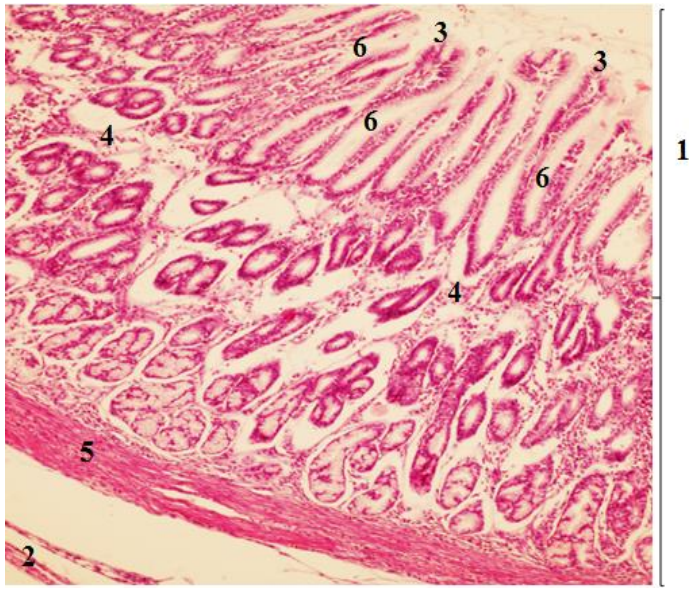

Fig. 2 Histological structure of the mucosa and submucosa in the swine stomach, 10x objective, HE stain;
1-mucosa; 2-submucosa; 3-simple prismatic epithelium; 4-lamina propria; 5-muscularis mucosae; 6-gastric crypts.

With the 20x lens is observed that the lamina propria glands are characteristic. Underlying glands are conjunctive condensed area (Figure 4,5,6) . The bulk of the gastric mucosa was occupied by the gastric glands which opened singly or in groups into the gastric pits. On the distal side of the limiting ridge, the stratified squamous epithelium of the non-glandular stomach transitioned abruptly to the simple columnar epithelium with interspersed surface mucous cells as reported earlier (Suckow et al., 2006).

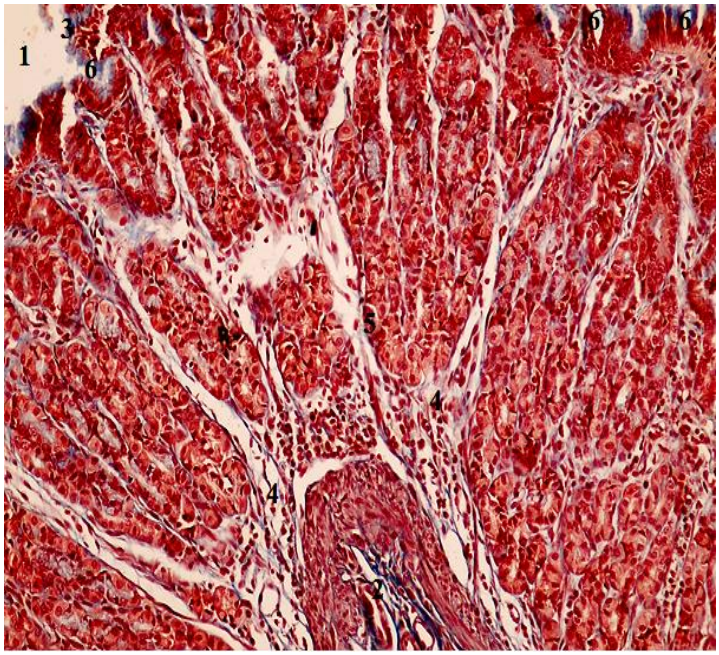

Fig. 3 Histological structure in swines, Mallory stain, 4x objective.
1-mucosa; 2-submucosa; 3-simple prismatic epithelium;
4-lamina propria; 5-muscularis mucoase; 6-gastric crypts.

The stomach of rat was divided into the proximal nonglandular and the distal glandular parts being separated by a fold of the non-glandular mucosa, the limiting ridge. The wall of the stomach was composed of mucosa, submucosa, muscularis and serosa as reported by (Sujin et al. 2008). With the 10x objective we examined gastric mucosal epithelium and noticed a simple prismatic epithelium that invaginate from place to place and forms the crypts gastrice (Nitovski A, Bisa Radović , Dragana Grčak , Valentina Milanović , Milena Potić , Milenković M , Grčak M, 2015). With the 10x objective we examined lamina propria composed of loose connective tissue infiltrated by lymphocytes and noticed that muscle lining is composed of smooth muscle fibers (Kierszenbaum A., 2011). With the 40x objective the apical pole of the cells are examined and observed that the secreted mucus accumulates in granular form from the apical pole of the cells (Solcan Carmen, 2006). The cardiac gland region was present at the junction of the fore-stomach and glandular stomach as a narrow band on the distal side of the limiting ridge (G. S. S. Chandana, 2013). The simple prismatic epithelium examined consists of two types of cells: high prismatic, located in the third round with core basal and basal cells that are grouped in the bottom of the crypts. We observed high prismatic cells with apical microvilli and basal cells from pole to pole dilated basal and apical

pole tapered, narrower allowing their location at the base of crypts. The fundic gland region was maximum and occupied the entire area between the cardiac and pyloric regions. The proper gastric glands were simple tubular and longer than cardiac glands (G. S. S. Chandana, 2013).

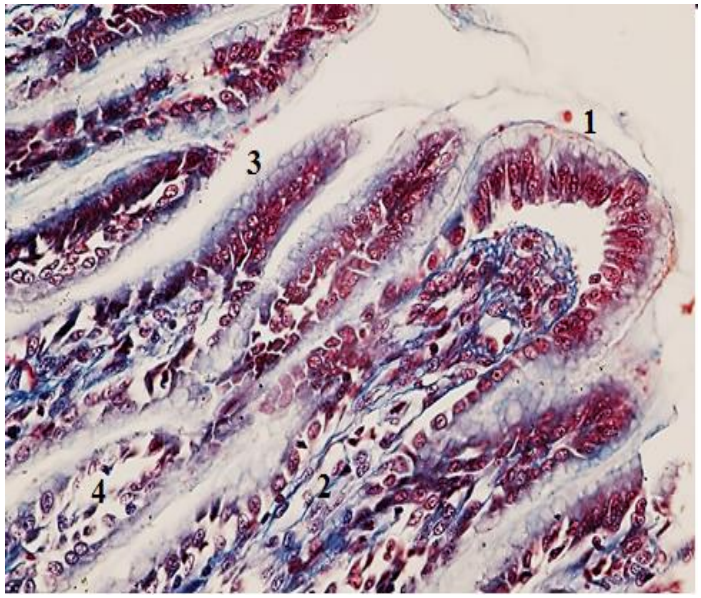

Fig. 4 Histological structure of the piloric mucosae in swines, Mallory stain, 20x objective. 1-simple prismatic epithelium; 2-lamina propria; 3-gastric crypts; 4-gastric glands.

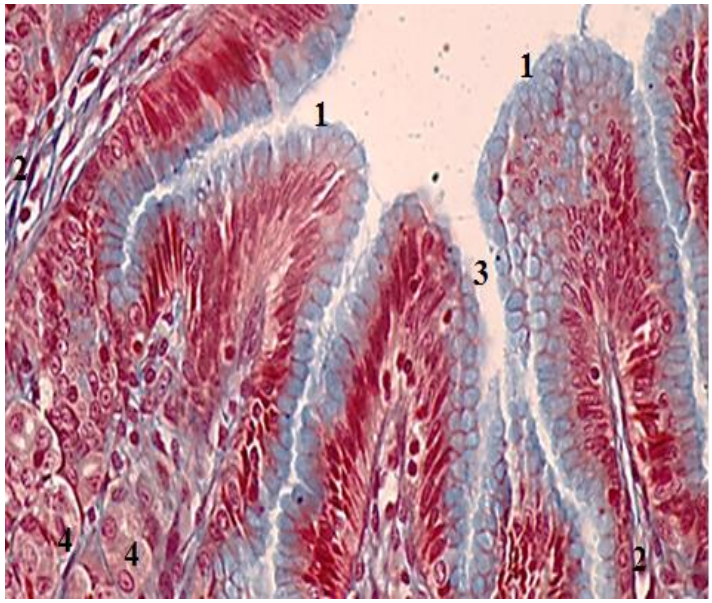

Fig. 5 Histological structure of the mucosa in the swine stomach (fundic region) , Mallory stain, 40x obiective; 1-simple prismatic epithelium; 2-lamina propria; 3-gastric crypts; 7-glandular cells.

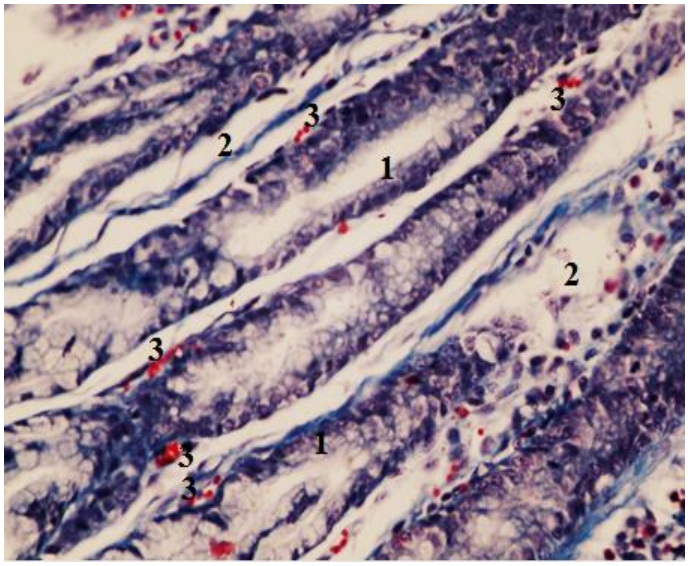

Fig. 6 Histological structure of piloric glands of the swine stomach,
Mallory stain, 40x objective;
1-glandular epithelium; 2-lamina propria; 3-capilaries.

Fundus the mucous membranes of the stomach pigs, horses and dogs is thicker than glandular mucous membranes in other regions of the stomach. It is darkly red, bumpy and educates the folds in the stomach.

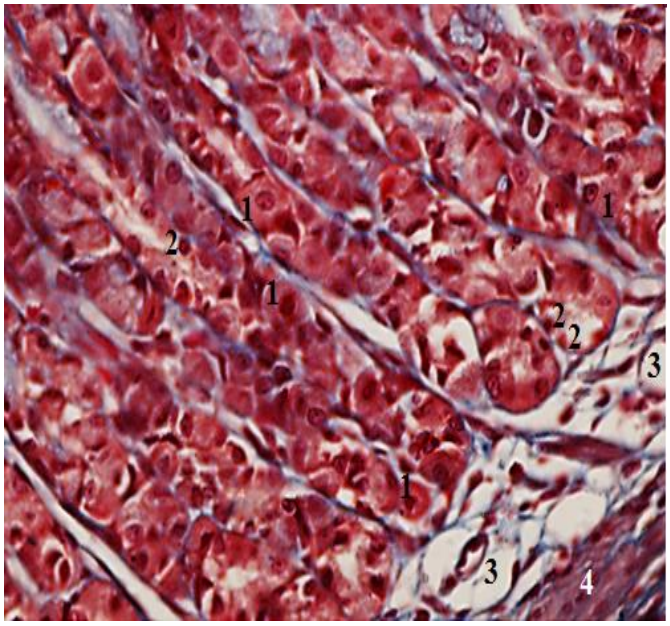

Fig.7 Detailed aspect of the gastric glands, Mallory stain, 40x objective.
1-parietal cells; 2-principal cells; 3-lamina propria;
4- muscularis mucosae.

These folds extend in different directions. On fundus mucose perceive the recess (foveoles gastricae) and furrows that share this area of mucous membranes in the lower fields (area gastricae). Landscape holdings mucous membrane (pars fundic) in pigs stretches along the ventral part of the large curvature of the stomach. It lines the cranial and caudal wall of the stomach, but does not reach the small curvature of the stomach. Fundus mucous membranes in the stomach of the horse represents about 2/3 to 3/5 of glandular mucosal his stomach (Nitovski A, et al., 2015). With the 40x objective is noted that the composition glands enter several types of cells: main basophils ; parietal cells , oxintic , delomorfe and undifferentiated cells .

Parietal cell (also called oksintic cells) contain highly branched intracellular tubules. Hydrochloric acid is produced on tufting outcrops in these ducts, and then sinks to the secretory tubules end cells (Arthur C. Guyton and John E. Hall, 2008).

With the 40x objective is noted that the base gland cells arranged principally they appear grouped into nests and are the most numerous cells (Figure 7).

These cells are cubic, small have basophil cytoplasm, nucleus euchromatic , small and round 40x objective is noted that prevails parietal cells in the body gland , they are round or oval , large that protrudes outside the gland. The glands of the cardiac and pyloric mucosal regions resemble those of the parietal area in structure but contain different cell types. The pyloric glands have noparietal cells but contain the gastrin - producing G cells. According to most reports, the pyloric glands to secrete pepsinogen. (James G. Cunningham and Bradley G. Klein, 2007). Muscle lining is made of two layers of smooth muscle organized on two levels: internal circular and external longitudinal (Cornilă, N., Raita Ștefania Mariana, 2013).

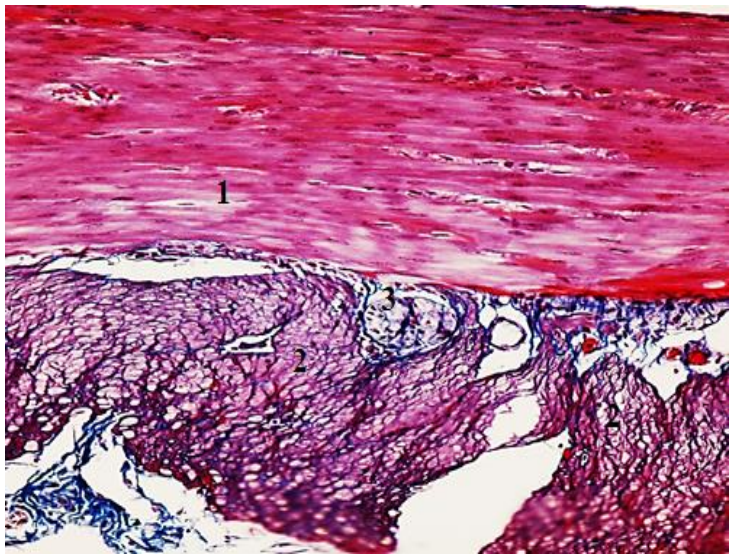

Fig. 8 Histological structure of the muscular tunic, 20x objective,
Mallory stain; 1-longitudinal muscular stratum; 2-transversal muscular stratum;
3-Auerbach nervous myenteric plexus.

Conclusions

On histological examination there is an overview of the stomach wall consisting of four tunics: mucosa, submucosa, muscular and serous.

Simple prismatic epithelium consists of two types of cells: high prismatic, located in the third round with core basal and basal cells that are grouped in the bottom of the crypts. We observed high prismatic cells with apical microvilli and basal cells from pole to pole dilated basal and apical pole tapered, narrower allowing their location at the base of crypts. Glands fund, which are the most numerous, straight appear in the upper and lower third bifurcated and these appear sectioned obliquely. The composition glands enter several types of cells: main basophils; parietal cells, oxintice, delomorfe and undifferentiated cells.

References

1. Arthur C. Guyton, John E. Hall (2008): Textbook of Medical Physiology, Translate Modern Administration, Belgrade, 2008, p. 771st.
2. Bacha, J.JR, 2011; Wood LM- Color atlas of veterinary histology. Third ed.,Ed.Willy-Blackwell.
3. Bancroft, J.D. and A. Stevens, 1986. Theory and Practice of Histological Techniques. ChurchillLivingstone, London.
4. Cornilă, N., Raita Ștefania Mariana, 2013- Biologie celulară, histologie și embriologie, Vol II, Ed.Ceres Bucuresti.
5. Dănacu Valerica, 2015- Histology and Embryology Animal Docendi Ars Publishing, Bucharest
6. Gartner I P., Hiatt J.L., 2011-Concise Histology,Saunders Elsevier.
7. G. S. S. Chandana, P. V. S. Kishore, N. K. B. Raju, M. Sreenu, G. Srinivasa Rao, 2013- Histological Studies on the Stomach of Albino Rat (Rattus norvegicus), Indian Journal of Veterinary Anatomy 25 (2): 107-108.
8. James G. Cunningham and Bradley G. Klein (2007): Textbook of Veterinary Physiology, Fourth Edition, Saunders Elsevier, p.300-302.
9. Lucian Ionita, Carmen Fierbințeanu Braticevici, Andrei Tănase, Carmen Ionita, Gheorghe Câmpeanu and Simona Ivana, (2009).-Preliminary experiment in the healing acceleration and tissue recovery in animals (rabbits) with the application in the plague of an extract of Benincasa hyspida. ARS Docendi, Bucharest, Romania, Romanian Biotechnological Letters.
10. Kierszenbaum A., 2011 -Histology and Cell Biology:An introduction to Pathology Ed.Elsevier Healt Sciences,.
11. Nitovski A, Bisa Radović , Dragana Grčak , Valentina Milanović , Milena Potić , Milenković M , Grčak M, 2015- Fluorescent Microscopy of Gastric Mucosal Tissue of Cattle and Pigs, International Journal of Agriculture Innovations and Research Volume 4, Issue 1, ISSN (Online) 2319-1473.
12. Solcan Carmen, 2006-Histology and Embryology, Ed.Performantica, Iasi,.
13. Seicaru Anca, 2016- The biodiversity of the mammary lymph nodes at ruminants, Scientific Works, Vet. Med Timisoara.

RESEARCH ON SWINE CHEEKS AND TONGUE HISTOSTRUCTURE

Valerica DANACU[1], Stefania Mariana RAITA[1], Viorel DANACU[2], Carmen IONIȚĂ[1], Luciana Madalina ICHIM[1]
[1]FMV Bucharest; [2]ANSVSA Bucharest
valericadanacu@yahoo.com

Abstract
In histological examination we noticed histostructural pigs cheeks, as evidanced by the buccal mucosa, muscle layer and skin. Connective tissue is dense semimodelat, predominantly collagen fibres arranged in bundles. Seromucoase is observed numerous small glands, blood supply and innervation rich. Lingual mucosa, stratified squamous epithelium presents a slightly keratinized. Lingual mucosa appears smooth on the ventral side of the tongue and the lingual papillae on the dorsal presents represented: conical papillae, filliform papillae, fungiform papillae, papillae and buds tinted circumvalate. The tongue is an organ formed musculo-membranous striated muscle tissue oriented in different planes, blood vessels, nervous and glandular formations. The tongue has a stratified squamous epithelium covered with a slightly keratinized tissue, and in the back of the tongue called pappilae are very protruding. The buccal mucosa consists of stratified squamous epithelium keratinized slightly, showing a histostructural lamina propria of loose connective tissue and glands tubulo-acinar forming intramural salivary glands. With 10x objective type mucosa is observed on the dorsal sensory, stratified squamous epithelium is keratinized and lingual papillae are four types: filiform, fungiform, tinted and circumvalate. Lamina propria under the epithelium and consists of dense connective tissue, salivary glands are presented thin lingual mucous or mixed type. Body mass is mostly muscular, skeletal muscle consists of bundles arranged in different planes Tongue muscle consists of striated muscle fibres bundles sectioned longitudinal, transverse or horizontal. Striated muscle fibres are oriented in different planes, with characteristic cross-banding. Between striated muscle fibres of connective tissue, are present numerous fibroelastic, blood vessels and nerves.
Key words*: stratified squamous epithelium keratinized, tubulo-acinar glands, skeletal muscle tissue*

Material and methods

The research was conducted on permanent histological preparations taken from pork tongue, clinically healthy. Histological specimens were prepared as follows: 10% formalin fixing, paraffin embedding and sectioning inclusion microtome. Large sections were stained on slides after staining following methods: hematoxylin eosin and Mallory (Bancroft, J.D. and A. Stevens, 1986).

By following successively and accordingly to the experimental plan, rigorous morphological studies were conducted using optical microscopy photomicrographs.

Histological preparations obtained were examined by light microscopy Labophot type 2 shooting device equipped with Nikon DX AFK-making photomicrographs.

Results and discussion

On histological examination it is noted that language is made up of striated muscle tissue oriented in different planes, blood vessels, nervous and glandular formations. With 4x objective is observed that tongue is covered with stratified squamous epithelium slowly keratinized, and in the back of the tongue rare lingual papillae are observed. With 10x objective sensitive type mucosa is observed in the back of the tongue and the epithelium is stratified squamous keratinized (Figure 1, 2).

Figure 1. Histostructural aspect of a foil papillae on the dorsal side of the tongue, ob.10x; HE coloration; 1-dorsal side; 2- foiled papilla; 3-lamina propria; 4-blood vessels; 5-conjunctive tissue.

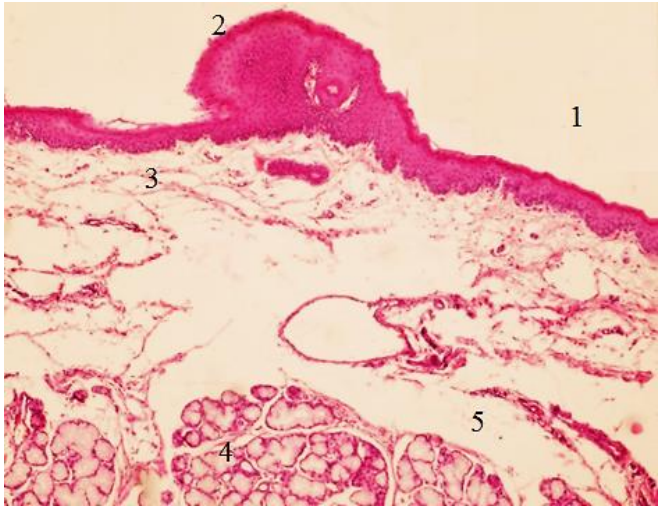

Figure 2.Histostructural aspect of a fungiform papillae on the dorsal side of the tongue, ob.10x; HE coloration; 1-dorsal side; 2- fungiform papilla; 3-lamina propria; 4- glands; 5-conjunctive tissue.

Lingual mucosa appears smooth on the ventral side of the tongue and lingual papillae are presented on the dorsal side, represented by: conical papillae, filiform papillae, fungiform papillae, foliated papillae and circumvalate papillae (Cornilă, N., Raita Ștefania Mariana, 2013).On histological examination we divided the tongue on three zone anterior, middle, and posterior parts (Saleh, K.Majeed ; Alaa , H.Saadon ; Samira A. Daaje, 2014). The anterior part covered externally by keratinized stratified sequamous epithelial tissue , deep to it lamina properia with skeletal cells and phagocytes with collagen fibers intermingled with skeletal muscle cells (Sh.A.Al-Zahaby , E.H.Elsheikh, 2014). Under skeletal muscle the adventitia

consist of adipose tissue while the middle part consist of stratified squamous tissue more cellular than anterior , the lamina properia consist of skeletal muscle intermingled with few collagen fiber. Lamina propria is under the epithelium and consists of dense, thin conjunctive tissue. With 40x objective is observed that in lamina propria lingual salivary glands are presented, mucous or mixed type (Figure 3, 4).

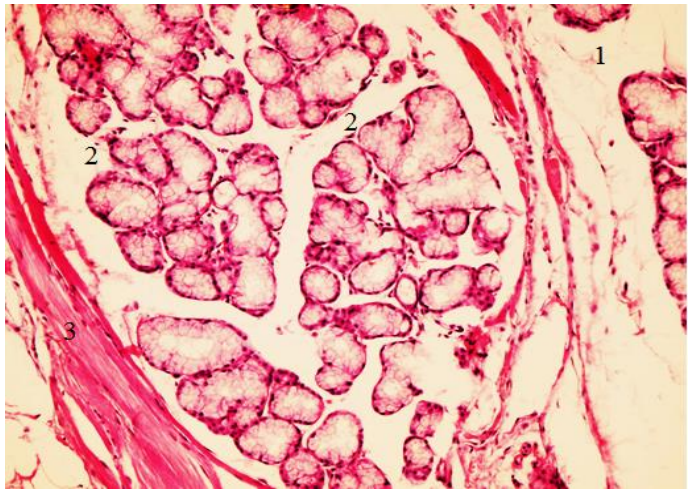

Figure 3.Histostructural aspect of lingual salivary gland and tongue musculature, ob.10x; HE coloration;1-lamina propria; 2-lingual salivary gland; 3- skeletal muscle tissue.

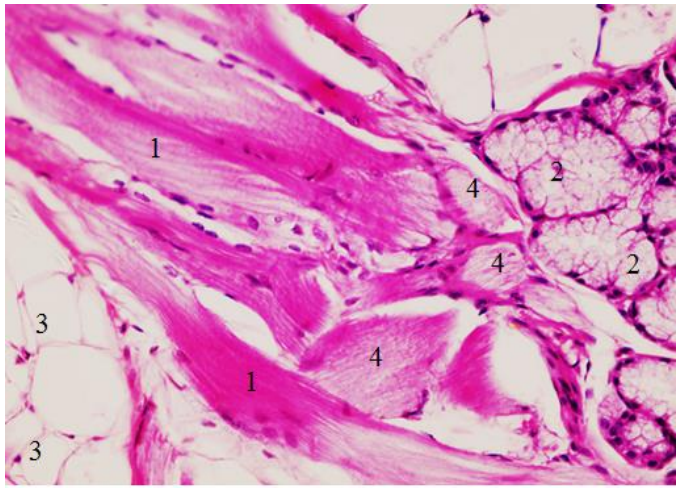

Figure 4. Histostructural aspect of tongue muscular tissue ob.40x; HE coloration; 1-longitudinal sectioned skeletal muscular tissue; 2- lingual salivary gland; 3-adipose tissue; 4-skeletal muscular tissue obliquely sectioned.

With 4x objective is noted that the organ mass is mostly muscular, consisting of skeletal muscle bundles arranged in different planes (Figure 5). In the submucosal layer, mucous salivary glands were surrounded by connective-tissue capsules, with septa dividing the glands into lobes (Guimarães JP; Maei, RB ; Carvalho , HS and Watanabe , IS. 2009).

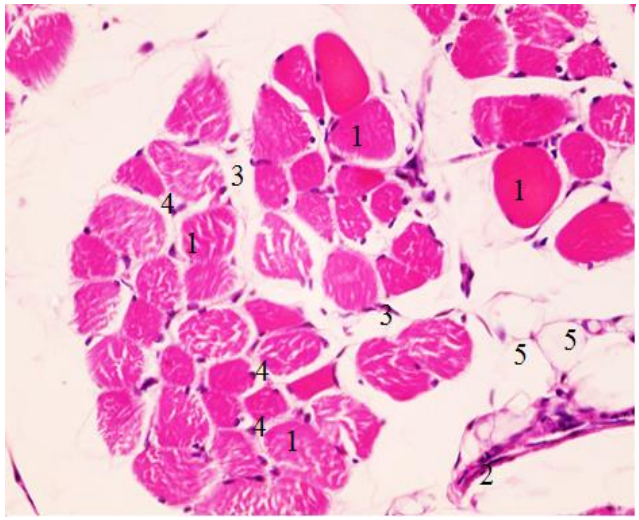

Figure 5. Detailed image of tongue skeletal muscular tissue ob.10x; HE coloration;
1-skeletal striated muscle fibers transversely sectioned; 2-epimisium;
3-perimisium; 4-endomysium; 5-adipose cells.

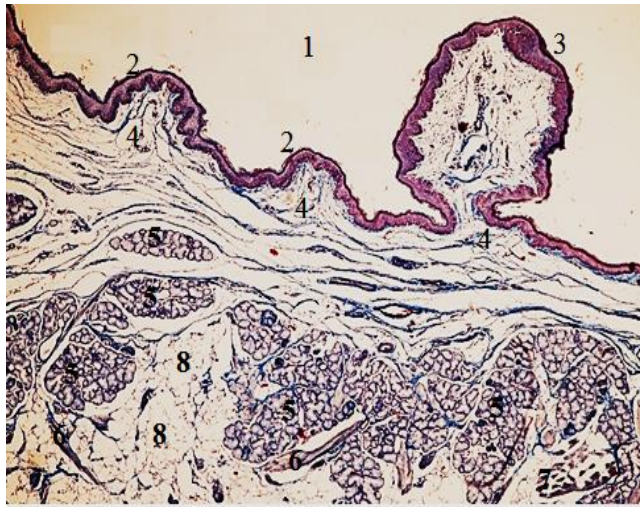

Figure 6. Histostructural aspect of the tongue, ob.4x; Mallory coloration;
1-dorsal side; 2- fungiform lingual papillae; 3-lingual filiform papilla;
4-lamina propria;5-lingual salivary gland; 6-striated muscle fibers longitudinally sectioned;
7-striated muscle fiber transversely sectioned; 6-white adipose tissue.

With 10x objective is observed that tongue musculature is made of striated muscular fiber bundles longitudinally, transversely or horizontally sectioned. Striated muscular fibers are oriented in different planes, with characteristic cross-banding. Between striated muscular fibers fibroelastic connective tissue fibers are presented with numerous blood vessels, nerves (Figure 6, 7).

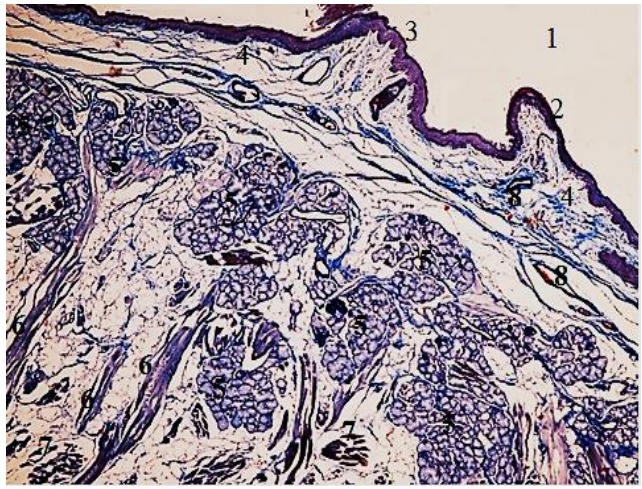

Figure 7. Histostructural aspect of the tongue, ob.4x; Mallory coloration; 1-dorsal side; 2-foiled lingual papilla; 3- circumvalată lingual papilla; 4-lamina propria; 5-lingual salivary gland; 6-striated muscle fibers longitudinally sectioned; 7-striated muscle fiber transversely sectioned; 8 blood vessels.

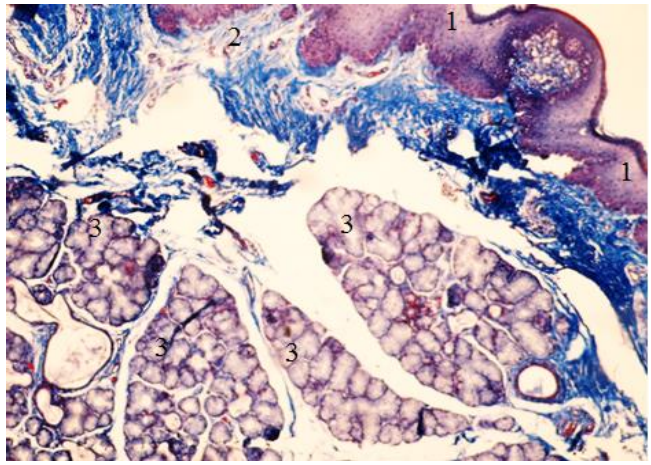

Figure 8. Histostructural aspect of the tongue, ob.10x; Mallory coloration; 1- stratified squamous keratinized epithelium ; 2-lamina propria; 3-lingual salivary glands;

With 10x objective is noted that the taste bud is an ovoid, intraepithelial formation. It is in contact with the basal membrane of the coating epithelium,it doesn't get to the surface and it opens through the pore mouth (Figure 8, 9).

With 40x objective is noted that the taste bud consists of several types of cells: on the basal menbrane, reserve, cubic cells are located, having a generator role.

Tall epithelial cells have supporting role and voluminous nucleus, also the cytoplasm is pale colored; epithelial cells acting as receptors are tall, very narrow, elongated, with heterocromatic nucleus.

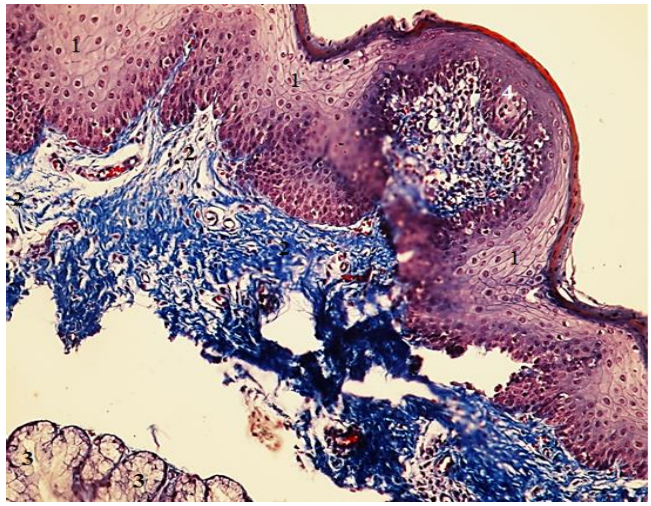

Figure 9. Detailed image of a fungiform lingual papillae and of a taste bud ob.20x; Mallory coloration; 1-stratified squamous keratinized epithelium; 2-lamina propria; 3-lingual salivary glands; 4-taste bud;

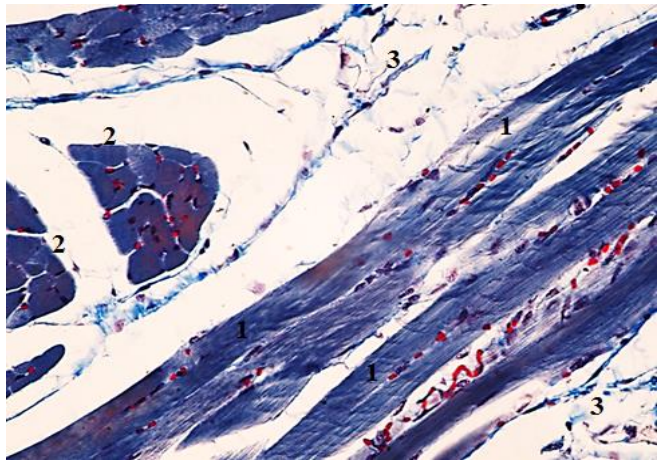

Figure 10. Skeletal muscular tissue from tongue, Mallory coloration, ob. 40x; 1-longitudinal section; 2 cross-section; 3- connective tissue fibers.

With ob.40x is observed that the nuclee are oval, peripheral alternating under the sarcolemma, heterochromatic and presents 1-2 nucleolus. In a musclar fiber are hundreds of thousands of myofibres arranged from end to end of muscular fiber, grouped into parallel beams forming Leydig colonette. With 40x objective is noted that cross-section beams appear as polygonal, point areas called Cohnheim fields. Each fiber is surrounded by a soft conjuctive tissue, called endomysium. Several adjoining muscular fibers fibers form a primary beam covered by perimisium, and the muscle as an organ is covered by epimisium (Figure 10).

Although stratification is a common feature of all parts of the oral epithelium of mammals, keratinization is normally associated with the masticatory oral mucosa that surrounds the dorsal part of tongue and seems to be related to the provision of protection against

damage through wear, to tissue (Stern, 1980). The labial and buccal mucosa, which lie very close to the opening of the mouth, persist in being non-keratinized (Abayomi T.A. et all, 2009).

Conclusions

Lingual mucosa, presents a slightly stratified squamous keratinized epithelium. Lingual mucosa appears smooth on the ventral side of the tongue and presents lingual papillae on the dorsal side, represented by: conical papillae, filiform papillae, fungiform papillae, foliated papillae and circumvalate papillae. In histological examination it was noticed that in the lamina propria lingual salivary glands are presented, mucous and mixed type.

On Mallory coloration, the taste bud is observed in the composition of a fungiform lingual papillae.

It is observed that taste bud is in contact with the basement membrane of the coating epithelium.

The muscular fibers are cylindrical, elongated, slightly rounded at the ends. It is noted that in striated muscular fiber structure are included: sarcolemma, or the skin cell, numerous nuclee and sarcoplasm and with 40x objective is observed that the nuclee are oval, peripheral alternating under the sarcolemma, heterochromatic and presents 1-2 nucleolus.

References

1. Abayomi T. A.; David A. Ofusori; Oladele A. Ayoka; Samson A. Odukoya; Emmanuel O. Omotoso; Frank O. Amegor; Sunday A. Ajayi; Gideon B. Ojo & Oladele P. Oluwayinka- . A comparative histological study of the tongue of rat (Rattus Norvegicus), bat (Eidolon Helvum) and pangolin (Manis Tricuspis). Int. J. Morphol., 27(4):1111-1119
2. Bancroft, J.D. and A. Stevens, 1986. Theory and Practice of Histological Techniques. ChurchillLivingstone, London.
3. Cornilă, N., Raita Ștefania Mariana, 2013- Biologie celulară, histologie și embriologie, Vol II, Ed.Ceres București.
4. Dănacu Valerica, 2015- Histology and Embryology Animal Docendi Ars Publishing, Bucharest
5. Guimarães JP; Maei, RB ; Carvalho , HS and Watanabe , IS. 2009. Structures of the dorsal surface of the Ostrich's(Struthio Camelus) tongue . J of Zoolog sci 26 (2) .
6. Iswasaki, S 2002. Evaluation of the structure and function of the vertebrate tongue. J of anatomy 201 : 1-14 .
7. Martinez, M.; Stefanini, M. A.; Martinez. F. E.; Guida, H. L.; Pinheiro, P. F. F.; Almeida, C. C. D. And Segatelli, T. M. 2003- Morphological study of the tongue of the budgerigar (Melopsittacus undulatus) . Int. J. Morphol., 21(2):117-122 .
8. Saleh, K.Majeed ; Alaa , H.Saadon ; Samira A. Daaje, 2014- Morphological , Anatomical and Histological studies on goose tongue, Basrah Journal of Science (B), Vol. 32(1),76-88.
9. Solcan Carmen, 2006-Histology and Embryology, Ed.Performantica, Iasi,.
10. Sh.A. Al-Zahaby , E.H. Elsheikh, 2014-Ultramorphological and histological studies on the tongue of the common kingfisher in relation to its feeding habit, The Journal of Basic & Applied Zoology
11. Seicaru Anca, 2015-The considerations on head and neck lymphocenters morphotopography in guineea pig, Scientific Works, Vet. Med Iasi.
12. Stern, I. B. Oral mucous membrane. In: Orban's Oral Histology and Embryology, 7th Ed. Bhaskar, S. N. (ed.), St. Louis, Mosby Co, 1980.

MORPHOLOGICAL AND TOPOGRAPHICAL PARTICULARITIES OF SOME LYMPH NODES FOR HOUSE RABBIT

Anca ŞEICARU
Faculty of Veterinary Medicine of Bucharest, SplaiulIndependenței 105, sector 5,
Email: ancaseicaru@gmail.com;

Abstract
In the present study it was investigated some lymph nodes in the: cephalic region, cervical region, limbs region, and also the cavitary lymph nodes - abdominal cavity. The lymph nodes have generally at this species a grey-ash colour being represented by several lymphonodal units. The lymph nodes at house rabbit have a lighter colour when compared to other rodents. The perilimfonodular amount of fat tissue is reduced compared with other laboratory rodents. Through the regional and stratigraphical dissection have been kept the physiological relations between lymphnodes and the formations close to them. In this investigated regions it was made also the dissection of the vascular-nervous formations of the musculature.
Keywords*: home rabbit, lymph nodes, dye, lymphatic vessels.*

Introduction

Extending the knowledge of the lymphatic system at leporidae brings additions and justifies the research in this field, and the new particularties described will supplement the scientific knowledge (Azargoshas B.K., 1963, Ciudin Elena, 1996, ViorelDanacu, et. al., 2013).

The laboratory rodents are commonly used for testing a vast array of drugs. Knowledge of the topography and morphology of the lymphatic system at this species can provide an assessment with respect to its pathological aspects. In laboratory, the examination of the lymphatic structures orientates from the necropsy point of view, not only for the diagnose establishing.These animals are also used as pets (Baciu I., 1977,Predoi, G., Belu, C., 1995, Predoi, G., Belu, C., 2001)

Materials and methods

For this study were usedfive house rabbits of both sexes, Oryctolaguscuniculus species, all clinically healthy. The rabbits belong to the Leporide family, Lagomorpha order, Glires supraorder. The animals were separated in the group of growth for three days before the injection of the dye.

For the morphotopographical study of some lymph nodes was used China ink solution 40% saline, 20 minutes filtered through a filter paper before using.

Injection of the dye solution was carried out in the following points of election: plantar and palmar pads until forming a local intradermic button (dose of 0.5 ml); tip of the nose, caudal face of the concha, lower lip (dose of 0.3 ml); nearby the flank region (dose of 0.2 ml).

Abdominal lymph nodes were stained by the method of intraperitoneal injection on the white line, in separate points, with ink dye in a dose of 1.5 ml, where syringes with atraumatic needle were used. The visualization of the lymphatic vessels after injecting the dye was needed because the dye was crossing them rapidly. The lymph nodes remain coloured for a long time.

The methods used were stratigraphical and regional dissection, using also the stereomicroscope Nikon.

Results and discussions

Cephalic lymph nodes

Mandibular lymph centres represented by rostral and aboral mandibular lymph nodes. The rostral mandibular lymphnode is represented by a lymphatic formation about 0.5 mm length with oval appearance. Is situated on the ventral and cranial edge of the jaw, nearby the facial vein, near the ventral edge of pterygoid medial muscle.

The aboral mandibular lymph nodes appear disposed behind the lingofacial vein. They are represented by two lymph nodes, in size of 0.6 mm and 0.4 mm respectively, with oval form, located close to each other*(figure 1).*

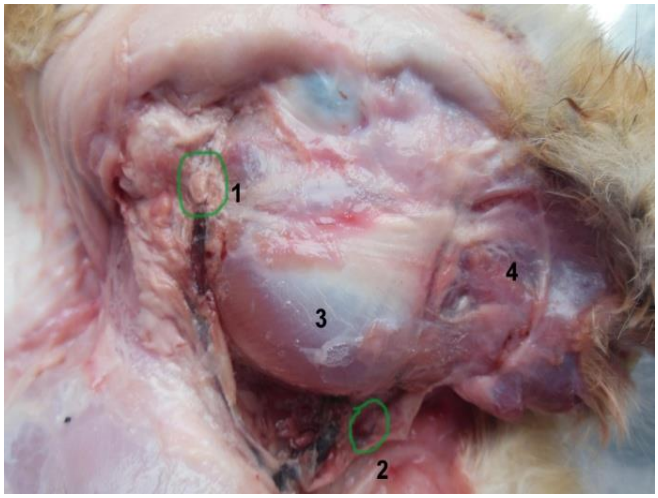

Figure 1– Mandibular lymph nodes
1 – Ln.parotidian at the origin of transversal face artery and vein;
2 – Ln.mandibular on the sublingual artery; 3 – M.masseter; 4 – M.buccinator.

Afferent lymphatic vessels are coming from the portion of the upper region of the neck. Efferent lymph vessels are tributaries for ventral superficial cervical lymph nodes.

Parotid lymph node is represented by an oval lymph node of about 0.7 mm along the course of the transversal face artery and vein. It is disposed caudal by the masseter muscle and anterior by the parotid gland and it is not covered by the parotid gland.

Afferent vessels come from the parotid region, the dorsal half of the head region, the mastoidian region. Efferent lymph vessels are tributaries to superficial cervical lymph nodes.

The anterior limb lymph centre

The axillary accessory lymph nodes are represented by twonearby unequal lymph nodes (0.3-0.5 mm), which are rounded. They are disposed close by thoracodorsal artery and vein.

Afferent lymphatic vessels are coming from the medio-caudal portion of the thoracic limb. The efferent lymhpatic vessels are tributary to the own axillary lymph node *(figure 2).*

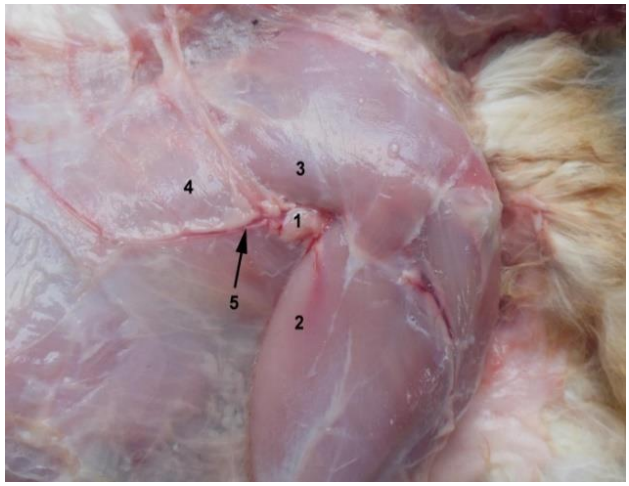

Figure 2 – Axillary accessory lymph nodes
1- Axillary accessory lymph nodes; 2 – The long portion of brachial triceps muscle;
3 – Subscapular muscle; 4 – Great wide dorsal muscle; 5 – Thoracodorsal artery and vein

The pelvic limb lymph nodes

The subiliac lymph node is disposed at the cranial edge of the fascia lata tensor muscle, near the ilium bone. Here appear two globular lymph nodes *(figure 3).* The subiliac lymph node is located on the deep circumflex iliac artery.

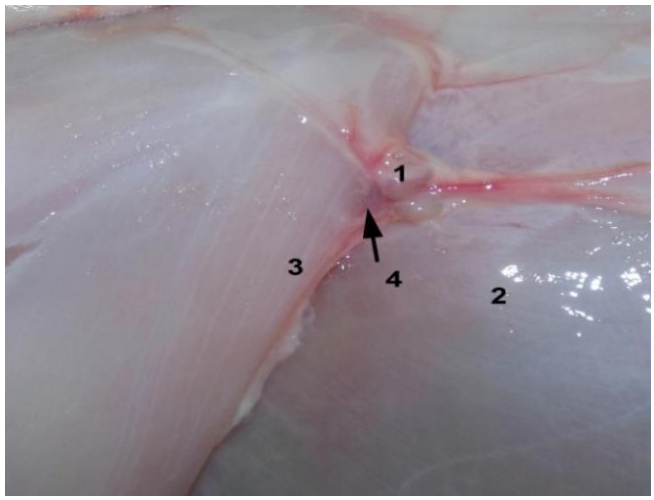

Figure 3. Subiliac lymph nodes
1 – Ln.subiliac; 2 – Ventrolateral abdominal musculature; 3 – Cranial edge of tensor of fascia lata muscle; 4 – The branch of deep iliac circumflex artery.

The abdominal cavity lymph centres

The cranial mesenteric lymph centres represented by a lymph centre, in size of 1.7 cm, on the origin of the cranial mesenteric artery *(figure 4).*

Afferent lymphatic vessels are collecting the lymph from the jejunum and ileum. Efferent lymph vessels participating in the formation of visceral lymphatic trunk.

Gastric lymph nodes are formed by two groups of lymph nodes of two ovoid lymphatic structures near the pylorus *(figure 5)*. This gastric lymph nodes have a dimension of 2 mm.

Jejunal lymph nodes appear on jejunal arteries path, perpendicular branch and have dimensions of about 2 mm.

Afferent lymphatic vessels come in from the jejunum and ileum. The efferent lymphatic vessels are tributary to the cranial mesenteric lymph centre (*figure 6*).

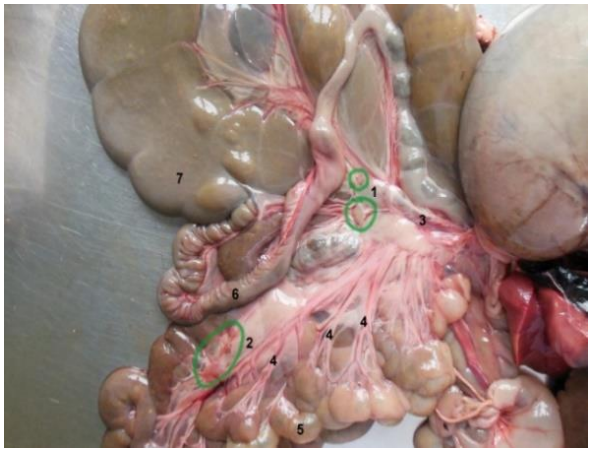

Figure 4 Cranial mesenteric artery

1 – Cranial mesenteric lymph nodes; 2 – Jejunal lymph nodes; 3 – Cranial mesenteric artery; 4 – Jejunal artery branches; 5 – Jejun; 6 – Ascending colon; 7 – Cecum.

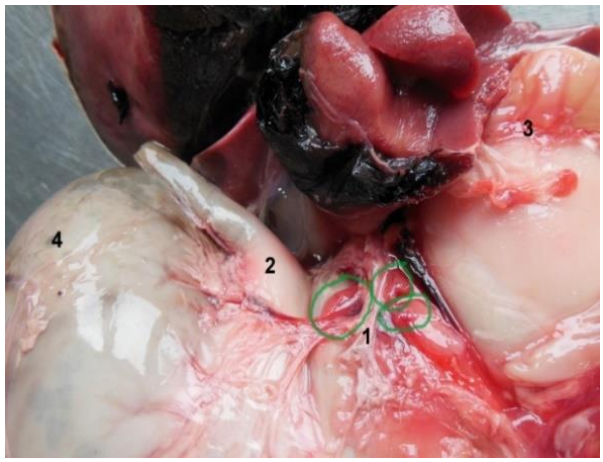

Figure 5 – Gastric lymph nodes

1 – Gastric lymph nodes; 2 – Oesophagus; 3 – Pylor; 4 – Left stomach extremity.

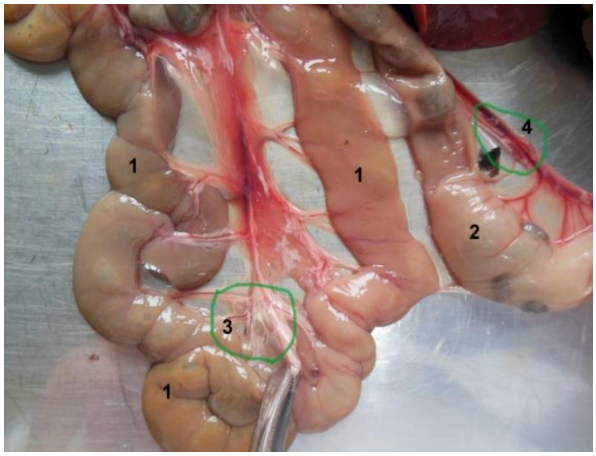

Figure 6 - Jejunal lymph nodes
1 – Jejunal; 2 – Descending colon; 3 – Jejunal lymph node; 4 –Small mesenteric.

Conclusions

At leporidae great epiploon is a lymphoid structure due to the existing peritoneal macrophages.

Subiliac lymph nodes are disposed at this species in the flank region, nearby the ilium bone and it can be palpated transcutaneous.

Mandibular lymph nodes cannot be palpable transcutaneous and are located in a small amount of fat.

The axillary accessory lymph node is located near the half tricipital lane.

The cranial mesenteric lymph centre ishighly developed, being formed by many small lymph nodes. This lymph centre in surrounding the origin of the mesenteric cranial artery, where is located.

Bibliogrphy

1. Azargoshas B.K. (1963) –Ductus Thoracicus lymph der Ratte. Ein Beitragzure xperimentallen Untersuchuna metodik der lymphogenen Kreb Metastasierung. Z. Gesauite, Exp. Met., 134, 541-553.
2. Baciu I. (1977) – Fiziologie, Ed. Did. Si Ped., Bucuresti.
3. Ciudin Elena, Marinescu, D. (1996) – Animale de laborator, Ed. All, Bucuresti.
4. Viorel Dănacu, Valerica Dănacu, A. T. Bogdan(2013) - Comparative morphotopographic research on popliteal lymphocenter in leporidae, Bulletin of University of Agricultural Sciences and Veterinary Medicine, Cluj-Napoca.
5. Predoi G., Belu C. (2001) – Anatomia animalelor domestice, Ed. All, București.
6. Predoi G., Belu C. (1995) – Cercetări asupra vascularizației venoase cefalice la caprine. Lucr. șt. UȘAMV, seriaC, vol. XXXVII, București.

MORPHOLOGICAL AND TOPOGRAPHICAL CONSIDERATION OF SOME LYMPH CENTRES OF THE PELVIC LIMB AT THE LABORATORY RAT

Anca ŞEICARU
Faculty of Veterinary Medicine of Bucharest, SplaiulIndependenței 105, sector 5,
Email: ancaseicaru@gmail.com;

Abstract
At the pelvic limb the lymph centres are represented by the following structures: popliteal lymph centre,ischiatic lymph centre, superficial inguinal lymph centre, deep inguinal lymph centre. Popliteal lymph node at rat is located at the proximal insertion of the gastrocnemius muscle. Ileofemoral lymph centre is represented by the lymph nodes that are located on the proximal side of the femoral triangle. Superficial inguinal lymph nodes are arranged on either side of the penis and the female near the mammary glands. Near the buttock point ischiatic lymph centre are screened. At 5% from the investigated animals it was described the presence of the ischiatic lymph nodes.Ischiatic lymph centre is located in the proximity of the proximal insertion of the biceps femoral muscle.
Keywords: *lab rat, lymph nodes, dye.*

Introduction

On the laboratory rats,it can be examined the macroscopic aspects of normal and pathological lymph nodes from the pelvic limb. Therefore, this rat is commonly used for laboratory testing (Apostoleano E., 1925, Barone, R, 1973 CastillorR.M., 1985, Ciudin Elena, MarinescuD., 1996).

The reactivity of the lymphatic system in pathological cases it is possible to be traced to muscular lymph nodes. The aspect of the lymph nodes are particularly important for study, as they indicate the organic homeostasis (BenetatoG., 1962, ValericaDănacu, et. al., 2014, G. Predoi,et. al., 2011)

This paper is intended as an addition to existing literature data. By injecting the dye can detect network of blood vessels and lymphatic system. After injecting the dye on the laboratory rats, one can detect the lymph nodes and lymph vessels, which appearembedded in a fairly large amount of adipose tissue, which has a grey colour.

Materials and methods

For testing were used ten mature laboratory rats of both sexes. Dye solution was used 40% China ink of previously filtered through a filter paper. Was used for injection syringes of 2 ml and atraumatic needles.

The dye was introduced into the plantar cushion, until they formed a local intradermal button.For the injection the animals were restrained, and the dye was injected, with a dose of 1.5 ml.

Demonstration of the lymphatic system formations was performed using the dissection and also using the stereo microscope and Nikon SMZ-2T. The research results communicated herein may underlie to conduct new research into the lymphatic system in laboratory rats.

The plantar pad was disinfected before the substance inoculation with sanitary alcohol. Beforethe injection with ink dye was done, the animals were isolated from the growth place.

Results and discussions

At laboratory rats, without the injection of a colourful substance, the lymph nodes have

a grey pink colour. The dimensions of this lymph nodes are relatively small.

Popliteal lymph centre was represented just by one lymph node at 2mm on the path of the caudal femoral artery. Efferent vessel drains to the femoral trunks. Popliteal lymph centre is located nearby the proximal insertion of the gastrocnemian muscles.

Inguinofemoral lymph centres were represented by the subiliac lymph node and superficial inguinal lymph nodes.

The subiliac lymphnodes were represented by two lymphonodular groups with elongated aspect disposed cranial by the tensor of fascia lata muscle, in the flank region. The subiliac lymph node is situated at the limit between the third half and the lower cranial edge of the tensor fascia lata muscle.

This lymph centre is embedded in fat tissue. The afferent vessels are coming from the lateral and dorsal sides of the abdominal cavity. This afferent vessels have a particularity, as they punch the flank musculature and in this way they reach the medial iliac lymph node. The efferent vessels were tributary to the lateral iliac lymph nodes. The subiliac lymph nodes are about 3.5 mm *(figure1)*.

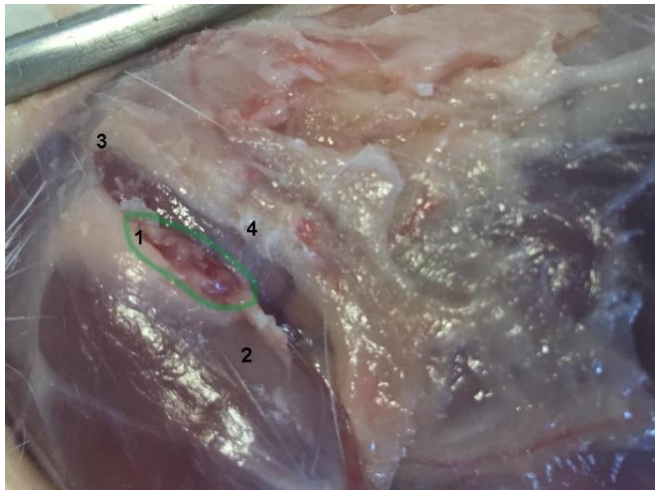

Figure 1 – Subiliaclymphnodes
1 – Subiliaclymphnodes; 2 –Quadriceps femoris muscle 3 –External iliac angle;
4 – Abdominal musculature

The superficial inguinal lymph nodesare represented by a single lymph node disposed by each part of the penis.

The scrotal lymph node is distanced from the saphenvasculonervous cordon. In 1% of the studied cases, a small lymph node was detected, with a size of 1.5 mm, disposed in lateral from the ischium bone.

At female, the superficial inguinal lymph nodes are represented by many globular formations about 2mm embedded in fat tissue. These mammary lymph nodes are disposed on the path of the cranial mammary artery.

The mammary afferent lymphatic vessels are coming from the nipples, glandular parenchyma, inguinal region and vulva.The efferent lymphatic vessels for the both sexes are tributary to the deep inguinal lymph nodes.

The deep inguinal lymph node is located nearby the saphen vasculo nervous cordon. It is represented by a single lymph node with a size of approximately 2 mm. The afferent vessels are coming from the medial side of the calf and thigh. The efferent vessels are tributary to the medial iliac lymph node (*figure 2*).

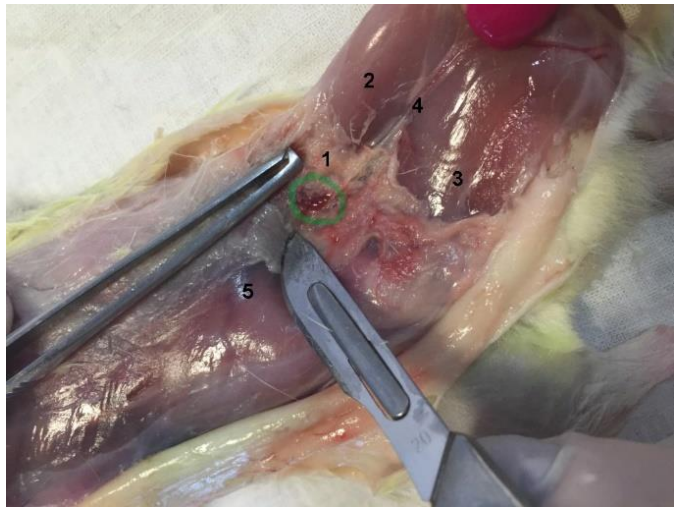

Figure 2 –Deep inguinal lymph nodes
1 – Deep inguinal lymph node; 2 – Quadriceps muscle; 3 –Sartorius muscle;
4 – Saphen vasculonervous cordon; 5 – Ventrolateral abdominal muscle

The ischiatic lymph node has a reduced dimension of approximately 1.5 mm.The ischiatic lymph nodes are situated under the medial gluteal muscle on the path of the caudal gluteal vessels. The ischiatic lymph node is located in relation with the biceps femoral muscle and sacrococcigian muscle.

The ischiatic lymph nodes has been detected in 1% of the cases.The afferent lymphatic vessels are draining the lymph from the tail region and thetight region. The efferent lymph nodes vessels are tributary to the medial iliac lymph node.

The inguinal superficiallymph nodes were distinguished through the ultrasound method *(figure 3)*.

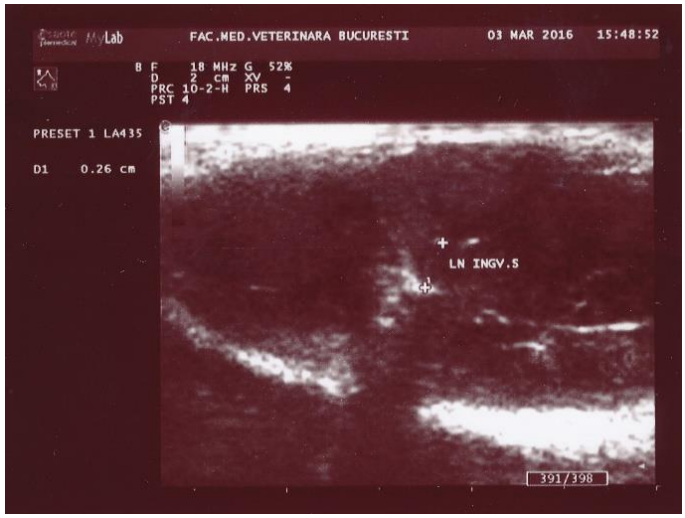

Figure 3 – Inguinal superficial lymph nodes

Conclusions

The popliteal lymph centre is situated nearby the proximal insertion of the gastrocnemian muscles.

The superficial inguinal lymph nodes can be palpated transcutaneous at female,when they present swellings.

The ischiatic lymph nodes are disposed close by the buttock, however for the laboratoryrats they appear inconstantly.

The subiliac lymphnodes have two enlongated formations, being situated on the deep circumflex iliac artery.

The deep inguinal lymph node is represented constantly by a single lymph node.

Bibliogrphy

1. Apostoleano E. (1925)–Contribution a l' étude du systène lymphatique mamaire ches les carnivores domestiques (Ètude Anatomique Physiologique et Pathologique),Thèse École Nationale Vètèrinaire d' Alfort.
2. Barone R. (1973) –Atlas d' anatomie du lapin, Ed. Masson et C-ie, Paris.
3. Benetato G. (1962)–Elemente de fiziologie normală şi patologică, Vol I, Ed. Medicală, Bucureşti.
4. Castillor R.M. (1985) –Animales de laboratorio en las investigaciones biomedicales, Ed.Cieucias medicas, Haleaua.
5. Ciudin Elena, Marinescu D.(1996) – Animale de laborator, Ed. ALL, Bucureşti.
6. Valerica Dănacu, S. Raita, V. Dănacu, C. Ioniță (2014) –Morphological studies on visceral lymph nodes of the abdominal cavity in the rabbit. Proceedings of the XXXth Congress of the European Association of Veterinary Anatomists Cluj-Napoca, Romania July 23–26, Anatomia,Histologia.
7. G. Predoi, B. Georgescu, C. Belu, I. Dumitrescu, Anca Şeicaru, Petronela Roşu (2011) – Anatomia Comparată a Animalelor Domestice,Ed. Ceres, Bucureşti.

BIOCHEMICAL ROLE OF POMEGRANATE MOLASSES IN MODULATION AND TREATMENT OF HYPERLIPIDEMIA ASSOCIATED WITH HYPERGLYCEMIA

Omayma A.R. ABOU ZAID*; SawsanM.EL.SONBATY, Neama M.A. HAMAM**
* Department, Faculty of Vet. Med. Moshtohor, Benha University, Egypt.
** Radiation Microbiology Dept, National Center for Radiation Research and Technology (NCRRT)

Abstract
Diabetes, when uncontrolled, causes dyslipidemia often followed by atherogenic abnormalities. The present study was aimed to determine the effect of Pomegranate molasses in diabetes-induced dyslipidemia. Diabetes in male rats induced by streptozotocin which showed increase in the treatment by Pomegranate molasses significantly reduced the elevated blood glucose and lipid profile levels. Thus, our study demonstrates that the consumption of Pomegranate molasses as a potential efficient natural therapeutic against induced type I diabetes accompanied with hyperlipidimic rats. Thirty two waster male rats divided into four equal groups of 8 rats. Group I (Control group): received no drugs, Group II (Pomegranate molasses (PM) group): received (500 mg /kg body weight/day) orally for 21 days. Group III (Streptozotocin (STZ) group): received intramuscular injection once by STZ (40 mg/kg body weight). Group VI :(Streptozotocin+ Pomegranate molasses (STZ+ PM)): received intramuscular injection once by STZ (40 mg/kg body weight) and after 3 days received orally PM (500 mg /kg body weight/day) daily. Treatment in groups for 21 days after diabetes induction blood. Blood samples and pancreatic tissue were collected at 22th day from treatment of PM. The obtained results showed that, rats treated with STZ showed a significant increase in glucose concentration with significant decrease in insulin level and G6PD activity. A significant increase in cholesterol, triglyceride, LDL with significant decrease in HDL levels. Also showed significant increase in MDA level and significant decrease in CAT, GPx, SOD activities and GSH level, where the liver enzymes ALT, AST significantly increased. Urea and creatinine (Kidney function) levels showed no significant changes. Animal's body weight was significantly decreased through experimental period. Histological studies of pancreatic tissue showed atrophy and pancreatic tissue damage in island of Langerhans cells. The data obtained shows that PM is potential antidiabeteic natural products and antihyperlipidemic associated with diabetes.

Key Words: *STZ, Pomegranate molasses, Diabetes, Anti-oxidant.*

Introduction

The number of patients suffering from diabetes (DM) worldwide has increased rapidly over the past few years and it is expected that the numbers will increase further from 171 million people suffering from diabetes in 2000, to 382 million in 2013 and to 592 million people by 2035 (International Diabetes Federation, 2013). Diabetes remains a major public health issue. In 2010, it was estimated that 4.787 million Egyptians suffer from diabetes, and that diabetes will increase to 8.615 million Egyptians by the year 2030 (Amer et al., 2011; Zaki et al., 2014). The costs of diabetes mellitus type I and type II are growing in all world countries. The disease management of patients with diabetes related chronic complications is very expensive (American Diabetes Association, 2013; Domeikienė et al., 2014).

Diabetes mellitus (DM) is a group of metabolic disorder and abnormally high blood glucose levels over a prolonged period and characterized by (hyperglycemia) resulting from defects in pancreatic insulin (Lin and Sun, 2010; ADA, 2012). Uncontrolled chronic hyperglycemia (Type I diabetes) or insulin resistance with or without insulin deficiency. (Type II diabetes) it is one of the primary causes of diabetic complications in a number of organs (Wang et al., 2012). This high blood sugar produces the symptoms of frequent urination, increased thirst, and increased hunger. Untreated, diabetes can cause many complications (Tang et al., 2008). Acute complications include diabetic ketoacidosis and nonketotic

hyperosmolar coma (Happich et al., 2007). Serious long-term complications include heart disease, stroke, kidney failure, foot ulcers and damage to the eyes (Tang et al., 2008). Diabetic peripheral neuropathy is the most common complication of long-standing diabetes mellitus, which frequently results in clinically significant morbidities e.g. pain, foot ulcers and amputations (Said, 2007).

Currently available therapies for diabetes include insulin and various oral antidiabetic agents such as sulfonylureas, biguanides, thiazolinedones, glinides, dipeptidyl peptidase-4-inhibitors, glucagon-like peptide-1 analogs and α -glucose inhibitors (Karow and Lang-Roth 2010).

The traditional herbal medicines plays important role in the management of diabetes mellitus. Herbal medicines have started to gain importance as a source of hypoglycemic agents (Patel and Srinivasan, 1997). Herbal products or plant products are rich in phenolic compounds, flavonoids, terpenoids, coumarins, and other constituents which show reduction in blood glucose levels (He et al., 2005; Jung et al., 2006; Ji et al., 2009).

The present work aimed to evaluate the effect of natural products as Pomegranate molasses (PM) reduce the side effects and toxicity accompanied with high potential in diabetes and hyperlipidemia.

Materials and method

Experimental animals:

Thirty two adult male Wistar strain rats of body weight 150 - 200 g. Rats were purchased from the Egyptian Holding Company for Biological Products and Vaccines (Cairo, Egypt). Rats were housed at the animal house of the national Centre of Radiation Research and Technology (NCRRT) (Cairo, Egypt). Animals were cared in accordance with the standards outlined in the guide for the Care and Use of Laboratory Animals (DHHS publication 85-23), and received food and water ad libitum. Animals were randomly divided into 4 groups (n=8).

Induction of diabetes:

Streptozotocine (STZ) powder manufactured by Sigma chemical Co. (St.Louis, USA) was used for induction of diabetes. After acclimatization for 7 to 10 days, rats were fasted for 12 hours an intramuscular injection of streptozotocine (40 mg/kg dissolved in citrate buffer, pH 4.0 body weight) once -Two days after STZ treatment, rats were considered diabetic after glucose level determination (Sri et al., 2003).

Experimental design:

Rats were randomly divided into four main equal groups, 8 rats each, placed in individual cages and classified as follow:-

1. Control group: received no drugs, served as control non-treated for all experimental groups.
2. Pomegranate molasses (PM): Rates were received PM orally (500 mg /kg body weight, in 1 ml water as a suspension) as suspension orally for 21th days (Huang, et al., 2005).
3. Streptozotocin group (STZ): Rats were intramuscular injected (40 mg /kg body weight) once at the first day of experiment by STZ (Sri et al., 2003).
4. Streptozotocin+ Pomegranate molasses (PM) group (STZ+PM): Rats were intramuscular injected with STZ and after 3 days they were injected with PM (500 mg /kg body weight, in 1 ml water as a suspension) orally for 21th days.

Sampling:

Blood samples and tissue specimens (pancreatic tissues) were collected at the end of experiment on 22th day for all groups.

Blood samples:

Directly, after animals were anaesthised using diethyl ether, blood samples were collected from the heart and put in tubes with and without EDTA and then centrifuged at 3500 rpm for 15 minutes. Serum, plasma and whole blood were collected and kept at (-20ºC).

Tissue samples (Pancreas tissue):

Specimens from pancreas tissue were fixed in 10% buffered neutral formalin solution, dehydrated, embedded in paraffin and then five-micron thick paraffin sections were prepared and fixed on glass slides. Slides were then stained with hematoxylin and eosin"H&E" by routine procedure. (Banchroft et al., 1996). Histological study for pancreas tissue was performed by Dr. Adel Bakir Medicine college, Cairo Universty.

Biochemical analysis:

We measured blood glucose, insulin, glucose-6-phosphate (G6PD). We also measured lipid profile (cholesterol, triglycerides, high-density lipoprotein (HDL) and low-density lipoprotein (LDL). In addition, measuring some antioxidants such as catalase (CAT), glutathione (GSH), superoxide dismutase (SOD), glutathione Peroxides (GPx), superoxide dismutase (SOD), glutathione Peroxides (GPx) and malondialdehyde (MDA). Also, measuring the activity of both liver enzymes (alanine aminotransferase (ALT) and aspartate aminotransferase (AST). Also, measure Urea and creatinine (Kidney function) in the blood. were analyzed according to the methods described by Trinder (Trinder, 1969) Rat insulin ELISA was measured using kit of accu-bindelisa microwells, Monobind Inc., Lake Forest, CA 92630, USA (Eastham, 1985).

Statistical analysis:

Statistical analysis of the results obtained was carried out using SPSS version 15-softwae programe**.**

Results

Biochemical effects of Pomegranate molasses (PM) treatment on some blood, serum and pancreatic tissue parameters of streptozotocin-induced diabetes in rats.

STZ group (positive control) results showed significant increase in the level of blood glucose, cholesterol, triglycerides, LDL, MDA, level of AST & ALT activity and significant decrease in insulin and G6PD, CAT, GSH, GPx and SOD with no changes in results of urea and creatinine levels. And a significant decrease in body weight of rats during the period of the experiment compared with the negative group.

In STZ groups administrated with PM results showed significant decrease in the level of blood glucose, cholesterol, triglycerides, LDL, MDA, level of AST & ALT activity and significant increase in insulin and G6PD, CAT, GSH, GPx and SOD with no changes in urea and creatinine levels. The results also showed significant increase in body weight of rats during the period of the experiment compared with the positive group.

Effect of PM treatment on pancreatic tissue of streptozotocin-induced diabetes in rats:

In figure (1), after injection of streptozotocin Show atrophy in pancreatic tissue and after treatment with PM make ameliorated pancreatic tissue.

Discussion

In this study, diabetic rats treated with Pomegranate molasses (PM) results compared with STZ group showed a significant decrease in glucose concentration with significant increase in insulin level and G6PD activity. On the other hand results showed significant decrease in cholesterol, triglyceride, LDL levels with significant increase in HDL level. A significant decrease in MDA level and significant increase in CAT, GPx, SOD activities and GSH level. Liver enzymes ALT, AST activities were significantly decreased. While Urea and creatinine (Kidney function) levels showed no significant changes. Results showed asignificant increase in animal body weight compared with STZ group. Histological studies of pancreatic tissue showed regression in cells atrophy caused by STZ with newly formed pancreatic β-cells.

Pomegranate molasses is a highly nutritive product, since it is processed as concentrate. Especially the presence of mineral content of the fruit are in higher concentration of the molasses, gives it an exceptional nutritional characteristic (Incedayi et al., 2010).

Some compounds in pomegranate seed, such as ellagic, gallic and ursolic acid, have been identified as having anti-diabetic actions as stated by Banihani et al., (2013). The effects of these plants may delay the development of diabetic complications and correct the metabolic abnormalities (Atta et al., 1989; Al-Rowais, 2002).

It has been demonstrated that, pomgranate shows hypoglycemic activity in diabetic animals (Jafri et al., 2000). This decrease may be the result of increased glycolysis (Snigur et al., 2008). Administration of Pomegranate increased plasma insulin levels in STZ-induced diabetic rats suggesting its possible action by increasing insulin release (Rao et al., 2010). Babu et al., (2008) found that, the activity of glucogenic enzyme glucose-6-phosphatase is increased which explain G6PD level reduction in this study.

Elberry et al., (2011) reported that Pomegranate administration resulted in lowering the plasma levels of cholesterol, LDL, and triglyceride with elevation of HDL level. Pomegranate molasses has recently been demonstrated to improve lipid profiles in type II diabetic patients with hyperlipidemia (Esmaillzadeh et al., 2004).

Pomegranate is a rich source of anthocyanins, ellagitannins and other phenolic compounds, which are already proved to have antioxidant activity (Perez-Vicente et al. 2004).

Presence of antioxidant compounds in Pomegranate reduce free radicals, oxidative stress and lipid peroxidation (Rosenblat et al., 2006). Pomegranate flavonoids increase activity of CAT, SOD, GPx and GR enzymes (Sudheesh and Vijayalakshmi, 2005). Also caused significant decrease in MDA (Turk et al., 2008).

The improvement of CAT, SOD and GPx enzyme activities could be possibly explained by antioxidant properties of Pomegranate molasses due to presence of bioactive polyphenolic compounds, which play a role in scavenging free radicals and also prevent DNA damage (Fyiad et al., 2012).

Kaur et al., (2006) reported that treatment with Pomegranate have a protective effect against hepatic injury with inhibition in serum of AST and ALT enzymes which may be due to potent antioxidant and hepatoprotective Properties of Pomegranate.

Chin et al., (1994) previously reported that Pomegranate is a growth factor for rats as shown by enhanced weight gain and improved feed efficiency. Thus, we consider that Pomegranate may have some growth promotional function.

In addition, the presence of one or more bioactive antihyperglycemic principles, such as flavonoids, isoflavones, and their synergistic effects (Manoharan et al., 2009). Pomegranate known to be natural antioxidants and thus protecting the existing β-cells from dying by their

free radical scavenzing action (Kaneto et al., 1999). That is in agreement with the histological findings in our study.

Conclusion & recommendations

From the present study we may conclude that Pomegranate molasses have anti-diabetic effect against pancreatic islets damage caused by STZ. In addition, repair/regeneration of β – cells in islets of Langerhans and induce insulin syntheses and secretion. Therapeutic effects of Pomegranate molasses are basically depends on their anti-oxidant properties and improving the anti-oxidant system work against STZ oxidative stress and its damage effect.

This study recommends the use of Pomegranate molasses natural materials as anti-diabetic agents for their antioxidant effect, anti-hyperglycemia and anti-hyperlipidemia and working on the formation of new β- cells in Islands of Langerhans.

Table 1

Effect of Pomegranate molasses treatment on some blood, serum and pancreatic tissue parameters of streptozotocin-induced diabetes in rats.

Experimental groups / Parameters	Control Normal group	PM group	STZ group	STZ+PM Group
Glucose (mg/dl)	88.0± 8.4^{b}	89.5± 8.70^{b}	418.0± 38.70^{a}	418.0± 38.70^{a}
Insulin (mIU/ml)	8.63± 0.83^{b}	7.90± 0.76^{b}	1.18± 0.09^{a}	8.57± 0.80^{b}
G6PD (U/g Hb)	39.5± 3.24^{b}	38.6± 3.41^{b}	16.0± 1.10^{a}	38.06± 3.42^{b}
Cholesterol (mg/dl)	106.7± 8.54^{b}	105.0± 8.21^{b}	183.0± 16.55^{a}	106.2± 10.58^{b}
TG (mg/dl)	63.3± 5.70^{b}	62.5± 5.16^{b}	176.8± 12.5^{a}	63.8± 3.95^{b}
HDL (mg/dl)	39.6± 3.37^{b}	38.6± 3.46^{b}	18.04± 1.55^{a}	39.0± 3.23^{b}
LDL (mg/dl)	54.4± 4.3^{b}	53.9± 3.8^{b}	129.3± 11.8^{a}	54.4± 4.9^{b}
GSH (mg/dl)	3.3± 0.25^{b}	3.2± 0.31^{b}	1.2± 0.91^{a}	3.6± 0.31^{b}
GPx (mU/ml)	5.6± 0.32^{b}	5.7± 0.55^{b}	3.1± 0.26^{a}	5.6± 0.41^{b}
MDA (nmol/L)	8.7± 0.65^{b}	8.8± 0.52^{b}	22.5± 2.12^{a}	8.9± 0.59^{b}
CAT (U/L)	618.0± 40.16^{b}	610.1± 50.06^{b}	316.4± 30.14^{a}	596.8± 40.47^{a,b}
SOD (U/ml)	25± 2.12^{b}	26± 1.98^{b}	10± 0.74^{a}	23± 2.12^{b}
ALT (U/L)	23.0± 2.55^{b}	24± 1.93^{b}	66.00± 4.7^{a}	24± 1.86^{b}

Values are expressed as means ± Standard Deviation (n=8).

AST (U/L)	55.0± 4.16[b]	55± 4.16[b]	86± 6.93[a]	56± 3.96[b]
Creatinine (mg/dl)	0.60± 0.06	0.5± 0.05	0.6± 0.05	0.6± 0.05
Urea (mg/dl)	24± 2.16	26± 2.55	25± 2.12	26± 1.58

[a] significant at p≤ 0.05 compared to control group.
[b] significant at p≤ 0.05 compared to STZ group.
Positive control group was compared to negative control group.
Diabetic group treated with tested drugs compared to positive control group (STZ group).

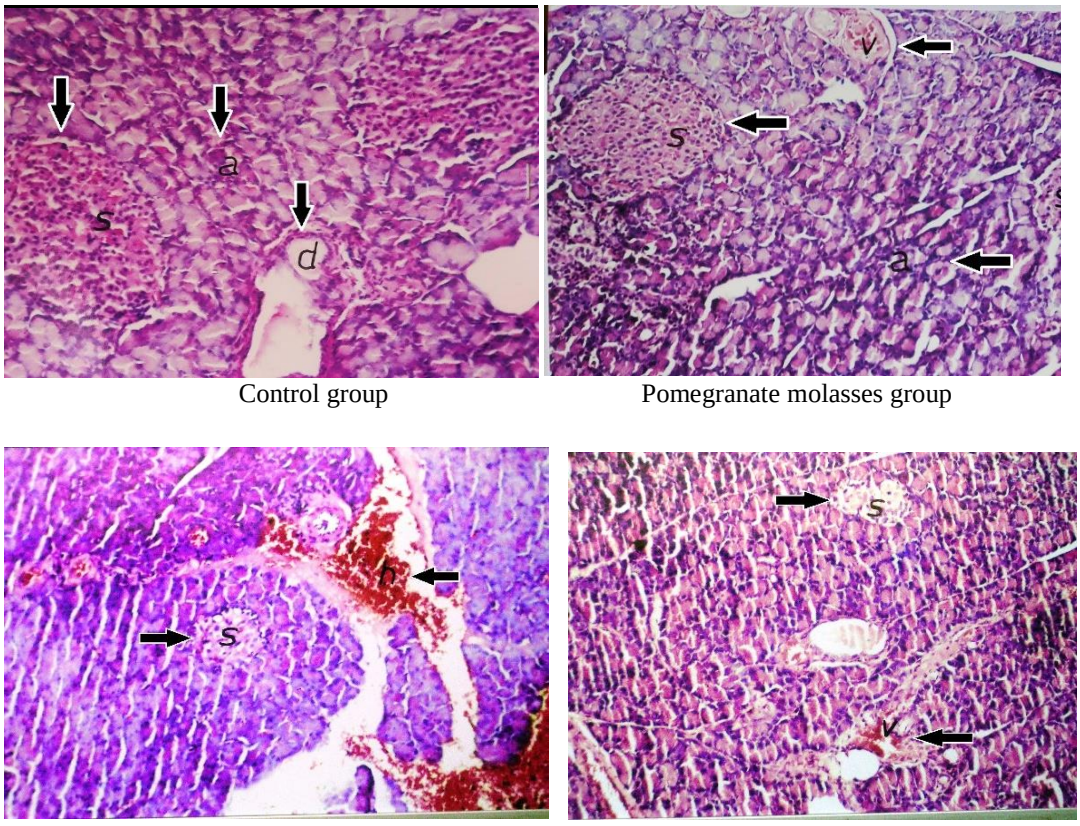

Control group | Pomegranate molasses group

Streptozotocin group | Streptozotocin + Pomegranate molasses group

Fig.1: Effect of Pomegranate molasses treatment on island of Langerhans cells.

References

1. Al-Rowais, N.A. (2002): Herbal medicine in the treatment of diabetes mellitus. Saudi Medical. 23: 1327-1331.
2. Amer, M.A.; Ghattas, M.H.; Abo-Elmatty, D.M and Abou-El-Ela, S.H. (2011): Influence of glutathione S-transferase polymorphisms on type-2 diabetes mellitus risk. Genetic Moliculav Research. 10: 3722-3730.

3. American Diabetes Association (2013): (ADA) Economic costs of diabetes in the U.S. in 2012. Diabetes Care. 36: 1033-1046.
4. American Diabetes Association, (2012): Diagnosis and classification of diabetes mellitus. Diabetes Care. 3: S64-S71.
5. Atta-Ur-Rahman, K. and Zaman, (1989): Medicinal plants with hypoglycaemic activity. Journal of Ethnopharmacol. 26: 1-55.
6. Babu, P.S.; Ignacimuthy, S. and Prince, P.S.M. (2008): Restoration of altered carbohydrate and lipid metabolism by hyponidd, aherbomineral formulation in streptozotocin-induced diabetic rats. Asian Journal of Biochemical. 3: 90-98.
7. Banihani, S.; Swedan, S. and Alguraan, Z. (2013): Pomegranate and type 2 diabetes. Nutrition Research Journal. 33(5): 341-348.
8. Chin, S.F.; Storkson, J.M.; Albright, K.J.; Cook, M.E. and Pariza, M.W. (1994): Conjugated linoleic acid is a growth factor for rats as shown by enhanced weight gain and improved feed efficiency. Journal of Nutrition. 124: 694-701.
9. Domeikienė, A.; Vaivadaitė, J.; Ivanauskienė, R. and Padaiga, Z. (2014): Direct cost of patients with type 2 diabetes mellitus healthcare and its complications in Lithuania. Medicina. 54-60.
10. Eastham, R.D. (1985): Bioghemical Values in Clinical Medicin, 7th Ed Bristol, John Wright &Sons, Ltd.
11. Elberry, A.A.; Harraz, F.M.; Ghareib, S.A.; Gabr, S.A.; Nagy, A.A. and Abdel-Sattar, E. (2011): Methanolic extract of Marrubium vulgare ameliorates hyperglycemia and dyslipidemia in streptozotocin-induced diabetic rats. International Journal of Diabetes Mellitus. 11: 1877-1878.
12. Esmaillzadeh, A.; Tahbaz, F.; Gaieni, I.; Alavi-Majd, H. and Azadbakht, L. (2004): Concentrated pomegranate juice improves lipid profiles in diabetic patients with hyperlipidemia. Journal of Medicinal Food. 7: 305-308.
13. Fyiad, A.A.; Abd El-Kader, M.A. and Abd El-Haleem, A.H. (2012): Modulatory Effects of Pomegranate Juice on Nucleic Acids Alterations and Oxidative Stress in Experimentaly Hepatitis Rats, Life Science Journal. 9(3): 676-682.
14. Happich, M.; Breitscheidel, L.; Benter, U. and Watkins, J. (2007): Cross-sectional analysis of adult diabetes type 1 and type 2 patients with diabetic microvascular complications from a German retrospective observational study. Current Medical Research and Opinion. 23: 1367-1374.
15. He, C.N.; Wang, C.L. and Guo, S.X. (2005): Study on chemical constituents in herbs of Anoectochilus roxburghii II. China Journal of Chinese Materia Medica. 30: 761-776.
16. Huang, T.H.; Peng, G.; Kota, B.P.; Li, G.Q.; Yamahara, J.; Roufogalis, B.D. and Li, Y. (2005): Pomegranate flower improves cardiac lipid metabolism in a diabetic rat model: role of lowering circulating lipids British. Pharmacology Journal. 145: 767-774.
17. Incedayi, B.; Tamer, E.C. and Copur, U.; (2010): A Research on the Composition of Pomegranate Molasses. Journal of Agricultural Faculty. 24 (2): 37-47.
18. International Diabetes Federation. (2013): IDF Diabetes Atlas, 6th Edn. Brussels, Belgium. Available at: http://www.idf.org/diabetesatlas.
19. Jafri, M.A.; Aslam, M.; Javed, K. and Singh, S. (2000): Effect of Punica granatum Linn., (flowers) on blood glucose level in normal and alloxan-induced diabetic rats. Journal of Ethnopharmacol. 70: 309-314.
20. Ji, H.F.; Li, X.J. and Zhang, H.Y. (2009): Natural products and drug discovery. EMBO Reports. 10 (3): 194-200.
21. Jung, M.; Park, Lee, H-Ch.; Kang, Y.; Kang, E.S. and Kim, S.K. (2006): Antidiabetic agents from medicinal plants, Current Medicinal Chemistry. 13: 1203-1218.
22. Kaneto, H.; Kajimoto, Y.; Miyagawa. J.; Matsuoka, T.; Fujitani, Y.; Umayahara, Y.; Hanafusa, T.; Matsuzawa, Y.; Yamasaki, Y. and Hori, M. (1999): Beneficial effects of antioxidants in diabetes: possible protection of pancreatic β–cells against glucose toxicity. Diabetes. 48: 2398-2406.
23. Karow, T. and Lang-Roth, R. (2010): Pharmakologie und Toxikologie. Thomas Karow.
24. Kaur, G.; Jabbar, Z.; Athar, M. and Alam, M.S. (2006): Punicagranatum (pomegranate) flower possesses potent antioxidant activity and abrogates Fe-NTA induced hepatotoxicity in mice. Food and Chemical Toxicology. 44(7): 984-993.
25. Lin, Y. and Sun. Z. (2010): Current views on type 2 diabetes. Journal of the Endocrinol. 204: 1-11.

26. Manoharan, S.; Kumar, R. Anish; Mary, A. Linsa; Singh, R. B.; Balakrishnan, S. and Silvan, S. (2009): Effects of punica granatum flowers on carbohydrate metabolizing enzymes, lipid peroxidation and antioxidants status in streptozotocin induced diabetic rats. The Open Nutraceuticals Journal. 2: 113-117.
27. Patel, K. and Srinivasan, K. (1997): Plant foods in the management of diabetes mellitus: vegetables as potential hypoglycemic agents. Nahrung. 41: 68-74.
28. Perez-Vicente, A.; Serrano, P.; Abellan, P. and Garcia-Viguera, C. (2004): Influence of packaging material on pomegranate juice colour and bioactive compounds, during storage. Journal of the Science of Food and Agriculture. 84 (7): 639-644.
29. Rao, M.U.; Sreenivasulu, M.; Chengaiah, B.; Reddy, K.J. and Chetty, CM. (2010): Herbal medicines for diabetes mellitus: a review. International Journal of Pharm Tech Research. 2(3):1883-1892.
30. Rosenblat, M.; Volkova, N.; Coleman, R. and Aviram, M. (2006): Pomegranate byproduct administration to apolipoprotein e-deficient mice attenuates atherosclerosis development as a result of decreased macrophage oxidative stress and reduced cellular uptake of oxidized lowdensity lipoprotein. Journal of Agricultural and Food Chemistry. 54: 1928-1935.
31. Said, G. (2007): Diabetic neuropathy-a review. Nature Clinical Practice Neurology. 3: 331-340.
32. Snigur, G.L.; Samokhina, M.P.; Pisarev, V.B.; Spasov, A.A.; Bulanov, A.E. (2008): Structural alterations in pancreatic islet snstreptozotocin- induced diabetic rats treated with of bioactive additive on the basis of Gymnema sylvestre. Morfologua. 133(1): 60-64.
33. Sri, M.B; Rukkumani, R. Meon, V.P. (2003): Protective effects of ferulic acid on hyperlipidemic diabetic rats. Acta Diabetol 40:118-122.
34. Sudheesh, S. and Vijayalakshmi, N.R. (2005): Flavonoids from Punica granatum potential antiperoxidative agents. Fitoterapia. 76(2): 181-186.
35. Tang, X.; Tang, G. and Özcan, S. (2008): Role of micro RNAs in diabetes. Biochimica et Biophysica Acta.1779: 697-702.
36. Trinder, P. (1969): Determination of blood glucose using an oxidaseperoxidase system with a non-carcinogenic chromogen. Journal of Clinical Pathology. 22 (2): 158-161.
37. Turk, G.; Sonmez, M.; Aydin, M.; Yuce, A.; Gur, S.; Yuksel, M.; Aksu, E.H. and Aksoy, H. (2008): Effects of pomegranate juice consumption on spermquality, spermatogenic cell density, antioxidant activity and testosterone level in male rats, Clinical Nutrition. 27: 289-296.
38. Wang, W.T.; Lee, P.; Yeh, H.W.; Smirnova, I.V. and Choi, I.Y. (2012): Effects of acute and chronic hyperglycemia on the neurochemical profiles in the rat brain with streptozotocin-induced diabetes detected using in vivo 1H MR spectroscopy at 9.4 T. Journal Neurochemistry. 121(3): 407-417.
39. Zaki, M.A.; Moghazy, T.F.; El-Deeb, M.M.K.; Mohamed, A.H. and Mohamed, N.N.A. (2014): Glutathione S-transferase M1, T1 and P1 gene polymorphisms and the risk of developing type 2 diabetes mellitus in Egyptian diabetic patients with and without diabetic vascular complications. Alexandria Journal of Medicin. Article in press.

BIOCHEMICAL EVALUATION ON PROPOLIS IN EXPERIMENTAL STZ DIABETIC RATS

Omayma A.R. ABOU ZAID[1], Khalid M. FARARH [2] , Aliaa H. ALI[3]

[1,3]Biochemistery Department, Faculty of Vet. Med. Moshtohor, Benha University, Egypt.
[2]Clinical pathology Department, Faculty of Vet. Med. Moshtohor, Benha University, Egypt

Abstract

This aim of study was to describe the antidiabetic activity of Propolis on 60 male rat and weighting 200 – 250 gm. the rat were divided into three equal groups of 20 male rats. Group 1: control Normal group (CN).Group 2: diabetic group (DN). Group 3: Propolis treated group orally (60 mg/kg bwt /day) for 50 days (8weeks). Blood samples were collected from all animal groups after 4 & 6 and 8weeks from the onset of treatment and processed directly for determination of Glucose, Urea, creatinine , Uric acid , Albumin , Cholesterol, triglyceride, HDL, LDL concentration in blood serum and activities AST, ALT in addition to MDA, GSH, and SOD activities in RBCs. The obtained results revealed a significant increase in Glucose , urea, creatinine, uric acid, Cholesterol, Trigyycreide, LDL , MDA level AST, ALT activity a marked significant depletion in GSH content and SOD activity in the blood of diabetic rat compared to control. Contrary results obtained in diabetic group (DN) treated with Propolis So, From the obtained results of the present study it could be concluded that administration of citrullus colocynthis to diabetic rat which may improve glucose, kidney function, liver enzyme, lipid profile, antioxidant enzyme.

Keywords*: experimental diabeties mellitus; Propolis, oxidative stress heptorenal function lipid profile.*

Introduction

Diabetes mellitus is a group of metabolic diseases characterized by hyperglycemia resulting from defects in insulin secretion, insulin action, or both. The chronic hyperglycemia of diabetes is associated with long-term damage, dysfunction, and failure of various organs, especially the eyes, kidneys, nerves, heart, and blood vessels (Robertson,. 2004).

Some medicinal plants have been reported to be useful in diabetes worldwide and have been used empirically as antidiabetic and antihyperlipidemic remedies (Huang, et al., 2005) .Antihyperglycemic effects of these plants are attributed to their ability to restore the function of pancreatic tissues by causing an increase in insulin output or inhibit the intestinal absorption of glucose or to the facilitation of metabolites in insulin dependent processes. However, searching for new antidiabetic drugs from natural plants is still attractive because they contain substances which take alternative and safe effect on diabetes mellitus. Most of plants contain glycosides, alkaloids, terpenoids, flavonoids, cartenoids, etc., that are frequently implicated as having antidiabetic effect (Loew, et al., 2002).

Propolis is traditional medicine and has been reported to exert abroad spectrum of biological functions including antioxidant activity (Benguedouar, et al., 2008) .Also, Propolis may improve disturbed metabolism associated with diabetes (Yamabe, et al., 2006) .

Accordingly, this study was performed to investigate the antidiabrtic, antioxidant and hypolipidemic effect of Propolis *on* experimentally diabetic rat.

Material and Methods

Animals:

60 male albinos Wister rats, weighting 200 – 250 gm were used in this study obtained from Laboratory Animals Research Center, Faculty of Veterinary Medicine, Benha University, Egypt. Rats were housed in separated metal cages 10-25 per cage and kept under the same constant environmental and nutritional condition through out the period of investigation; water

was supplied *ad Libitum*, in the special laboratory animal room at Faculty of Vet. Med. Moshtohor, Benha University.

***Chemicals*:** streptozotocin were purchased from Segma (USA). for trading chemicals, medicines and medical appliances, Egypt. Other chemical and kits purchased from Diamond, Vitro (Egypt).

Nutraceuticals preparation:

PE was prepared by mixing 50 g of the propolis powder with 100 ml of deionized water and shaking or left at room temperature for three days then filters the mixture. Collect the filtrate and resuspend the precipitate in 100 ml distilled water with shaking at 40 ºC for three days then filter the mixture. collect the filtrate and resuspend the precipitate in 50 ml acetone at 40 ºC for two days till a smooth paste formed and then mix it with the previously collected filtrate and complete with distilled water to obtain the required concentration) (Park, et al., 1998).The obtained PE was administrated orally at a dose of 300 mg/kg b.w (Basnet, etal., 1996a).

***Preparation of streptozotocin*:** Rats were fasted for 18 hr and allowed free access of water the experimental induction of diabetes in male was induced by intrapertinoel (i.p) injection dose of 60 mg/kg of streptozotocin (STZ) (Sigma chemical co. P.O Box. 14508, st. Lowis, U.S.A.) For 3 successive days (dissolved in citrate buffer 0.1 mol/l, PH 4.2) .(Abdel-Hassan, et al., 2000).

***Experimental design* :** the rats were divided into the following groups:The animals were divided into 3 groups: control group & diabetic group and citrullus colocynthis treated group (CCT) group.

1- *GroupI: (control group):* Comprised of 20 male rats, injected with citrate buffer only served as control group.

2- *GroupII: (Diabetic group):* Comprise 20 rats fed with normal diet injected with streptozotocin intrapertinoel dissolved in citrate buffer PH (=4.2) at dose 60 mg/kg bwt for 3 successive days.

3- *GroupIII*: (diabetic Propolis treated group(PT) : Comprised 20 diabetic male rats received propolis by oral gavages daily at a dose of 300 mg/kg body weight after five weeks from the onset of diabetes induction.

Blood sampling:

Rats were fasted over night, collected blood in coated glass tubes via reto – orbital bleeding for each animal and each sample was collected into two tubes, heparinized and non–heparinized. The non heparinized blood samples were allowed to coagulate and then centrifuged at 3000 r.p.m. for 10 minutes. The separated serum used for the estimation of serum glucose (Trinder ,1969), urea (Patton ,et al., 1977), creatinine (Murray , 1984c), uric acid (Teitz ,1995), albumin (Doumas, et al., 1971), AST, ALT (Frankel, 1995) , cholesterol, Triglycerides (Schettler, et al.,1975), cholesterol HDL (Gordon, et al., 1977), cholesterol LDL (Friedewald, et al., 1972) and L-Malondialdehyde(L-MDA) (Esterbauer ,et al., 1982), Super oxide dismutase (SOD) (Beutler ,et al., 1963), Glutathione (GSH) determination (Nishikimi, et al., 1972).

Preparation of erythrocytes:

Washing of erythrocytes *:* Red blood cells were washed according to the method described by(Trinder ,1969).To 0.2 ml of collected heparinized blood, 2 ml of sodium chloride solution was added, mixed well and centrifuged for 15 minutes at 3000 r.p.m the plasma and buffy coat were discarded by careful suction (this process was repeated 3 times) After centrifugation, aliquots were used for L-Malondialdehyde (L-MDA), Super oxide dismutase (SOD), Glutathione (GSH) determination (Kornberg, et al., 1955).

Statistical analysis:

Statistical analysis was done using SPSS software version 15. The inter-group variation was measured by one way analysis of variance (ANOVA) followed by Post Hoc LSD test. Results were expressed as mean ± SEM. The mean difference is significant at the $p \leq 0.05$ level (Snedecor , et al., 1969).

Results

Effect of propolis on changes of glucose , Kideny function, Liver function, lipids profiles, Lipid peroxidation and antioxidants in diabetic rats.

The obtained results in table 1, 2, and 3 showed decrease in glucose concentration, urea, creatinine, uric acid concentration, AST, ALT activity, Cholesterol, triacylglycerol, LDL and L-MDA concentration compared to diabetic rats. And increased albumin, HDL concentration, and GSH, SOD activity compared to diabetic rats after 4, 6 and8 weeks of Citrullus colocynthis administration.

Discussion

Diabetes mellitus is associated with microvascular, macro vascular and non-vascular complications (Montilla, et al., 2005) .Increase production of reactive oxygen species plays a role in pathogenesis and pathophysiological mechanisms that trigger diabetic complications (Nobecourt, et al.,2005).

Some serum glucose concentrations in diabetic rats showed significant increase in serum glucose concentrations in experimental diabetic rats all over the periods of the experiments. These results were nearly similar to those reported by (Yoshida,et al., 2008) after the STZ had been injected. They attributed this increase to the diabetogenic action of STZ due to the direct result of irreversible damage to the pancreatic beta cells resulting in degranulation and loss of capacity to secrete insulin.

Treatment with propolis in experimental diabetic rats showed decrease in glucose concentration in diabetic groups treated with Propolis due to the water extract of propolis (200 mg/kg) prevented β cells destruction by inhibiting IL-1β generation and NO synthase activity). Propolis may control blood glucose and modulate glucose and lipid metabolism, leading to decreased outputs of lipid peroxidation and scavenging the free radicals in diabetic rats (Fuliang, et al., 2005).

Concerning to kidney function markers, there was significant increase in the concentration of urea, creatinine and uric acid in diabetic rats compared to the control ones after 4,6,8 weeks this results agree with previously reported data were predominantly the increase in kidney function in patients with type I diabetes due to impaired glomerular filtration rate (Ross,1988).The increased concentration of urea, creatinine and uric acid were attributed to the renal damage caused by abnormal glucose regulation, including elevated glucose and

glycosylated protein tissue levels, hemodynamic changes within the kidney tissue, and increased oxidative stress. Also, Mild hyperuricemia was further shown to induce renal microvascular disease independent of blood pressure, as consequence of activation of the renin–angiotensin–aldosterone system, (Mazzali ,et al., 2002).

Treatment with propolis in experimental diabetic rats showed significant reduction in kidney function.(Nirala, et al.,2008). These decrease in kidney function after treatment with propolis that propolis may prevent hepatorenal injury by inhibiting lipid peroxidation and enhancing the activities of antioxidant enzymes (Abo-Salem ,et al., 2009).

Concerning to liver function markers, there was significant increase in the activities of AST and ALT in diabetic rats compared to the control ones after 4,6,8 weeks,which albumin showed significant decrease. These results agree with previously reported data (Jorda ,et al., 1982). The increased activities of AST and ALT were attributed to increased protein catabolism accompanying gluconeogenesis and urea formation in diabetic rat. Moreover loss of insulin effect on the liver leads to glycogenolysis with high hepatic glucose production, which may enhance the increase in AST and ALT (Begum, 1978).

Treatment with propolis in experimental diabetic rats showed significant decrease in activities of AST and ALT (Bhadauria, et al., 2007) . this improvment by propolis may be due to hepatoprotective role of propolis through reducing oxidative stress in living system. Also, dietary intervention with propolis preparations reduces free-radical-induced lipid peroxidation in liver (Bhadauria, et al., 2008).

Concerning to lipid profile markers, there was significant increase in the concentration of cholesterol, triacylglycerol and LDL in diabetic rats compared to the control ones after 4,6,8 weeks, which HDL showed significant decrease. These results agree with previously reported data were predominantly the increase in Liver function in patients with type I diabetes may be due to this increase to hypercholesterolemia is common in diabetes, contributing to the high prevalence of coronary heart disease (Gentile, et al., 2000).

Treatment with propolis in experimental diabetic rats showed significant reduced in Cholesterol ,Triacylglycerol, LDL-C and increased in HDL concentration. The decease in lipid profile is due to propolis reducing some of the major risk factors of cardiovascular disease. So, propolis preparations could modulate lipid metabolism and reduce the syndrome caused by blood lipid abnormalities. Also, the antioxidant effects of propolis have amelioration affect on diabetes (Abo-Salem,et al.,2009) . this improvement of serum HDL and LDL to propolis inhibits oxidative damage in various tissues of streptozotocin-induced diabetic animals (El-Sayed ,et al., 2009).

Concerning to antioxidant enzymes markers, there was significant decrease in and a significant decrease in GSH content, and SOD activity in diabetic rats compared to the control ones after 4,6,8 weeks, which L-MDA concentration showed significant increased.These results agree with previously reported data (Knoll, et al., 2005) who reported that the increase in the level of MDA were attributed to Increased formation of ROS may occur in diabetes for reasons possibly related to an increase in glucose concentrations in plasma and tissues and agreement with (Dallak, , 2011).who attributed this decreased in GSH content in diabetic rats' liver were observed significantly (GSH acts as an antioxidant and its level are reduced in diabetes mellitus. Decreased GSH levels represent increased utilization due to increased oxidative stress. Also (Yoshida, ,et al.,2008).who attributed this decrease in SOD may be due to the utilization of antioxidant enzymes in the removal of released H_2O_2 released so that

Hyperglycemia reduces the synthesis and activities of a number of antioxidant enzymes including SOD presumably by glycation

Treatment with propolis in experimental diabetic rats showed significant reduced L-MDA The obtained results agree with those recorded by(Yang, et al., 2009) who attributed this improvement in L-MDA activity to propolis which has strong antioxidative activity and is confirmed to inhibit increase of MDA level and improve antioxidase activity in the animal model and patients (Kanbur, et al., 2009) this increase in erythrocyte reduced GSH content this increase in GSH activity is due to the protective effect of propolis on hepatorenal function is partially attributed to antioxidant activity and it may act by affecting the mitochondrial respiratory chain. In addition, (Eraslan, et al., 2008). this increase in SOD activity to the effects of Caffeic acid phenethyl ester (CAPE), which is a component of propolis, on lipid peroxidation and antioxidant enzymes in a diabetic rat. They found that in the untreated diabetic group, the SOD activity level were significantly decreased, while the GSH activity was increased in the CAPE-treated diabetic rats compared to those observed in untreated diabetic rats (Okutan,etal., 2006)

Conclusion

It can be concluded that, propolis plays an important role in experimental diabetic rat, because it shows preventive action against its secondary complications due to: hypoglycaemic, antioxidant and Hypolipidemic action.

References

1. Abdel-Hassan, I.A., Abdel-Barry, J.A., and Mohammeda, S.T. 2000. The hypoglycaemic and antihyperglycaemic effect of Citrullus colocynthis fruit aqueous extract in normal and alloxan diabetic rabbits. J. Ethnopharmacol., 71: 325-330.
2. Abo-Salem, O.M.; El-Edel, R.H.; Harisa, G.E.; El-Halawany, N. and Ghonaim M.M. 2009. Experimental diabetic nephropathy can be prevented by propolis: Effect on metabolic disturbances and renal oxidative parameters. *Pak. J .Pharm Sci*, 22(2):205-10.
3. Abo-Salem, O.M.; El-Edel, R.H.; Harisa, G.E.; El-Halawany, N. and Ghonaim M.M. 2009. Experimental diabetic nephropathy can be prevented by propolis: Effect on metabolic disturbances and renal oxidative parameters. *Pak. J .Pharm Sci*, 22(2):205-10.
4. Basnet, P.; Matsushige, K.; Hase, K.; Kadota, S. and Namba, T. 1996 a. Potent antihepatotoxic activity of dicaffeoyl quinic acids from propolis. Biological and Pharmaceutical Bulletin; 19(4): 655- 657.
5. Begum, N., and Shanmugasundaram, K.R. 1978. Transaminases in experimental diabetes. Arogya J Health Sci; 4:116-22.
6. Benguedouar, L.; Boussenane, H.N.; Kebsa, W.; Alyane, M.; Rouibah, H. and Lahouel, M. 2008. Efficiency of propolis extract against mitochondrial stress induced by antineoplasic agents (doxorubicin and vinblastin) in rats. *Indian JExpBiol;* 21:112-9.
7. Beutler, E.; Duron, O. and Kelly, M.B. 1963. Improved method of estimation of blood) yglutathione. Lab. Clin. Med., 61(5): 882.
8. Bhadauria, M.; Nirala, S. K. and Shukla, S. 2007. "Propolis protects CYP 2E1 enzymatic activity and oxidative stress induced by carbon tetrachloride," *Molecular and Cellular Biochemistry*, vol. 302, no. 1-2, pp. 215–224.
9. Bhadauria, M.; Nirala, S. K. and Shukla, S. 2008. "Multiple treatment of propolis extract ameliorates carbon tetrachloride induced liver injury in rats," *Food and Chemical Toxicology*, vol. 46, no. 8, pp. 2703–2712.
10. Dallak, M., in vivo, 2011. hypolipidemic and antioxidant effects of Citrullus colocynthis pulp extract in alloxan-induced diabetic rats. African Journal of Biotechnology; 10(48): 9898-903.
11. Doumas, B. T.; Watson, W. and Biggs, H. G. 1971. Albumin stan- dards and the measurement of serum albumin with bromcresol green. Gun. Chim. Acta 31,87

12. El-Sayed, S.M.; Abo-Salem, O.M.; Aly, H.A. and Mansour, A.M. 2009. Potential antidiabetic andhypolipidemic effects of propolis extract in streptozotocin-induced diabeticrats. *Pak JPharm Sci*, 22:168–174. 38-48.
13. Eraslan, G.; Kanbur, M.; Silici, S.; Altinordulu, S. and Karabacak, M. 2008. "Effects of cypermethrin on some biochemical changes in rats: the protective role of propolis," *Experimental Animals*, vol. 57, no. 5, pp. 453–460.
14. Esterbauer, H.; Cheeseman, K. H.; Danzani, M. U.; Poli, G. and Slater, T. F. 1982. Separation and characterization of the aldehyde products of ADP/Fe^{+2}C stimulated lipid peroxidation in rat liver microsomes. Biochem. J; 208: 129-140.
15. Frankel, E. 1995. Nutritional benefits of flavonoids. International Conference on food factors: Chemistry and Cancer Prevention, Hamamatsu, Japan. Abstracts, C6-2. Mangili R., 1998. MJcroalbuminuria in diabetes. Clin, Chem, Lab, Med, 63 (12); 941 – 6.
16. Friedewald W.T., Levy, R.I. and Fredrickson, D.S. 1972. Estimation of the concentration of low-density lipoprotein cholesterol in plasma, without use of the preparative ultracentrifuge.Clin. Chem.; 18:499–502.
17. Fuliang, H. U.; Hepburn, H. R.; Xuan, H.; Chen, M.; Daya, S.; and Radloff, S. E. 2005. "Effects of propolis on blood glucose, blood lipid and free radicals in rats with diabetes mellitus," *Pharmacological Research*, vol. 51, no. 2, pp. 147–152.
18. Gentile, S., Turco, S., and Guarino, G. 2000. Comparative efficacy study of ator-vastatin vs. simvaslatin, provastatin, lovastnlin and placebo in type 2 diabetic patients with hypercholcslerolemia. Diabetes, 2: 355-362.
19. Gordon, T.; Castell, W. P.; Hjortland, M. C.; Kannel, W. B. and Dawber, T. R. 1977. High-densitylipoprotein as a protective factor against coronary heart disease. Am. J. Med., 62, 707-714.
20. Huang, T.H., Kota, B.P., Razmovski, V., and Roufogalis, B.D. 2005. Herbal or natural medicines as modulators of peroxisome proliferator-activated receptors and related nuclear receptors for therapy of metabolic syndrome. Basic Clin. Pharmacol. Toxicol., 96: 3-14.
21. Jorda, A., Gomez, M., Cabo, J., and Gandrisolia, S. 1982. Effect of streptozotocin Journal of Immunology 68: 216-27.
22. Kanbur, M.; Eraslan, G. and Silici, S. 2009. "Antioxidant effect of propolis against exposure to propetamphos in rats," Ecotoxicology and Environmental Safety, vol. 72, no. 3, pp. 909–915.
23. Knoll, K.E., Pietrusz, J.L., and Liang, M. 2005. Tissue-specific transcriptome responses in rats with early streptozotocin-induced diabetes. *Physiol Genomics*, 21:222-9.
24. Kornberg, A. and Horecker, B. L. 1955. Glucose 6 phosphate dehydrogenase. In Methods in Enzymology, Vol. 1, edited by S. P. Colowick and N. 0. Kaplan, pp. 323-325. Academic Press, New York.
25. Loew, D., and Kaszkin, M. 2002. Approaching the problem of bioequivalence of herbal medicinal products. Phytother. Res., 16: 705-711.
26. Mazzali ,M.; Kanellis, J.; Han, L.; Feng, L.; Xia, Y.Y.; Chen, Q.; Kang, D.H.; Gordon, K.L.; Watanabe, S.; Nakagawa, T.; Lan, H.Y. and Johnson, R.J. 2002. Hyperuricemia induces a primary renal arteriolopathy in rats by a blood pressure-independent mechanism. Am J Physiol Renal Physiol; 282:F991–F997.
27. Montilla, P.; Barcos, M.; Munoz, M.; Castaneda, I. and Tunez, I. 2005. Red wine prevents brain oxidative stress andnephropathy in streptozotocin-induced diabetic rats. *J. Biochem. Mol. Biol.,* 38(5): 539-544.
28. Murray, R. 1984c. Creatinine; in Kaplan et al., (1984): The C.V. Mosby Co. St Louis.Toronto. Princeton: 1261-1266 and 418.
29. Nirala, S. K.; Bhadauria, M. and Shukla, S. 2008. "Pharmacological intervention of tiferron and propolis to alleviate berylliuminduced hepatorenal toxicity," Fundamental and Clinical Pharmacology, vol. 22, no. 4, pp. 403–415.
30. Nishikimi, M.; Roa, N.A. and Yogi, K. 1972: Measurement of superoxide dismutase. Biochem. Biophys. Res. Common, 46:849-854.
31. Nobecourt, E.; Jacqueminet, S.; Hanset, B.; Chantepie, S.; Grimaldi, A.; Chapman, M.J. and Kontush, A. 2005. Defective antioxidative activity of small dense HDL 3 particles in type 2 diabetes: relationship to elevated oxidative stress and hyperglycemia. *Diabetologia*, 48(3): 529-538.

32. Okutan, H.; Ozcelik, N.; Yilmaz, R.H. and Uz, E. 2006. Effects of caffeic acid phenethyl ester on lipid peroxidation and antioxidant enzymes in diabetic rat heart. Clin Biochem. ; 38(2):191–196.
33. Park, Y. K. and Ikegaki, M. 1998. Preparation of water and ethanolic extract of propolis and evaluation of the preparation. Biosci. Biotech. Biochem. 62: 2230-2232.
34. Patton, C. L. and Crouch, S. R. 1977. Colorimetric determination of Urea. Analytical Chemistry., 49, 464 469.
35. Robertson, R.P. 2004: Chronic oxidative stress: a central mechanism for glucose toxicity in pancreatic islet beta cell in diabetes. J. Biol. Chem. 279: 4235-2354.
36. Ross, D. 1988. Glutathione, Free radicals and chemotherapeutic agents. Mechanisms of free radical induced toxicity and Glutathione dependant protection. Pharmocol. Ther, 37: 231-249.
37. Schettler, G. and Nüssel, E. 1975. Colorimetric determination of Triglycerides and cholesterol. Arb. Med. Soz. Med. Präv. Med. 10, 25.
38. Snedecor, S. and Cochran, A. 1969. Statistical method 6th ed. The Iowa State University, Press, Iowa, USA.
39. Snedecor, S., and Cochran, A. 1969: Statistical method 6th ed. e Iowa State University., Press, Iowa, USA.
40. Teitz, N. W.; Clinical guide to laboratory tests, W.B. 1995. SaundersCo, Philadelphia, PA, 3rd Edn, p. 238.
41. Trinder, P. 1969. Determination of glucose in blood using glucose oxidase with an alternative oxygen acceptor. *Ann Clin Biochem.*; 6:24-7
42. Yamabe, N.; Yokozawa, T.; Oya, T. and Kirn, M. 2006. Therapeutic potential of (-)-epigaliocatechin 3-Ogallate on renal damage in diabetic nephropathy model rats, Journal of. Pharmacology & Experimental. *Ther*., 319(1): 228-236.
43. Yang, Y.; He, X.; Chen, S.; Wang, L.; Li, E. and Xu, L. 2009. Changes of serum and urine neutrophil gelatinase-associated lipocalin in type-2 diabetic patients with nephropathy: one year observational follow-up study. *Endocrine*, 36(1):45-5.
44. Yoshida, S.I., Hashimoto, T., Kihara, M., Ima, N., Nomur, K., Hirawa, N., Toya, Y., Kitamura, H., and Umemura, S. 2008: Urinary oidative stress markers closely reflect the efficacy of Candesartan treatment for diabetic nephropathy. *Nephron Exp Nephrol*, 111:20-30.
45. Yoshida, S.I., Hashimoto, T., Kihara, M., Ima, N., Nomur, K., Hirawa, N., Toya, Y., Kitamura, H., and Umemura, S. 2008. Urinary oidative stress markers closely reflect the efficacy of Candesartan treatment for diabetic nephropathy. *Nephron Exp Nephrol*, 111:20-30.

Table 1.

Effect of propolis on some biochemical blood parameters of diabetic rats after four weeks of administration:

	Glucose (mg/dl)	Urea (mg/dl)	Creat. (mg/dl)	Uric acid (mg/dl)	ALT (U/ml)	AST (U/ml)	Albumin (g/dl)	Chol. (mg/dl)	Tri. (mg/dl)	HDL (mg/dl)	LDL (mg/dl)	MDA (nmol /ml)	GSH (mmol/ /gm Hb	SOD U/gm Hb
Control group (CN group)	109.00 ± 2.96 ^{b}	49.21 ± 21.42 ^{b}	0.85 ± 9.36 ^{b}	2.18 ± 0.39 ^{b}	10.00 ± 0.53 ^{c}	10.86 ± 0.67 ^{c}	3.96 ± 0.12 ^{a}	145.33 ± 4.00 ^{c}	58.14 ± 6.93 ^{b}	40.56 ± 1.23 ^{a}	94.71 ± 7.96 ^{b}	76.33 ± 1.88 ^{d}	46.10 ± 1.92 ^{b}	23.57 ± 1.83 ^{b}
Diabetic group (DN group)	568.71 ± 37.92 ^{a}	81.10 ± 37.92 $^{a b}$	3.00 ± 4.88 ^{a}	9.58 ± 0.41 ^{a}	23.86 ± 2.40 ^{b}	61.43 ± 6.60 ^{b}	1.93 ± 0.17 ^{c}	221.71 ± 5.80 ^{b}	169.43 ± 4.28 ^{a}	22.87 ± 2.60 ^{c}	161.63 ± 7.48 ^{a}	160.77 ± 2.52 ^{a}	16.73 ± 0.41 ^{d}	18.33 ± 0.50 ^{c}
Propolis treated group	535.71 ± 25.27 ^{a}	97.13 ± 10.01 ^{a}	2.87 ± 0.12 ^{a}	8.97 ± 0.49 ^{a}	34.43 ± 1.70 ^{a}	89.86± 7.83 ^{a}	2.10± 0.14 $^{b c}$	242.57 ± 4.05 ^{a}	184.29 ± 4.05 ^{a}	33.09 ± 1.45 ^{b}	173.47 ± 4.04 ^{a}	122.90 ± 0.67 ^{b}	29.31± 0.86 ^{c}	28.59 ± 2.097 ^{a}

- Data are present as mean Mean± SE
- Mean values with different superscripts within the same column indicate statistical significant differences between groups at $p \leq 0.05$.

Table 2.

Effect of propolis on some biochemical blood parameters of diabetic rats after six weeks of administration:

	Glucose (mg/dl)	Urea (mg/dl)	Creat. (mg/dl)	Uric acid (mg/dl)	ALT (U/ml)	AST (U/ml)	Albumin (g/dl)	Chol. (mg/dl)	Tri. (mg/dl)	HDL (mg/dl)	LDL (mg/dl)	MDA (nmol /ml)	GSH (mmol/ /gm Hb	SOD U/gm Hb
Control group (CN group)	108.57 ±3.12 ^{c}	27.94 ± 2.78 ^{c}	1.27 ± 0.33 ^{c}	2.73 ± 0.53 ^{b}	11.14 ± 0.51 ^{c}	7.57 ± 1.02 ^{b}	4.27 ± 0.16 ^{a}	163.14 ± 8.58 ^{b}	57.29 ± 5.85 ^{c}	37.00 ± 0.97 ^{a}	122.54 ± 10.20 ^{b}	78.10 ± 2.04 ^{d}	40.33 ± 0.79 ^{b}	26.73 ± 1.64 $^{a b}$
Diabetic group (DN group)	572.7 ±34.16 ^{a}	97.43 ± 5.57 ^{a}	3.01 ± 6.66 ^{a}	8.46 ± 0.31 ^{a}	28.29 ± 2.47 $^{a b}$	72.29 ± 6.41 ^{a}	1.93 ± 0.12 ^{c}	217.71 ± 9.11 ^{a}	195.71 ± 5.54 ^{a}	20.39 ± 1.95 ^{c}	165.14 ± 9.02 ^{a}	161.84 ± 2.58 ^{a}	18.00 ± 0.51 ^{d}	14.80 ± 0.99 ^{b}
Propolis treated group	369.71 ± 30.61 ^{b}	78.14 ± 5.46 $^{a b}$	2.50 ± 0.12 $^{a b}$	8.34 ± 0.52 ^{a}	31.00 ± 1.68 ^{a}	62.57 ± 6.24 ^{a}	2.64 ± 0.14 ^{b}	226.00 ± 3.91 ^{a}	175.43 ± 4.28 ^{b}	31.56 ± 2.28 ^{b}	172.43 ± 4.29 ^{a}	117.13 ±1.34 ^{b}	31.29 ±0.98 ^{c}	30.43 ±1.67 $^{a b}$

- Data are present as mean Mean± SE
- values with different superscripts within the same column indicate statistical significant differences between groups at $p \leq 0.05$.

Table 3.

Effect of propolis on some biochemical blood parameters of diabetic rats after eight weeks of administration:

	Glucose (mg/dl)	Urea (mg/dl)	Creat. (mg/dl)	Uric acid (mg/dl)	ALT (U/ml)	AST (U/ml)	Albumin (g/dl)	Chol. (mg/dl)	Tri. (mg/dl)	HDL (mg/dl)	LDL (mg/dl)	MDA (nmol /ml)	GSH (mmol/ /gm Hb	SOD U/gm Hb
Control group (CN group)	107.00 ± 3.89 c	25.14 ± 2.48 c	0.96 ± 7.17 c	3.44 ± 0.24b	9.86 ± 0.59 c	10.00 ± 0.58 c	4.14 ± 0.19 a	170.00 ± 12.12 b	52.29 ± 4.85 c	36.71 ± 1.84 b	145.57 ± 6.54 a b	92.83 ± 13.06 b	44.89 ± 1.24 b	28.04 ± 2.12 b
Diabetic group (DN group)	728.57 ± 83.78 a	108.01 ± 6.79 a	2.99 ± 5.49 a	7.76 ± 0.23 a	46.00 ± 2.33 a	77.29 ± 6.61 a	1.95 ± 7.80 c	198.00 ± 4.72 a	210.29 ± 11.17 a	19.91 ± 1.89 c	162.81 ± 7.65 a	155.10 ± 7.54 a	19.60 ± 1.09 d	12.90 ± 0.78 c
Propolis treated group	370.14 ± 22.37 b	70.14 ± 4.17 b	2.38 ± 0.16 b	7.70 ± 0.43 a	25.00 ± 2.49 b	50.71 ± 5.74 b	3.04 ± 4.59 b	203.00 ± 2.02 a	167.00 ± 4.13 b	33.11 ± 1.88 b	153.36 ± 5.25 a b	105.77 ± 3.23 b	33.84 ± 0.72c	32.84 ± 1.70 a

- Data are present as mean Mean± SE
- values with different superscripts the same each column indicate statistical significant differences between groups at $p \leq$